

For Reference

---

NOT TO BE TAKEN FROM THIS ROOM

# For Reference

NOT TO BE TAKEN FROM THIS ROOM

## Ex LIBRIS UNIVERSITATIS ALBERTAENSIS













THE UNIVERSITY OF ALBERTA

A PHOTOGRAPHIC STUDY OF CAPSULE BEHAVIOR IN A PIPELINE

by

R. T. LIDDLE, B. SC.

A THESIS

SUBMITTED TO THE FACULTY OF GRADUATE STUDIES

IN PARTIAL FULFILLMENT OF THE REQUIREMENTS FOR THE DEGREE

OF MASTER OF SCIENCE

DEPARTMENT OF CIVIL ENGINEERING

EDMONTON, ALBERTA

DATE May 23, 1968



UNIVERSITY OF ALBERTA  
FACULTY OF GRADUATE STUDIES

The undersigned certify that they have read, and recommend to the Faculty of Graduate Studies for acceptance, a thesis entitled "A Photographic Study of Capsule Behavior in a Pipeline" submitted by R. T. Liddle in partial fulfillment of the requirements for the degree of Master of Science.



### ACKNOWLEDGEMENTS

The author wishes to express his gratitude to Dr. G. F. Round, of the Research Council of Alberta and Dr. T. Blench of the University of Alberta for their patient and constructive assistance in their supervision of this investigation.

The author is indebted to the Research Council of Alberta for the financial arrangements made to support this investigation.

The technical assistance of Mr. L. White, Mr. W. Withers, and Mr. K. Grunert, of the Research Council of Alberta, in construction and operation of the experimental equipment, and of Mr. A. Chernick, Technical Services, University of Alberta, in printing of photographs, is gratefully acknowledged.





## ABSTRACT

In the first part of the study, flow patterns around static cylindrical capsules in a 1 1/4" acrylic pipeline were visualized by addition to the water of pigmented acrylic particles which fluoresced under ultra violet light. Measurements were made of the characteristic features of the pattern; namely, vortex dimensions point of separation at the capsule rear and separation of streamlines as they pass over the capsule edge into the annulus. These values were plotted and shown to tend to equilibrium values with increasing water velocity. Pressure drop measurements were also made and correlated with the five different diameter ratios employed. Experiments were performed over a range of fluid velocities from 0.1 ft./sec. to the threshold velocities of the various capsules tested. The maximum threshold velocity was 3 ft./sec. for the smallest diameter capsule.

In the second part of the study clearances of cylindrical capsules from the pipe wall were studied. A theoretical method was outlined for predicting the relation between clearance, velocity, and pressure drops when the liquid flowing in the pipeline was turbulent. The principal assumption was that the flow around the capsule was of Couette type modified by a pressure gradient in the direction of flow. For calculation, the flow condition was separated into two components: a simple Couette flow and an annular flow due to the pressure gradient. The annular space was divided into small radial sectors with the flow in each increment being calculated. Each of these small areas was tested for laminarity using a criterion based on a local Reynolds number.

Experimentally, clearances were measured for capsules of density



ratios 1.01, 1.02, 1.05, 1.10, and 1.15, diameter ratios of 0.70, 0.80 and 0.90 and lengths of 3" and 6", for velocities ranging from 0.2 to 12 ft./sec. The clearance was characterized by two distinct regimes: first where the clearance was small and measurable only through a microscope, with neither nose or tail predominating, and second where the clearances were visible with the unaided eye. In this second regime the capsule always traveled with a large nose-up clearance. The capsule velocity at the point of "nose lift off" varied from 0.70 ft/sec. with a 3" long, 0.90 diameter ratio, 1.01 density ratio capsule to 8.60 ft./sec. with a 6" long, 0.70 diameter ratio, 1.15 density ratio capsule. These "nose lift off" velocities were correlated with density ratio, diameter ratio and capsule length for the range of variables used.

The average clearance was shown to increase with

- (a) decreasing capsule density
- (b) decreasing capsule length
- (c) increasing capsule diameter ratio
- (d) increasing liquid velocity

Capsule pressure drops were shown to decrease with increasing clearance. A confirmation of the hypothesis that the flow is laminar in the capsule pipe annulus was obtained for the 6" long, 0.90 diameter ratio capsules when negative pressure drops were recorded.



# TABLE OF CONTENTS

	Page
List of Tables	i
List of Figures	ii
I INTRODUCTION	1
II LITERATURE REVIEW Flow Patterns	3
III LITERATURE REVIEW Clearances	8
IV THEORY	22
V EXPERIMENTAL APPARATUS	44
VI EXPERIMENTAL PROCEDURE	58
VII DISCUSSION OF EXPERIMENTAL RESULTS - Flow Patterns	60
VIII ANALYSIS AND DISCUSSION OF EXPERIMENTAL RESULTS - Clearances	85
IX CONCLUSIONS	119
X NOMENCLATURE	121
XI BIBLIOGRAPHY	124
Appendices	
AI Velocity Calibrations	127
AII Pressure Cell Calibration	128
AIII Camera - Microscope Calibrations	136
AIV Basic Data Tabulation - Flow Patterns	143
AV Basic Data Tabulation - Clearances	152





i

LIST OF TABLES

<u>TABLE</u>		<u>PAGE</u>
1	Details of Experimental Equipment	50
2	Capsule Dimensions Flow Patterns	51
3	Capsule Dimensions Clearances	81
4	Macro Lift off Velocities	93
A-1	Velocity Calibration Data	127
A-2	Pressure Cell Calibration Data	133
A-3	Camera Microscope Calibration Data	136
A-4	Basic Data Flow Patterns	143
A-5	Basic Data Clearances	152



## LIST OF FIGURES

FIGURE		PAGE
1	Pipe-Concentric Capsule - Charles	9
2	Pipe-Concentric Capsule - Kennedy	11
3	Capsule-Pipe Annulus	23
4	Detail of Clearances	23
5	Forces on Capsule	25
6	Turbulent Flow in Capsule-Pipe Annulus	26
7	Radial Distribution of Shear Stress	27
8	Ratio of $U_{\max}/V_{av}$ vs $k$	29
9	Maximum Point Velocities Relative to Radial Position	31
10	Position of Maximum Velocity Points	32
11	Turbulent Velocity Profiles with Capsule Superimposed, $k = 0.70$ ,	41
12	Turbulent Velocity Profiles with Capsule Superimposed, $k = 0.90, 0.80$	42
13	Forces on Capsule	43
14	Photographic Apparatus Schematic	47
15	Schematic of Test Apparatus	48
16 A,B	Photograph - overall test line	52
17	Photograph - Capsule and Particle Injection Apparatus	53
18	Photograph - Pump & Storage Tank	53
19 A,B,C	Photograph - Photographic Apparatus	54
20	Photograph - Flow Control Board	55
21	Photograph - Differential Pressure Cells	56
22	Photograph - Test Capsules Flow Patterns	56
23 A,B,	Photograph - Test Capsules Clearances.	57
24 A,B,C	Photograph - Flow pattern side view, capsule rear	61
25	Photograph - Flow pattern top view, capsule rear	64
26 A,B,C, D	Photograph - Flow pattern side view, capsule nose	65
27 A,B	Photograph - Flow pattern top view, capsule nose	70



28	Photograph -- Separation Top Capsule Rear	71
29	Vortex "X" and "Y" Dimensions $k = .625$	72
30	Vortex "X" and "Y" Dimensions $k = .675$	72
31	Vortex "X" and "Y" Dimensions $k = .718$	73
32	Vortex "X" and "Y" Dimensions $k = .765$	73
33	Vortex "X" and "Y" Dimensions $k = .866$	74
34	Schematic - Capsule Flow Patterns	76
35	Stagnation Point	77
36	Separation at Top Rear Edge	78
37	Wake Downstream of Capsule Nose	80
38	Correlation Capsule Pressure Drops; Static Condition	83
39	Basic Data Plot Full View Run	87
40	Basic Data Plot Microscope Run	88
41	Typical Photographs Full View Run	89
42	Typical Photographs Microscope Run	90
43 A	Capsule Macro Lift Off Velocities $V_c$	94
43 B	Capsule Macro Lift Off Velocities $V_{av}$	95
44	Capsule Clearance vs. $V_c$ $k = .90$ $L_c = 3"$	98
45	Capsule Clearance vs. $V_c$ $k = .90$ $L_c = 6$	99
46	Capsule Clearance vs. $V_c$ $k = .80$ $L_c = 3$	100
47	Capsule Clearance vs. $V_c$ $k = .80$ $L_c = 6$	101
48	Capsule Clearance vs. $V_c$ $k = .70$ $L_c = 3$	102
49	Capsule Clearance vs. $V_c$ $k = .70$ $L_c = 6$	103
50 A	Correlation of Capsule Macro Lift Off Velocities on $V_c$ Basis	105
50 B	Correlation of Capsule Macro Lift Off Velocities on $V_{av}$ Basis	106
51	Capsule Clearance vs. $VR:k = .90$ , $L_c = 3"$	107
52	Capsule Clearance vs. $VR:k = .90$ , $L_c = 6$	108
53	Capsule Clearance vs. $VR:k = .80$ , $L_c = 3$	109
54	Capsule Clearance vs. $VR:k = .80$ , $L_c = 6$	110
55	Capsule Clearance vs. $VR:k = .70$ , $L_c = 3$	111
56	Capsule Clearance vs. $VR:k = .70$ , $L_c = 6$	112
57	Correlation Capsule Velocity to Fluid Velocity	114
58	Capsule Pressure Drop vs. $V_c$ $k = .90$ $L_c = 6"$	116
59	Capsule Pressure Drop vs. $V_c$ $k = .80$ $L_c = 6$	117





## I INTRODUCTION

Capsule pipelining is defined as a method by which solid materials shaped into, or contained in, basic cylindrical or spherical shapes are transported by liquid flowing in the pipeline.

The concept evolved from observations made during the course of investigation of two-phase flow of water and an immiscible oil conducted at the Research Council of Alberta in 1959, and published in 1961 (1). It was noted that a condition existed wherein the water carried cylindrical shaped "slugs" of oil concentrically in the pipeline with total energy requirements comparable to that for water alone.

Since 1959, a series of experimental and theoretical investigations have been carried out at the Research Council of Alberta. In these experimental investigations measurements of capsule and liquid velocities and pressure gradient have been made for capsules flowing in 3/8", 1/2", 1 1/4", and 4" diameter pipelines.

In the initial studies (2, 3), the capsule densities were equal to the liquid density (water and various oils) with variations being made in capsule diameter, length and shape, all in a 1 1/4" pipeline. A theoretical analysis of the equal density capsule condition was also performed at this time (4).

Later experimental work ( 5, 6 , 7 , ) extended the investigations to other diameters of pipeline (3/8", 1/2", and 4") as well as to capsule densities up to twelve times the densities of the carrier liquids, water and oil. Observations of the capsule orientation within the pipeline were made during these studies but no actual measurements were taken. In conjunction with the experimental work, theoretical studies for laminar flow conditions were made which give a means of predicting the capsule and liquid velocities and pressure gradients, and the clearance of the capsule from





the pipe wall ( 8, 9).

At this stage, in May 1966, the author entered the investigations. In 1967 a 4-inch diameter, 3900 ft. long pilot pipeline including a 5° incline, a 5° decline, a 60-foot radius bend and horizontal test sections was constructed. This facility allowed experimentation with trains of capsules up to 100 feet in length and also included methods of injecting, bypassing of pumps, and retrieval of capsules from a pipeline. Results of this investigation are not yet published.

From prior experimental observations and theoretical analysis it is evident that a knowledge of capsule orientation relative to pipe wall for different capsule velocities, densities, diameters and lengths is required to understand the hydrodynamics of the system. From a practical viewpoint a knowledge of capsule orientation, particularly clearance from the pipe bottom, is important in that in any commercial application of capsule pipelining it would be desirable to have the maximum possible clearance to minimize capsule-pipe abrasion. The following thus is an investigation of the orientation of a capsule in the pipeline. The basic problem is outlined in terms of the variables involved. Based on a review of relevant literature, a theoretical method is outlined for predicting the capsule behaviour. Experimental investigations were performed on both the flow patterns existing around a stationary capsule and the orientation within a pipeline of a moving capsule. The results of these investigations are presented and discussed. Conclusions are made based on this investigation along with recommendations for future work.



## II LITERATURE REVIEW Flow Patterns.

To the author's knowledge there are no other published papers regarding flow patterns around capsules in a pipeline. There are of course numerous papers published in the general field of flow visualization. Recent literature was searched in an attempt to find a satisfactory method of flow visualization. It was decided to look for a method that would not restrict the flow visualization to stationary capsules. This consideration ruled out any method which would require any apparatus in the interior of the pipe, such as bubble generation from a wire, or dye injection needles. Any method involving ejection of dye or particles from the capsule body was also ruled out since this meant that no pattern would be observed downstream or upstream of the capsule depending on which direction the flow at the capsule surface was moving. This meant that the method used would have to employ particles as a tracing medium.

A paper by Clayton and Massey (10) reviewing past and current techniques for flow visualization in water, discussed the advantages and disadvantages of various techniques. Particular attention was paid to methods using tracer particles and the following materials were considered:

- (1) aluminum powder
- (2) lycopodium powder
- (3) polystyrene spheres
- (4) air bubbles

For all these methods, the recommended form of lighting was an intensely-lit plane parallel to the direction of flow and perpendicular to the desired axis of photography. Aluminum powder, though highly reflective, is considerably denser than water and the particles tend to be quickly tarnished





by an oxide film. Polystyrene spheres can be obtained in densities close to that of water, but their size (.01 to .02 in.) is fairly large in relation to a  $1\frac{1}{4}$ " pipe diameter and the size of annulus involved when a capsule is present. The air bubble technique, although versatile is limited because of the necessity of introducing apparatus inside the pipe.

A particular modification of the technique employing polystyrene spheres was developed by Van Meel and Vermij (11) to obtain a third dimension (i.e. into the plane of the photograph). They achieved this by passing white light through multi color filters which broke the light into ten adjacent, parallel but differently-colored beams. A velocity into or out of the plane of the photograph can then be detected by observing changes in the apparent color of the polystyrene spheres as they travel from one plane to another.

The technique of streaming birefringence is also discussed in (10). Visualization is achieved by the shear forces causing preferred orientation of the particles. The method is not well suited for any flow in which significant third dimensional motion occurs, which is the case in the present study. Also there are practical disadvantages involved in the physical preparation of birefringent solutions since very fine size colloidal suspensions are required.

The Schlieren method, which is widely used in gas flow visualization is applicable to water flows as well if a density gradient is induced in the water by means of non-uniform heating of the water in the areas of interest.

Chemical methods involving luminescent reactions may also be employed. Such reactions can be produced by the reaction between 3-aminophthalhydrazide and hydrogen peroxide. In this particular reaction,





a 0.1% solution of 3-aminophthalhydrazide is ejected in a jet along with 0.1% solution of potassium ferricyanide into a dilute solution of sodium hydroxide and hydrogen peroxide.

A similar chemiluminescent reaction can be produced by applying an electric potential to a solution of luminol (5-amino-2, 3-dihydro-1, 4-phthalazinedione) with hydrogen peroxide as the oxidizing agent and potassium chloride added to increase conductivity.

A "time reaction" method where a definite time interval elapses before a reaction occurs has been used to create stationary visualizations of flow patterns. The line of separation between colored and colorless fluid is a direct measure of the distance the fluid has travelled. This type of reaction will occur between an acidified solution of potassium iodate and a solution of sodium sulphite containing a little starch.

The classical method of introducing dye filaments is best suited to laminar flow since in turbulent flow the filament is rapidly dispersed. Another form of tracer may be formed from droplets of a second liquid different from water which are immiscible in the water. Such droplets can be formed by mixing carbon tetrachloride with glycol, benzene or nitrobenzene.

Gas bubble generation is discussed by Clayton and Massey (10) at some length. A method using a tellurium wire as a cathode generates bubbles of oxygen as well as intensely black particles of elemental tellurium. The method has drawbacks in that the tellurium wires are fragile and shortlived due to the electrolytic process, additionally toxic tellurium oxide fumes are produced. Although the tellurium particles have very good optical properties, it is suggested that equally good results can be achieved more simply using the hydrogen bubble technique. In the hydrogen bubble technique, hydrogen is liberated at a cathode, which is usually a very thin platinum



wire. The method is very versatile in that pulsing the electrical supply allows visualization of velocity profiles. Filaments of bubbles can also be produced by crimping of the wire which concentrates the bubbles at the bent points. Clayton and Massey (10) list several different applications that have successfully used this technique. Also, theoretical work done to determine the reliability of the technique indicates that even for complex three dimensional shapes, accuracy within 4 to 5% of the actual flow velocity can be obtained.

Apart from the methods discussed by Clayton and Massey, Popovich and Hummel (12) describe a technique using flash photolysis to produce a filament of blue dye in a solution of 2-(2,4-dinitro benzyl)-pyridine in a 95% ethyl alcohol solution. The blue filament produced by an intense flash is photographed a few milliseconds later by a second flash. This method is suited to obtain velocity information very close to solid boundaries, which would be impossible with other techniques.

For the purposes of this study, it was decided that a method using tracer particles would be best. Some earlier attempts had been made at the Research Council to obtain flow visualizations using filaments of fluorescent dye under ultraviolet light. The dye filaments were not suitable for turbulent work, but did show up well under the ultraviolet light. This suggested that particles which would fluoresce would be needed for turbulence work. A quantity of a fluorescent powdered acrylic pigment used in plastic manufacture was obtained and found to be suitable for qualitative flow pattern observations.

Representative of a study carried out using flow visualization was that of Macagno and Hung (13) who studied, both theoretically and experimentally, the characteristics of the captive annular vortex occurring at the corners of an abrupt expansion of a conduit. The captive annular vortex thus formed is comparable to the vortex region in the wake of a stationary capsule.





The parameters used to describe the vortex were length as measured along the conduit divided by smaller conduit diameter, position of vortex center measured along the conduit length divided by smaller conduit diameter, relative vortex intensity, and relative vorticity, all plotted against Reynolds number,  $Re$ . The length parameters were both found to increase linearly with increasing Reynolds numbers. The values of vortex intensity and vorticity were found to approach asymptotically to maximum values which indicated that although the vortex grew with  $Re$ , its strength did not. The theoretical and experimental data agreed well, verifying the correctness of the theoretical approach used in solving the Navier-Stokes equations.

Experimentally, both dye and aluminum powder were used in visualizing the flow patterns. Only the aluminum powder runs were photographed.

Representative of the type of work carried out in flow pattern visualization around bodies in infinite flow fields is the paper of Kaneda (14) investigating the wake behind spheres at low (laminar) Reynolds numbers. Again the parameters used to describe the vortex were its length and position of centre relative to sphere diameter, although in this case the variations were linear with log of Reynolds number. Kaneda points out that work with a circular cylinder had shown a variation directly with Reynolds number, which he suggests is related to the fact that the cylinder represents a two dimensional case, whereas the sphere is three dimensional.



### III LITERATURE REVIEW Capsule Clearances

The study of the capsule pipelining concept originated from the observation of the flow patterns occurring in two-phase flow of immiscible liquid such as oil and water, especially those conditions in which "slugs" of oil were observed to form and remain stable in a water carrier as they moved down a pipeline. From this work reported by Charles, Govier and Hodgson (1), further studies were carried out, almost exclusively at the Research Council of Alberta to determine the characteristics of a flow system in which the observed slugs of oil were replaced by solid bodies basically of cylindrical or spherical shape. This work has been presented as a series of papers, Part 1 - Part 9 (Ref. 2 to 9 incl., 13)

This series of papers presents the basic research done to date. Of the theoretical papers (4, 8, 9), (4) is restricted to concentric flow and as such its applicability is limited to equal density capsules. (12) and (9) deal with eccentric capsule conditions in laminar flow.

Charles, in Part 2 (4) defines four mathematical models to describe the possible flow regimes existing in a capsule system, where the capsule is concentric within the pipe (i.e. equal density capsules). These models are:

1. Laminar flow both in free pipe and capsule-pipe annulus
2. Turbulent flow both in free pipe and capsule-pipe annulus
3. Turbulent flow in free pipe, laminar flow in capsule-pipe annulus.
4. Laminar flow in free pipe - turbulent flow in capsule-pipe annulus.

The 4th model is not applicable except for a very small region near Reynolds numbers of 1800 and capsule diameter ratios of 0.57, and as such is not considered for analysis of theoretical velocities or pressure





gradients. Charles (1) has theorized that a capsule will attain a velocity, both in laminar and turbulent flow such that the capsule will have a velocity,  $V_c$ , equal to the point velocity in a free pipe velocity profile at the radial point in the pipe corresponding to the capsule boundary. The profile used for turbulent flow is according to Blasius' 1/7 power law, i.e.

$$u' = u'_{\max} \left( \frac{r_p - r}{r_p} \right)^{1/7} \quad (1)$$

where  $u$  = point velocity

$r$  = radius

$r_p$  = pipe radius

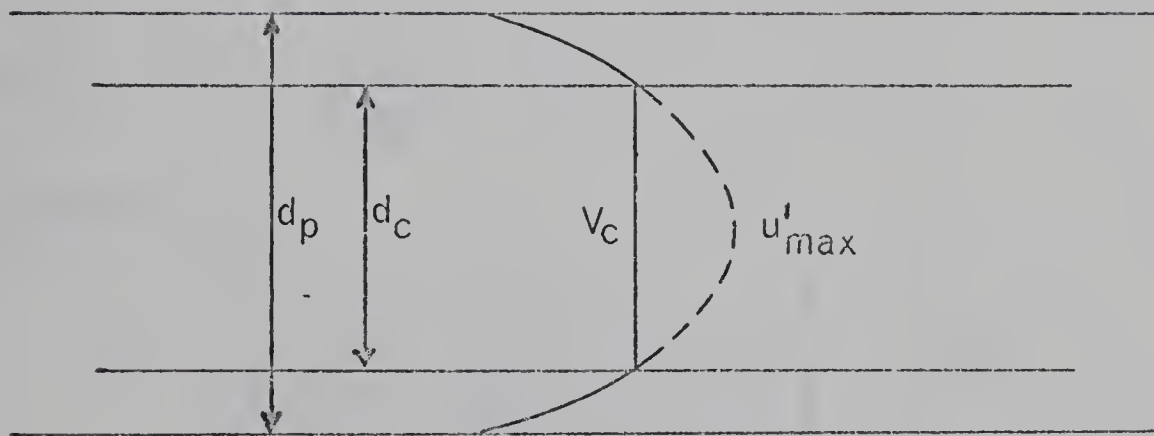


Fig. 1

$d_p$  = pipe diameter

$d_c$  = capsule diameter

$u'_{\max}$  = hypothetical point velocity

$V_c$  = capsule velocity

$V_{av}$  = average liquid velocity

$k = \frac{\text{capsule diameter}}{\text{pipe diameter}}$



From this, the velocity ratio can be calculated by summing the average velocity in the annulus and the capsule velocity which will give the overall average velocity of the system. The velocity ratio is then  $V_c/V_{av}$ . Depending on the diameter ratio,  $k$ , a particular velocity ratio is calculated for any specific liquid velocity. The velocity ratio calculation is dependent only on the condition of the fluid in the annulus, i.e. whether it is laminar or turbulent. The equations for the velocity of the capsules are:

$$V_c = \left( \frac{2}{1+k^2} \right) \cdot V_{av} \quad \text{or} \quad 2 V'_{av}(1-k^2) \quad (2)$$

Where  $V'_{av}$  = hypothetical average liquid velocity based on profile in Fig. 1.

$$\text{So that} \quad V'_{av} = \frac{1}{(1-k^4)} \cdot V_{av} \quad (3)$$

for laminar flow

$$V_c = \left[ \frac{1}{\frac{7}{4} k(1-k) + \frac{49}{60} (1-k)^2 + k^2} \right] \cdot V_{av} \quad (4)$$

$$\text{and} \quad V'_{av} = \left[ \frac{0.82}{(1-k)^{1/7} \left[ \frac{7}{4} k(1-k) + \frac{49}{60} (1-k)^2 + k^2 \right]} \right] \cdot V_{av} \quad (5)$$

for turbulent flow

To calculate pressure ratios, Charles uses the relationship that  $\left( \frac{\Delta P}{L} \right)_f \sim V_{av}$  in laminar flow. The capsule pressure gradient  $\left( \frac{\Delta P}{L} \right)_c$  will vary as  $V'_{av}$ , calculated from the hypothetical velocity profile as shown in Fig. 1. For turbulent flow, the same approach was used, except that  $\left( \frac{\Delta P}{L} \right)_f \sim V_{av}^{1.75}$  and  $\left( \frac{\Delta P}{L} \right)_c \sim V'_{av}^{1.75}$ . The pressure ratios calculated on this basis for the three models are:



$$1. \quad \left(\frac{\Delta P}{L}\right)_{cL} = \frac{1}{1-k^4} \left(\frac{\Delta P}{L}\right)_f \quad (6)$$

$$2. \quad \left(\frac{\Delta P}{L}\right)_{ct} = \left( \frac{0.82}{(1-k)^{1/7} \left[ \frac{7}{4} k(1-k) + \frac{49}{60} (1-k)^2 + k^2 \right]} \right)^{1.75} \left(\frac{\Delta P}{L}\right)_{ft} \quad (7)$$

$$3. \quad \left(\frac{\Delta P}{L}\right)_{cL} = \frac{202}{(1-k^4) \frac{V_{av} \rho}{\mu}^{3/4}} \left(\frac{\Delta P}{L}\right)_{ft} \quad (8)$$

where  $\mu$  = dynamic viscosity  
 $\rho$  = liquid density

Kennedy (16) has questioned the assumptions made by Charles for Model 2 (turbulent-turbulent flow) by pointing out that if there is to be any transfer of shear outward from the capsule to the fluid in the annulus, there must be a slip velocity,  $V_s$  existing along this boundary.

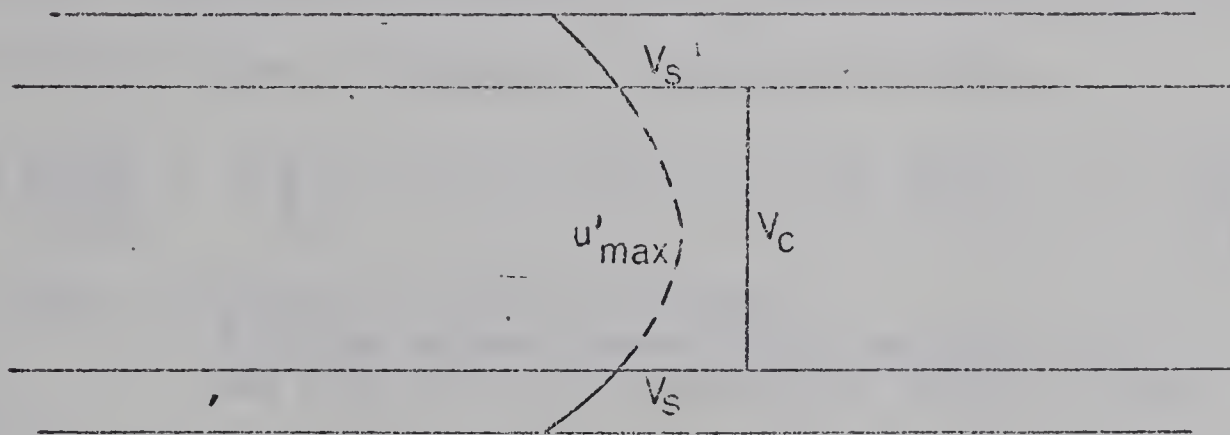


Fig. 2

Kennedy calculates that  $V_s = B \sqrt{\frac{\tau_c}{\rho}}$ ,  $\tau_c = \frac{r_c}{2} \left(\frac{\Delta P}{L}\right)_c$

where  $B = 12$  (a dimensionless constant)  
 $\tau_c$  = shear intensity on capsule



Including this correction, Kennedy modifies Charles' equation (5) to read

$$V_c = \left[ \frac{V_{av} + V_s \frac{7}{4} k(1-k) + \frac{49}{60} (1-k)^2}{\frac{7}{4} k(1-k) + \frac{49}{60} (1-k)^2 + k^2} \right] \quad (9)$$

where

$$V_s = \left[ \frac{B \cdot \frac{V_c}{2} \cdot \left( \frac{\Delta P}{L} \right)_c}{1.22 (1-k)^{1/7} \frac{7}{4} k(1-k) + \frac{49}{60} (1-k)^2 + k^2 + \frac{Bk^2}{V_{av}} \frac{r_c}{2} \left( \frac{\Delta P}{L} \right)_c} \right] \quad \dots \dots (10)$$

Similarly equation (7) is modified by Kennedy to read

$$\left( \frac{\Delta P}{L} \right)_{ct} = \left[ \frac{0.82}{(1-k)^{1/7} \frac{7}{4} k(1-k) + \frac{49}{60} (1-k)^2 + k^2} \right]^2 \left( \frac{\Delta P}{L} \right)_{ft} \quad (11)$$

In Part 3 (2) Ellis investigated experimentally the transport of single equal density cylindrical and spherical capsules in a water carrier. He performed a dimensional analysis of the variables involved in the general case of moving a capsule flowing in a pipeline obtaining

$$V_c \text{ or } \left( \frac{\Delta P L}{L} \right)_c = \phi \left( V_{av} \sigma, \rho, \mu, L_c, d_c d_p \text{ end shape, } j, \epsilon_c, \epsilon_p \right) \quad (12)$$

where  $j$  = factor to take into account  
friction between capsule pipe surfaces  
and also lubricating quality of carrier liquid

$\epsilon_c$  = capsule roughness height

$\epsilon_p$  = pipe roughness height

By dimensional analysis Ellis obtained

$$\frac{V_c}{V_{av}} = 2 \left( \frac{V_{av} d_p \rho}{\mu}, \frac{\sigma - \rho}{\rho}, \frac{d_c}{d_p}, \frac{L}{d_c}, \text{ end shape, } \frac{\epsilon_c}{d_c} \frac{\epsilon_p}{d_p} \right) \quad (13)$$

or using  $\left( \frac{\Delta P}{L} \right)_c$ ,  $\frac{V_c}{V_{av}}$  is replaced by  $\left( \frac{\Delta P}{L} \right)_c \frac{d_p g_c}{V_{av}^2}$

The experimental work was limited to equal density capsules thus





eliminating  $\frac{\sigma-\rho}{\rho}$  as an independent variable and  $\left(\frac{\Delta P}{L}\right)_c$  was not measured. The effect on  $V_c/V_{av}$  of  $\frac{V_{av}d_p\rho}{\mu}$ ,  $\frac{d_c}{d_p} - \frac{L}{d_c}$  and end shape were determined. It was found that:

- (1)  $\frac{V_c}{V_{av}}$  or VR was independent of Reynolds number. However, a region of instability was noted at Reynolds numbers of approximately  $10^4$  at which the value of  $V_c$  changed sharply from minimum to maximum values.

Ellis attributed this instability to a possible displacement of the point of separation of the boundary layer to the rear of the capsule

- (2) VR increased with decreasing  $\frac{d_c}{d_p}$  (k)
- (3) VR increases with increasing  $\frac{L_c}{d_c}$
- (4) End shape had limited effect for large diameter ratios, but showed more effect for small diameter ratios.

In Part 7(6) Ellis & Bolt repeated experiments with equal density capsules in an oil carrier and found generally the same effects as noted with the water carrier. However the region of instability at Reynolds numbers of  $10^4$  observed in the water carrier work did not appear in the oil carrier experiments.

Data taken in the laminar range with the oil carrier showed good agreement with the laminar theory as proposed by Charles (4).

Parts 4(3) and 5(5), deal with cylinders and spheres, denser than a water carrier, and Part 8(7), deals with cylinders and spheres denser than an oil carrier, relate experimental results in terms of velocity ratios as they are affected by changes in the system parameters.

In Part 4(3), a discussion was presented of the forces involved



in the case of the eccentric cylinder, but no quantitative theory was attempted. The experimental data showed, for both laminar and turbulent flow, the following essential points:

1. The effect of increasing diameter ratio was, in general, to increase velocity ratio except for small diameter ratios at high velocities where the reverse was true.
2. Increase in density ratio decreased velocity ratio markedly at low velocities. All density ratios tend to the same velocity ratios at higher velocities.
3. The effect of increasing length was to decrease the velocity ratio at low fluid velocities but to increase velocity ratios at high fluid velocities.
4. The effect of end shape was slight. Ellipsoidal noses tended to be slightly detrimental to the velocity ratio for small diameter ratios at low liquid velocities but improved the velocity ratios for higher liquid velocities.
5. Rougher surfaces tended to reduce velocity ratios at low velocities, but this effect disappears at higher velocities

Of particular relevance to this study were the predictions and observations made regarding the presence of a liquid film between the capsule and pipe bottoms. Particularly for smaller diameter capsules, especially in laminar flow, it was observed that the capsules lifted clear of the pipe bottom, first in tail-up positions and at a higher velocity, to a nose-up position. It was noted that at sufficiently high velocities this visible lift-off would occur for larger diameter ratios and heavier capsules. The observed effects in point 2 and 5 above were also stated as criteria for suggestions that the liquid film beneath the capsule must





increasingly thicken to the extent that the capsule is fully supported by the liquid film or layer, thus eliminating the effects of surface roughness and its effect on the frictional retarding force. An analogy is drawn between this and lubrication effect, although it was pointed out that the geometry of the capsule pipe system precluded any rigorous application of lubrication theory.

In Part 6(8), with particular application to clearances, Newton, Redberger and Round used a numerical analysis approach to investigate the effect of axial displacement (i.e. clearance), end configuration and length, deformations of the capsule cross-section and frictional effect between the capsule and pipe wall for capsules in laminar flow. In their investigation, a significant effect on capsule performance was found for all the above variables except for capsule end configuration and length.

For the analysis the following assumptions were made: incompressible fluid of constant viscosity and density, time independence, constant axial pressure gradient and no inertial effects. With these assumptions the Navier-Stokes equations are reduced to

$$\Delta^2 V = \left( \frac{\Delta P}{L} \right)_c \quad \text{where } \Delta \text{ is the operator } \frac{\partial}{\partial x}, \frac{\partial}{\partial y}, \frac{\partial}{\partial z}$$

For solution, the above equation was put into a finite difference form corresponding to a mesh system best suiting the capsule and pipe configuration, and the equation was solved by standard applied iterative methods using an IBM 1620 computer.

The effect of clearance was to increase the capsule velocity/average fluid velocity ratio as the capsule became closer to a concentric position in the pipeline. As this velocity ratio increased, the ratio of the pressure required to move the capsule compared with the pressure re-





quired for fluid alone was shown to decrease. Another ratio was introduced to compare the effect of two opposing moment systems on the capsule. The moment tending to twist the eccentric free flowing capsule from an axial position,  $M_c$ , was evaluated as the integrated shear forces acting along the capsule surfaces.

$$M_c = \int u \frac{\partial v}{\partial r} r_c \sin \theta r_c d\theta \quad (14)$$

It was held that this force tends to tip up the capsule nose. An opposing moment,  $M_o$  was held to be the moment produced by the pressure differential across the capsule ends

$$M_o = \pi r_c^3 \left( \frac{\Delta P}{L} \right)_c \quad (15)$$

There was assumed to be no frictional force. This moment ratio  $M_c/M_o$  was shown to increase as clearance decreased, with the maximum rate of change occurring for the smaller diameter ratio capsules. This was taken to show that smaller diameter ratio capsules will lift most readily.

With regard to friction, it was shown, as would be expected, that increasing frictional forces decreased capsule velocities, and subsequently velocity ratios. The frictional force was shown as a relative friction defined as the ratio of the friction force to the total forces propelling the capsule.

For consideration of capsule ends and length effects, the analysis was limited to considerations of an concentrically flowing capsule. In this analysis, it was again assumed that the inertial terms in the Navier-Stokes equations could be ignored. Secondly, it was assumed that at any point in the flow, the axial pressure gradient is proportional to the velocity at that point:



$$\frac{dp(r,z)}{dz} = \frac{dp(r,z)}{dz} = \frac{u(r,z)}{u(r,z_0)} \text{ where } r, z \text{ are polar co-}$$

ordinates, where  $p(r,z)$  and  $V(r,z_0)$  are pressures and velocities at equivalent points in the undisturbed flow. The resulting analysis showed negligible effects of capsule length and end configuration.

The results obtained in the study of capsule distortion have no relevance in the present study.

A later paper, Part 9, by Kruyer, Redberger and Ellis (9) applies an analytical approach to the solution of the case of an infinitely long cylinder in laminar flow, at varying clearances.

The analysis employs the equations developed by Bentwich, Epstein & Kelly (17) describing the velocities of the cylinder and fluid in the annulus under any pressure gradient. The equations derived by Bentwich et al. are:

For the liquid in the annulus the discharge is:

$$Q_{\text{ann}} = A \left( \frac{\Delta P}{L} \right) c \left[ (1-k^2)^2 + 2k^2 \frac{C}{d_p}^2 - \left\{ 8 k \sinh(a + \beta) \right\} \times \right. \\ \left. \left\{ \sum_{n=1}^{\infty} \left[ \coth \eta (a - \beta) \right] \left[ \frac{2 \eta \frac{C}{d_p} \sinh \beta - k^2}{e^{2n\beta} + e^{2na}} + \frac{k^2}{e^{2na}} \right] \right\} \right] \quad (16)$$

$$\text{where } a = \cosh^{-1} \left\{ \frac{1-k^2 - \frac{C}{d_p}^2}{2 k \frac{C}{d_p}} \right\}$$

$$\beta = \cosh^{-1} \left\{ \frac{1-k^2 + \frac{C}{d_p}^2}{2 \frac{C}{d_p}} \right\}$$



For the cylinder the discharge is

$$Q_c = A \left( \frac{\Delta P}{L} \right)_c \times 4k^3 \sinh(a - \beta) \quad (17)$$

In laminar flow in a cylinder free pipe, the discharge is:

$$Q_p = A \left( \frac{\Delta P}{L} \right)_f \quad (18)$$

where  $C$  = clearance between capsule and pipe

$$A = \text{constant} = \frac{d_p^4 g_c}{128 \nu}$$

Equating the flow in a free pipe with  $Q_c + Q_{\text{ann}}$  gives:

$$\frac{\left( \frac{\Delta P}{L} \right)_c}{\left( \frac{\Delta P}{L} \right)_f} = \frac{1}{\text{function} \left( k, \frac{C}{d_p} \right)} = \text{PR for } Q \text{ constant} \quad (19)$$

If instead the pressure gradients are equated, then

$$\frac{Q_p}{Q_c + Q_{\text{ann}}} = \frac{\left( \frac{\Delta P}{L} \right)_f}{\left( \frac{\Delta P}{L} \right)_c} = \frac{1}{\text{function} \left( k, \frac{C}{d_p} \right)} \quad (20)$$

which shows that for a given capsule pipe diameter ratio and clearance, the pressure ratio at constant throughput is equal to the flow ratio at constant pressure gradient. Using this relationship, pressure and velocity ratio calculations were made for a range of diameter ratios from 0.25 to 0.97 and clearances varying from fully eccentric to concentric capsule positions. The resulting calculations showed PR to be very nearly linear when plotted against VR. Clearances were also plotted against VR and PR independently for a number of diameter ratios. Experimental data from 1/2 inch, 1 1/4 inch and 4 inch pipelines were plotted on a PR-VR basis and found to agree very well with the theoretical predictions given by equations (16) to (20) above.





Although the experimental capsules were of varying lengths, the agreement with the theoretical prediction of pressure and velocity ratios was equally valid. However, large differences do appear when capsules of equal diameter ratio and density were compared on a basis of pressure or velocity ratio vs. capsule velocity. On this basis it was seen that at a given capsule velocity, the shorter capsules produced lower pressure ratios and higher velocity ratios. It is implicit in the theory that such changes can only be caused by an increase in clearance, i.e. nose or tail lift occurring at a lower capsule velocity with the short capsules. The fact that the agreement with the theory on the PR-VR basis still holds for the short capsules, which were finite in length and probably non-parallel to the pipe, suggests that the governing parameter may not be primarily the clearance, but rather the particular velocity ratio the capsule achieves. The shorter capsules may be able to achieve this higher velocity ratio due to the contribution of the ends being of significant importance in producing a more efficient energy transfer from the fluid to the capsule.

Studies have also been carried out on the flow of coal paste slugs in oil (18). In these studies trains of pasted coal slugs were tested and results plotted in the same fashion as for the rigid cylinder work. Since deformation of these pasted slugs did occur it was not possible to compare these results directly with work performed for rigid cylinders.

Several other papers investigating economics and technical problems have also been published at the Research Council of Alberta (20-38 incl.), but essentially they did not delve into any different aspects of the theory or experimental data pertinent to the present study





beyond that already reviewed in the Parts 1-9 series.

Apart from the Research Council of Alberta, an experimental study of capsule clearances has been conducted by Suhr (39). The conditions were limited to laminar flow in water (velocities 0.2 ft./sec. and less) and a density range extending from equal density to  $32 \times 10^{-5}$  greater than equal density. On a theoretical basis, Suhr developed an expression for predicted clearances based on the Navier-Stokes equations with the following assumptions:

1. Fully laminar flow
2. Steady state
3. No slip at boundaries
4. Thin film between capsule & pipe (i.e. large capsule diameter ratio)
5.  $\frac{\partial p}{\partial y} = 0$  (i.e. velocity across film is zero)
6. No external forces act on the film
7. All other velocity gradients are small compared to  $\frac{\partial V_x}{\partial y}$  and  $\frac{\partial V_z}{\partial y}$
8. Newtonian incompressible fluid
9.  $\frac{\partial p}{\partial z} \ll \frac{\partial p}{\partial x}$
10. Forces on the cylinder in vertical direction are due to pressure forces acting over a portion on the top half of the cylinder and a portion of the bottom half of the cylinder. This assumes that the vertical components of shear forces are small compared to the pressure forces.

Based on these assumptions, and assuming an angle of attack,  $\alpha$ , for the capsules Suhr obtains the equation for clearance:



$$C = \frac{6 L_c \mu V_c}{a (\sigma - \rho)} r_c^2 g_c \quad (21)$$

where  $L_c$  = capsule length

$\sigma$  = capsule density

Suhr points out that his assumptions (particularly 9, and 10) may rule out his formula for quantitative prediction, but should not impair its value for qualitative work.

Suhr's experimental work was done for density ratios (i.e.  $\frac{\sigma - \rho}{\rho}$  of 1.00009, 1.00014, 1.00018 and 1.00032). Clearance, measured at capsule mid point, increased with increasing Reynolds number and decreased with increasing capsule density. All other factors were held constant. Suhr stated that it was evident that for a higher density, a point would be reached where the capsule would never measurably lift off, which is contrary to observations made in earlier mentioned studies. (3) It is necessary to point out that the range of velocities and density ratios studied by Suhr were both extremely limited.



#### IV THEORY

Part 9 in the capsule flow series of the Research Council of Alberta (9) provides a theoretical approach for analysing the case of an eccentric capsule in laminar flow conditions.

It is proposed to outline an empirical approach to produce a method for analysis of the case of turbulent flow in the pipe and laminar/turbulent flow in the pipe-capsule annulus. First, an essentially physical argument will be given as a basis for the remainder of the empirical analysis.

For the concentric case, Charles (4) set out mathematical models, assuming either turbulent or laminar flow in the annulus. However, it has been observed that a capsule with a density even slightly greater than the carrier fluid travels on or very near the bottom of the pipeline. In this eccentric case we have a very small clearance between the capsule and the pipe bottom. In this area, unless we have very high velocities, or very low viscosities, it is reasonable to assume that laminar flow conditions will prevail. Thus, even though the pipe flow may be highly turbulent, it is unlikely that flow in the capsule-pipe annulus will be fully turbulent. This assumption of laminar conditions in a portion of the annulus has been stated for studies of eccentric fixed annuli (40).

Having made this assumption, it will be necessary to adopt a criterion for determining the point of change from laminar to turbulent flow in an annulus. The conventional criteria for Reynolds number is that the length dimension to be used is  $4R$  where  $R$  is the hydraulic diameter (area/wetted perimeter) to make it comparable to the classic free





pipe Reynolds number.

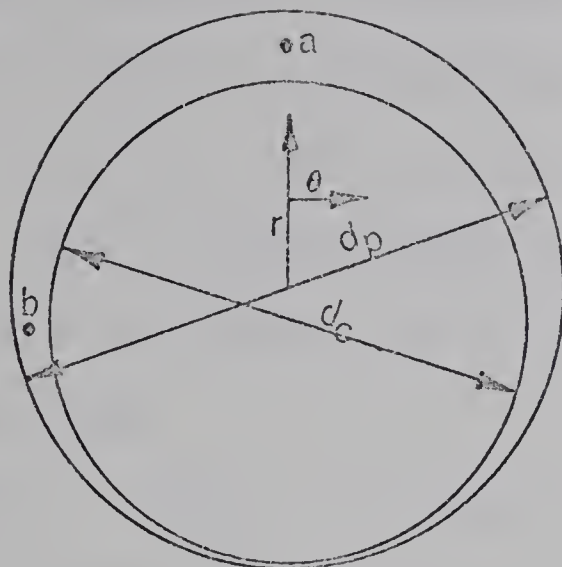


Figure 3

Considering particles at "a" and "b" in Fig. 3 and using polar coordinates, it is obvious that a particle at "a" while restricted in the "r" direction, is much less restricted than a particle at "b". This would mean that flow in an annulus would become turbulent at a lower velocity in the area of largest clearance.

For this analysis it is proposed that a local Reynolds number,  $Re_{Loc.}$ , be determined for any given section of the annulus. Then if the hydraulic radius method is used we would have :

$$\text{Area} = \frac{r_c + r_p}{2} d\theta C$$

$$\text{Wetted parameter} (r_c + r_p) d\theta$$

$$Re_{Loc} = \frac{4 u_{ann} \frac{C}{2}}{\nu} = \frac{2 u_{ann} C}{\nu} \quad (1)$$

where  $\nu$  = kinematic viscosity

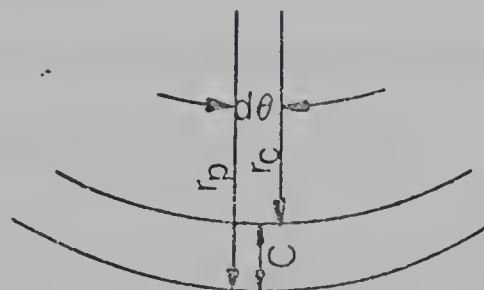


Fig. 4



This criteria will be used to determine the point of transition from laminar to turbulent flow. The velocity profile in the laminar case in the annulus is described in part 6 (8). The velocity given there can be used to determine the point of transition.

Since the flow in the annulus when the clearance is small is primarily due to the motion of the capsule, it presents an approximation of Couette flow. Using a Reynolds number criterion of  $\frac{u_{ann} C}{2}$ , Couette (41) found transition to turbulent flow at Re of 460. By our definition of Re this would be 1840.

Reichardt, in plane Couette flow experiments found the critical Reynolds number to be 750, corresponding in our definition to 3000. These Reynolds numbers suggest a range of transition 1840 - 3000 somewhat similar to that encountered in pipe flow. As a first approximation a value of 2400 will be used as a cutoff between laminar and turbulent flow.

It will be further assumed that the remainder of the annulus flow which is turbulent may be represented by the superposition of Couette flow and an eccentric annulus flow. The assumption of Couette flow is of doubtful validity for small diameter ratios and should not be used for diameter ratios  $< .70$ , since the difference in curvature between capsule and pipe becomes excessive.

Both the annulus flow and the Couette flow will be determined by the pressure gradient acting on the annular area and the capsule cross-section area respectively. The total shear force on the capsule surface and the pipewalls must equal and oppose the pressure gradient at any section.



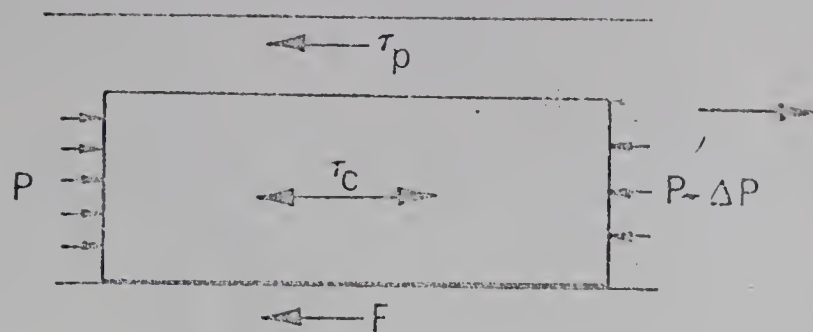


Fig. 5

It can immediately be seen that  $\tau_p$  will always be negative, but depending on the relative capsule motion,  $\tau_c$  can be positive or negative, and can be both on different areas of the capsule. The net amount of shear, its direction and the position of its point of action will produce a moment couple on the capsule which in a finite length capsule will either tend to lift the nose or tail.

As the first step in evaluation of these forces, flow in an eccentric annulus with a fixed core will be examined. Regarding shear forces, Jonsson and Sparrow (40) prepared plots of

$$\frac{\tau_{c\theta} r_c}{\tau_{ave} (r_c + r_p)} \quad \text{and} \quad \frac{\tau_{p\theta} r_p}{\tau_{ave} (r_c + r_p)}$$

versus radial position.

$\tau_{ave}$  is the average total shear stress on both walls of the annulus, derived from the relation,  $\tau_{ave} = \frac{f \rho V_{ave ann}^2}{8}$  (2).

where  $f$  is given as a function of  $Re$  and  $k$  in Figure 2 of the above mentioned reference. (40)

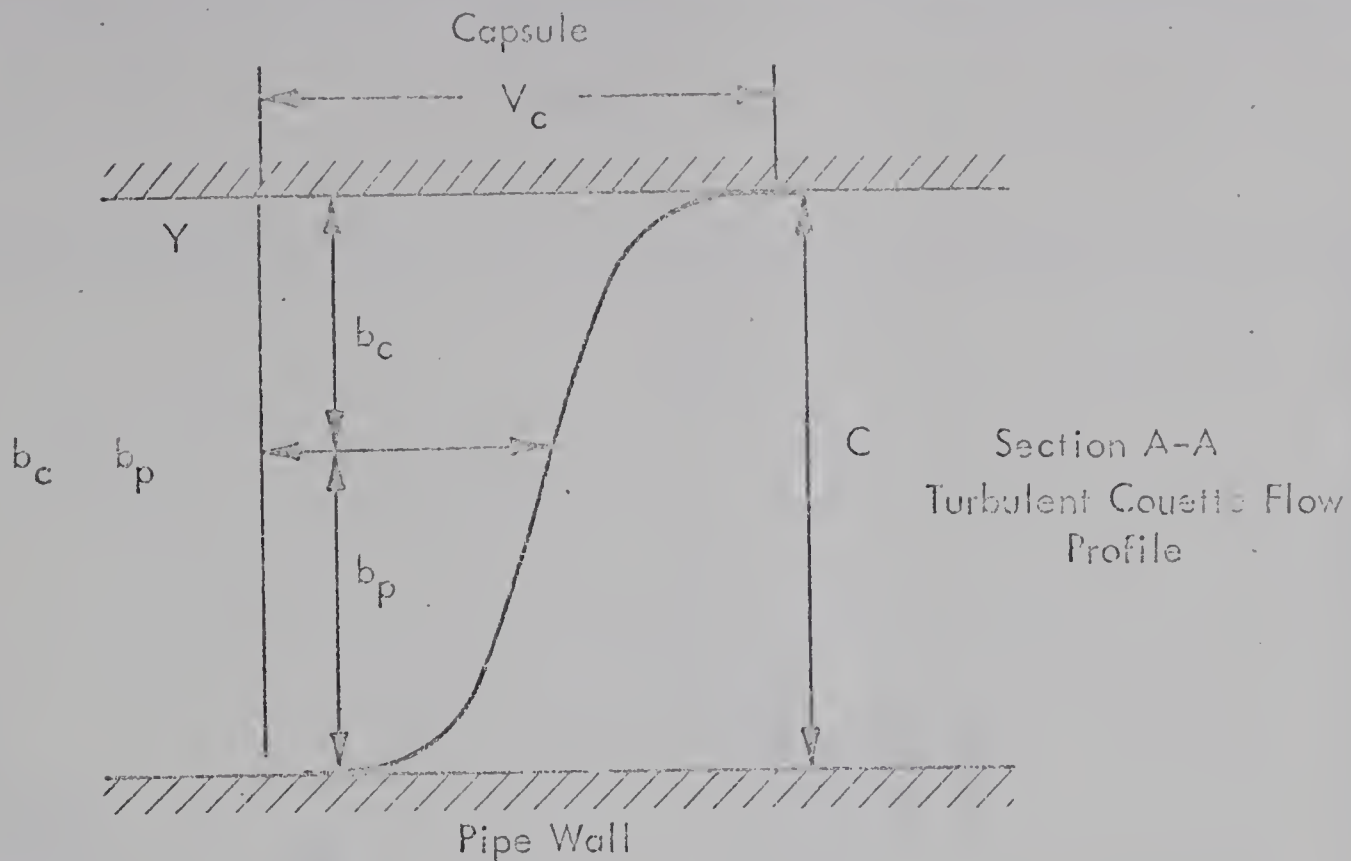
Referring to the dimensionless groupings above it was found that by plotting the ratio of local value to maximum value of  $\tau$ , and plotting against a  $D/D_{max}$  parameter where  $D$  is the length of a line orthogonal to the equal velocity contours in the annulus (Ref. Fig. 6) the following relationship was derived. (Fig. 7)

$$T_c = \frac{\frac{\tau_{c\theta} r_c}{\tau_{ave} (r_c + r_p)}}{\frac{\tau_{c\theta} r_c}{\tau_{ave} (r_c + r_p)}_{max}} = \left( \frac{D}{D_{max}} \right)^{1.177} \quad (3)$$

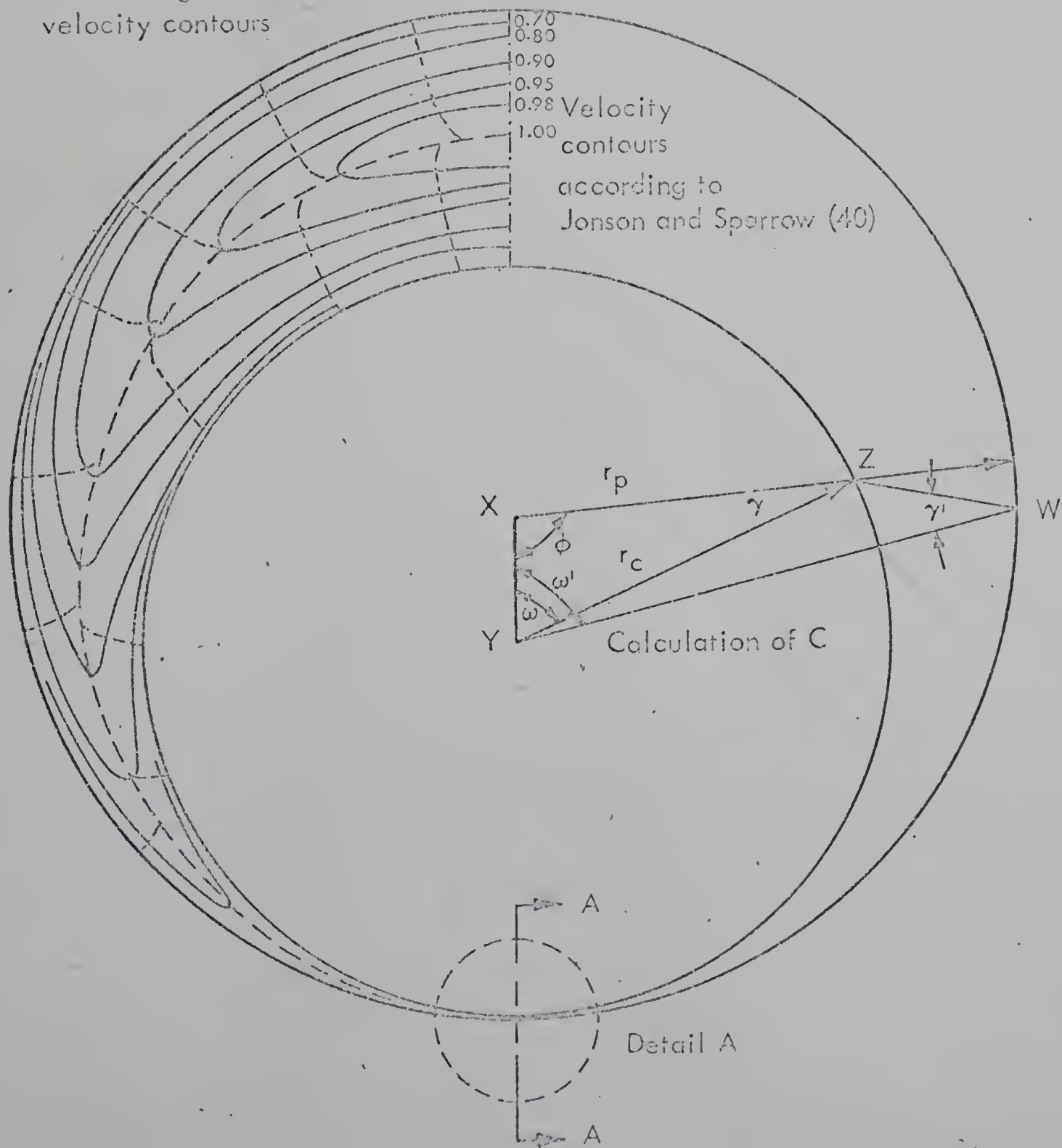




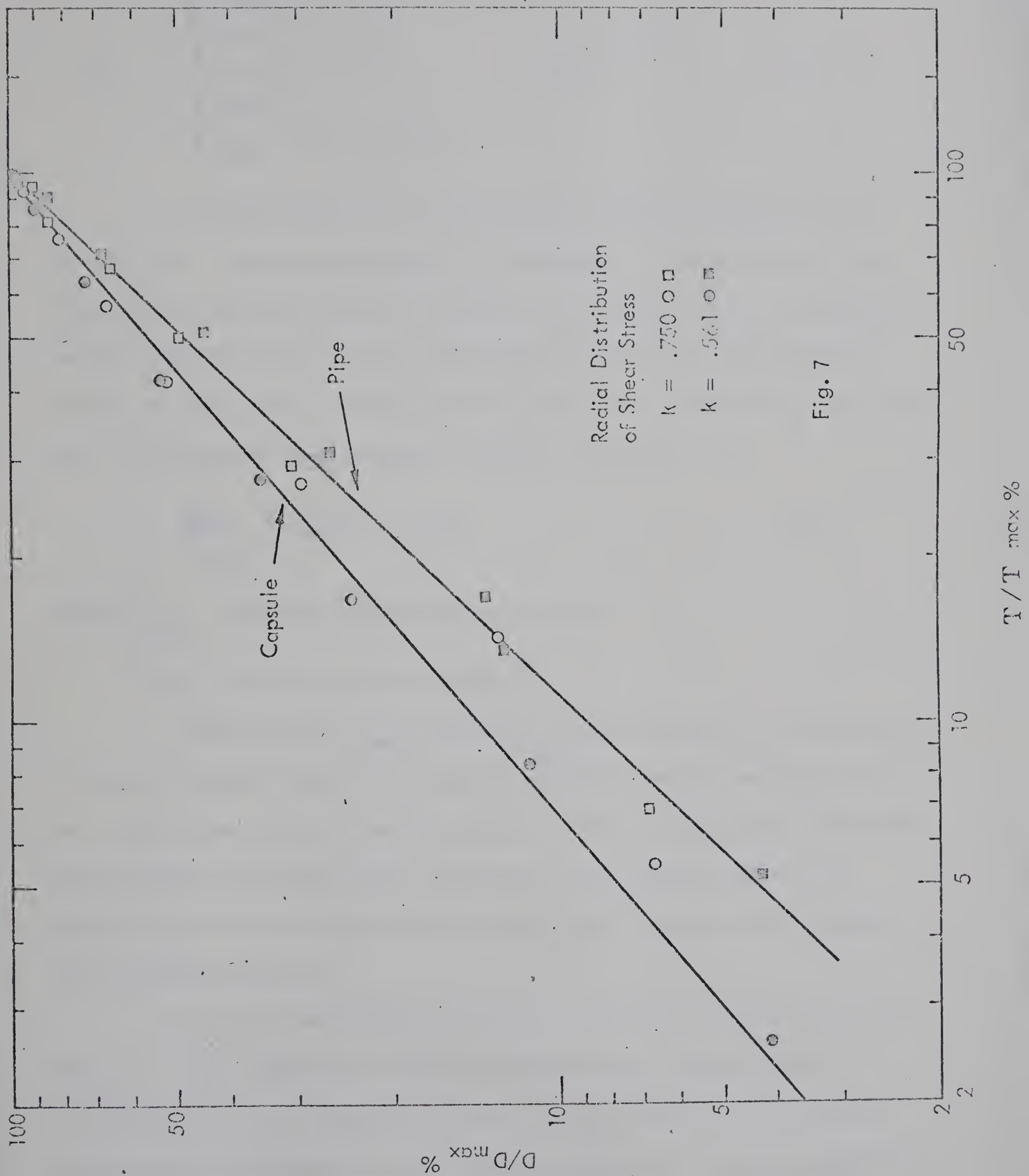
Turbulent Flow in Capsule - Pipe Annulus Fig. 6



Line orthogonol to velocity contours









$$T_p = \frac{\left( \frac{\tau_{p\theta} r_p}{\tau_{ave} (r_c + r_p)} \right)}{\left( \frac{\tau_{p\theta} r_p}{\tau_{ave} (r_c + r_p)} \right)_{max}} = \left( \frac{D}{D_{max}} \right)^{.957} \quad (4)$$

The next step is to determine the velocity profile in the annulus when flow in the annulus is turbulent. For the annulus flow  $V_{ave1}$  due to pressure gradient acting on the annular space an analysis of the extensive experimental data taken by Jonsson & Sparrow (40) for annuli of .281, .561 and .750 diameter ratios was performed by the author and the following relationships obtained. (See Fig. 8 ).

$$\frac{U_{max}}{V_{ave1}} = 1.077 + .353k \quad (5)$$

where  $U_{max}$  = maximum annular point velocity

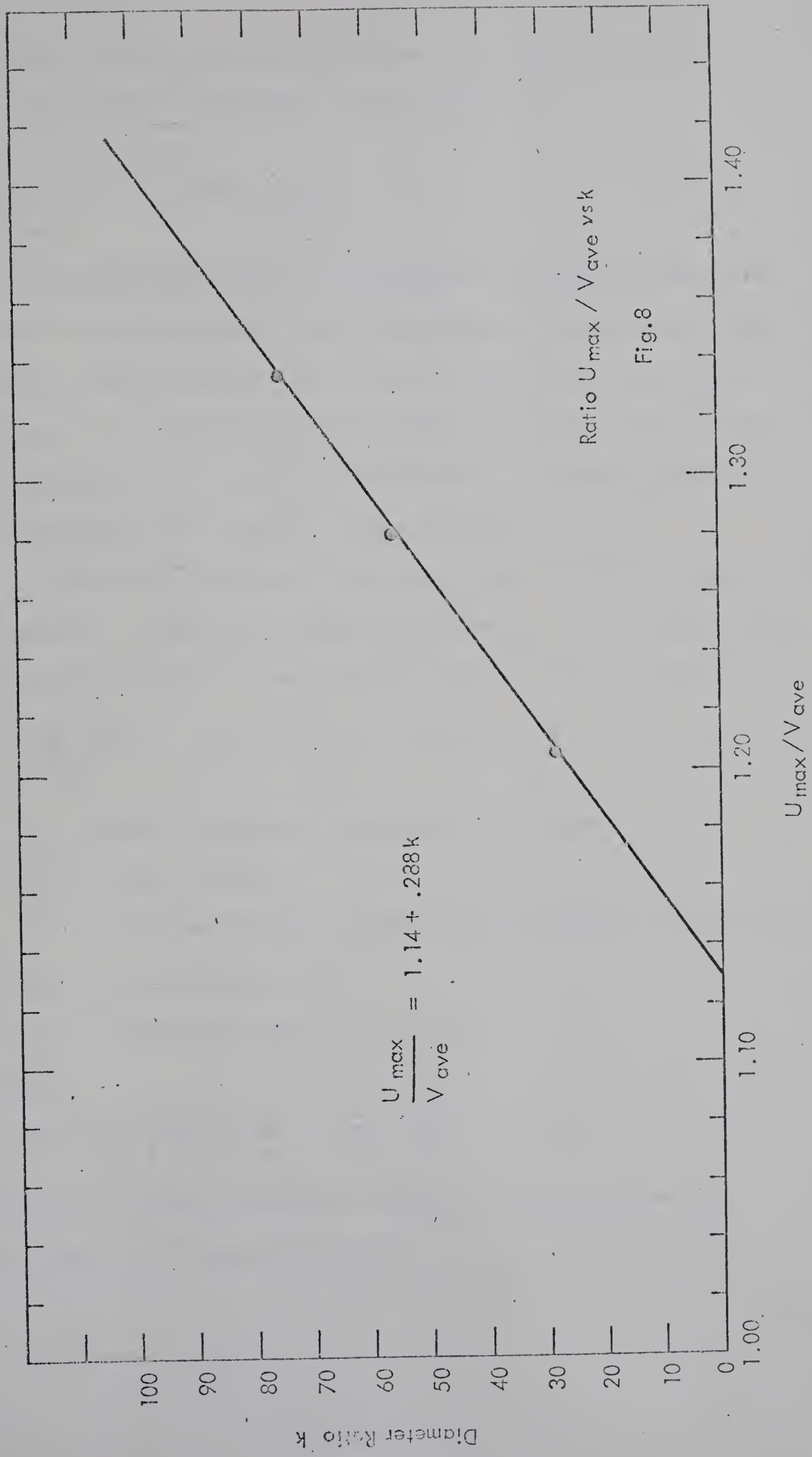
$V_{ave1}$  = average annulus velocity

This velocity ( $U_{max}$ ) occurs at the widest gap in the annulus. Jonsson & Sparrow plotted the velocity profiles for the entire annulus, and using these points it was possible to deduce a logarithmic relationship between the maximum point velocity at any radial position as measured on the inner cylinder compared to the maximum point velocity at the maximum clearance.

It was found that by plotting a "velocity deficiency" of the form,  $1 - \frac{U}{U_m}$  (where  $U$  is the maximum velocity at any value of ( $U = U_m$  @  $\theta_c = 0$ ) against the ratio of the length of the gradient line  $D$  (line orthogonal to equal velocity contours) to maximum gradient line length,  $D_{max}$ , (i.e.  $d_p - d_c$ ) a reasonably straight line fit could be achieved. By multiplying the velocity deficiency by  $\frac{1}{k}$ , the straight lines









for the three diameter ratios could be made coincident (Fig. 9).

The equation resulting from this plot is

$$\frac{1}{k} \left( 1 - \frac{U}{U_{\max}} \right) = 1.16 \log \frac{D}{D_{\max}} \quad (6)$$

Regarding the position of the points of maximum velocity at any point of the annulus Heyda (42) has performed a rigorous analysis to determine the position of these points. In the same report (42) Heyda refers to an observation by Noyes that these points are in fact closely approximated by the mid-points of arcs of circles orthogonal to the capsule and pipe surface. (See Figure 10).

Equation (6) describes the maximum point velocity at any radial position. Jonsson and Sparrow (40) found that the defect law of Hinze (43), best described the velocity profile across the annulus.

$$\frac{U_{\theta} - u_{\theta}}{u_{\tau}} = -2.44 \ln \frac{y}{y_m} + 0.8 + h \frac{y}{y_m} \quad (7)$$

where  $u_{\theta}$  = point velocity at position for a given  $y$

$u_{\tau}$  = shear velocity

$y$  = distance measured outward from the capsule or pipe wall.

$y_m$  =  $y$  at which  $u_{\theta} = U_{\theta}$

$h$  = correction factor (see ref. 43)

Rearranging

$$u_{\theta} = u_{\tau} \left[ 2.44 \ln \frac{y}{y_m} - 0.8 - \frac{hy}{y_m} \right] + U_{\theta} \quad (8)$$

It is required to know the average velocity,  $V_{\text{ave ann}}$  across the annulus at any  $\theta$ . Integrating we have:



Maximum Point Velocities  
Relative to Radial Position

$k = .750$  ■

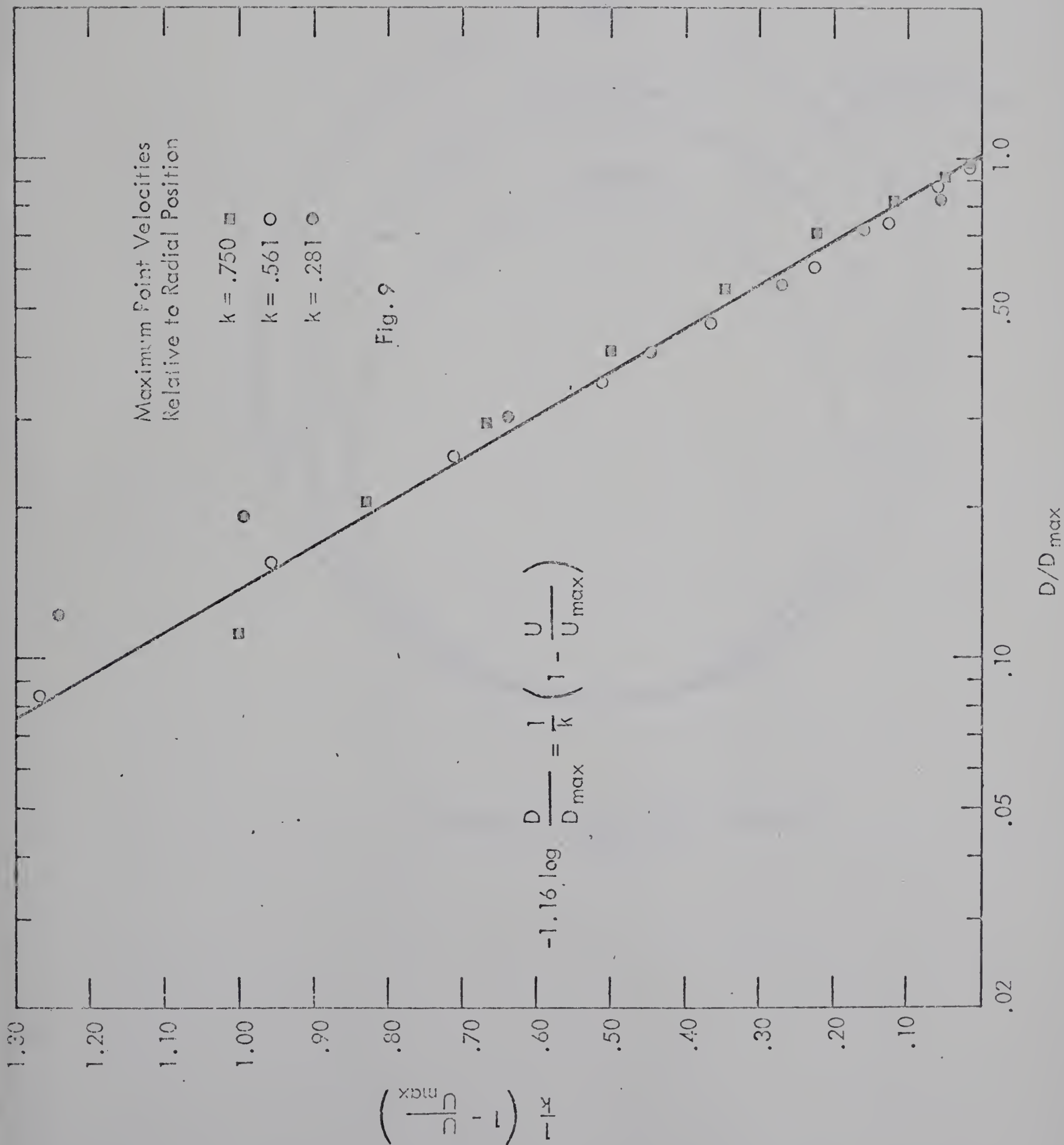
$k = .561$  ○

$k = .281$  ●

Fig. 9

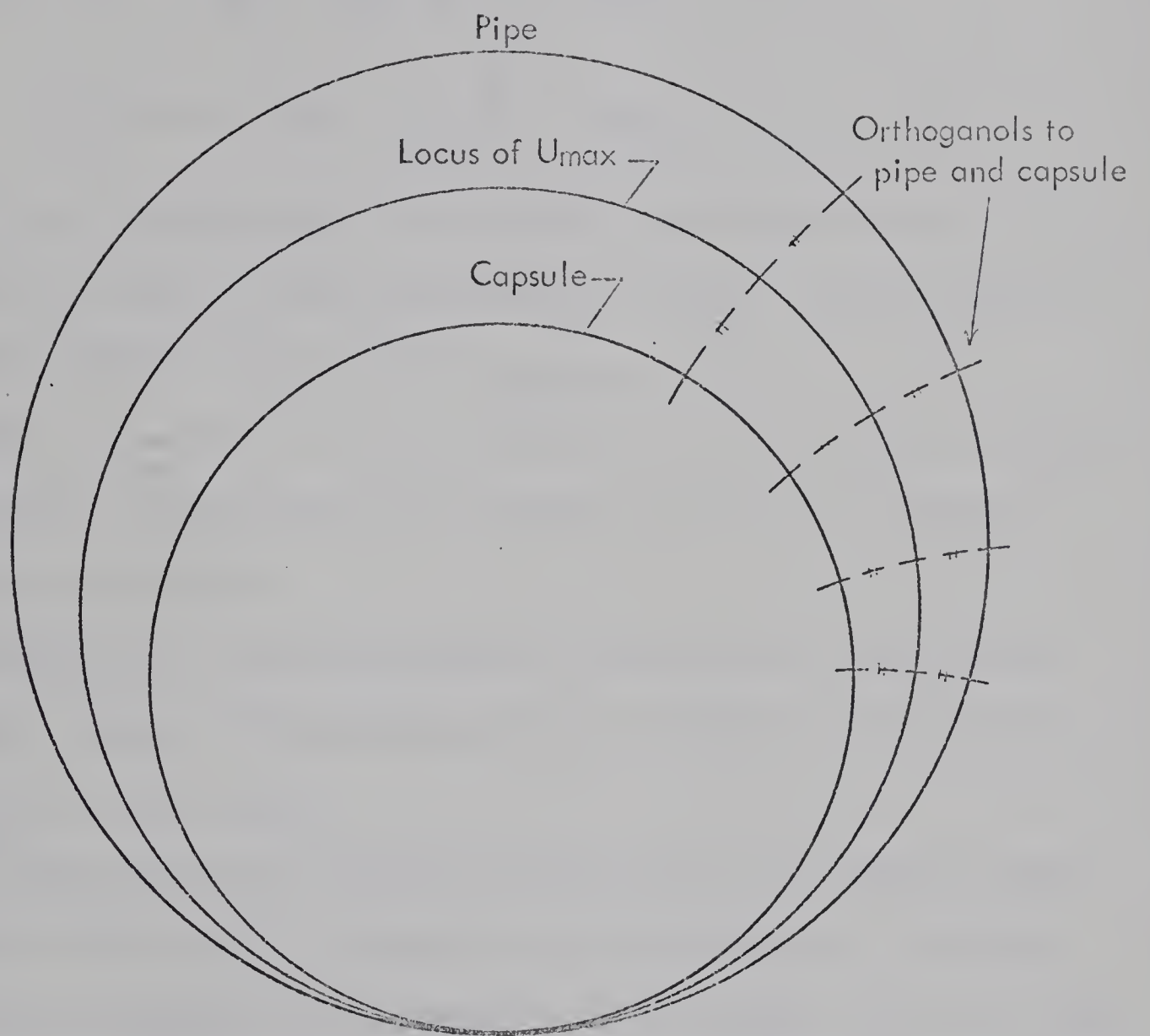
$$-1.16 \log \frac{D}{D_{\max}} = \frac{1}{k} \left( 1 - \frac{U}{U_{\max}} \right)$$

$D/D_{\max}$









Position of Maximum Point Velocities  
Fig. 10



$$\begin{aligned}
u_{\text{ave ann}} &= \int_0^{y_m} u_{\theta} dy = \int_0^{y_m} \left( u_{\tau} \left[ 2.44 \ln \frac{y}{y_m} - 0.8 - \frac{hy}{y_m} \right] + U_{\theta} \right) dy \\
&= \left\{ u_{\tau} \left[ 2.44 \frac{y}{y_m} \ln \frac{y}{y_m} - \frac{y}{y_m} - 0.8y - \frac{hy^2}{2y_m} \right] + U_{\theta} y \right\}_0^{y_m} \\
&= u_{\tau} \left[ -2.44 - 0.8y_m - \frac{h}{2} y_m \right] + U_{\theta} y_m \quad (9)
\end{aligned}$$

This integration procedure must be carried out from both the capsule and pipe walls to the point in the annulus where  $u = u_{\text{max}}$ . The two portions would then be summed to give a total  $V_{\text{ave ann}}$ .

This now provides a means to represent both the velocity and the shear at any point in the annulus for the flow caused by the pressure differential in the annulus.

Turning now to the flow caused in the annulus by the movement of the capsule, similar relationships will be developed to describe the flow and shear in these cases.

It has already been stated that the flow in the annulus caused by the capsule motion can be represented by a Couette flow. In Couette flow, the shear intensity on both boundary walls is equal. This will hold true for the case where the two surfaces are truly parallel. However, in the present case, the surfaces are not completely parallel, and the inside of the pipe representing one plate and the outside of the capsule representing the other are different in area according to the ratio of diameters,  $k$ . Since the total shear stress on the capsule and on the outer wall must be equal, the unit shear stress intensity on the outer wall must be less than that on the inner wall.



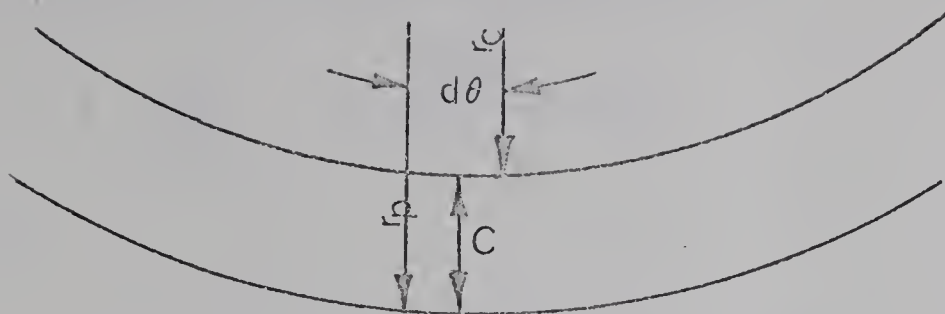


Fig. 6 Detail A

Area of inner surface =  $r_c d\theta$

Area of outer surface =  $(r_c + C)d\theta$

Ratio of area =  $\frac{r_c}{r_c + C}$

C is only a constant in the case of the capsule being concentric within the pipe. Otherwise C will be as shown in Fig. 6

Using sine law in  $\triangle XYZ$  (known XY, YZ,  $\phi$ )

$$\frac{YZ}{\sin \phi} = \frac{XZ}{\sin \omega} = \frac{XY}{\sin \gamma}$$

Solve for  $\gamma$ , then W and XZ

Then in  $\triangle XYW$  (Known  $\phi$  XW, XY)

$$\text{Solve for } YW = \sqrt{(XY)^2 + (XW)^2 - 2(XY)(XW)\cos \phi}$$

Then solve for  $\omega$ ,  $\gamma$

$$\therefore C = \frac{(XZ - r_c) + (WY - r_c)}{2} \quad (10)$$

Robertson (44) has performed experimental tests on plane Couette flow.

He has also compared his solutions with those obtained by other re-

searchers (45, 46, 47, 48, 49). Following a basically empirical approach,

Robertson found the following solutions to most satisfactorily describe





the velocity profile in turbulent Couette flow:

$$1 - \frac{u}{u_z} = E \sqrt{\frac{c_{fr}}{2}} (1 - y/b) \quad (11)$$

with  $E = 4.1$

$$\text{and } \sqrt{\frac{c_{fr}}{2}} = \frac{0.19}{\log Re} \quad \text{where } Re = \frac{u_z b}{\nu} \quad b = C/2 \quad u_z = \frac{V_c}{2} \quad (12)$$

Substituting for  $\sqrt{\frac{c_{fr}}{2}}$  in (11)

$$\text{we have} \quad 1 - \frac{u}{u_z} = E \left( \frac{0.19}{\log \frac{u_z b}{\nu}} \right) \left( 1 - \frac{y}{b} \right) \quad (13)$$

and

$$\tau = c_{fr} u_z^2 \quad (14)$$

Squire (49) as part of his unified theory of turbulent flow has theoretically analysed the plane Couette flow case, deriving expressions for velocity in both the velocity defect and universal velocity distribution forms. He found that neither expression completely agrees with the experimental data of Reichhardt or Robertson. Until such time as more extensive experimental data becomes available, it is not possible to state conclusively which, if any, of the velocity distribution formulae best describe this condition.

For this study, Robertson's experimentally derived formula will be used.

Shear at  $y = C$  must be larger than the shear at  $y = 0$  by a ratio of  $\frac{r_c + C}{r_c}$ . Since  $\tau = c_{fr} u_z^2$ , this means that one of the factors involved in  $\tau$  must change by an amount sufficient to bring about the necessary reduction in  $\tau$ . So it would be reasonable to assume that the change will shift the position of the point at which  $u = u_z = 1/2 V_c$ . This



could be expected to move inwards towards the capsule thus producing the required increase in shear intensity. Ref. Fig. 6

We have  $\sqrt{\frac{c_{fr}}{2}} = \frac{0.190}{\log Re}$

or  $\frac{c_{fr}}{2} = \left( \frac{0.190}{\log Re} \right)^2 = \left( \frac{0.0361}{\log \frac{b u_z}{\nu}} \right)^2$

∴ our desired relation would be

$$\frac{\left( \log b_p \frac{u_z}{\nu} \right)^2}{\left( \log \frac{b_c u_z}{\nu} \right)^2} = \frac{r_c + C}{r_c} \quad (15)$$

Subscripts c and p denote pipe wall and capsule, and  $b_p + b_c = 2b = C$ .

For each section of the annulus, the values of  $b_p$  and  $b_c$  will have to be calculated according to the value of C for that section.

To obtain the net fluid flow through any section of the annulus it will be necessary to integrate the velocity profile in two sections: For the portion from the pipe wall to  $b = b_p$  we have

$$u = u_z \left[ 1 - \left\{ E \left( \frac{.190}{\log \frac{u_z b_p}{\nu}} \right) \left( 1 - \frac{y}{b_p} \right) \right\} \right] \quad (16)$$

$$= u_z \left( 1 - A + \frac{y}{b_p} A \right)$$

where  $A = E \left( \frac{.190}{\log \left( \frac{u_z b_p}{\nu} \right)} \right)$

Now to integrate over the area for the total flow:

$$\int_0^{b_p} \int_{\theta_1}^{\theta_2} u dy d\theta = u_z \left[ \left( 1 - A + \frac{y}{b_p} A \right) (r_c + C - y) \right] d\theta dy$$

$$= u_z \left[ r_c A r_c + y \frac{r_c}{b_p} A + C - AC + \frac{C y}{b_p} - y + A - \frac{y^2}{b_p} A \right] d\theta dy$$



$$= u_z \left[ \int_0^{b_p} r_c y - A r_c y + \frac{y^2 r_c A}{2 b_p} + C y - A C y + \frac{C y^2}{2 b_p} A - \frac{y^2}{2} + A y - \frac{y^3 A}{3 b_p} \right] d\theta$$

$$= u_z \left[ r_c b_p - A r_c b_p + \frac{b_p^2 r_c}{2 b_p} + C b_p - A C b_p + \frac{C b_p^2}{2 b_p} - \frac{b_p^2}{2} + A b_p - \frac{b_p^3 A}{3 b_p} \right] d\theta$$

$$= u_z b_p \left[ r_c - A r_c + \frac{r_c}{2} + C - A C - \frac{C}{2} - \frac{b_p}{2} + A - \frac{b_p}{3} A \right] (\theta_1 - \theta_2)$$

$$= u_z b_p \left[ 3/2 r_c - A r_c + 3/2 C - A C - \frac{b_p}{2} + A - \frac{b_p}{3} A \right] (\theta_1 - \theta_2) \quad (17)$$

In the area from  $y = b_1$  to the capsule wall the equation actually measures the velocity deficiency  $V_c - u$

$$\therefore u = V_c - u_z \left( 1 - B + \frac{y}{b_c} B \right) \quad (18)$$

$$\text{where } B = E \left( \frac{.190}{\log \frac{u_z b_c}{\nu}} \right)$$

Integrating as before, remembering that  $y$  is now measured outward from the capsule:

$$\int_0^{b_c} \int_{\theta_1}^{\theta_2} u dy d\theta = \left[ V_c - u_z \left( 1 - B + \frac{y}{b_c} B \right) (r_c + y) \right] dy d\theta$$

$$= \left\{ V_c r_c + V_c y - u_z \left[ r_c - r_c B + \frac{r_c y}{b_c} B + y - y B + \frac{y^2 B}{b_c} \right] \right\} dy d\theta$$

$$= \int_0^{b_c} \left[ V_c r_c y + \frac{V_c y^2}{2} - u_z \left( r_c y - r_c B y + \frac{r_c y^2 B}{2 b_c} + \frac{y^2}{2} - \frac{y^2 B}{2} + \frac{y^3 B}{3 b_c} \right) \right] d\theta$$

$$= \left\{ V_c r_c b_c + \frac{V_c b_c^2}{2} - u_z \left[ r_c b_c - r_c B b_c + \frac{r_c b_c^2}{2 b_c} + \frac{b_c^2}{2} - \frac{b_c^2 B}{2} + \frac{b_c^3 B}{3 b_c} \right] \right\} (\theta_1 - \theta_2)$$





$$= \left\{ V_c b_c \left[ r_c + \frac{b_c}{2} \right] - u_z b_c \left[ r_c - \frac{r_c B}{2} + \frac{b_c}{2} - \frac{b_c B}{6} \right] \right\} (\theta_1 - \theta_2) \quad (19)$$

$d\theta$  is chosen small enough so that the value of  $C$  does not change appreciably allowing  $b_p$  and  $b_c$  to be treated as constants. Alternatively the value of  $C$  could be placed in the equation in relation to radial position and the integration carried throughout the whole annulus.

Having now obtained an equation for the velocities in both the inner and outer portions of the Couette flow, the overall average Couette flow in the annular space will be the sum of 17 and 19 divided by the total area, which is

$$\left[ \frac{r_c (\theta_1 - \theta_2) + r_c + C (\theta_1 - \theta_2)}{2} \right] C = \frac{2 \left( \frac{r_c C}{2} + C^2 \right)}{2} (\theta_1 - \theta_2) \quad (20)$$

Add to this the velocity at the same radial position due to the pressure flow in the annulus, so that the  $u_{ave \text{ ann1}} + u_{ave \text{ ann2}}$  = the average velocity across an annular section at any given radial position.

It is now possible to outline a procedure to establish pressure gradients, velocity ratios, etc. for a capsule pipe system where all or a portion of the flow in the annulus is turbulent.

#### Procedure

1. Choose a diameter ratio  $k$ , and a clearance  $C$ .
2. Choose an applied  $\left( \frac{\Delta P}{L} \right)_c$ , and a  $V_c$ .
3. Determine velocity in the annulus as described by laminar flow equations (Part 6 or Part 9) based on  $V_c$ .
4. Determine point of transition to turbulent flow with criterion

$$\frac{2u_{ann \text{ ave}} C}{\nu} < 2400.$$





5. For region of annulus in laminar flow determine  $\tau_{cL}$  and  $\tau_{pL}$ .
6. For turbulent portion of annulus, determine amount of annulus flow  $u_{ann\ ave1}$  due to  $\left(\frac{\Delta P}{L}\right)_c$  based on  $f$  values taken from Jonnson & Sparrow (40).
7. Solve for  $U_{max}$  from Fig. 8.
8. Solve for  $U$  and  $u_{ann\ ave1}$  for radial sections to the point of transition defined in (3).
9. Solve for  $\tau_{ct1}$  and  $\tau_{pt1}$ , for the various radial positions from Fig. 6.
10. Determine amount of annulus flow due to capsule motion,  $u_{ave\ ann2}$  (i.e. Couette flow) by use of equations (15), (17) and (19).
11. Calculate  $\tau_{ct2}$  and  $\tau_{pt2}$  according to equations.
12. Sum  $\tau_{cL}$ ,  $\tau_{ct}$ ,  $\tau_{ct2}$  and compare to  $\left(\frac{\Delta P}{L}\right)_c k^2$ . If not equal, choose different  $\left(\frac{\Delta P}{L}\right)_c$  and repeat (2) to (12) until satisfactory  $\left(\frac{\Delta P}{L}\right)_c$  is found.
13. Knowing  $V_c$ ,  $k$  and  $V_{ann\ ave}$  solve for  $V_{av}$ 

$$V_{av} = k^2 V_c + 1 - k^2 (V_{ann\ ave}), \quad VR = \frac{V_c}{V_{av}}$$
14. Knowing  $V_{av}$ , we can solve for  $\left(\frac{\Delta P}{L}\right)_f$  and PR.
15. Change  $V_c$  in preset increments and repeat (2) to (14).
16. Change clearance and repeat (2) to (15).
17. Change  $k$  and repeat 2 to 16.

The above procedure will produce PR-VR clearance relationships which are dependent on  $V_c$ ,  $k$ ,  $dp$ ,  $\nu$ , unlike the fully laminar theory, which is dependent only on  $k$ .

For a single capsule of finite length, there will be end effects, particularly at the capsule nose. If we examine the velocity profile in



the free pipe, we see that the capsule is encountering slower moving fluid in the lower portion of the turbulent free pipe profile.

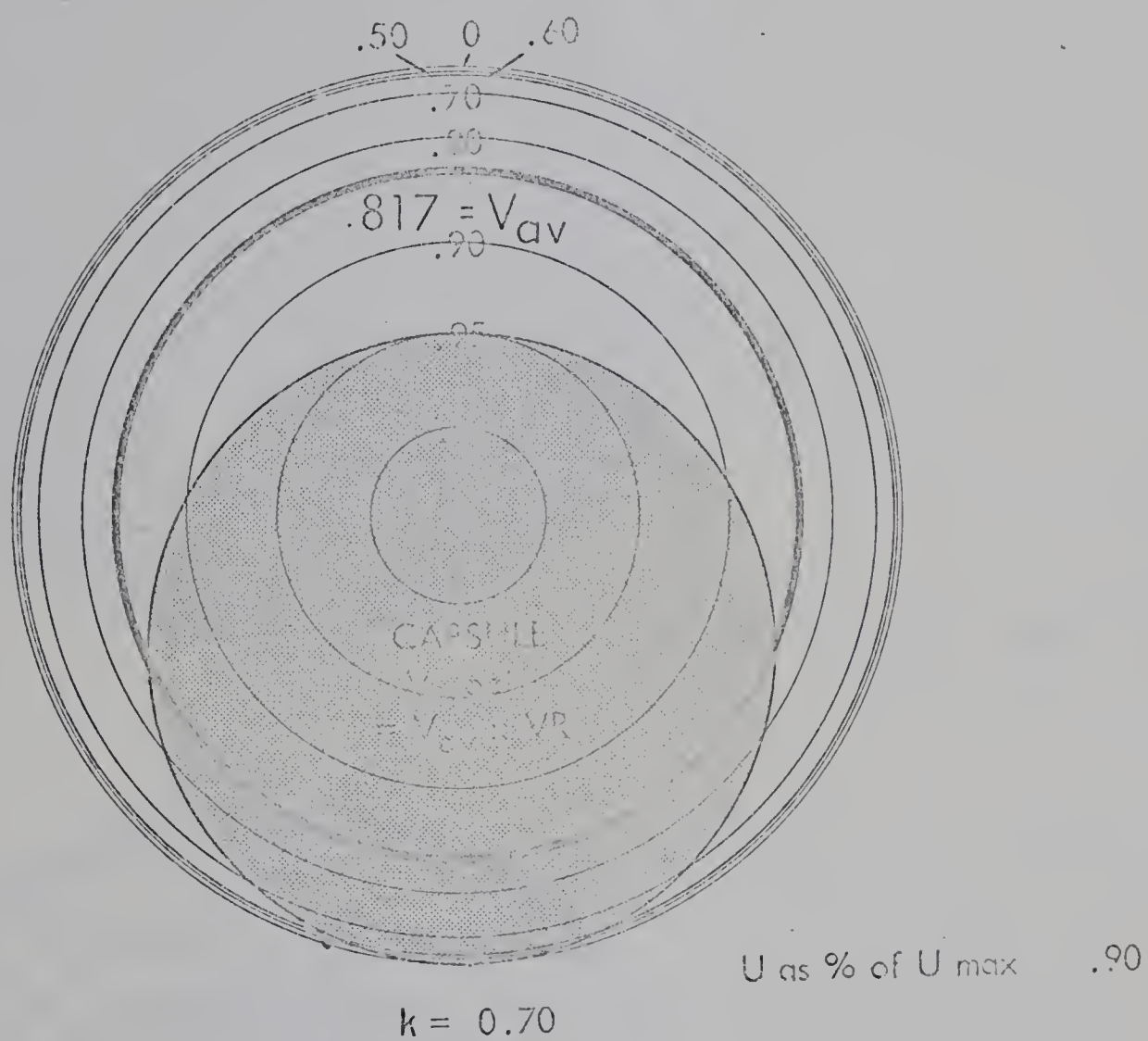
(Fig. 11, 12 ). This fluid must be displaced in an upward direction into velocity deficient areas in front of the capsule or into the upper regions of the annular area. This upward movement of fluid must produce an upward shear on the capsule nose.

This force acts at the nose of the capsule, and produces a lifting moment about a fulcrum at the tail of the capsule. At the tail of the capsule, the profile must again return to a free pipe turbulent profile, thus requiring a net downward shear. However, this transference must occur primarily in the wake of the capsule where it would have no effect on the capsule body.

The existence of this type of force is the only thing that can explain the observed phenomenon of nose lift. Considering the earlier assumptions of the flow system as being represented by a combination of annulus pressure flow and Couette flow it is seen that:

- (1) Shear force on capsule due to annulus flow is always positive (i.e. tail lift), also for any eccentric condition, the net line of action of this shear force will be above the capsule centerline.
- (2) Shear force on the capsule due to Couette flow is always negative (i.e. producing a nose lift). For any eccentric case the net line of action of this force will be below the capsule centerline.



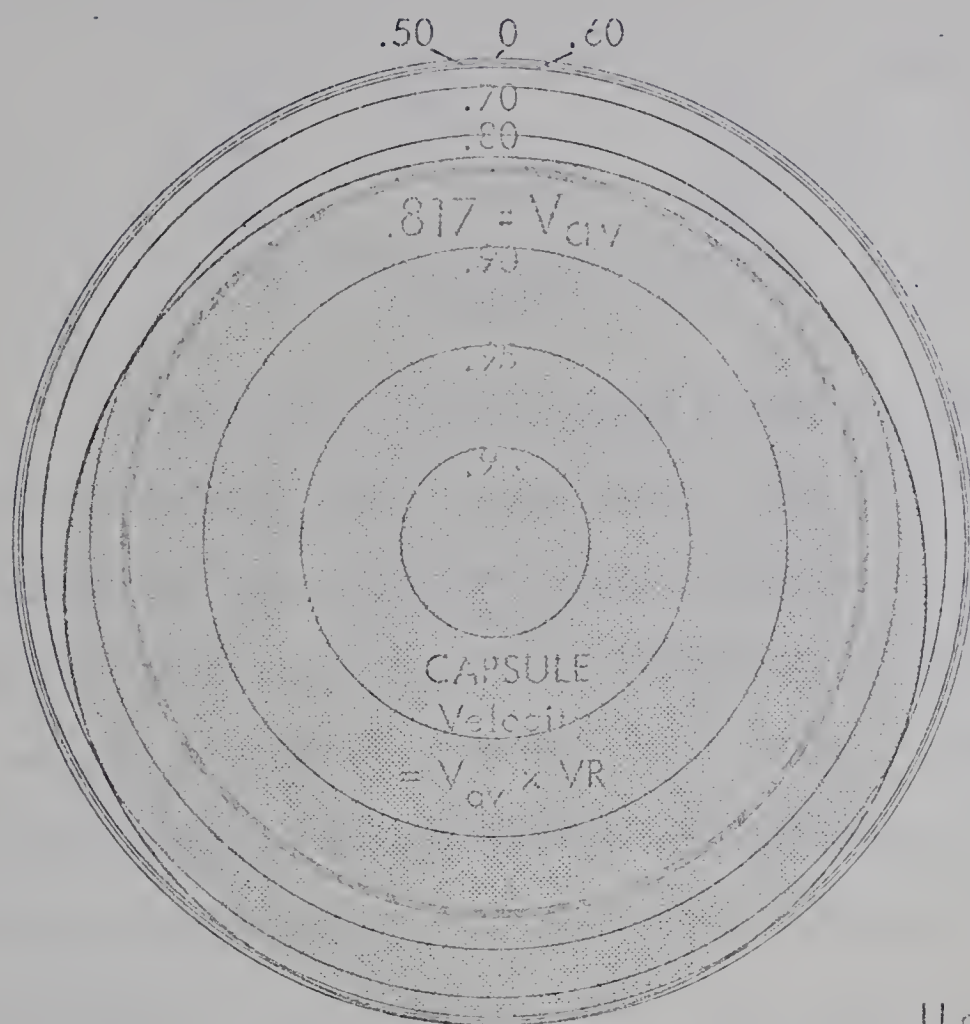


TURBULENT VELOCITY PROFILE  
WITH CAPSULE SUPERIMPOSED

Fig. II

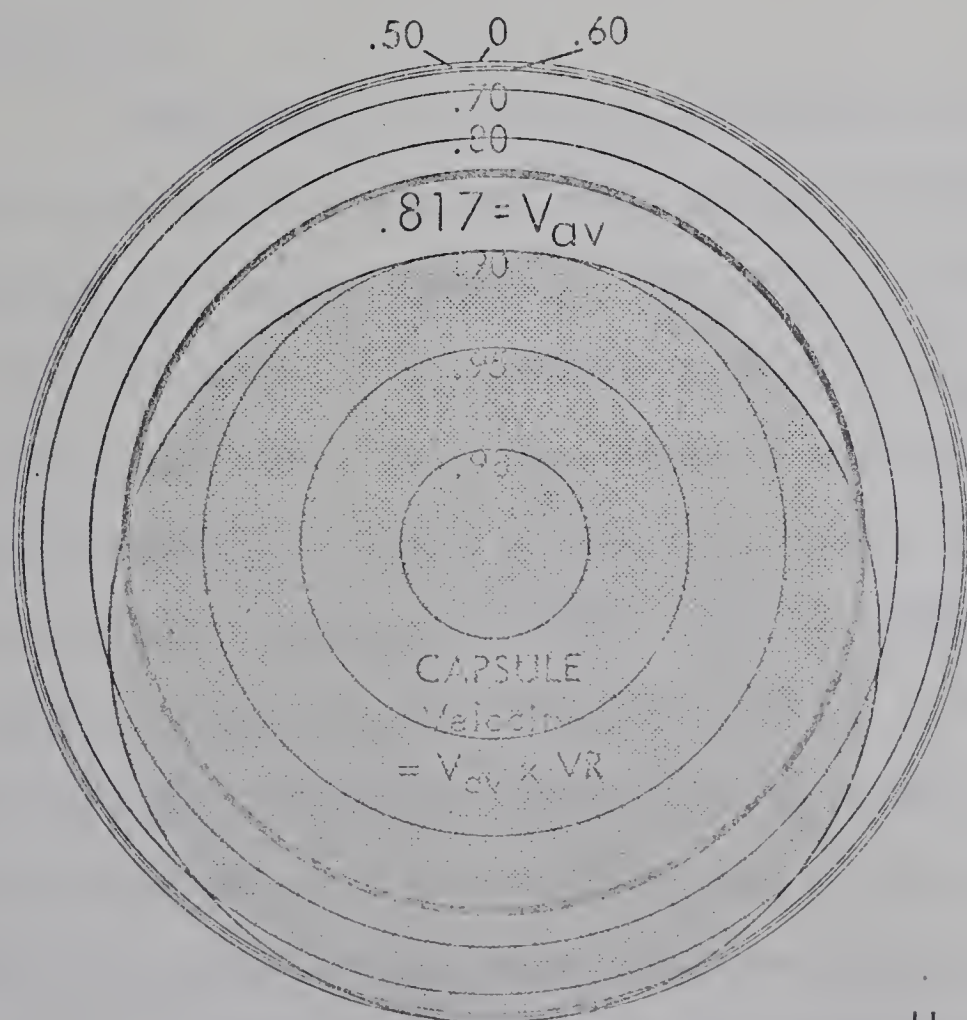






$k = 0.90$

U as % of  $U_{max}$  .90



$k = 0.80$

U as % of  $U_{max}$  .90

TURBULENT VELOCITY PROFILES  
WITH CAPSULE SUPERIMPOSED



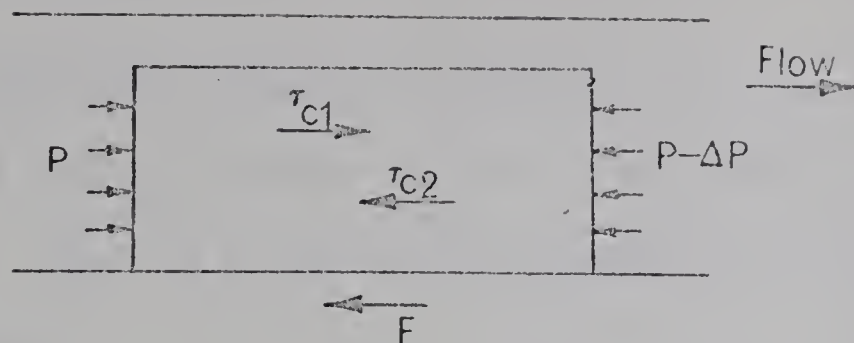


Fig. 13

A force balance will yield that  $\Delta P + \tau_{c1}$  must equal  $\tau_{c2} + F$ . Also it is evident that the net moment from these forces alone must be a tendency to lift the capsule tail. Therefore shear due to the fluid transfer in the nose area must be the force which eventually produces the capsule nose lift. Once this lift begins to occur, then the angle of attack provided will allow for the beginning of "lubrication" effect under the capsule which will aid in the lifting process, as outlined by Suhr (39). It is also possible that an angle of attack is provided by roughnesses of the pipe interior which would tend to lift up the capsule nose.

There must be, of course, a lifting force under the capsule even in the case where it is freely flowing parallel to the pipe, which maintains the capsule clearance. This force must be produced by circumferential variation in the pressure such that  $P_{\text{bottom}} - P_{\text{top}} = \sigma - \rho$  per projected unit area. It is reasonable to expect that higher pressures would be obtained in the area under the capsule where the velocity gradients are most severe, since  $\frac{\Delta P}{L} \sim \frac{\partial u}{\partial y}$ . Jonsson and Sparrow (40) did find a circumferential pressure variation in fixed eccentric annulus, with the higher pressures corresponding to regions of higher velocity. Since the upward and downward forces must balance each other in any equilibrium state, this circumferential variation of the pressure forces should not produce any net moment on the capsule.





## V EXPERIMENTAL APPARATUS

The basic apparatus is shown in Figs. 14 & 15 with the accompanying Table 1 giving pertinent details of the pumping and measuring equipment used. Figs. 16 to 22 are photographs of the various sections of the test equipment.

An attempt was made to improve the internal diameter tolerances of the available acrylic tubing (1 1/4" nominal dia.) by cutting it into 6 in. sections and internally machining each section to a dimension of 1.310 in. The ends of each 6 in. joint were prepared for lap jointing with glue. The pipeline, along with pressure tap fittings, was aligned over an internal mandrel and glued joint by joint. The pipeline was polished with a polishing compound to produce as smooth a line as possible.

For photographic purposes, a viewing cell was placed around the pipeline within the test section to minimize distortion of the images by refraction and diffraction.

The first viewing cell thus constructed consisted of an acrylic box 4 in. x 4 in. x 4 ft. 0 in. long placed over the pipeline and filled with glycerine. This was used for the first portion of the flow pattern work, but was replaced for the remainder of the work by a solid acrylic viewing cell which was found to give less diffraction and refraction by minimizing the number of interfaces involved.

The photographic equipment employed included three 35 mm. single lens reflex, focal plane shutter cameras and two monocular microscopes. Specifications are given in Table 1. Illumination was provided by three mercury arc lamps equipped with collimating and condensing lens to provide maximum illumination within a small area of interest. For that portion of the experimental work requiring synchronization of two or three cameras, a



photocell activated solenoid apparatus simultaneously fired cable releases connected to the cameras. (See Fig. 14)

For the flow pattern pictures, the tracing material employed was a -80 mesh pigmented acrylic powder which fluoresced under ultraviolet light. This material was originally received as a very fine powder which was found unsuitable for use as the tracing medium. However, if the acrylic was melted down, recrushed and screened, a usable product was obtained. The fluorescent particles were intensely illuminated by the mercury arc light, which is rich in the ultraviolet portion of the spectrum.

The capsules used for the static flow pattern work were nickel-plated, solid steel cylinders as listed in Table 2. For the clearance measurements work, hollow aluminum capsules with removable ends to allow weighting of the capsules to any desired density were used. Details of these capsules are given in Table 3.

### Calibrations

The various components of the system were calibrated in the following manner.

#### 1. Flowmeter

An approximate flowrate was obtained from rotameters. A more exact measurement was made by means of measurement of the pressure drop across orifices of six different diameters. For each orifice diameter a series of time-weight samples were taken at different velocities within the orifice range. The time was taken by a photo cell activated mechanical millisecond clock, which recorded the time required to obtain a known weight of water.

The photocells were activated by the moving needle of a Toledo platform scale thus allowing a running sample to be taken and avoiding any





errors due to start up or shut down. Velocity calibrations for the six different orifices are shown in Figs. A-1 to A-3. Data is listed in Table A-1.

## 2. Pressure Cells

All three pressure transducers were calibrated against an air over water manometer (see Figs. A-4 and A-5 and Table A-2.)

## 3. Cameras

The amount of distortion in the viewing cell was measured by means of introducing a scale held between two snugly fitting cylinders into the viewing cell and photographing the scale in both the vertical and horizontal positions. Measurements were then made from the photograph and compared with the actual scale. It was found that in the vertical plane, measurements were .869 of actual size.

To calibrate the microscopic pictures a capsule with brass discs of known larger diameter than the capsule attached concentrically to each end of the capsule was placed in the pipeline in front of the microscopes and a photograph taken of this artificial clearance. This was done for each of the three capsule diameters used (see Figs. A-6, 7, 8, Table A-3.)

To calibrate the synchronization of the cameras, photographs were taken of the running millisecond clock and the photographs from the three cameras compared. Results showed variations of less than two milliseconds between camera firings.



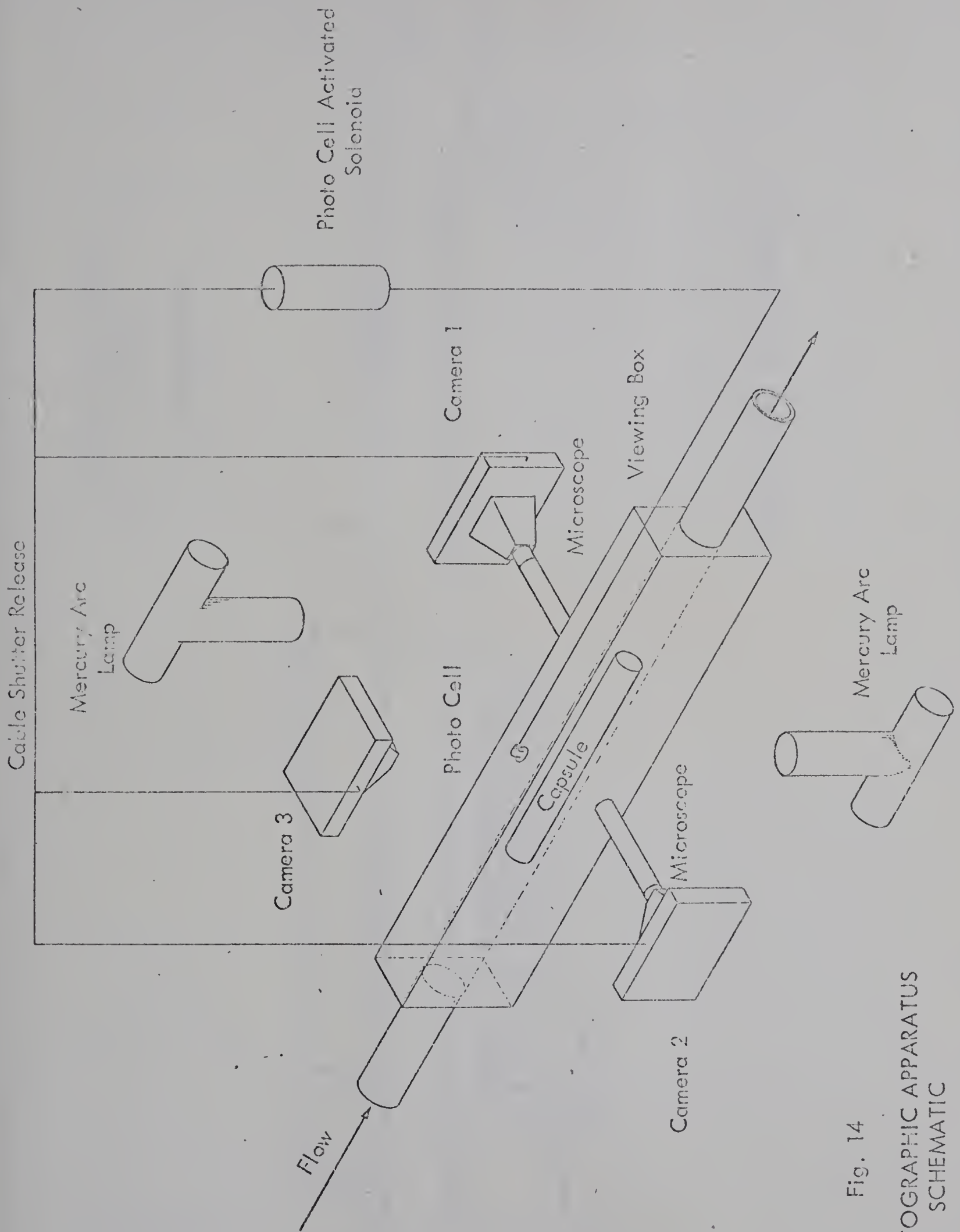


Fig. 14  
PHOTOGRAPHIC APPARATUS  
SCHEMATIC

N.T.S.



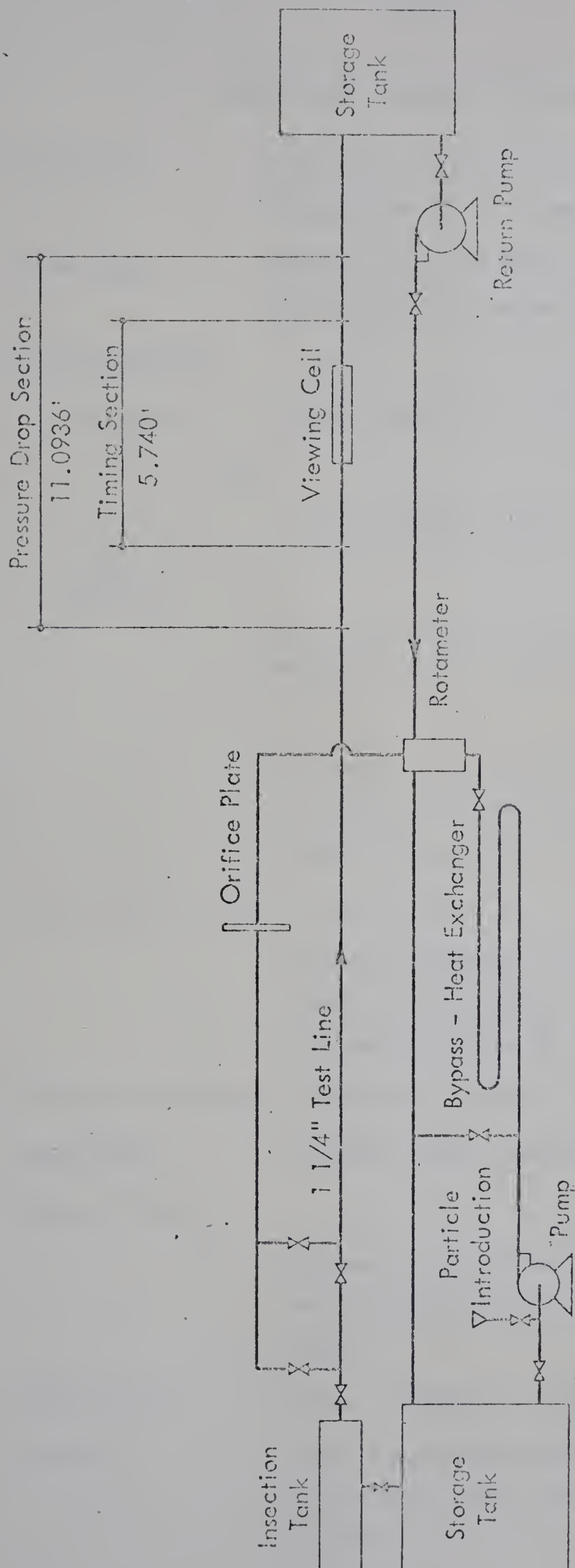


Fig. 15

SCHEMATIC OF TEST APPARATUS

N.T.S.





Table 1

Details of Experimental Equipment

Main Pump	Viking Model 18 LS 2" Gear pump powered by Westinghouse 20 hp electric motor.
Return pump	Gardner Denver 1" 3500 r.p.m. centrifugal pump powered by Tamper 10 hp. electric motor.
Flow measurement	
- Rotameters	- Brooks Model 13 1110
	and
	Brooks Model 8 1110
Orifice	
	- Variable diameter brass plate orifice (3/16", 1/4", 3/8", 1/2", 3/4", 1")
	- pressure drop measured by Foxboro pneumatic differential pressure cell model 13-LA-1-205, range 0 to 200" of water
Test Section Pressure Differential	
	- Foxboro pneumatic differential pressure cells, model 15 A-1-5 range 0 to 2" water and model 15-LA-1-20 range 0 to 20" water
Pressure Differential Recorder	- Foxboro three pen Model 5430
Temperature	- Rochester Dial Thermometer Range 0 to 100° F
Capsule Timing	
	- Photocells and 6 volt bulbs, through relay box to Standard millisecond electro mechanical clock.
Illumination	- Three -- CENCO 110 volt Mercury Arc Lamps.
Cameras	- 35 mm Focal Plane Shutter Miranda Model G.
	- 35 mm. Focal Plane Shutter Exacta Model IHA 6EE



- 35 mm. Focal Plane Shutter Asahiflex No.  
79862

Microscopes - Bausch & Lomb Optical Co. Monocular  
Microscope Barrel No. 138480

- Bausch and Lomb Optical Co.  
Monocular Microscope Barrel No. 157004

Camera Firing - Photocell activated solenoid to depress  
cable releases to three cameras.

Table 2

Capsule Dimensions - Static Flow Patterns Investigation

	Capsule diameter (inches)	Capsule length (inches)	Capsule diameter Ratio
1.	1.129	4.010	.862
2.	1.002	4.010	.765
3.	.941	4.015	.718
4.	.885	4.010	.675
5.	.817	4.012	.625

Table 3

Capsule Dimensions - Clearance Investigation

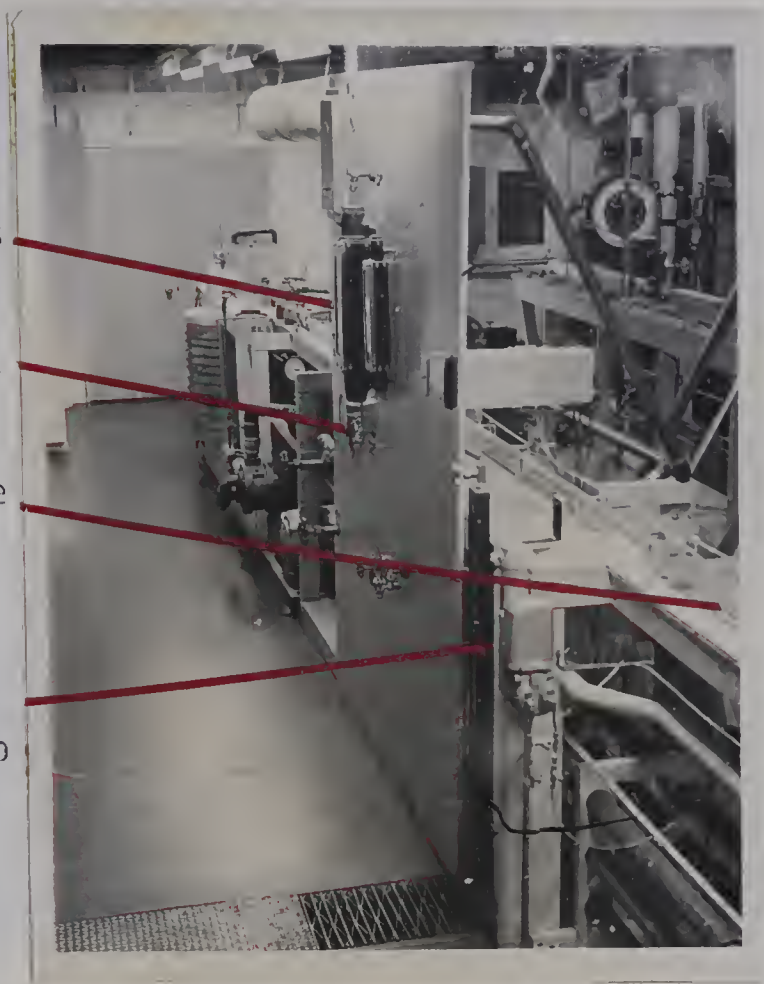
Capsule diameter inches	Capsule Length inches	Capsule diameter Ratio	Capsule weight gms.	Density Ratio
.918	3.006	.701	32.30	1.000
			32.62	1.010
			32.95	1.020
			33.92	1.050
			35.53	1.100
			37.05	1.147
.918	6.007	.701	64.72	1.000
			65.35	1.010
			66.01	1.020
			67.96	1.050
			71.21	1.100
			74.43	1.155
1.050	3.010	.802	42.41	1.000
			42.86	1.011
			43.36	1.022



Capsule diameter inches	Capsule Length inches	Capsule diameter Ratio	Capsule weight gms.	Density Ratio
1.050	6.010	.802	44.53	1.050
			46.65	1.100
			48.74	1.149
			84.81	1.000
			85.65	1.010
			86.31	1.020
			89.05	1.050
			93.30	1.100
			97.52	1.150
1.181	3.003	.902	53.51	1.000
			54.03	1.010
			54.58	1.020
			56.19	1.050
			58.85	1.100
			61.56	1.150
1.181	6.000	.902	106.91	1.000
			107.98	1.010
			109.03	1.020
			112.25	1.050
			117.61	1.100
			123.01	1.151



Rotameters  
Flow Control  
1 1/4" Test Line  
D/P cell to measure  
orifice pressure drop



Photographic  
Enclosure

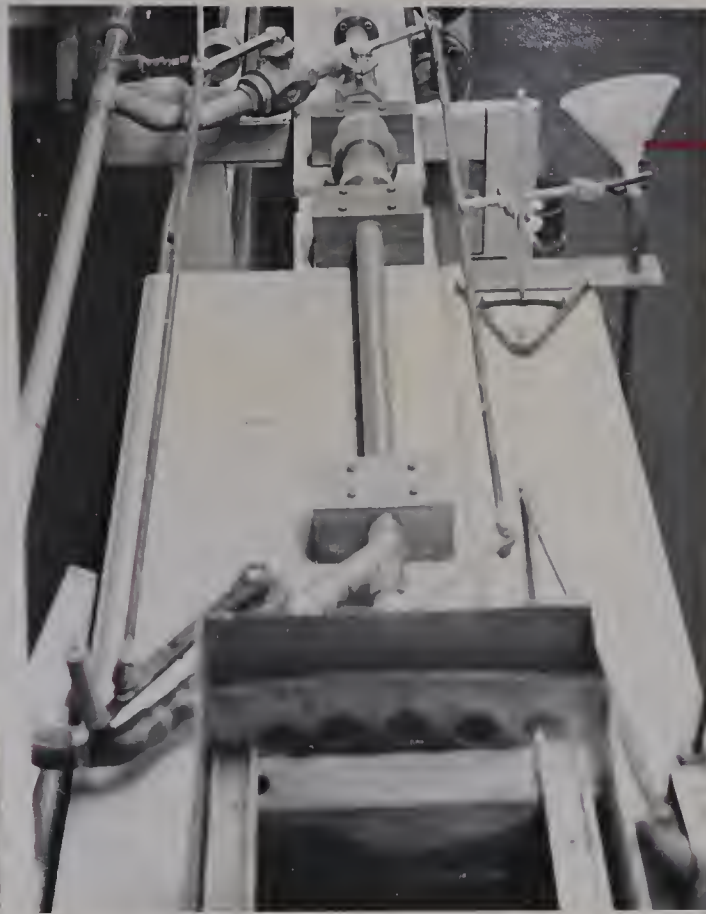


Receiving Tank

OVERALL VIEW - TEST PIPELINE - FIGURE 16

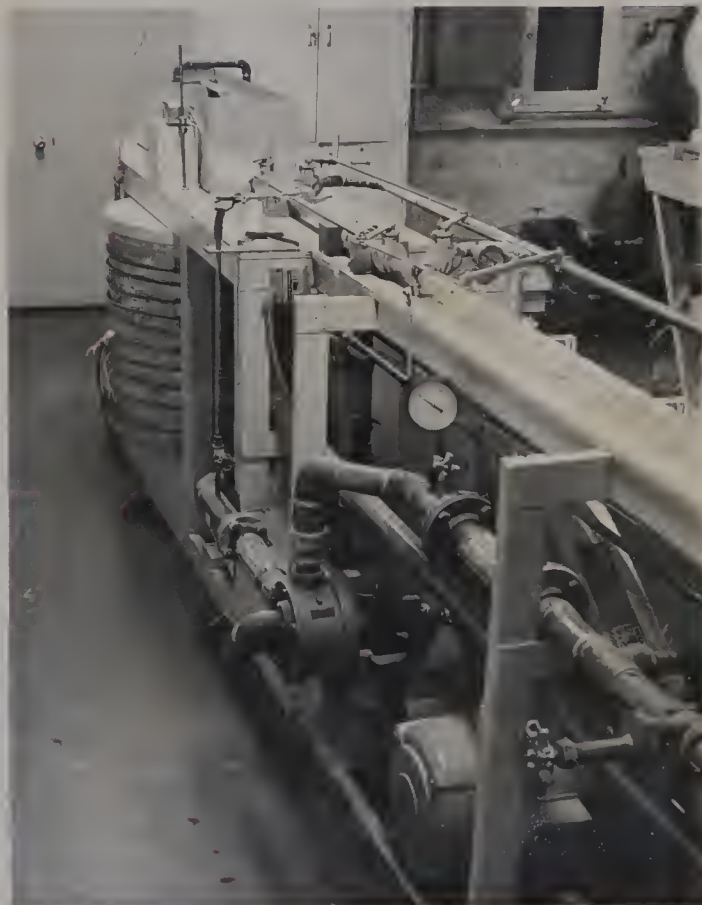






Particle  
Injection  
Point

INJECTION TANK AND VALVES - FIGURE 17



PUMP AND STORAGE TANK - FIGURE 18

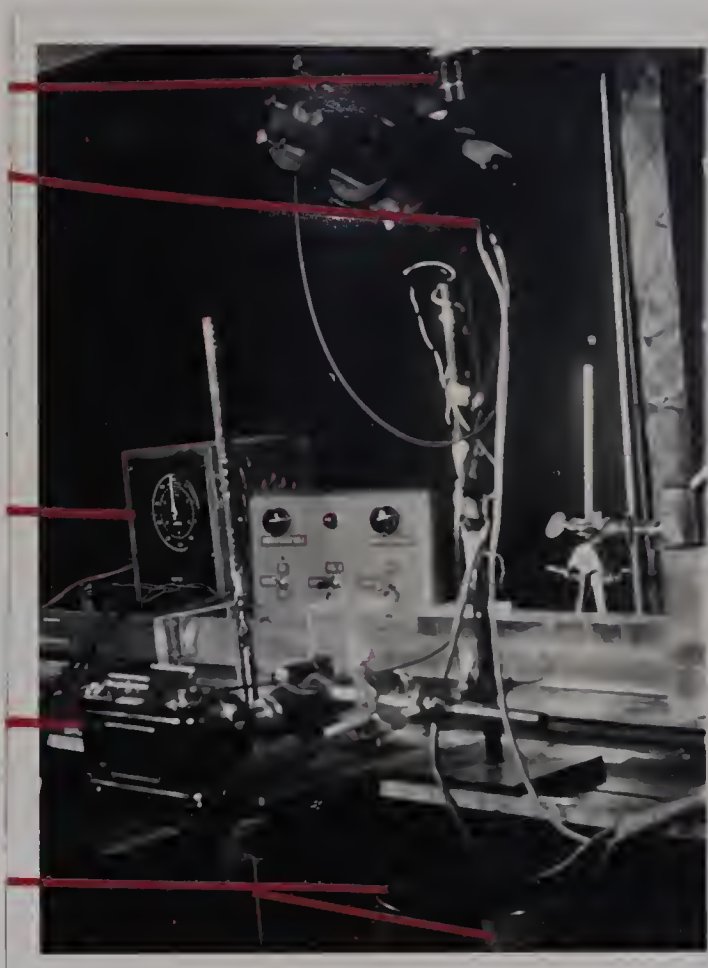


Camera No. 3  
Camera Firing Solenoid

Timing Apparatus

Camera No. 2 and  
Microscope

Lower Mercury Arc  
Lamps



PHOTOGRAPHIC APPARATUS - FIGURE 19A

Upper Mercury Arc  
Lamp  
Solenoid Power Supply  
Solenoid Release  
Photocell  
Viewing Cell  
Camera No. 1 Position  
Solenoid Fire Photocell  
Camera No. 2

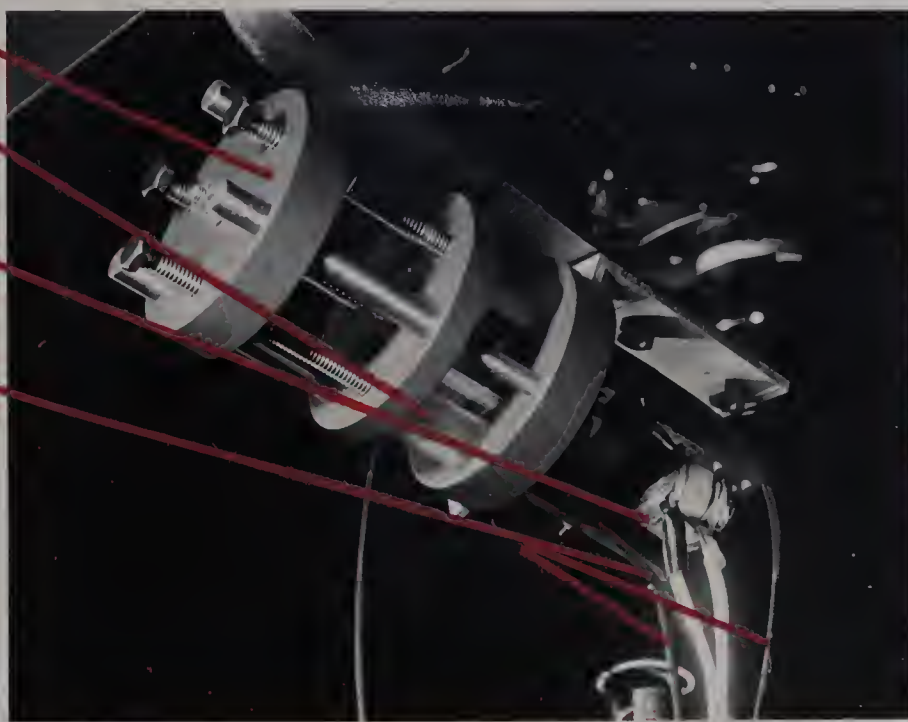


PHOTOGRAPHIC APPARATUS - FIGURE 19B





Moveable Plate  
 Cable Heads  
 Solenoid  
 Cables to Cameras  
 Solenoid fires,  
 pulling moveable  
 plate, depressing  
 cable head,  
 firing cameras.



PHOTOGRAPHIC APPARATUS - SOLENOID - FIGURE 19c

Rotameters  
 Chart Recorder  
 Flow Control  
 Heat Exchanger  
 Control

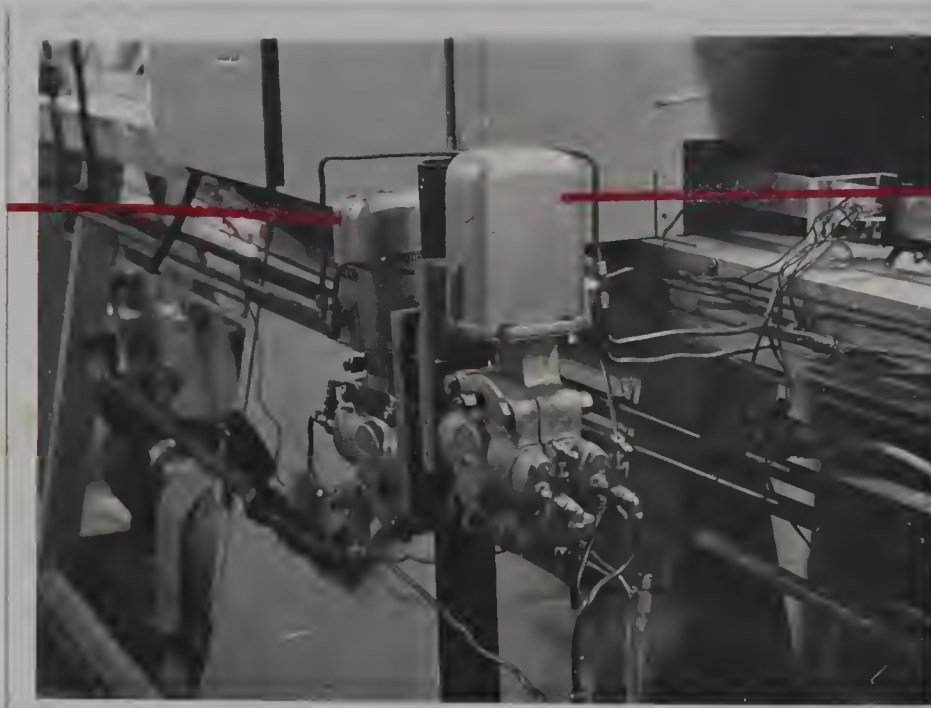


CONTROL BOARD - FIGURE 20





2 inch  
range



20 inch  
range

PNEUMATIC DIFFERENTIAL PRESSURE CELLS

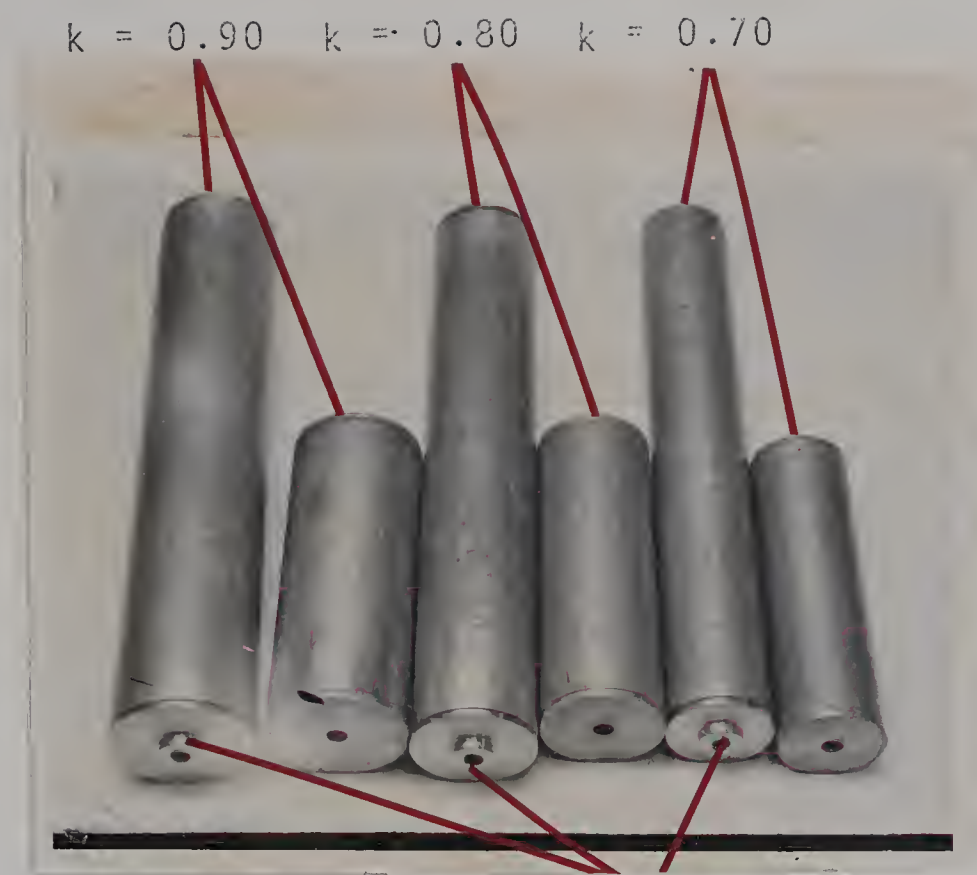
FIGURE 21



$k = .625$     $k = .715$     $k = .765$     $k = .866$

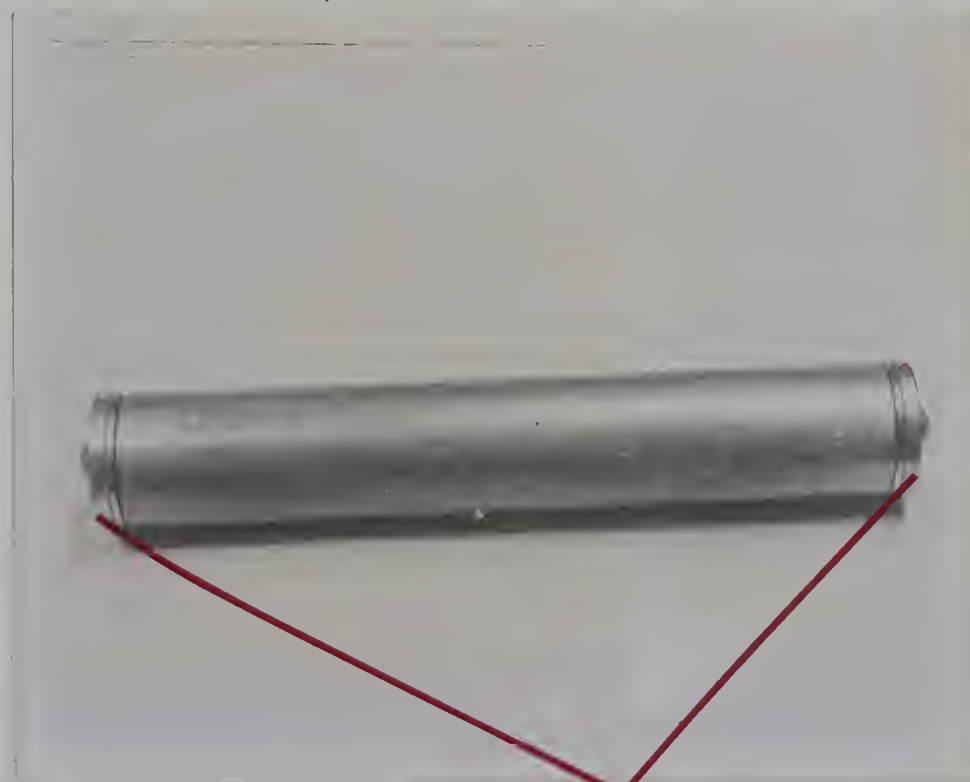
TEST CAPSULES - FLOW PATTERNS - FIGURE 22





Ends in Place for Calibration Discs

TEST CAPSULES - CLEARANCE FIGURE 23A



Calibration Discs

TEST CAPSULE WITH CALIBRATION DISCS IN PLACE

FIGURE 23B



## VI EXPERIMENTAL PROCEDURE

### Flow Patterns

The fluorescent particles were introduced into the line in a concentrated solution through a standpipe connected to the pump suction. They dispersed quickly throughout the system.

A capsule was then positioned in the pipeline and the viewing cell and the mercury arc lamps were set to illuminate the desired section of the pipeline. For each of the five capsules examined, a series of photographs were taken for horizontal and vertical sections at both the nose and the tail of the capsule.

A number of velocity settings were used for each capsule up to the point at which the capsule began to move down the pipe. At each velocity setting, a photograph was made and a trace of the velocity and pressure were recorded. In these series a single camera was used and was mounted on a movable slide apparatus for vertical section pictures and an adjustable rack apparatus for horizontal section pictures.

### Clearances

For the clearance part of the investigation three synchronized photographs were required. First a series of photographs were taken which included a complete view of the capsule and pipeline from the side on one camera and a similar shot from the top on a second camera. These photographs were used to determine the overall position of the capsule within the pipe, particularly that condition where the capsule lifted at the nose to form a wedge (on the Macro scale). Following this series, a second set of runs was made to obtain data regarding microscale clearances under the capsules.

In this series, two cameras, one on each side of the viewing cell





at a known distance apart horizontally took photographs through microscopes. The third camera remained in position above the pipeline to take a full view shot of the capsule and pipeline. This enabled a calculation to be made of the position along the capsule at which the microscopic pictures were taken.

Each series of photographic runs was done at ten velocity settings. The velocities were chosen such that they included a velocity sufficient to produce lift off of the capsule on a macro scale.

All photographs were taken on ASA 400 Tri-X Kodak Pan film which was developed in Bauman Diafine two bath developer giving an effective ASA rating of 2400.





## VII DISCUSSION OF EXPERIMENTAL RESULTS Flow Patterns

The study of flow patterns around stationery capsules of sizes as listed in Table 2 extended from low velocities, up to velocities just smaller than the threshold velocities of the capsules. Photographs were taken of both the nose and tail regions, from the side and from the top of the pipeline. Typical photographs are shown in Figures 24 to 28

Discussing first the tail regions, we will consider three main features:

- (1) vortex existing at the bottom of the capsule
- (2) point of stagnation on capsule face
- (3) separation of flow as it passes over sharp edge  
of the capsule

Regarding (1), the parameter used for describing the vortex was the position relative to the bottom of the pipe and the face of the capsule. These Y and X dimensions were expressed in terms of fraction of capsule diameter so that the different capsules could be compared. These dimensions were plotted against  $V_{av}$  (in Figs. 29 to 33). From the plots we see that for all diameter ratios the vortex is smaller for increasing values of  $V_{av}$  ( and pressure gradient).

However, for all diameter ratios, the values of X and Y tend to become constant for increasing values of  $V_{av}$ , showing that the vortex size tends to an equilibrium value.

Pictures taken from the top of the pipe at the capsule showed no vortex motion in the horizontal plane. The only motion evident was the symmetric division of streamlines around the capsule. The vortex observed in the side view pictures extends to the sides of the capsules



Stagnation

Vortex Center



$$V_{av} = .098 \text{ ft./sec.}$$

$$k = .675$$

Stagnation

Vortex Center



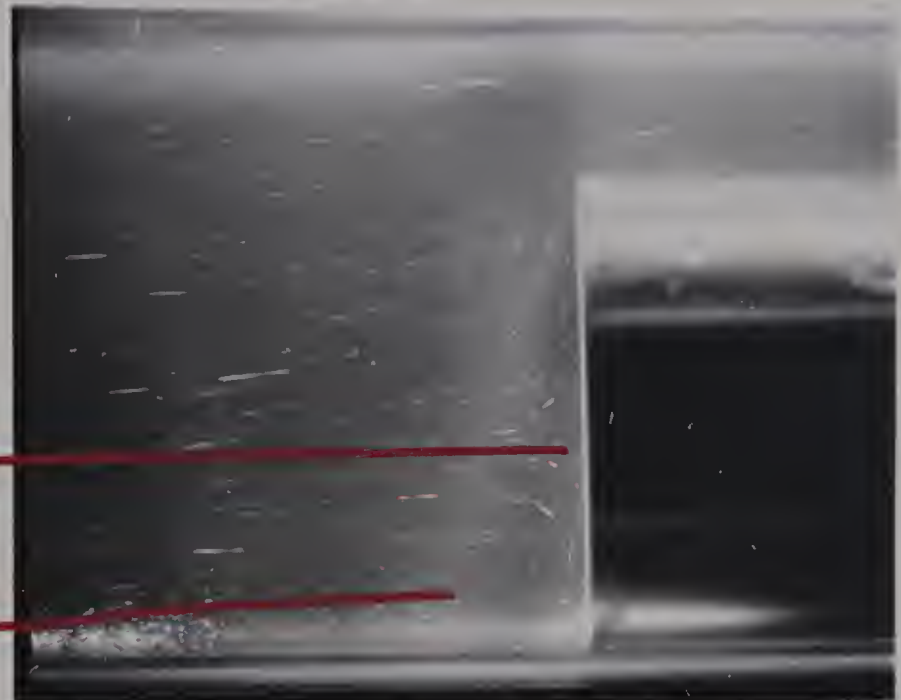
$$V_{av} = .201 \text{ ft./sec.}$$

$$k = .765$$

REAR VORTEX LAMINAR FLOW FIGURE 24A



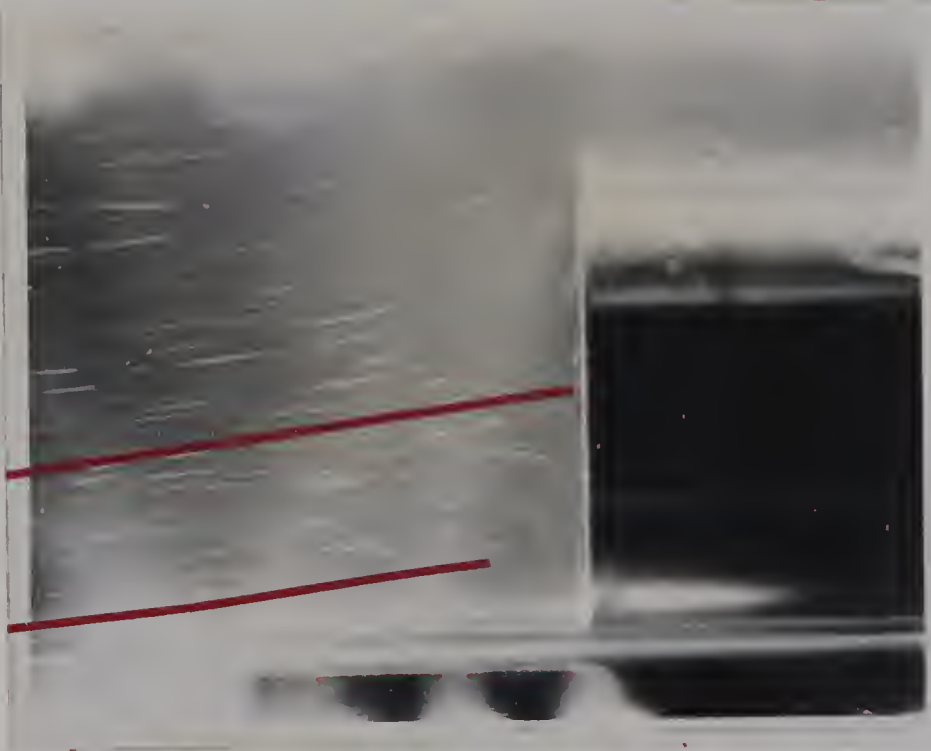
Stagnation  
Vortex Center



$$V_{av} = .635 \text{ ft./sec.}$$

$$k = .765$$

Stagnation  
Vortex Center



$$V_{av} = 1.168 \text{ ft./sec.}$$

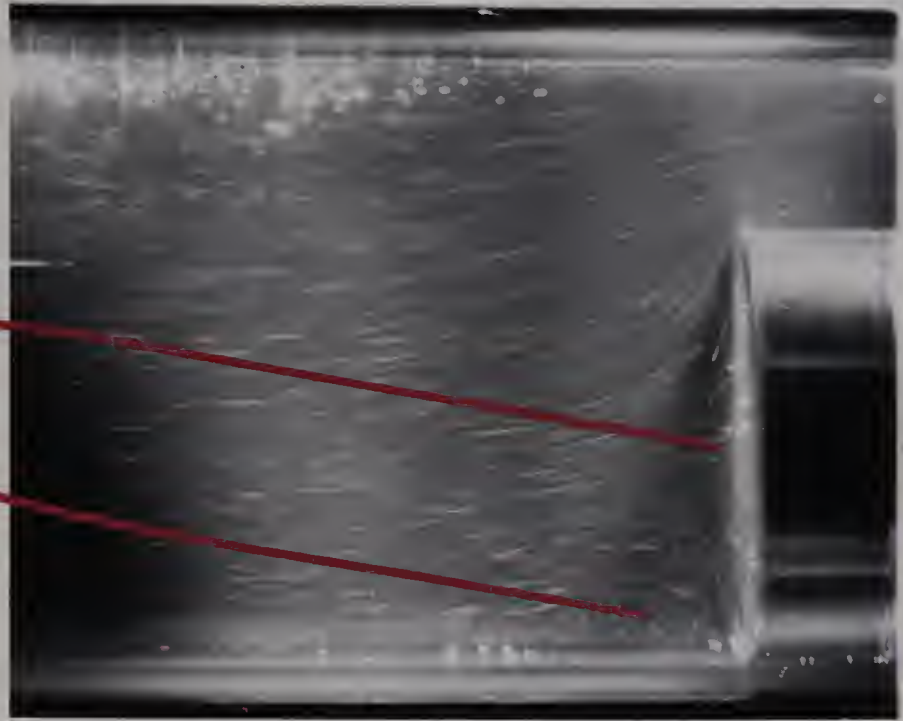
$$k = .765$$

REAR VORTEX TURBULENT FLOW - FIGURE 24B





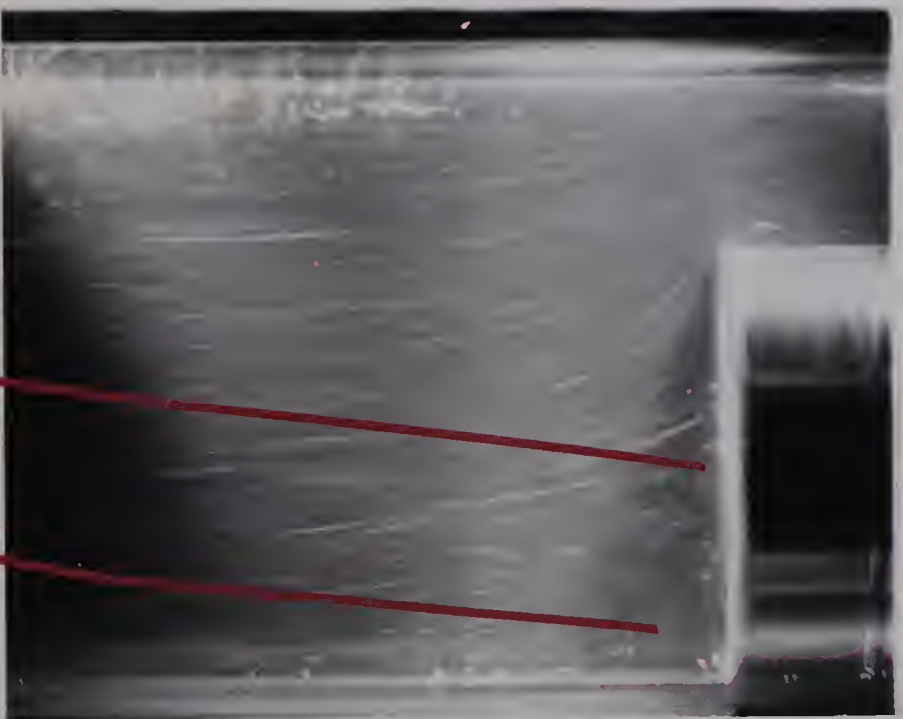
Stagnation  
Vortex Center



$$V_{av} = 1.30 \text{ ft./sec.}$$

$$k = .718$$

Stagnation  
Vortex Center



$$V_{av} = 2.275 \text{ ft./sec.}$$

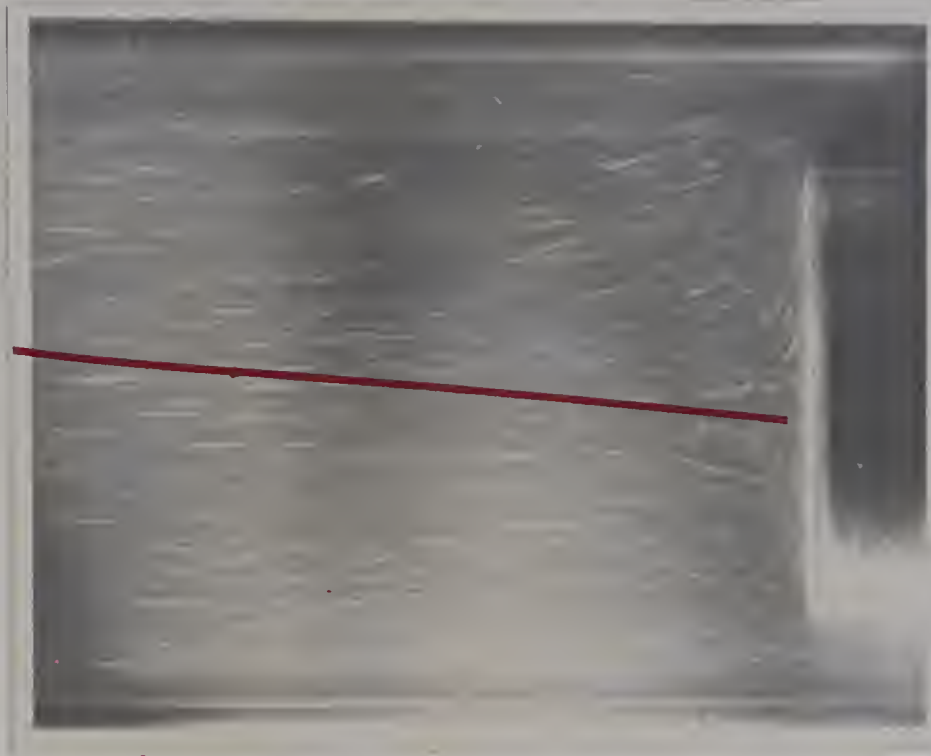
$$k = .718$$

REAR VORTEX TURBULENT FLOW FIGURE 24C

8-1-2020

10/1/2020

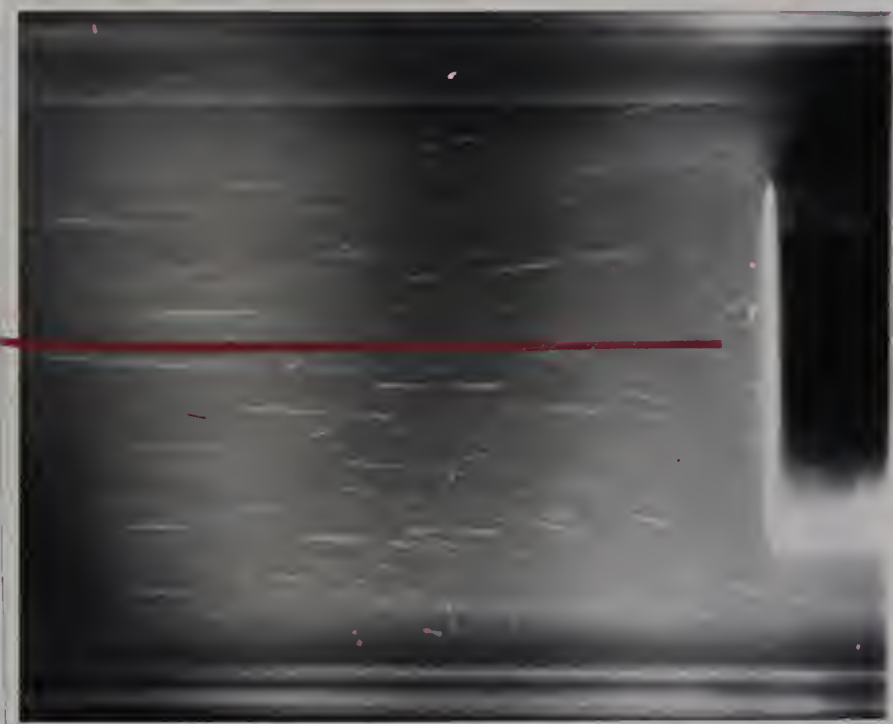
Stagnation



$$V_{av} = 1.820 \text{ ft./sec.}$$

$$k = .765$$

Stagnation

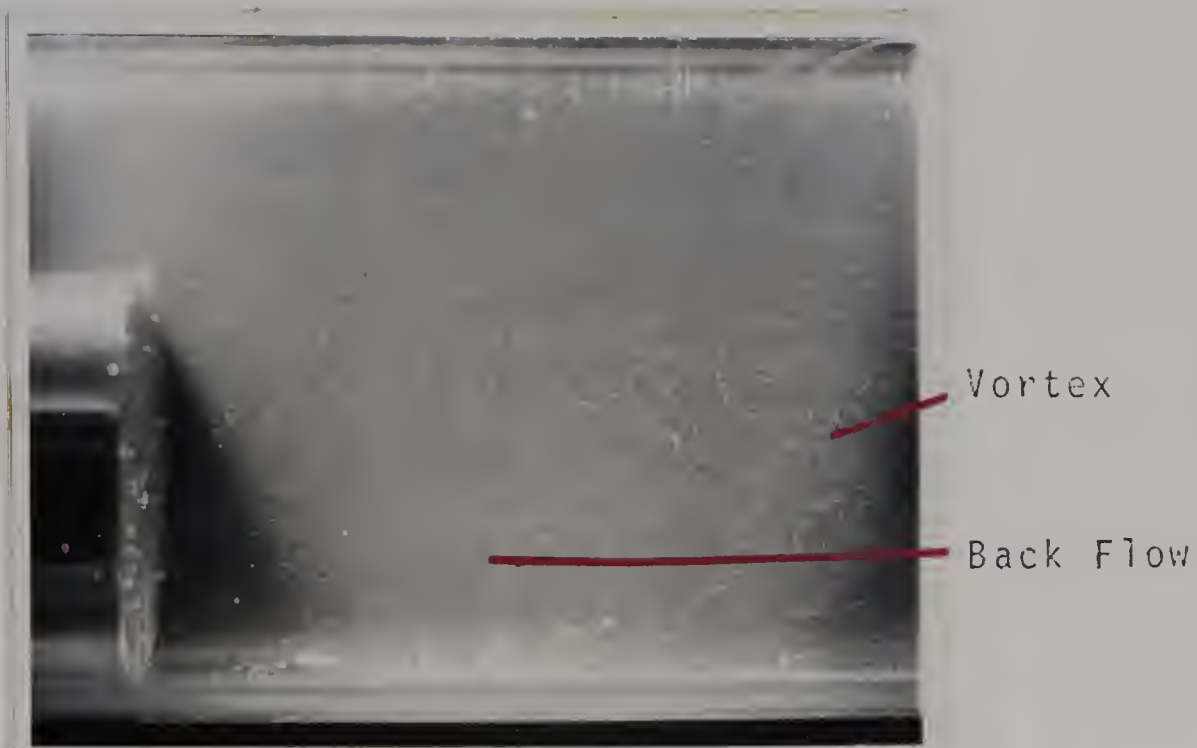


$$V_{av} = 2.95 \text{ ft./sec.}$$

$$k = .625$$

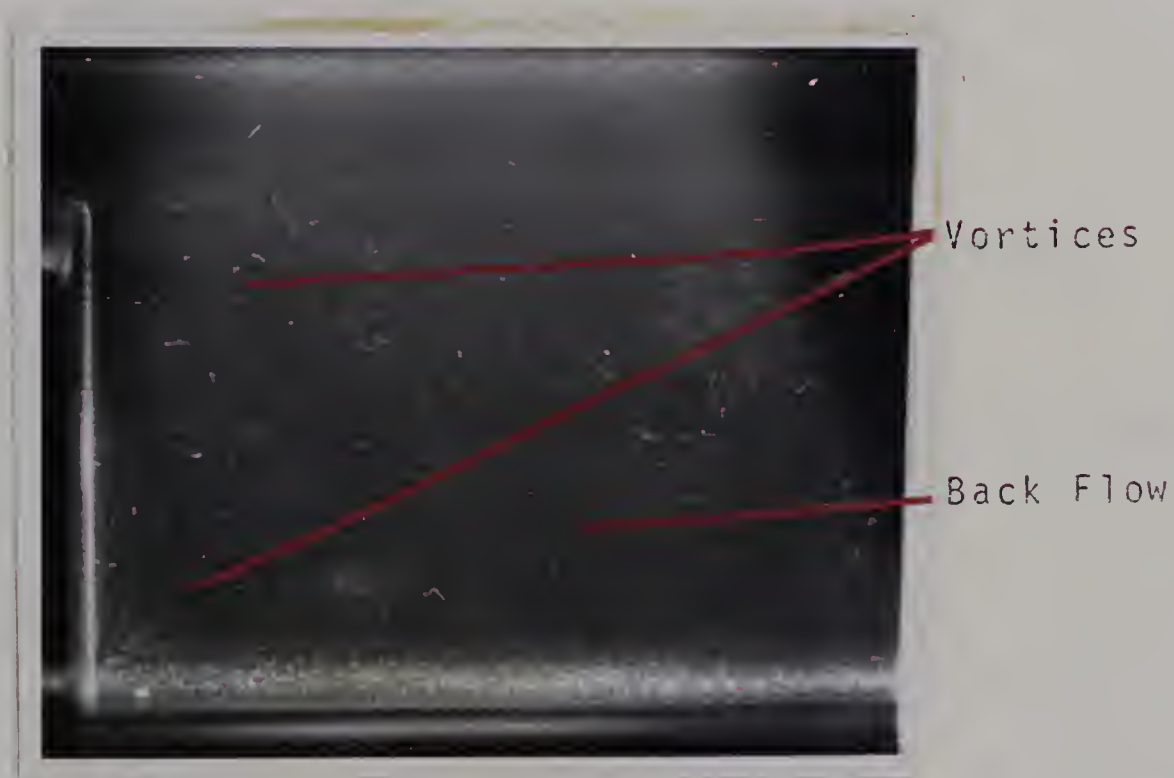
REAR OF CAPSULE - TOP VIEW FIGURE 25





$$V_{av} = .238 \text{ ft./sec.}$$

$$k = .675$$



$$V_{av} = .232 \text{ ft./sec.}$$

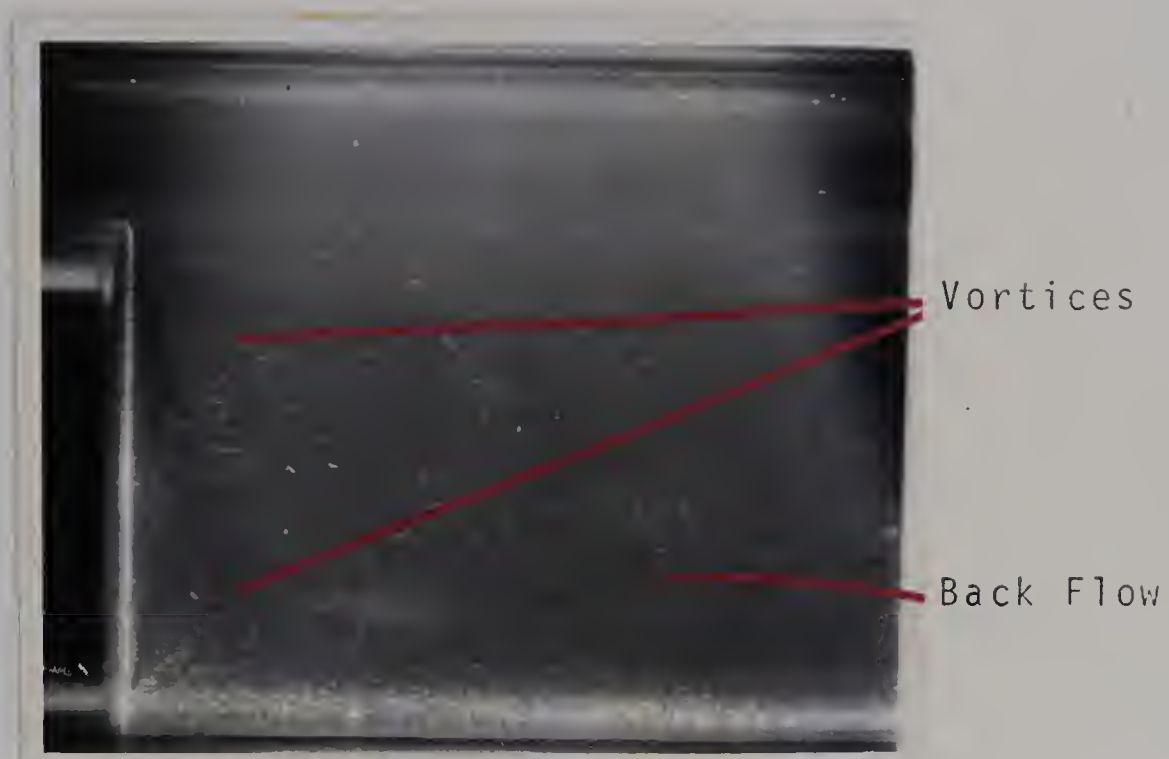
$$k = .765$$

WAKE AT NOSE OF CAPSULE SIDE VIEW

FIGURE 26A

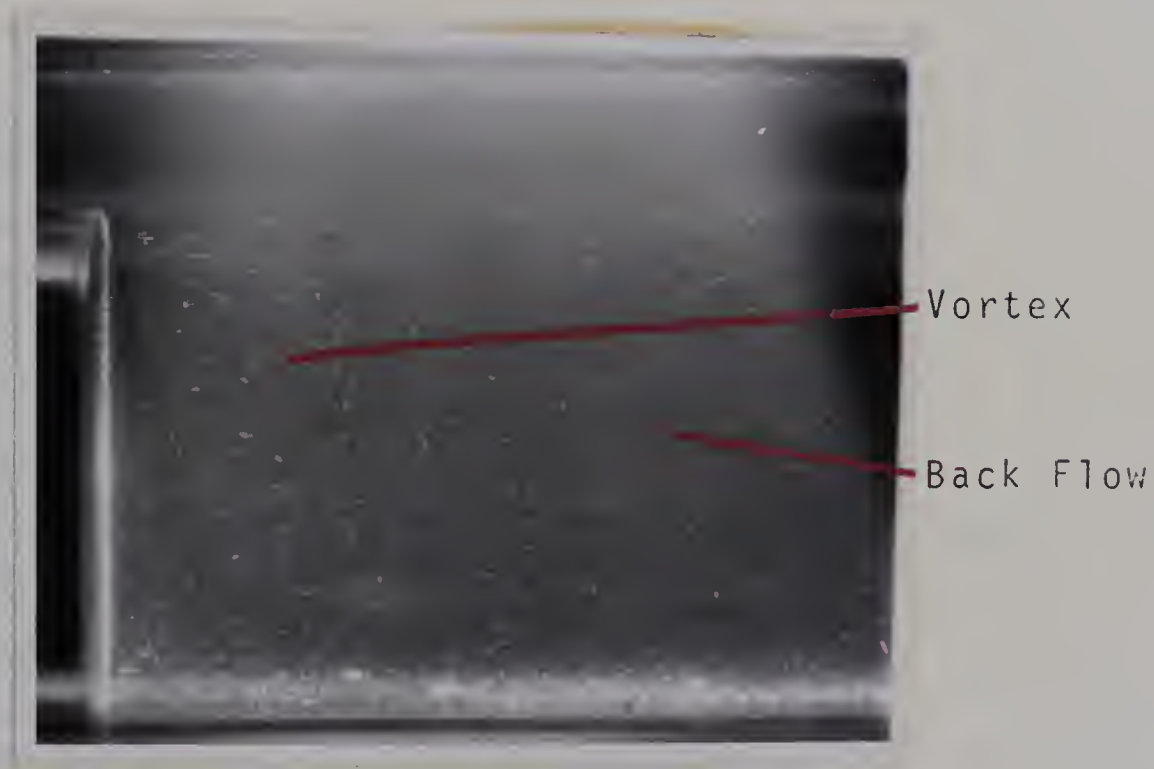






$$V_{av} = .232 \text{ ft./sec.}$$

$$k = .765$$



$$V_{av} = .137 \text{ ft./sec.}$$

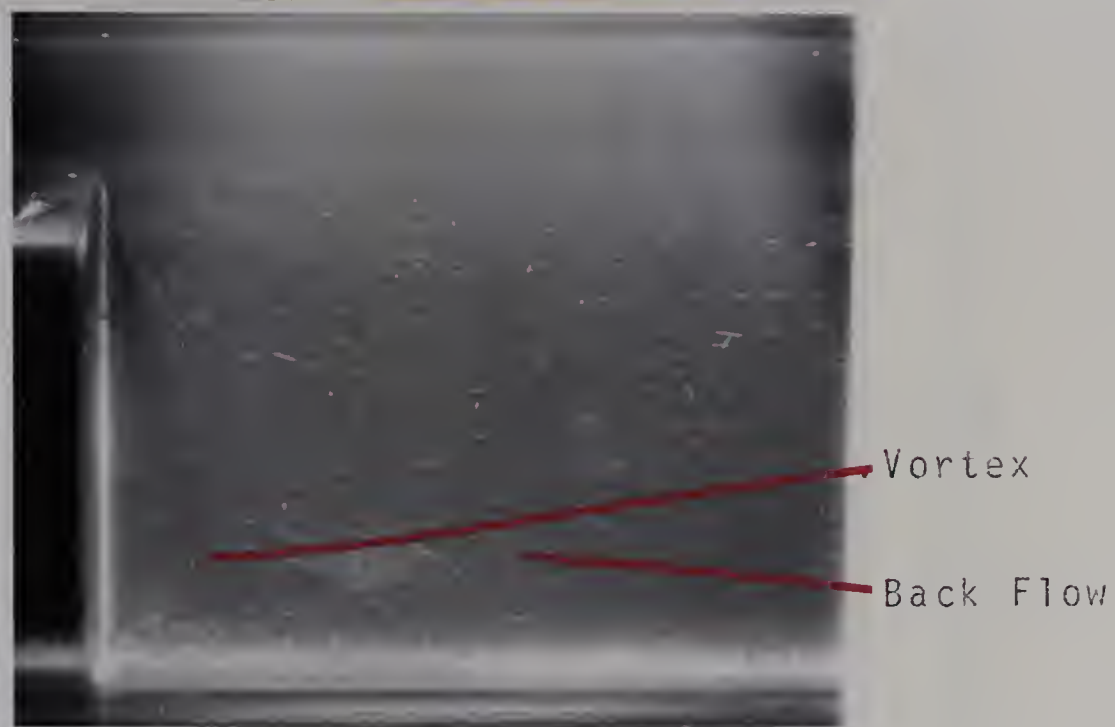
$$k = .765$$

WAKE AT NOSE OF CAPSULE SIDE VIEW

FIGURE 26B







$$V_{av} = .058 \text{ ft./sec.}$$

$$k = .768$$



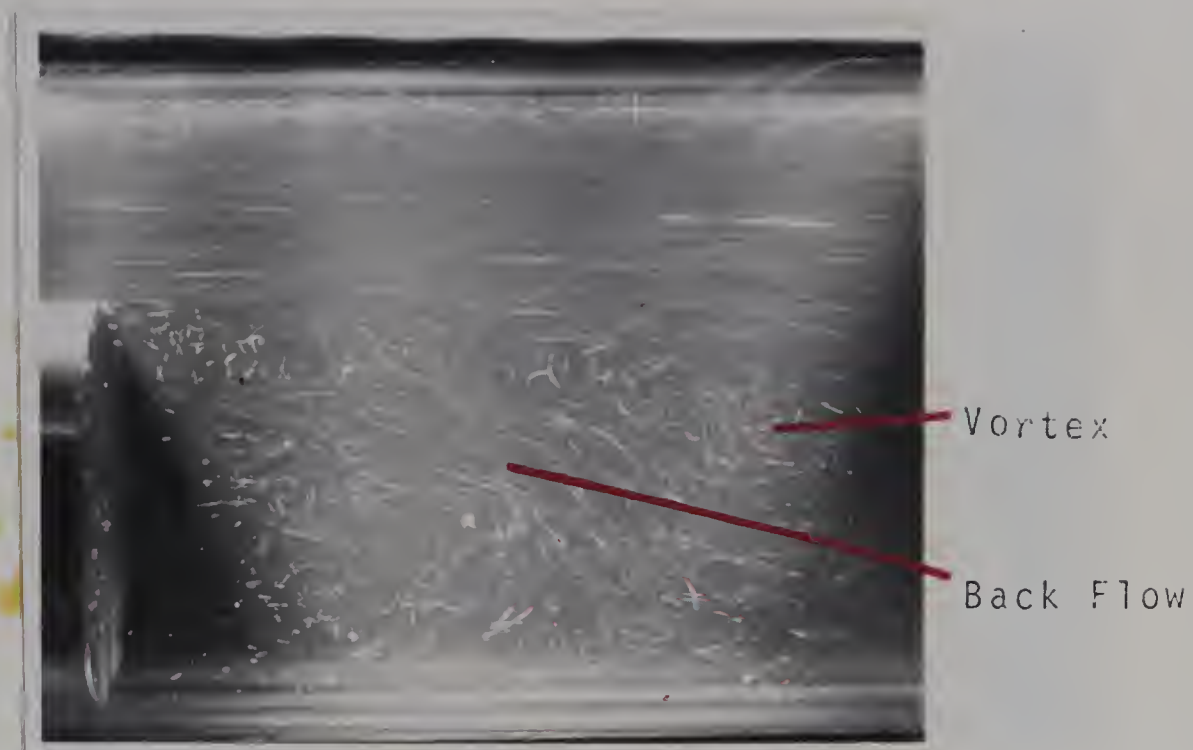
$$V_{av} = 1.732 \text{ ft./sec.}$$

$$k = .765$$

WAKE AT NOSE OF CAPSULE SIDE VIEW

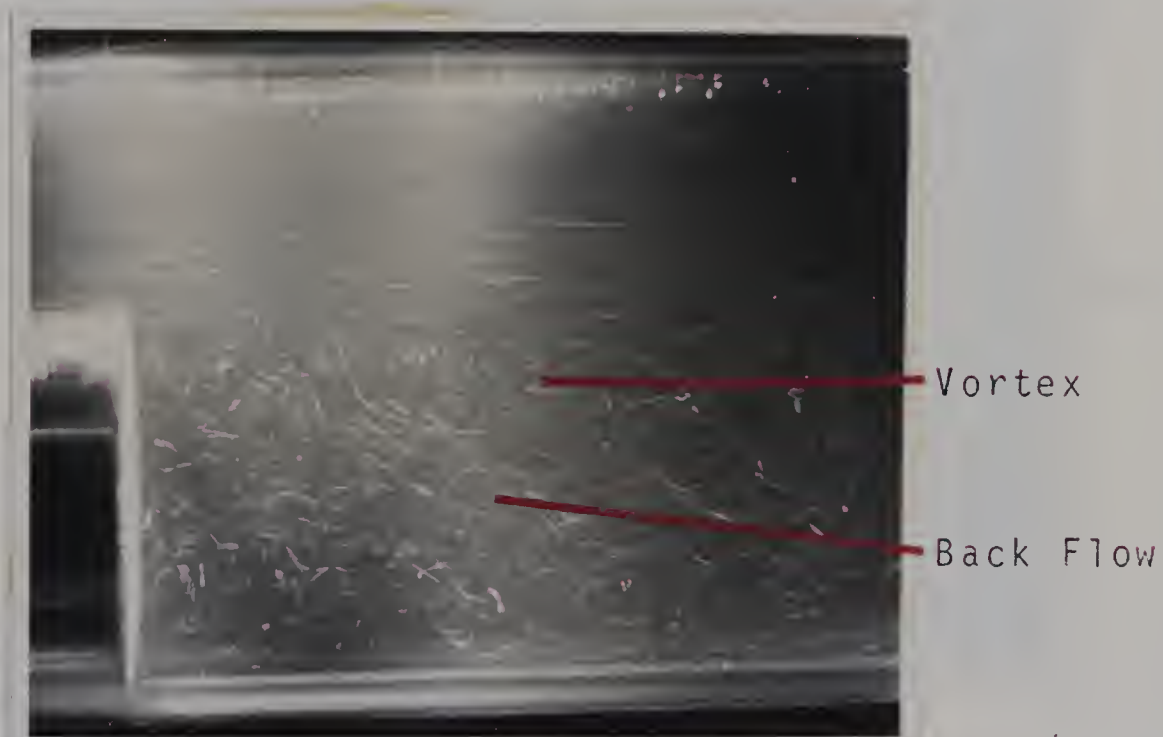
FIGURE 26C





$$V_{av} = 1.265 \text{ ft./sec.}$$

$$k = .675$$



$$V_{av} = 1.645 \text{ ft./sec.}$$

$$k = .625$$

WAKE AT NOSE OF CAPSULE SIDE VIEW

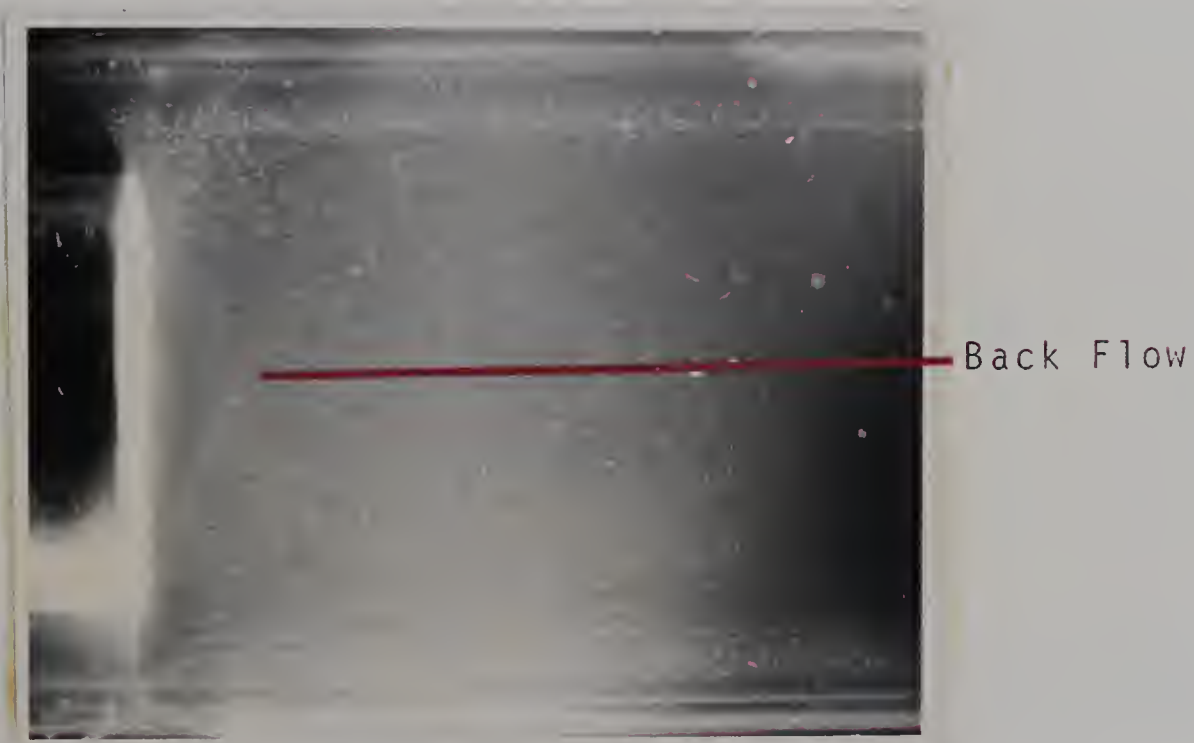
FIGURE 26D





$$V_{av} = .245 \text{ ft./sec.}$$

$$k = .625$$



$$V_{av} = .264 \text{ ft./sec.}$$

$$k = .718$$

WAKE AT NOSE OF CAPSULE TOP VIEW

FIGURE 27A







Back Flow

$$V_{av} = .884 \text{ ft./sec.}$$

$$k = .866$$



Back Flow

$$V_{av} = .921 \text{ ft./sec.}$$

$$k = .765$$

WAKE AT NOSE OF CAPSULE TOP VIEW

FIGURE 27B

1

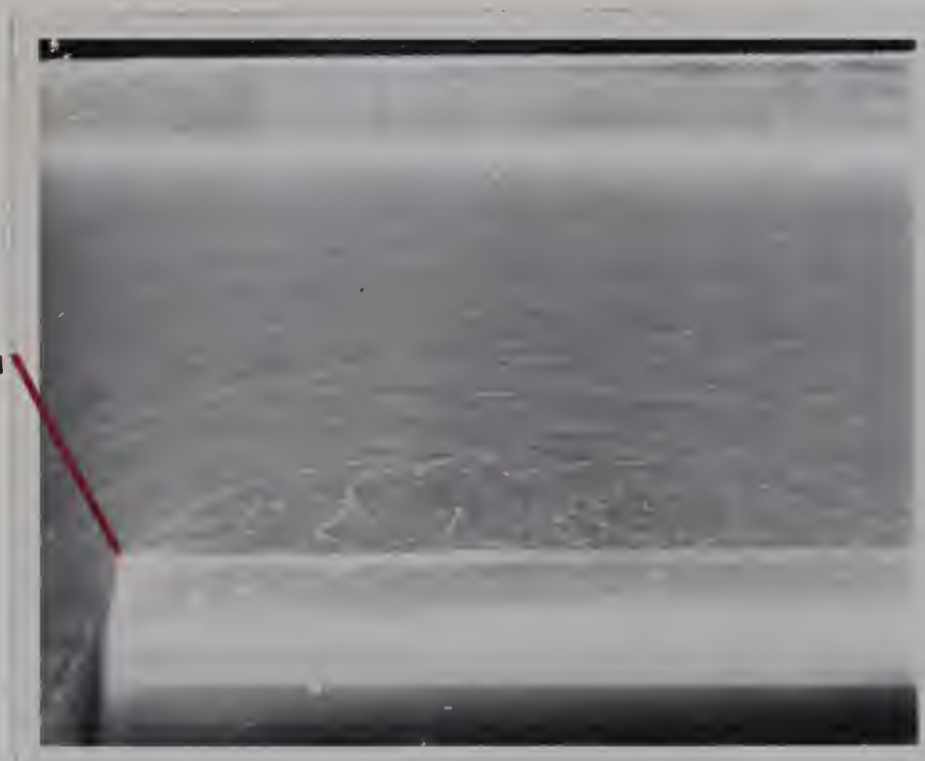
Separation



$$V_{av} = 1.470 \text{ ft./sec.}$$

$$k = .675$$

Separation



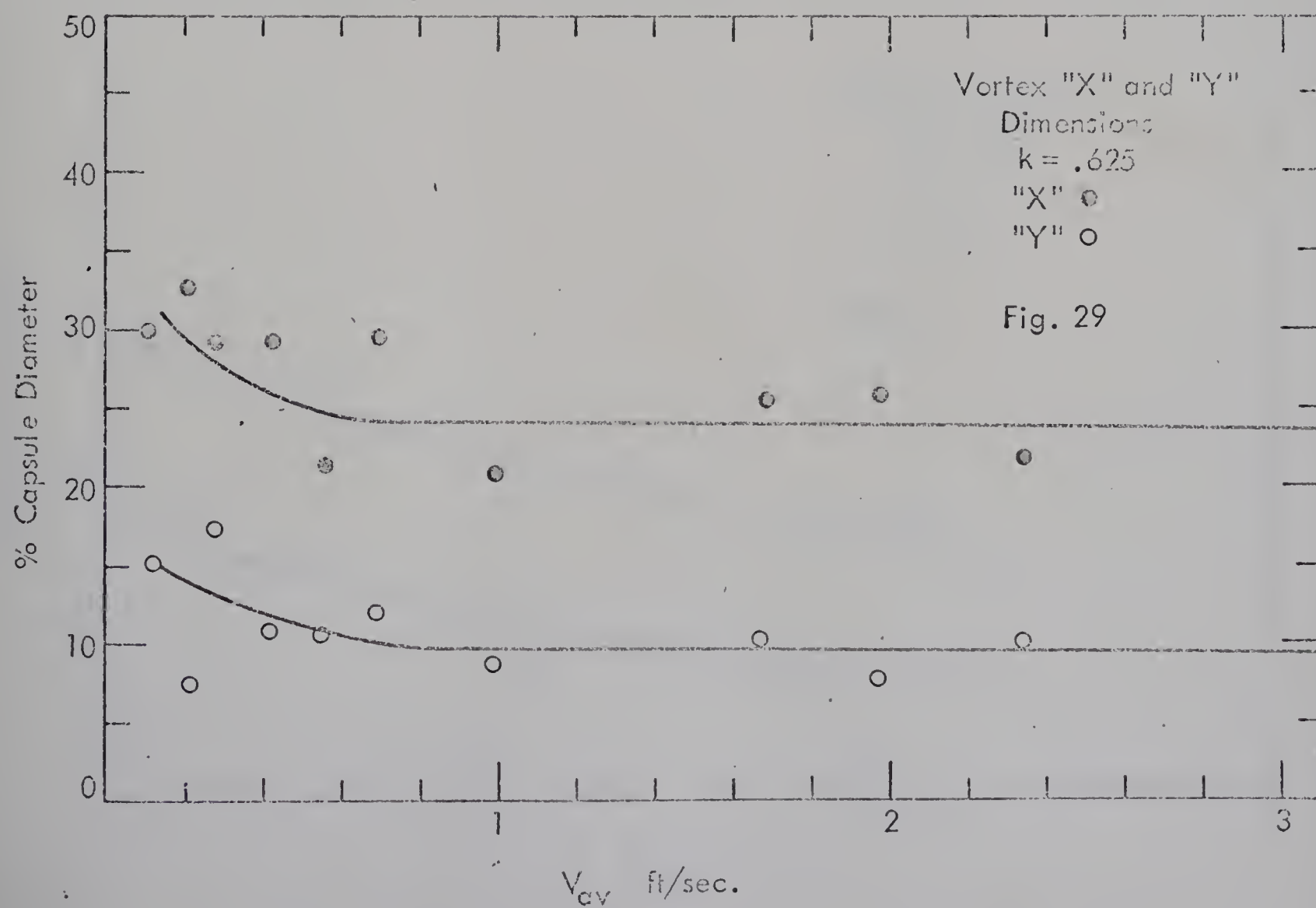
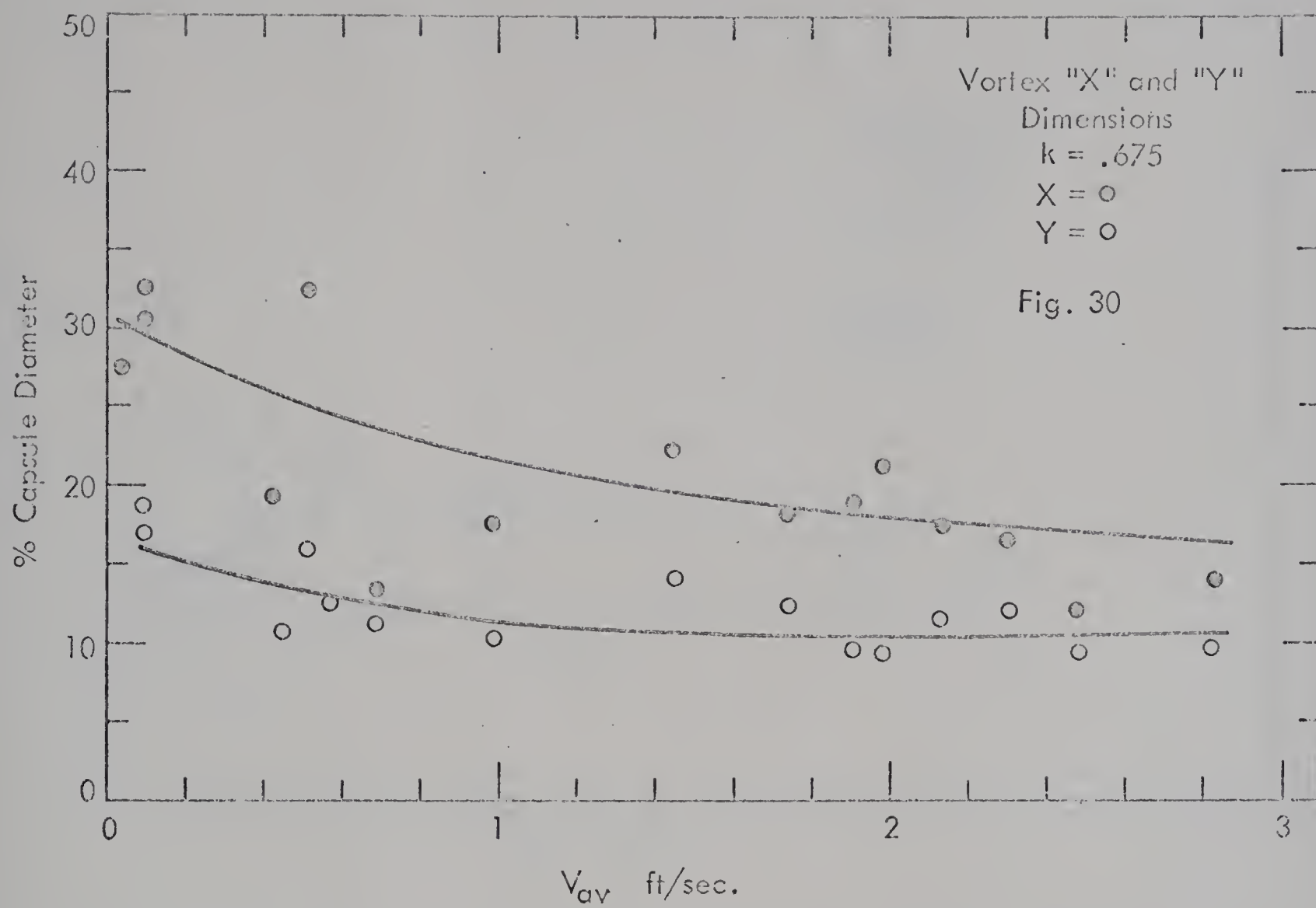
$$V_{av} = 2.480 \text{ ft./sec.}$$

$$k = .718$$

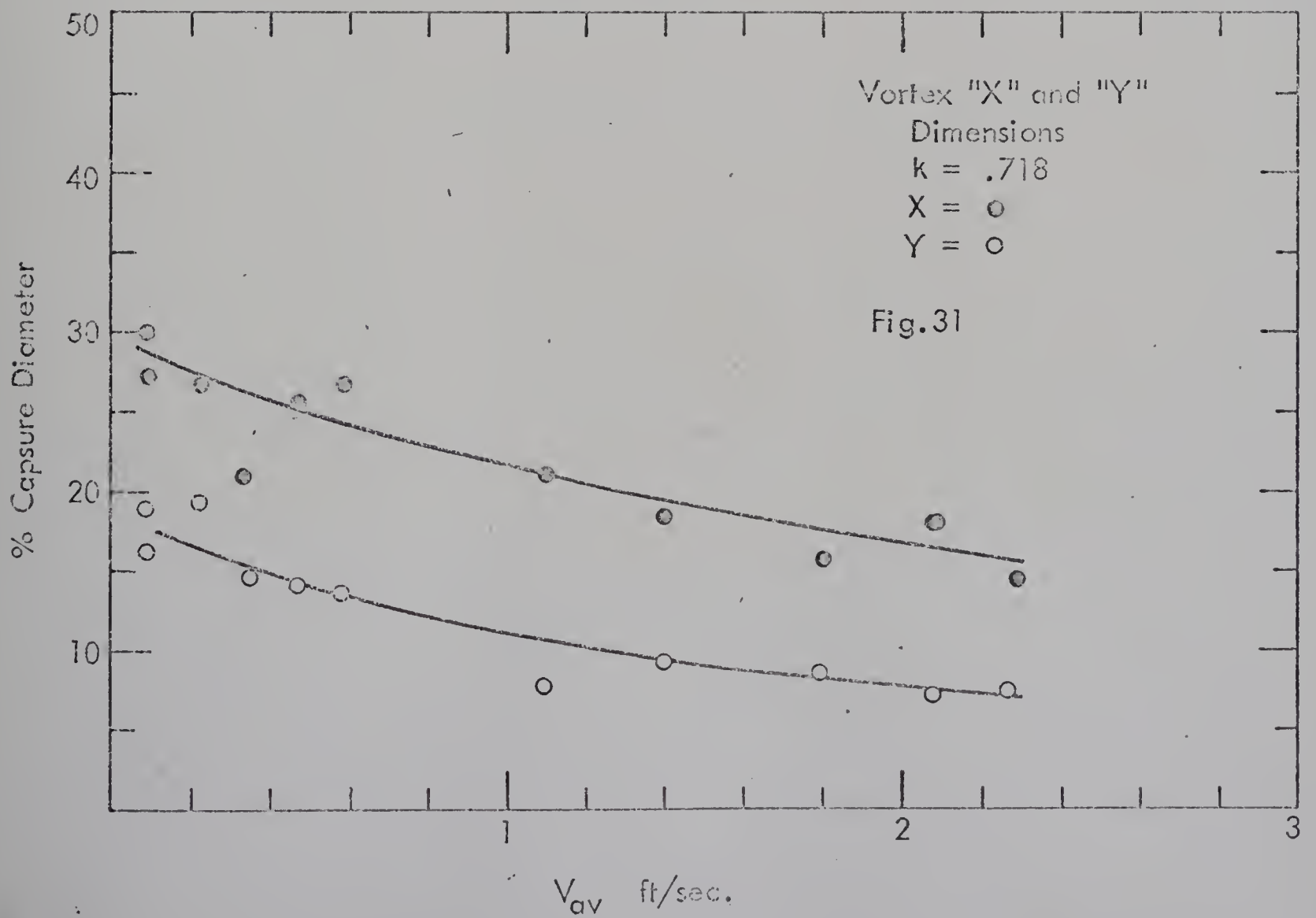
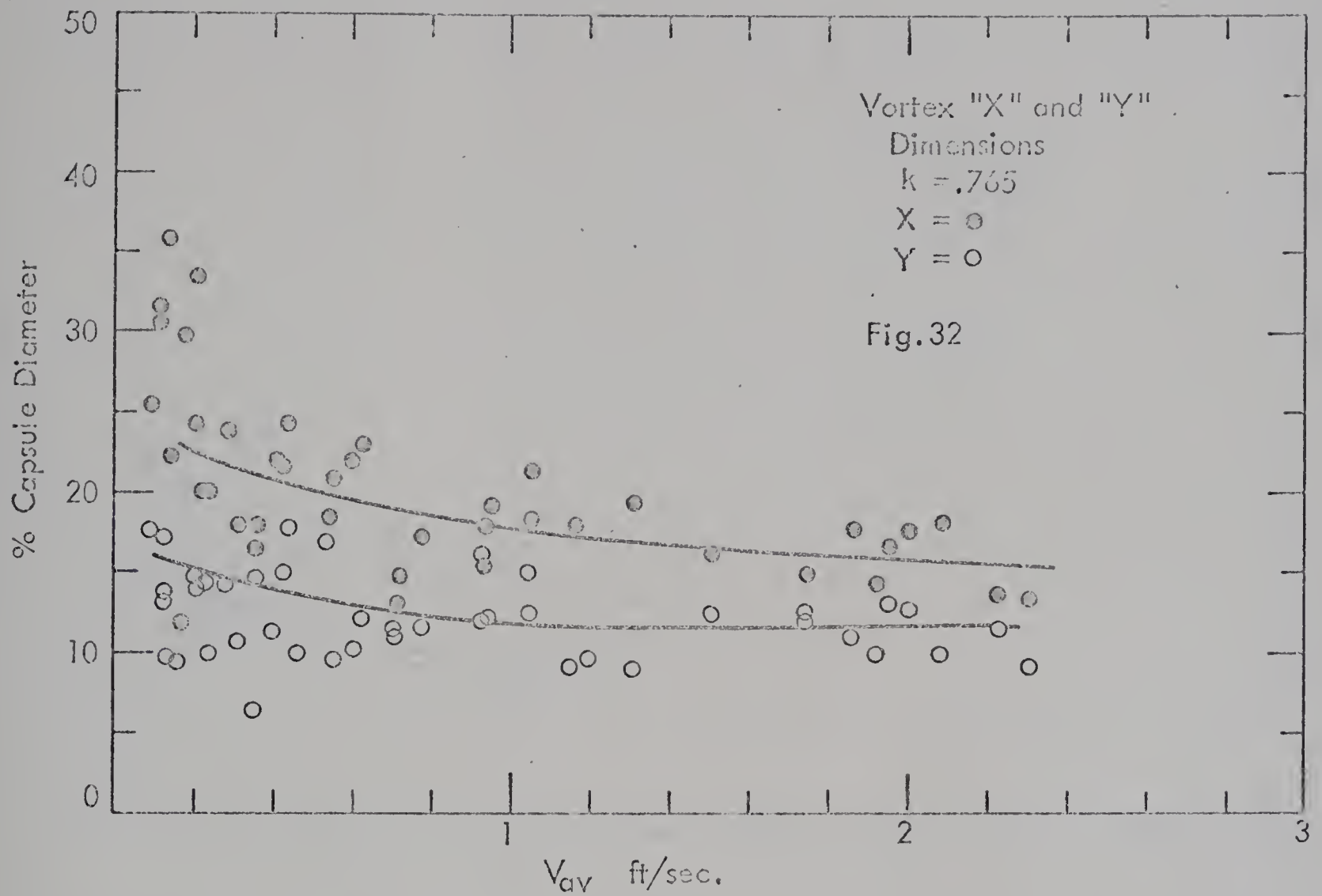
SEPARATION AT CAPSULE TOP REAR EDGE

FIGURE 28



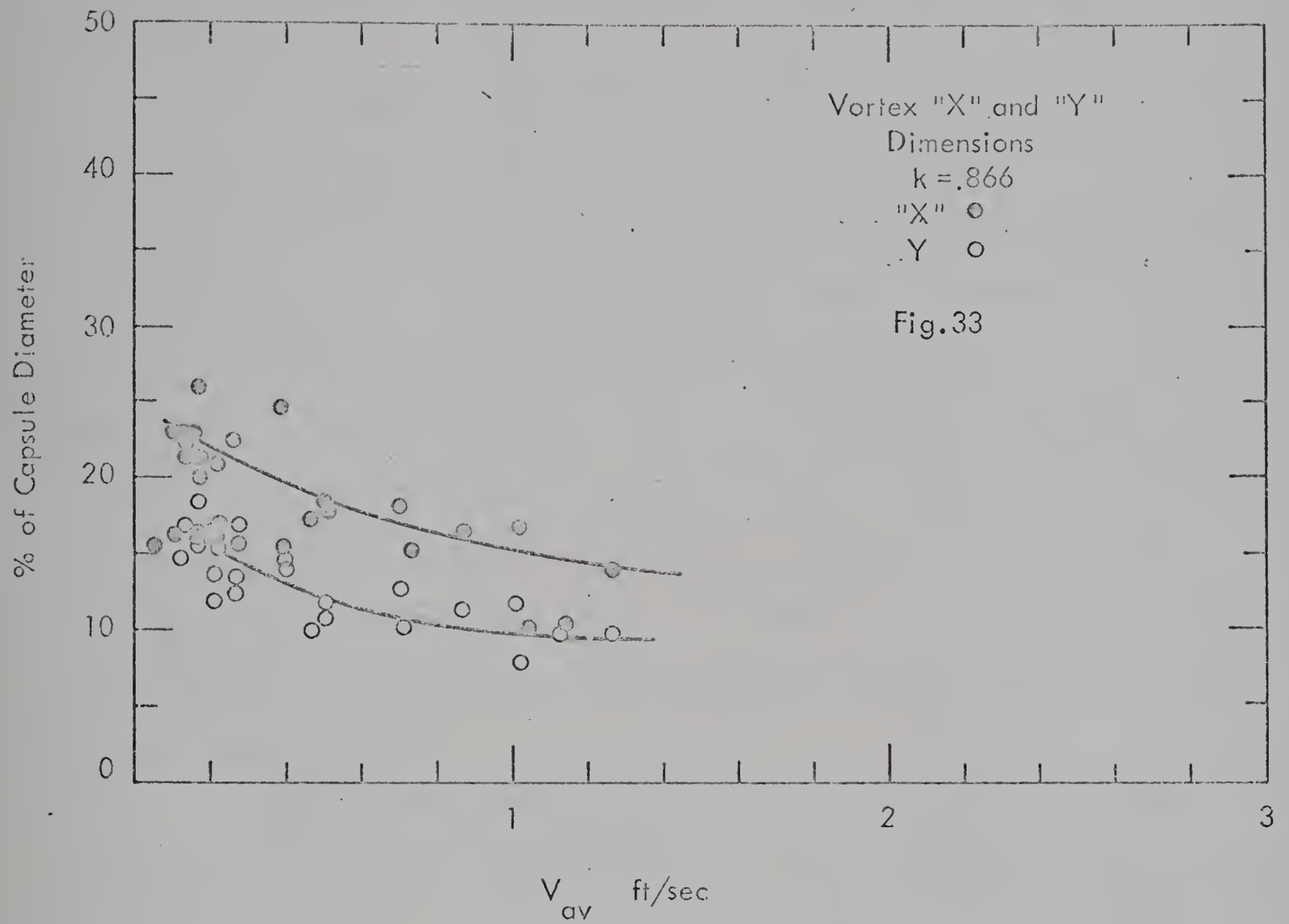














with decreasing dimensions, and disappears at the edge of the capsule.  
(See fig. 34)

Regarding point (2), the stagnation point was also plotted as a fraction of the capsule diameter. As would be expected the stagnation point rises higher on the capsule tail face, as the dimension of the vortex increases. The position of this stagnation point relative to the capsule diameter is plotted against  $V_{av}$  in Fig. 35. It can be seen from the figure that there is not much difference in the stagnation values for the different diameter ratios: The value at higher velocities was about .40 with a slow rise to a value of about .60 at low velocities in the laminar range. The stagnation point in the horizontal plane was on the capsule centerline and showed no tendency to be displaced from this point.

The third variable studied, the separation of the flow lines at the rear edge of the capsule, was plotted as a percentage of  $d_p - d_c$  against  $V_{av}$  in Fig. 36. The amount of separation is shown to be less for the .625 and .675 diameter ratios, and reaching a maximum value of approximately 33% for the .718 .765 and .866 diameter ratios. Also, in general the separation is less for the lower velocities, but does tend toward a constant value for increasing velocities.

At the nose of the capsule, there were no specific repeatable patterns appearing similar to the vortex at the capsule tail. In the side and top views, there were vortices being continually formed by a high velocity fluid stream flowing through the annulus. As this high velocity stream comes through the annulus it immediately puts into motion the fluid which takes the place of the capsule wall. To maintain continuity conditions a reverse flow is then set up along the central lower portions of the pipe in front of the capsule, thus starting a general circulation



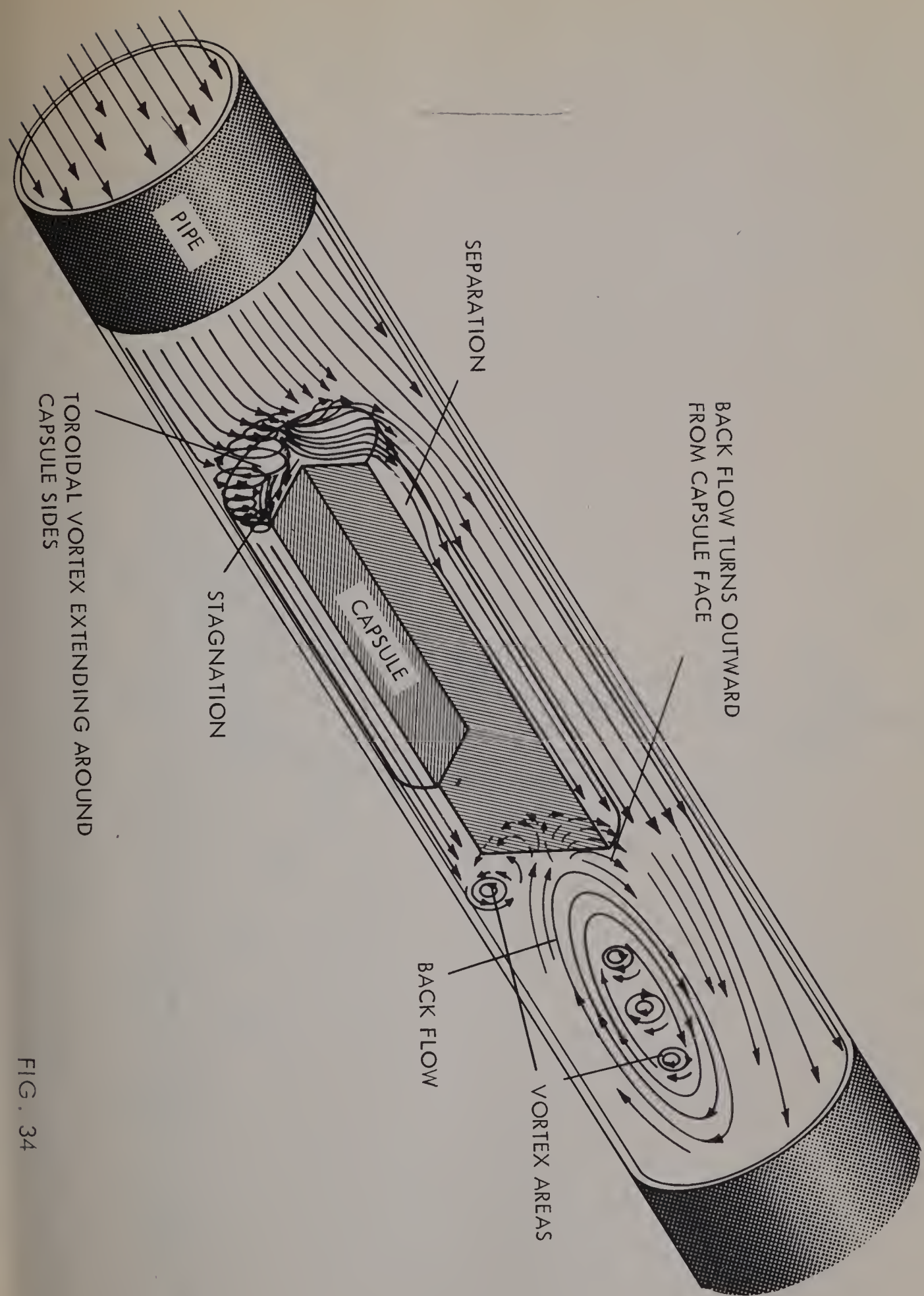
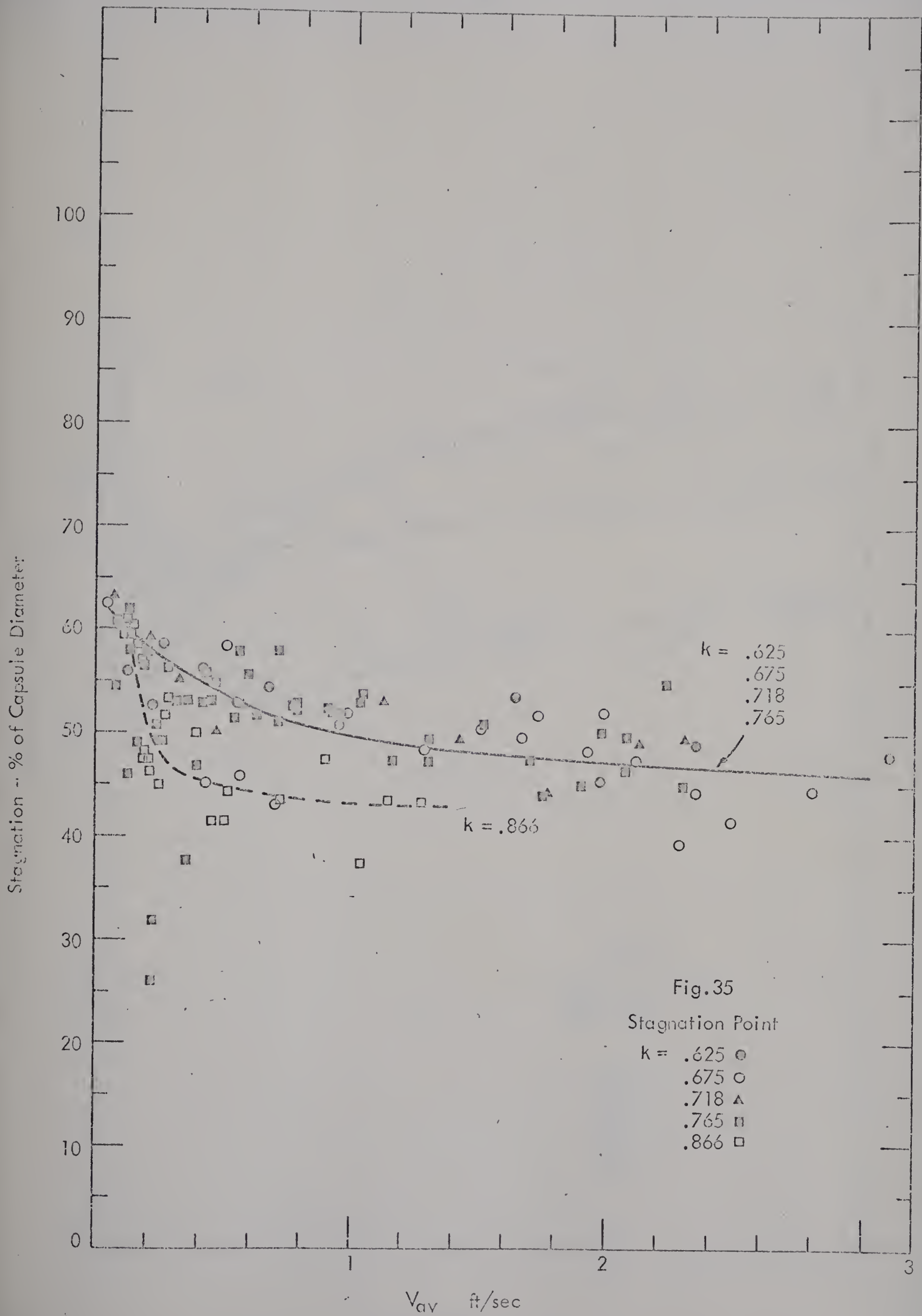


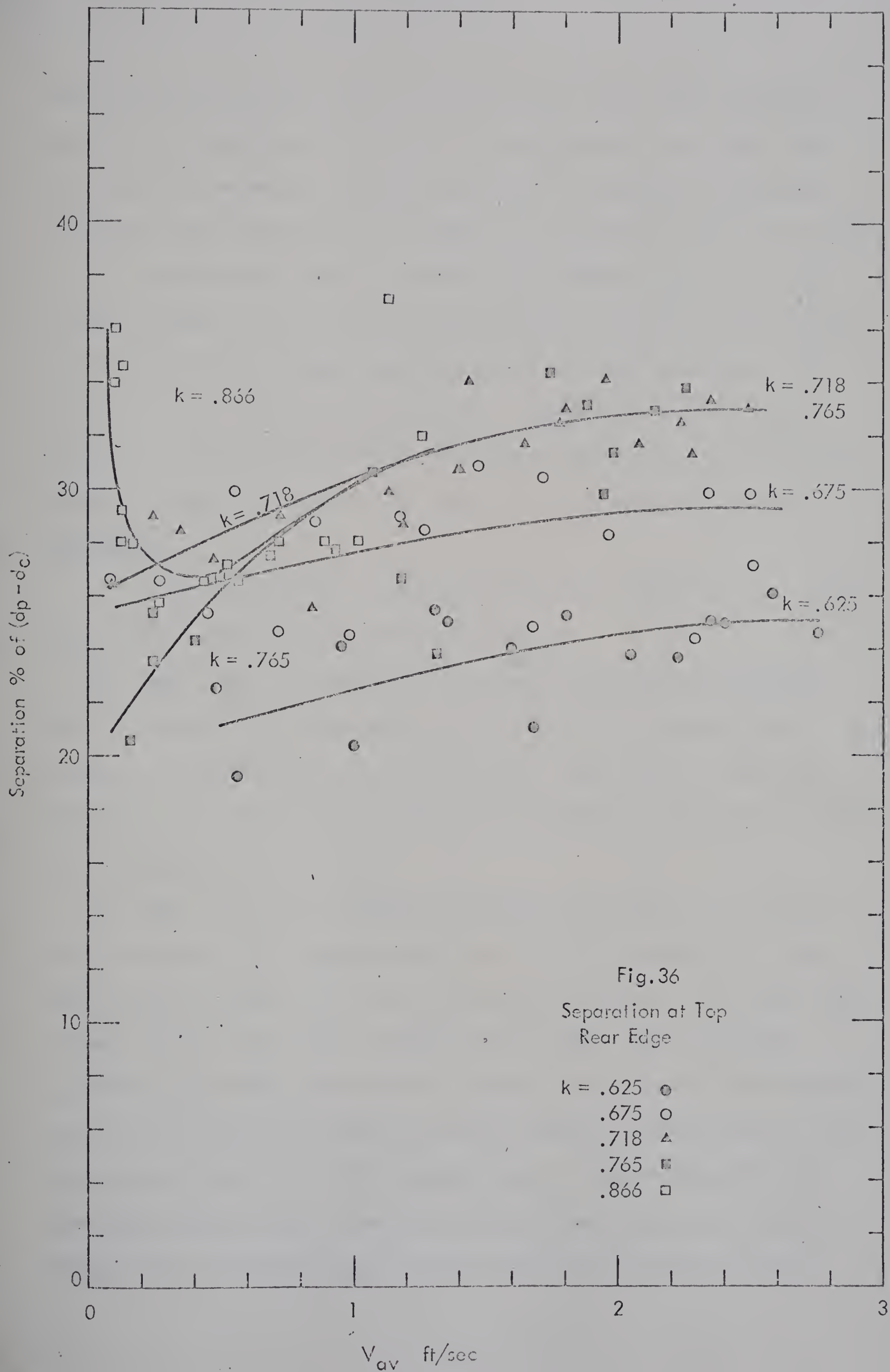
FIG. 34













which continually gives birth to new vortices. This back flow and the vortices were particularly evident in some photographs (see Fig. 26B). For three set velocities, pictures were taken at successive increments downstream from the capsule. The distance downstream at which the effect of the capsule could still be observed, for different velocities and a capsule diameter ratio of .866 is shown in Fig. 37. It is seen that the wake effect extends further downstream for the lower velocities. This seems contrary to what one would expect. However the overall higher level of turbulence at the higher velocities must eliminate the specific effects of the capsule wake at a faster rate than they are carried downstream.

The actual forces that the observed flow patterns would cause on a single capsule can be outlined as follows:

(a) Rear - The fluid stream is deflected up and over the capsule body producing a net upward shear on the wall of the capsule in the annulus. The upper rear face of the capsule experienced a similar upward force, but the lower rear face will experience a downward force due to the presence of the vortex.

(b) Nose - The fluid flowing out through the annulus will produce a downward force on the capsule walls, as it starts to return to a free pipe velocity profile. The back flow along the bottom of the pipe, rises to meet the annulus stream in front of the capsule nose. At lower velocities, this back flow tends to come all the way back to the capsule nose, and as it rises to meet the annulus stream, it will produce an upward shear on the face of the capsule nose. At higher velocities the back flow tends to rise to meet the annulus stream downstream from the capsule nose. In this case, a smaller circulation pattern is set up



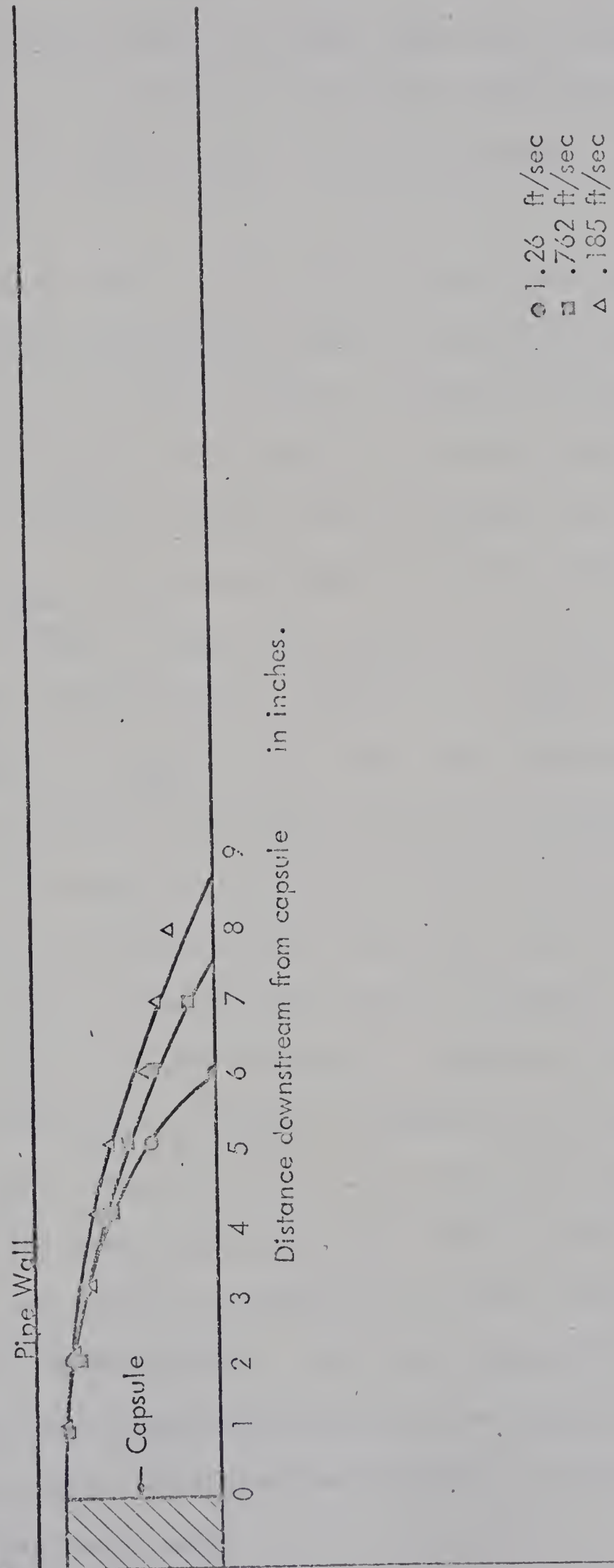


Fig. 37

Wake downstream of capsule nose





between the capsule nose and the rising back flow. This smaller circulation pattern may give rise to a simple vortex with a downward motion against the capsule nose, or two or more vortices with both upward and downward forces on the capsule nose. These various types of pattern are shown in Fig. 34.

Referring to Figs. 11 and 12 in the theory section, we can make some observations regarding the type of flow pattern which would occur in the case where a single capsule is moving in the pipeline. Let us assume that our capsule is travelling at a velocity ratio of one (i.e.  $V_c = V_{av}$ ). We will consider first the capsule rear. Along the line of  $u = .817 U_{max} = V_{av}$ , we know that the capsule velocity equals the point fluid velocity. Inside this  $V_{av}$  line, the fluid velocity will be larger than the capsule velocity, giving at any time an excess of fluid flow. Outside the  $V_{av}$  line, the point fluid velocities are less than the capsule velocity, thus giving at any time a deficiency of fluid flow. Obviously there must be a movement of fluid from the velocity excess areas to the velocity deficient areas, that is a movement of fluid from the core region down the capsule rear face, forming a vortex as in the static condition, and outward around the capsule into the annulus.

At the nose of the capsule, we again have the condition where the fluid velocity is deficient in the area outside the line of  $u = V_{av}$  and in excess in the area inside this line. Since in the velocity deficient areas, the capsule is overtaking the fluid, this fluid must move into areas of velocity excess. This then will produce a movement of fluid upward at the capsule nose from the lower region of the pipe in front of the capsule. This again would produce a pattern similar to what we have in the static case.



Pressure drop readings were taken during the course of the experimental runs. Since there were no basic changes in the flow pattern, it would not be expected that any basic change would occur in the pressure drops and it should be possible to correlate the pressure drops obtained for the different diameter ratios with liquid velocity,  $V_{av}$ .

First consider the factors involved in the pressure drop in turbulent flow. It is expected that it will vary according to the square of the liquid velocity in the annulus, which produces a shear drag. The liquid velocity in the annulus will be a function of the relative annulus area (i.e.  $1-k^2$ ). For a single capsule, there will also be a form drag which will vary according to the relative area of the capsule ends (i.e.  $k^2$ ). Taking both these factors,

$$(\Delta P)_{c-f} \sim \left( \frac{k^2}{1-k^2} \right)^2$$

where,  $(\Delta P)_{c-f}$  = increase in pressure drop with capsule  
above pressure drop for liquid alone

Then for a given  $V_{av}$ ,

$$(\Delta P)_{c-f} = \text{constant} \left( \frac{k^2}{1-k^2} \right)^2$$

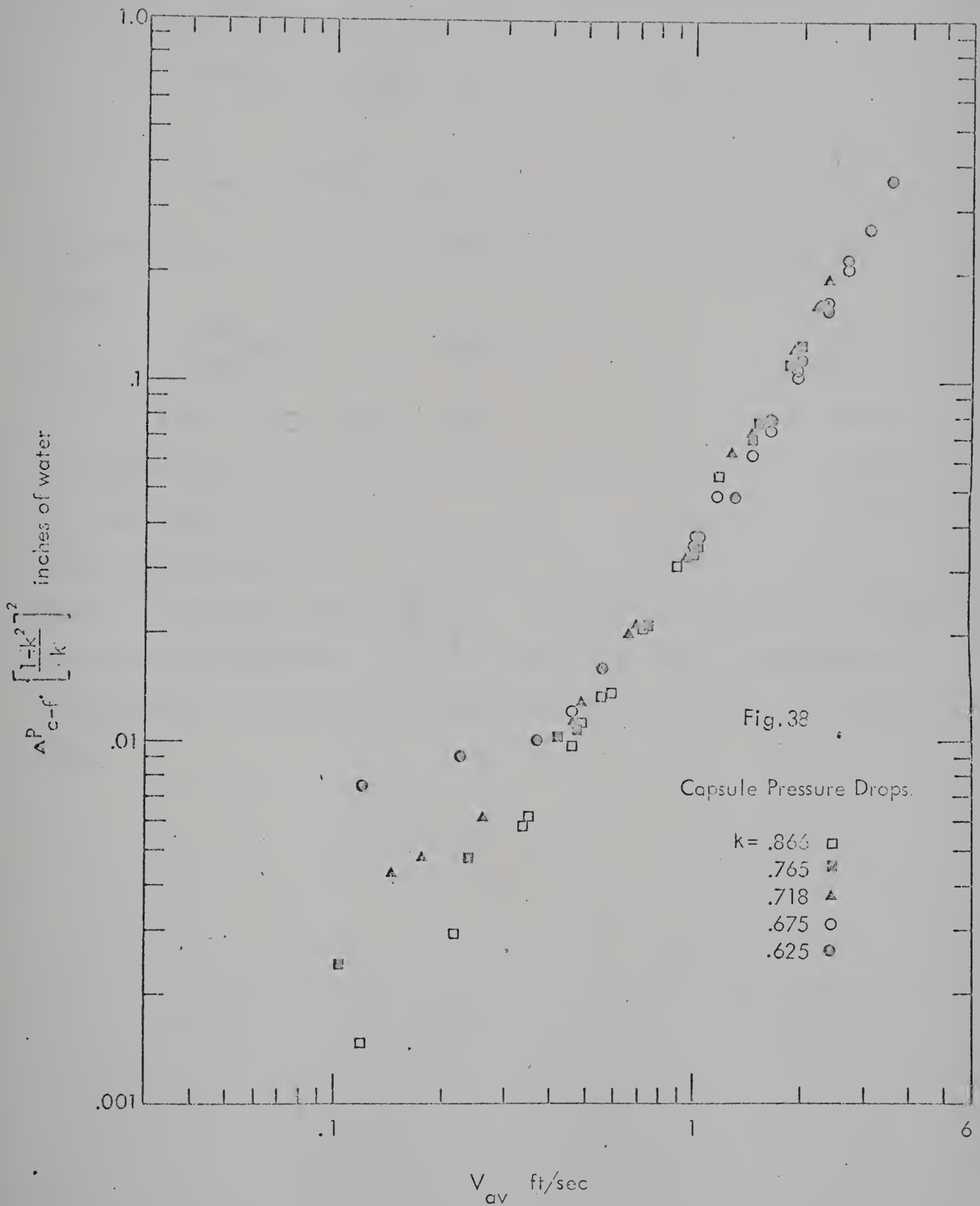
$$\text{or constant} = (\Delta P)_{c-f} \left( \frac{1-k^2}{k} \right)^2$$

Plotting this against  $V_{av}$  on Fig. 38 we get a linear relation on a log-log plot

$$.355 V_{av}^{1.70} = (\Delta P)_{c-f} \left( \frac{1-k^2}{k} \right)^2 \quad (1)$$

This relationship shows good agreement with the data except for the low









values of  $V_{av}$ , where  $(\Delta P)_{c-f}$  shows a divergence. In this range, flow in the capsule pipe annulus may be laminar, and as such  $(\Delta P)_{c-f}$  would be expected to vary directly with velocity

$$(\Delta P)_{c-f} L \sim \frac{k^2}{1-k^2} V_{av}$$

or

$$V_{av} \sim \frac{1-k^2}{k^2} \frac{\Delta P}{L} \quad (2)$$

Comparing this with the turbulent condition in equation (1) the ratio becomes

$$\frac{(\Delta P)_{c-f} L}{(\Delta P)_{c-f} t} = \frac{1-k^2}{k^2} V_{av}^{1-n} \quad (3)$$

Since all the data was plotted on a turbulent basis, it would be expected from 3 that the laminar range data will diverge. At a given  $V_{av}$ , the highest values of  $(\Delta P)_{c-f} L$  will be for the lowest values of  $k$ , which agrees with the plot in Fig. 38. The data could have been presented as a pressure gradient  $\left(\frac{\Delta P}{L}\right)_{c-f}$  by dividing by the capsule length. However since the pressure drop due to the capsule ends is independent of capsule length, it was held to be more logical to present the total pressure drop.



VIII ANALYSIS AND DISCUSSION OF EXPERIMENTAL RESULTS Clearance

Regarding the clearance, it became apparent during the course of the data acquisition that two types of clearance existed. For the lower velocities, the clearance, if any, that existed was only microscopic in scale, and could only be detected by the microscope. A second range of velocities occurred which produced a clearly visible lift-off of the capsule nose, which is referred to as a macroscopic clearance. This point of the inception of macroscopic clearance represented the most well defined and repeatable feature of the experimental work.

The method of analysis for the photographs will be described for the two types of series taken.

1. Full view of capsule - the capsule was photographed from the side and top simultaneously. From these photographs direct measurements could be taken of the capsule clearance, and apparent pipe diameters from the photographs. (Ref. Fig. 41)
2. Microscopic pictures - In this series of pictures, three pictures were taken simultaneously: one full capsule view from the top and two views of the capsule - pipe wall clearance, taken from the opposite sides of the capsule (Ref. Fig. 14, 42)

Measurements made on the microscopic photographs were compared to the calibration curves to get an actual measurement of clearance. These measurements were then used in the same way as those taken in (1) to compute the capsule nose and tail clearances and angles.

Having made these measurements, the data, along with pressure and velocity information, was punched onto computer tape for reduction



to desired calculated quantities and plotted. The variables calculated were:

- (1) Nose and Tail Clearance (in terms of fraction of pipe diameter).
- (2) Capsule Angle (positive for nose up)
- (3) Fluid Velocity
- (4) Capsule Velocity
- (5) Fluid Pressure Drop
- (6) Capsule Pressure Drop

In order to isolate any effects from imperfect balancing the capsules had been run twice at each velocity setting with opposite ends of the capsule as the nose. These alternating runs were identified in the data and kept separate for the basic plots prepared.

The basic plot prepared from this data consisted of nose and tail clearance, capsule angles and fluid velocity,  $V_{av}$ , all plotted against  $V_c$  as an abscissa. A separate plot of this nature was prepared for each data run. A typical plot for one full view run and one microscope run are shown in Fig. 39 and 40. Data for all the runs are tabulated in Appendix A-5.

Before trying to interpret this data, the basic hydraulic problem as stated by Ellis (2) is restated here for convenience.

$$V_c \text{ or } \left( \frac{\Delta P}{L} \right)_c = (V_{av}, \mu, \sigma, \rho, g_c, L_c, d_c, d_p, \text{end shape}, j, \epsilon_c \epsilon_p) \quad (1)$$

The gravitational constant  $g_c$  has been added by the author.

Similarly, clearance,  $C$ , is a function of the same independent variables.

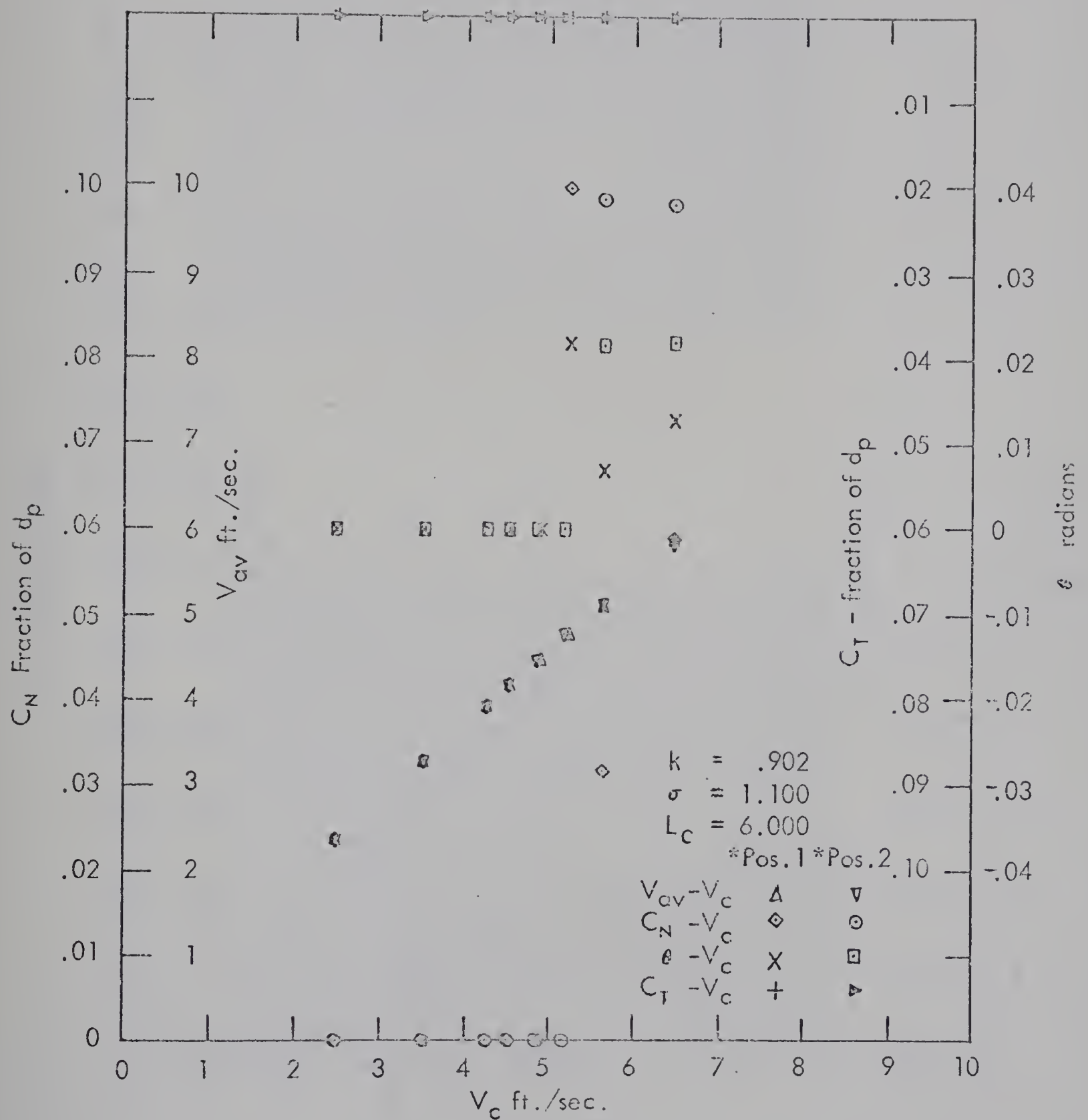
One possible dimensionless grouping of the above independent variables is:

$$\frac{C}{d_p} = \left( \frac{V_{av} d_p \rho}{\mu}, \frac{V_{av}^2}{g_c d_p}, \frac{\sigma - \rho}{\rho}, \frac{L_c}{d_p}, \frac{d_c}{d_p}, \text{end shape}, \right)$$





\*Pos. 1 and Pos. 2 symbols separate data for reverse capsule positions in the pipeline.



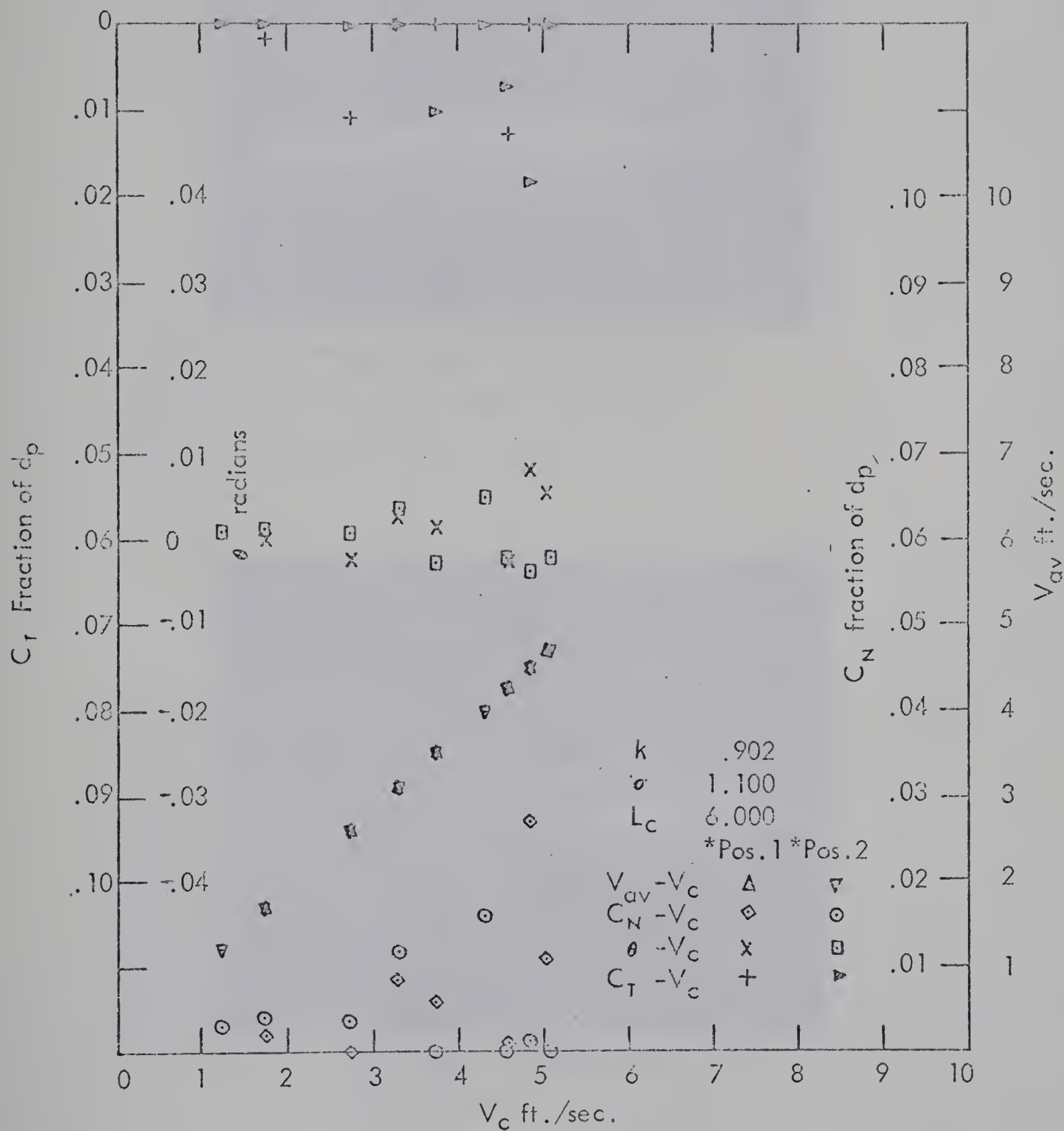
Basic Data Plot  
Full View Run

Fig. 39



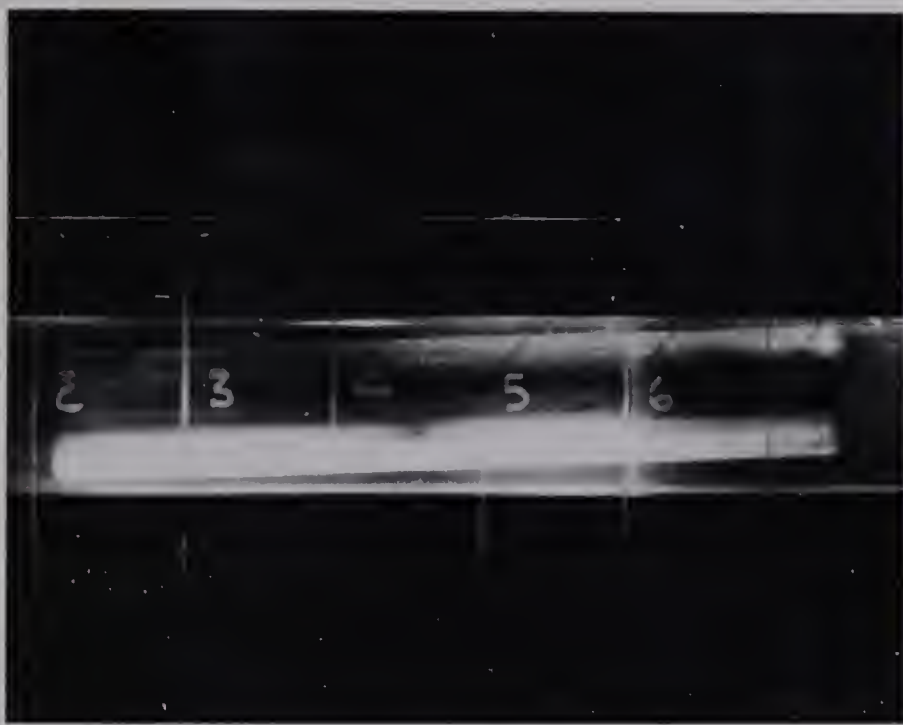


\*Pos. 1 and Pos. 2 symbols separate data for reverse capsule positions in the pipeline.

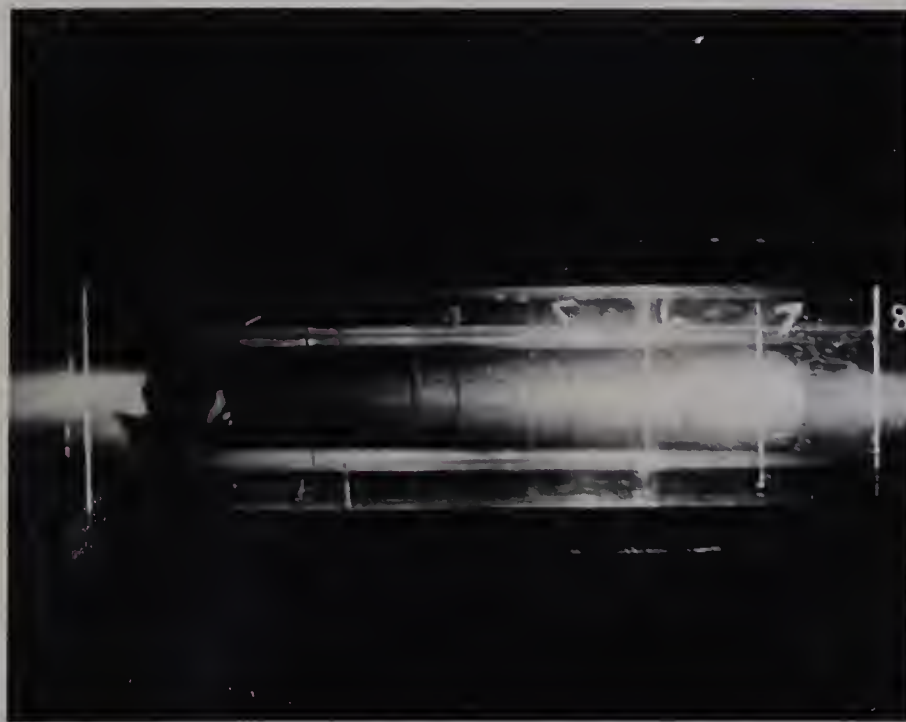


Basic Data Plot  
Microscope Run  
Fig. 40





SIDE VIEW - CAMERA NO. 2  
 $k = 0.80$        $L = 6''$



TOP VIEW - CAMERA NO. 3  
 $k = 0.80$        $L_c = 6''$

TYPICAL FULL VIEW PHOTOGRAPHS - FIGURE 41





Capsule

Clearance

Pipe Wall

Camera No. 1

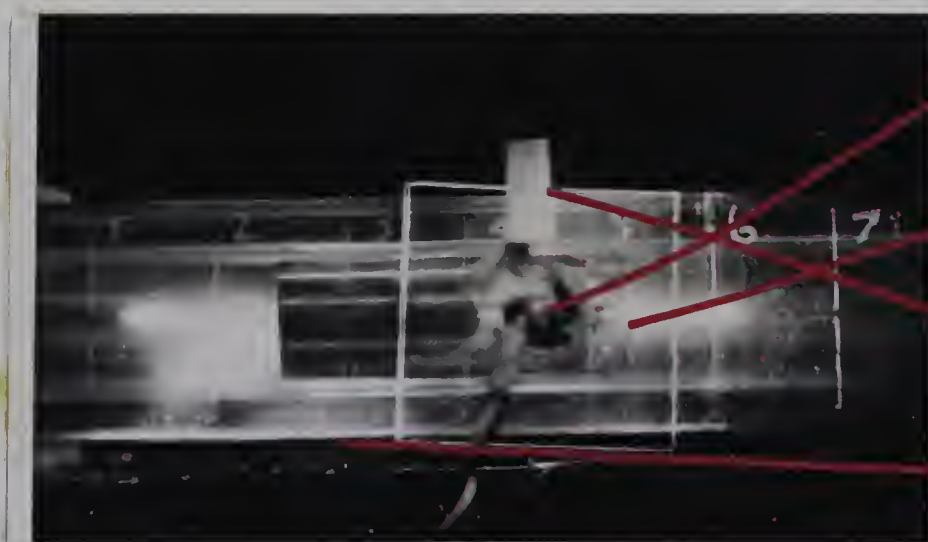


Capsule

Clearance

Pipe Wall

Camera No. 2

Capsule Firing  
Photocell

Capsule

Microscope No. 1  
PositionMicroscope No. 2  
Position

Camera No. 3





$$j, \frac{\epsilon_c}{d_p}, \frac{\epsilon_v}{d_p} \quad (2)$$

In the experimental runs, end shape,  $j, \frac{\epsilon_c}{d_p}, \frac{\epsilon_v}{d_p}$  were all held constant.

This leaves a six dimensional problem. For any given experimental run,

the groups  $\frac{\sigma-\rho}{\rho}, \frac{L_c}{d_p}, \frac{d_c}{d_p}$  were also held constant, leaving  $\frac{C}{d_p}$  as a function of  $\frac{V_{av} d_p \rho}{\mu}$  and  $\frac{V_{av}^2}{g_c d_p}$ . Since  $d_p, \mu, \rho, g_c$  were all constant,

this in effect means that  $\frac{C}{d_p}$  is a function of  $V_{av}$ . The analytical

solution for laminar flow presented in Part 9 (15) and referred to earlier

in the Literature Review chapter related  $\frac{C}{d_p}$  to VR (i.e.  $\frac{V_c}{V_{av}}$ ).

Similarly the solution proposed for turbulent flow in the theory chapter also relates  $C$  to  $V_c$  as well as  $V_{av}$ .

The clearance is measured at the bottom of the pipe, where the local liquid velocity is low compared to the average liquid velocity,  $V_{av}$ , in the overall pipe. This suggests that  $V_c$  would be the more important velocity, although it must be remembered that  $V_c$  itself is a function of  $V_{av}$ . In fact, as was evidenced on the Basic Data plots, the  $V_c$  versus  $V_{av}$  plot showed a linear relation in all cases such that  $V_c = -A + B V_{av}$ , where  $A$  is a measure of the threshold velocity of the capsule and  $B$  is the slope of the line. With the density ratios used in this study, the threshold velocities were low ( $< .50$  ft./sec.), so that  $V_c$  was nearly equal to  $B V_{av}$ , with  $B$  varying according to the diameter ratio,  $k$ . Thus, whether the clearance measurements were plotted against  $V_c$  or  $V_{av}$ , the type of relationship shown varies only as the change in the constant  $B$ . The clearance measurements presented in this study have been plotted against  $V_c$ . During the experiments, it was



observed that the point of inception of the macroscopic clearance for any given capsule was approximately proportional to  $(V_c)^2$  and this feature was in fact used as a guide for determining the velocity settings to be used for the microscopic and full view runs. The values of  $V_c$  and  $V_{av}$  at the point of macro lift-off are given in Table 4 below.

Table 4.

k	$L_c$	$\frac{\sigma - \rho}{\rho}$	$V_c$ at lift off ft./sec.	$V_{av}$ at lift off ft./sec.
0.701	3.006	1.010	1.80	1.65
		1.020	2.50	2.30
		1.050	3.80	3.37
		1.100	3.00	4.30
		1.147	6.00	5.30
0.701	6.007	1.010	2.30	2.04
		1.020	3.30	2.88
		1.050	5.60	4.82
		1.100	7.30	6.40
		1.155	8.50	7.45
0.802	3.010	1.011	1.40	1.33
		1.022	1.80	1.69
		1.050	2.60	2.42
		1.100	4.20	3.83
		1.149	5.60	5.10
0.802	6.010	1.010	1.80	1.65
		1.020	2.50	2.27
		1.050	4.60	4.02
		1.100	6.70	5.90
		1.150	8.00	7.18
0.902	3.003	1.010	0.70	0.68
		1.020	1.30	1.22
		1.050	2.30	2.14
		1.400	3.60	3.40
		1.150	4.50	4.17
0.902	6.000	1.010	1.20	1.12
		1.020	1.84	1.71
		1.050	2.90	2.68
		1.100	5.00	4.57
		1.151	6.00	5.62

Plotting values of  $V_c$  lift off as obtained from the basic data plots



vs.  $\frac{\sigma-\rho}{\rho}$  (Fig. 43A) the point of lift off was proportional to  $V^n$ , but  $n$  was not constant for the different diameter ratios. The actual values of  $n$  obtained were :

$L_c = 3$	$k = 0.70$	$n = 2.24$
$L_c = 6$	$k = 0.70$	$n = 2.10$
$L_c = 3$	$k = 0.80$	$n = 1.80$
$L_c = 6$	$k = 0.80$	$n = 1.78$
$L_c = 3$	$k = 0.90$	$n = 1.51$
$L_c = 6$	$k = 0.90$	$n = 1.58$

Similarly the macroscope lift-off point may be plotted against  $V_{av}$ , Fig 43B. The same type of relationship occurs as on the  $V_c$  plot, but the values of  $n$  are slightly different.

$L_c = 3$	$k = 0.70$	$n = 2.38$
$L_c = 6$	$k = 0.70$	$n = 2.02$
$L_c = 3$	$k = 0.80$	$n = 1.76$
$L_c = 6$	$k = 0.80$	$n = 1.84$
$L_c = 3$	$k = 0.90$	$n = 1.56$
$L_c = 6$	$k = 0.90$	$n = 1.65$

Turning now to the microscopic clearances, we do not have any definitive point such as the inception of the macroscopic clearance in the full view pictures. The clearance measured up to the point of macroscopic clearance remained relatively small ( $<.02$  pipe diameters) and then showed rapid increase as macroscopic clearance occurred. The clearances were calculated for both the capsule nose and tail and plotted separately against  $V_c$ . Generally, the clearances of both nose and tail showed an increase, as capsule velocity increased, although the scatter of the data was of the same magnitude as the quantities being

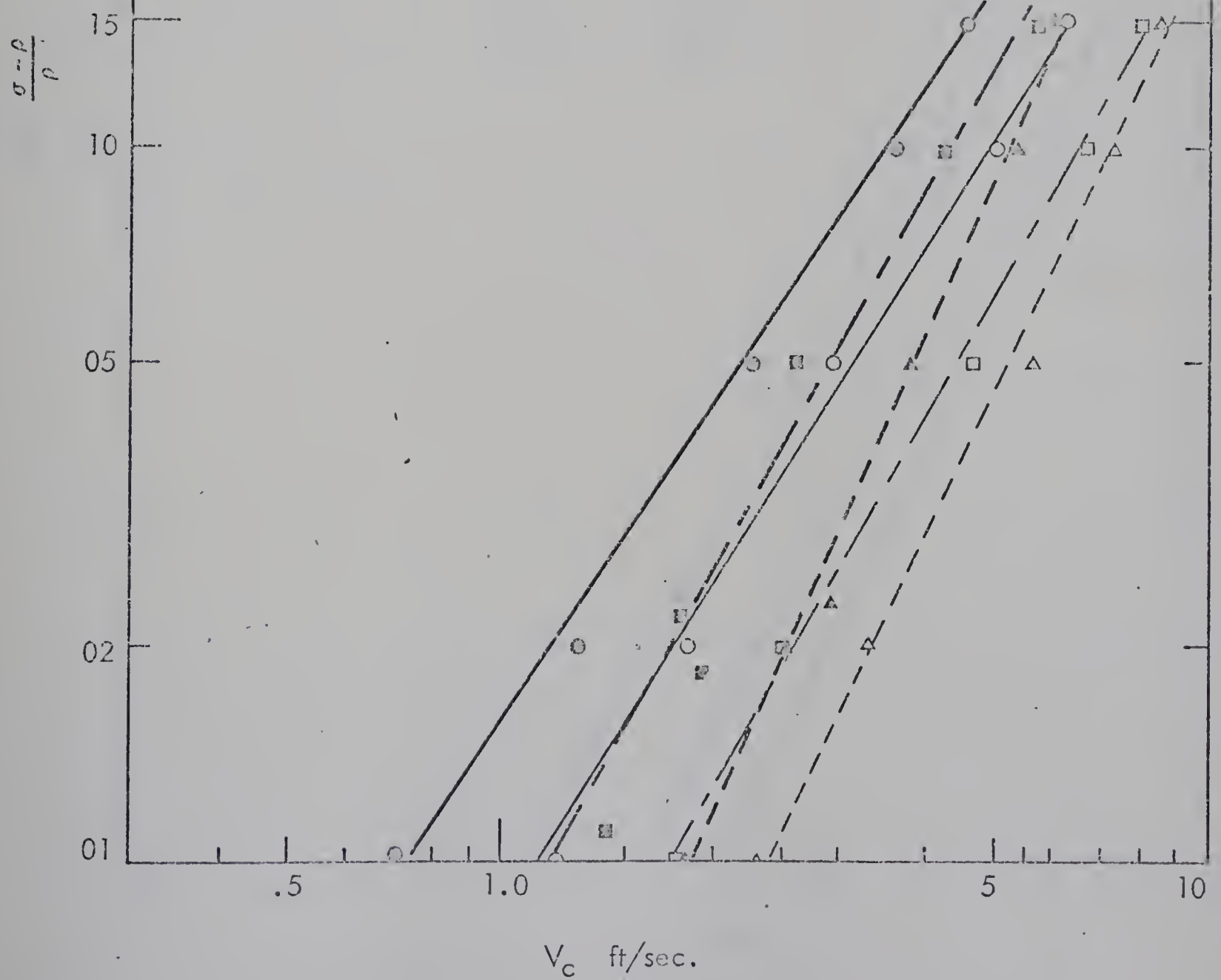


Fig. 43A

Capsule Macro Lift-off Velocities

vs

$k = 0.90$   $L = 6$   $\circ$   
 $L = 3$   $\odot$   
 $0.80$   $L = 6$   $\square$   
 $L = 3$   $\blacksquare$   
 $0.70$   $L = 6$   $\triangle$   
 $L = 3$   $\blacktriangle$

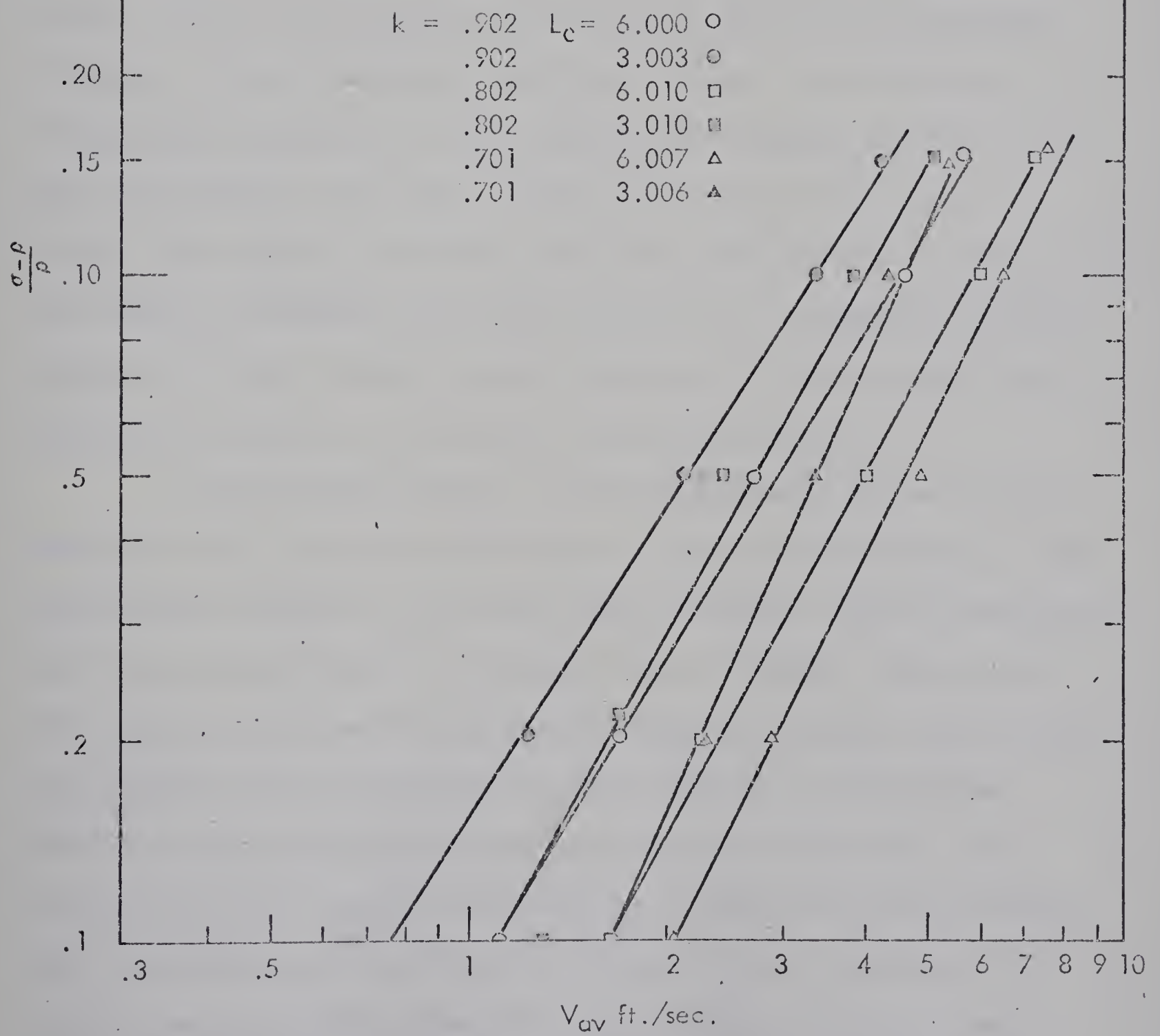






Liquid Velocities at  
Capsule Micro Lift off

Fig. 43B





measured. The capsule nose tended to be at a larger clearance than the capsule tail in the case of the 0.80 and 0.90 diameter ratios, but for 0.70 diameter ratios the clearance of the tail was larger relative to the nose. The resulting capsule angle was also plotted against  $V_c$ . As  $V_c$  increased, the magnitude of the angle increased. In particular, the maximum negative angle usually occurred just prior to the inception of the macroscopic lift off. At this maximum negative angle, the clearance of the nose was zero.

The fact that the angle of the capsule tended to alternate between positive and negative values probably represented an unstable condition. As was outlined in the theory section, the net moment on a capsule due to pressure and shear forces on the capsule parallel to the pipe must produce a tail lift. However, the forces at the nose of a single finite capsule are on the other hand trying to lift the capsule nose, thus trying to counteract the tail-lifting force. An unsteady condition persists until the velocity becomes sufficient to produce nose-lifting forces that completely overcome the tail-lifting forces.

An interesting feature of the experimental data, was the sensitivity of the clearance to the center of gravity of the capsule. The capsules were balanced in the equal density case, but were not rebalanced with the subsequent addition of copper wires as weights. However, the clearance data did show for particular capsules, a definite trend depending on which end of the capsule was placed forward in the pipeline, resulting either in larger clearances at the nose or the tail. This sensitivity of the capsule to the position of centre of gravity suggests that the forces providing the capsule clearance must themselves be distributed nearly uniformly along the capsule length, otherwise a small shift in the capsule centre of gravity would not change the capsule



orientation so markedly. This type of sensitivity would not occur if the primary force causing the capsule clearance was concentrated at either the capsule nose or tail. To obtain an average value of the capsule clearance,  $\frac{C_N + C_T}{2}$  was calculated and plotted against  $V_c$

(See Fig. 44 to 49) The value of  $\frac{C_N + C_T}{2}$  was plotted on a logarithmic

basis to allow the small values of clearance measured in the microscopic runs to be plotted along with the macroscopic clearances measured in the full view runs. Also, plotting the data in this way will indicate whether the point of inception of the macroscopic clearance is really as marked as it appears on an arithmetic plot or whether there is a relation of clearance to  $V_c^n$  in such a way that  $n$  remains constant over the range of  $V_c$ .

All runs for a particular diameter ratio and length were plotted on the same sheet in order to illustrate the effect of density change. (Figs. 44 to 49). As expected, the increase in density resulted in increased  $V_c$  to obtain the same average clearance.

The clearance data lying above the point of inception of macro nose lift off do appear to give a steeper slope referred to  $V_c$  than the clearance data lying below the macro lift off point. This change in slope was more evident for the plots of 6" capsule length, for 0.80 and 0.90 diameter ratios, and the higher densities.

#### Velocity Clearance Correlations

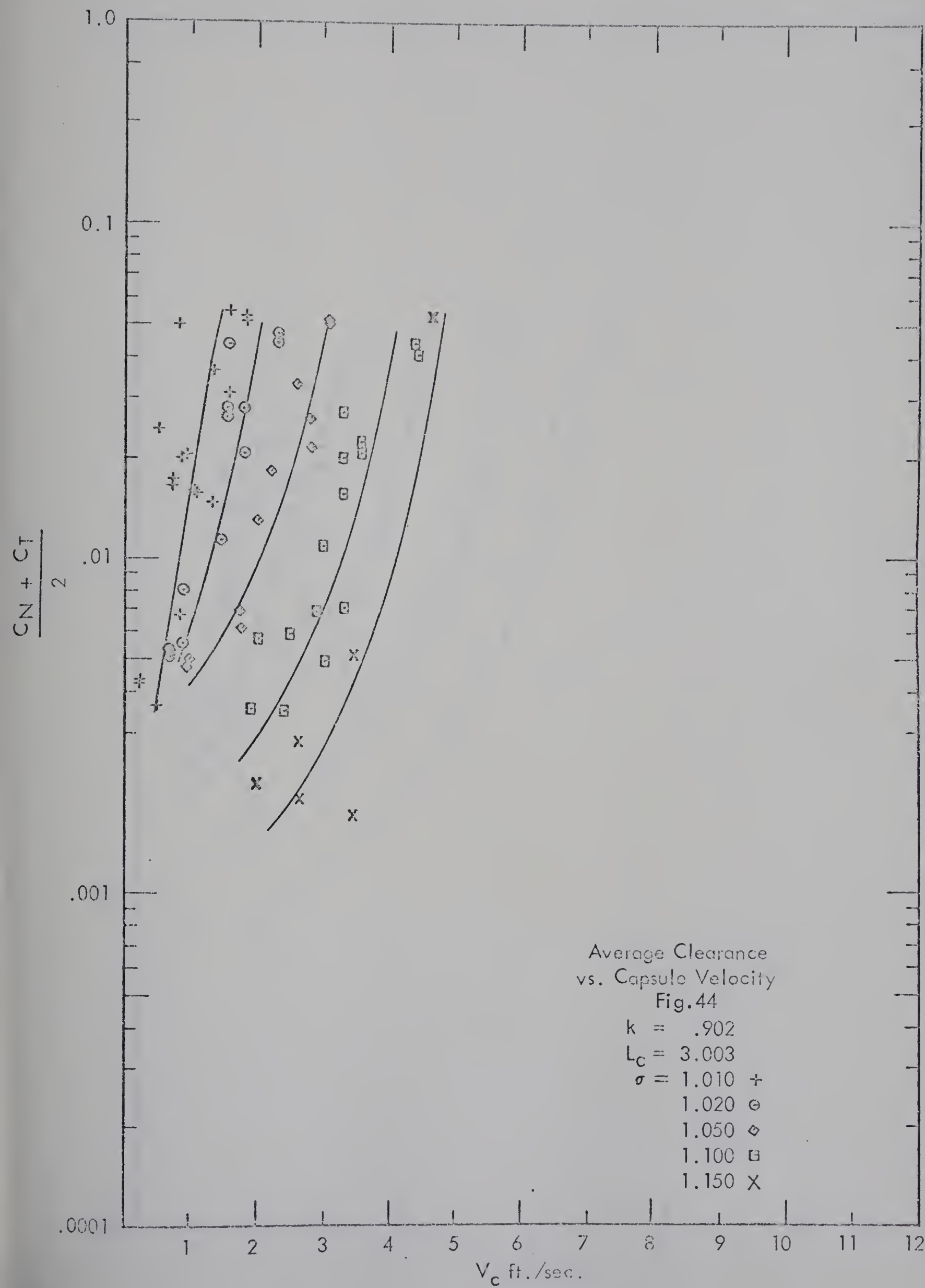
It was stated earlier (page 86) that

$$\frac{C}{d_p} = \left( \frac{V_{av}^2}{g_c d_p}, \frac{V_{av} d_p \rho}{\mu}, \frac{\sigma - \rho}{\rho}, \frac{L}{d_p}, \frac{d_c}{d_p} \right)$$

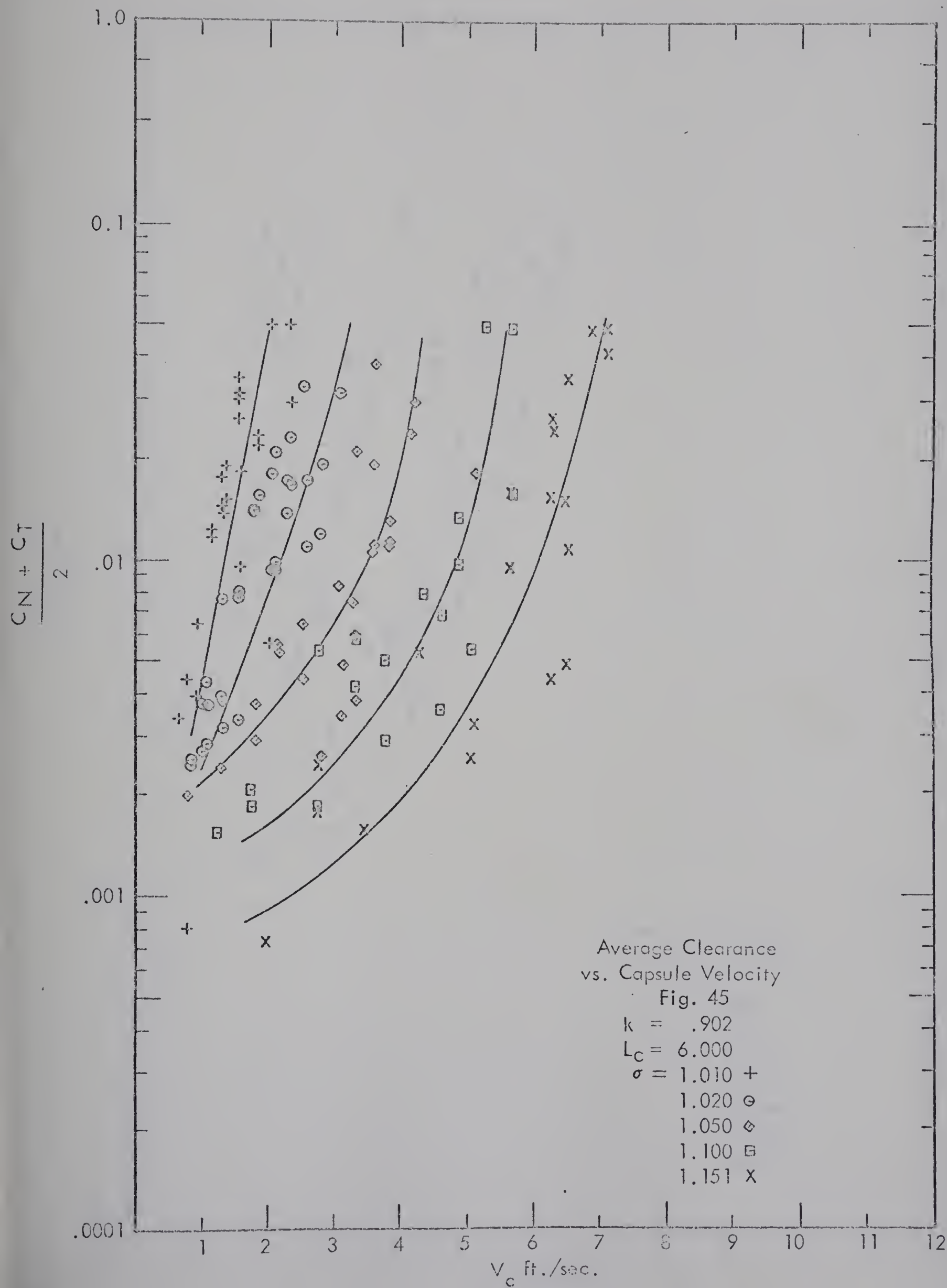
It was also argued that  $V_c$  is just as useful a velocity



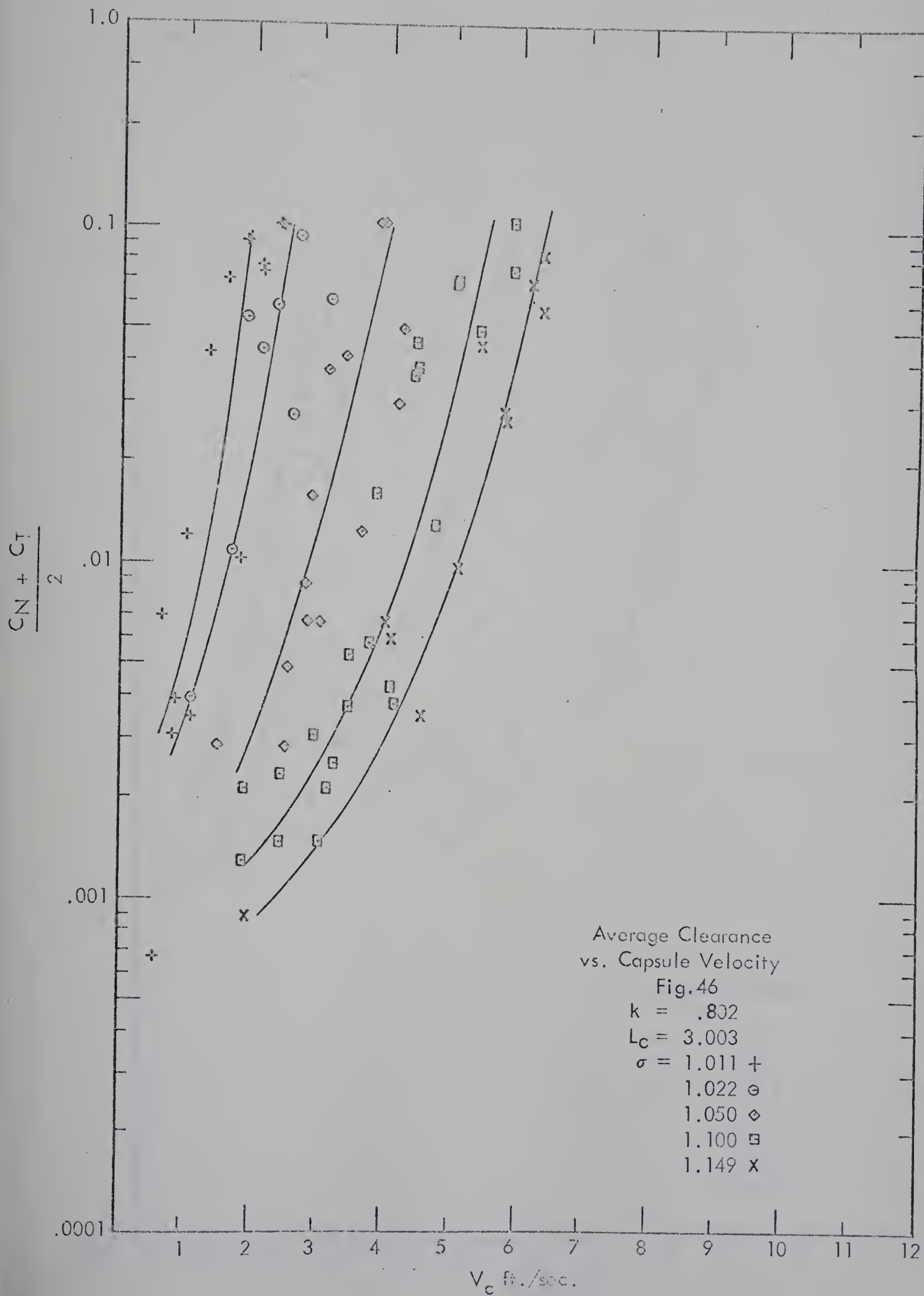




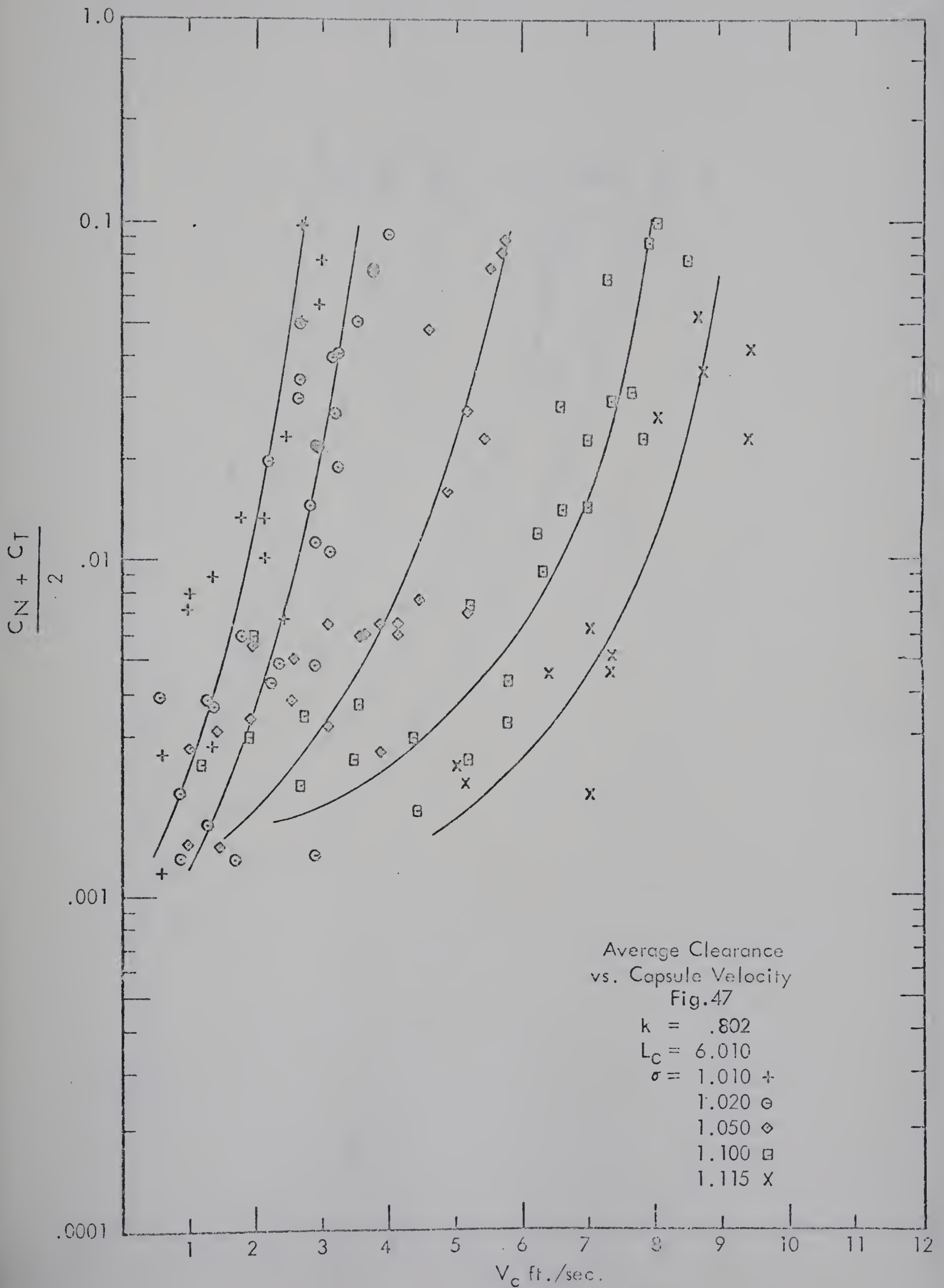






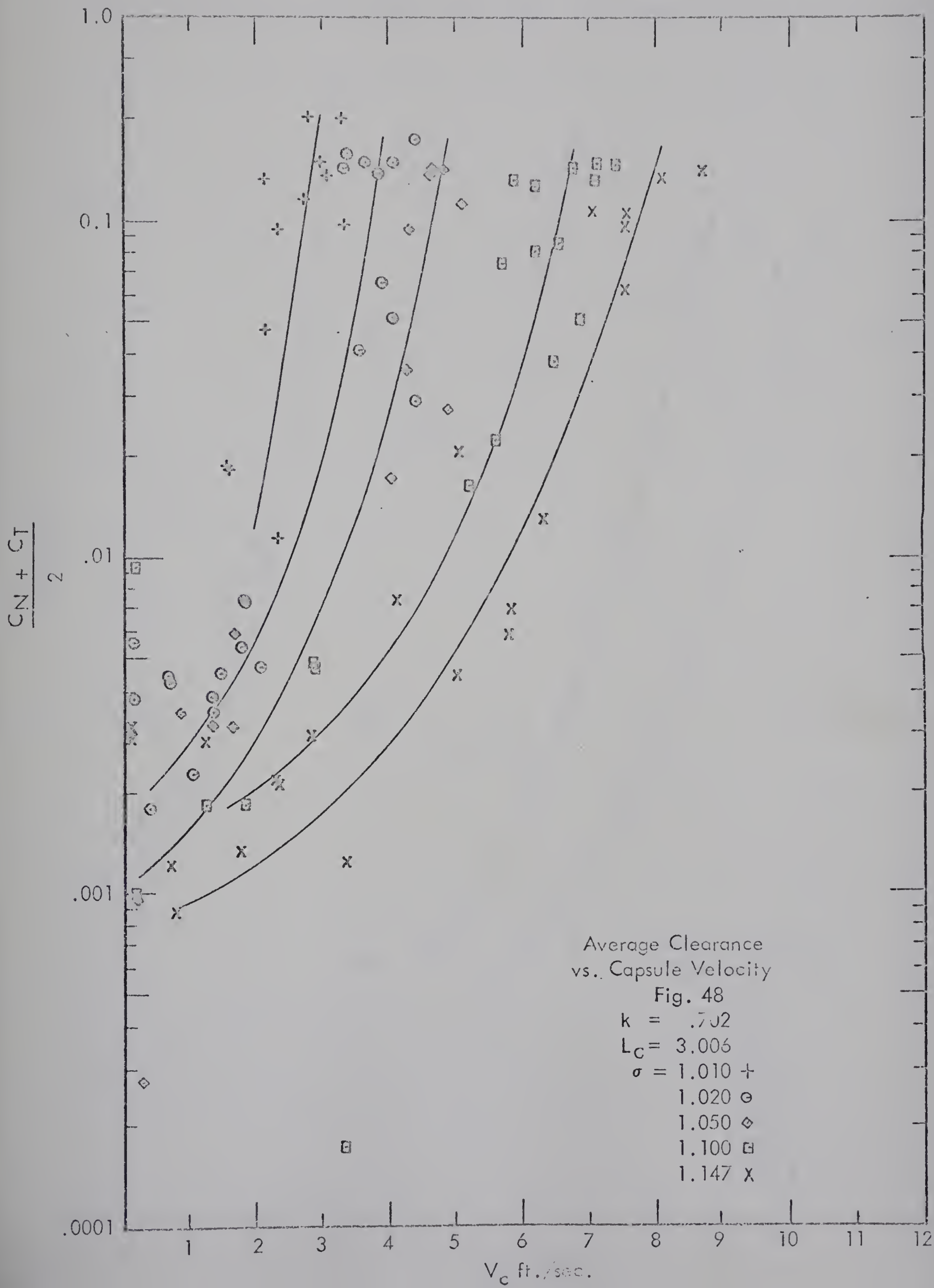




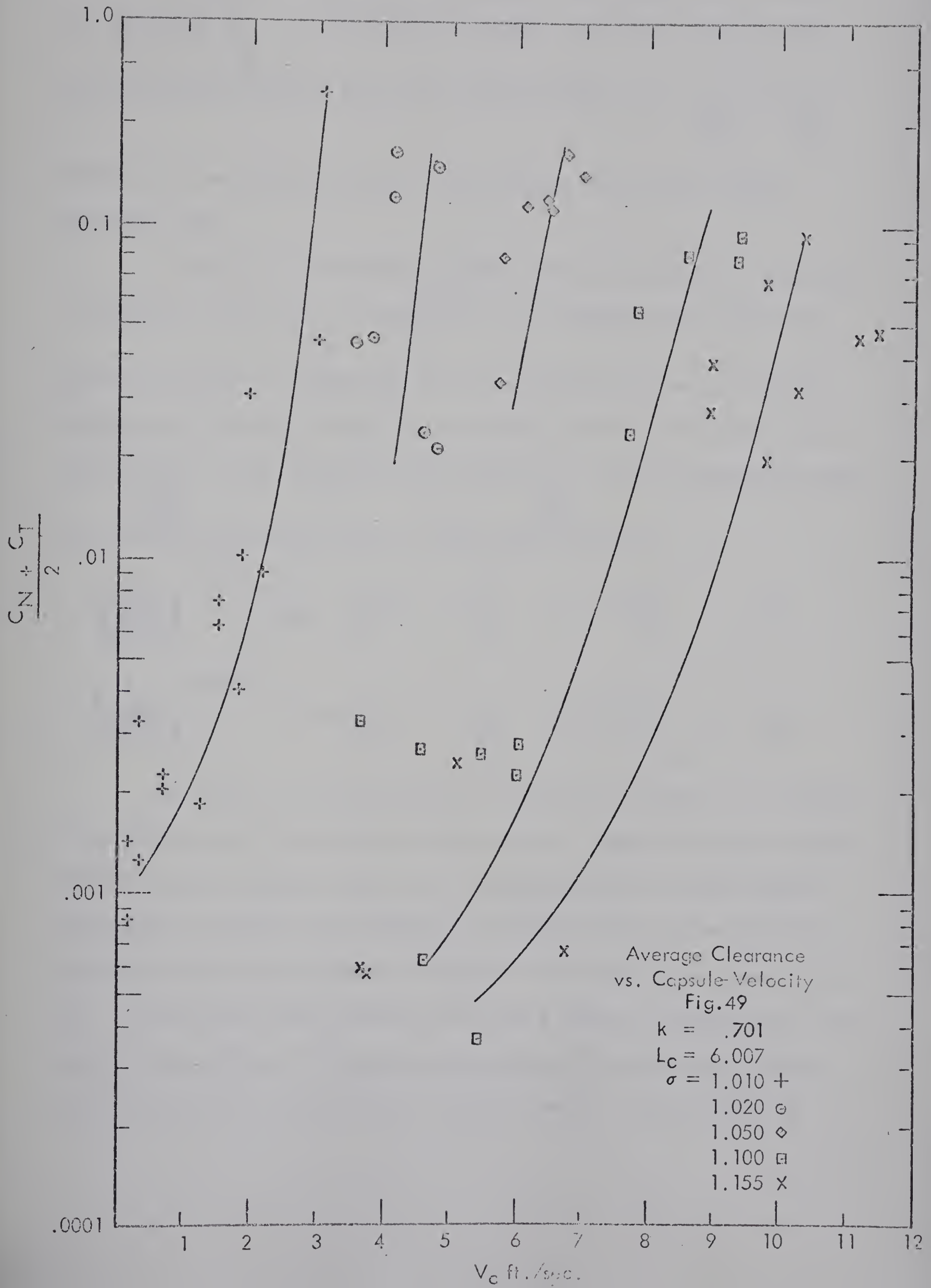














parameter as  $V_{av}$ . For correlation purposes it is held that to relate the clearance  $\frac{C}{d_p}$ , to the other groupings, the proper dimensionless

group including velocity would be a Froude number (i.e.  $\frac{V_{av}^2}{g_c d_p}$  or  $\frac{V_c^2}{g_c d_c}$

rather than the Reynolds number, since gravity forces must play an important part.

The point of inception of macro lift off was held to represent a "constant" value of  $\frac{C}{d_p}$ , since this point represents the particular velocity (capsule or liquid) at which nose lifting forces completely overcome tail lifting forces. A correlation of either the pipe Froude number  $\frac{V_{av}^2}{g_c d_p}$ , or the capsule Froude number  $\frac{V_c^2}{g_c d_c}$  with the remaining groups was developed (Figs. 50A, 50B). These relations were

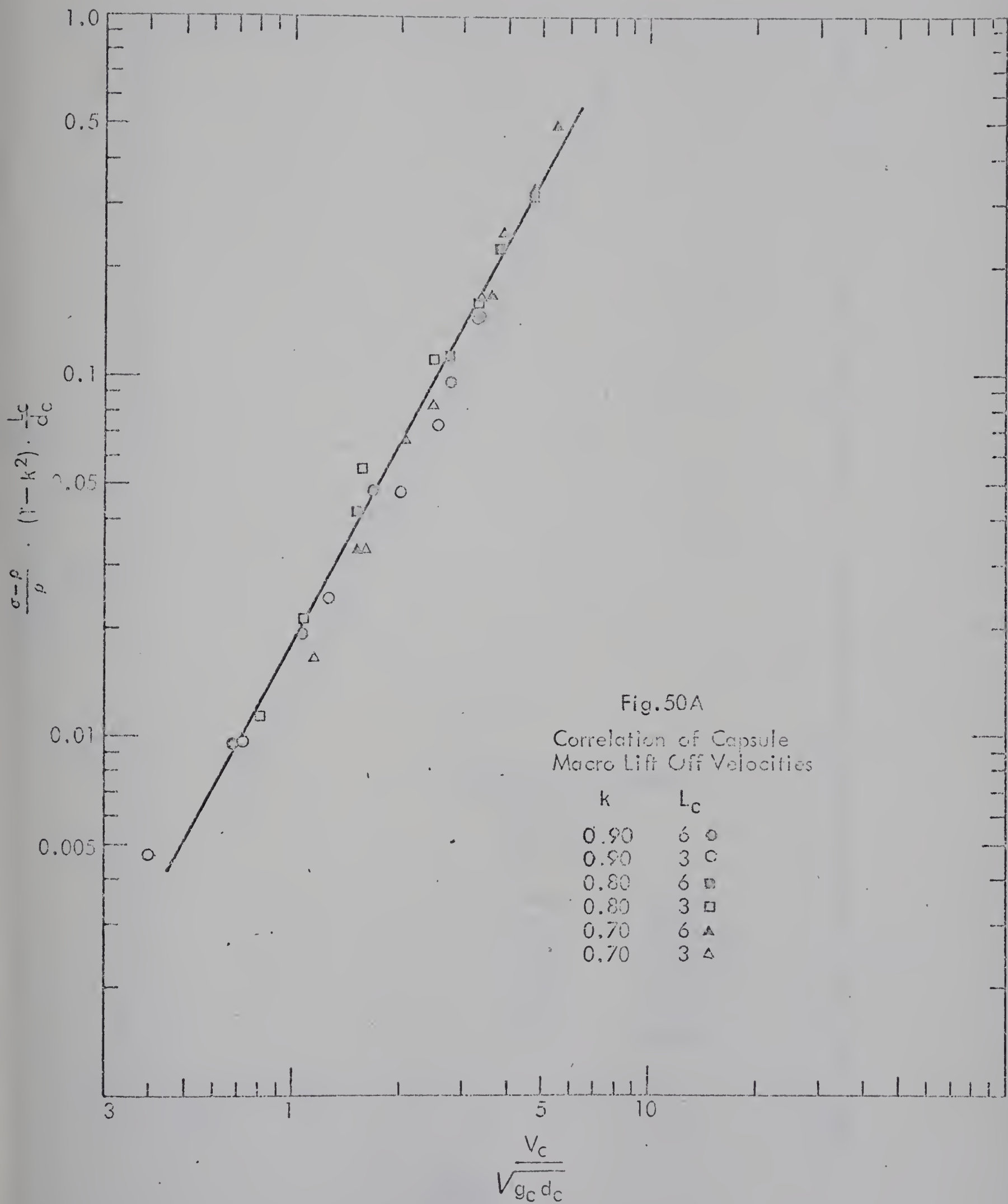
$$\left( \frac{V_{av}}{\sqrt{g_c d_p}} \right)^{1.95} = 55.5 \left( \frac{\sigma - \rho}{\rho} \times \frac{L_c}{d_p} \times (1-k^2) \right) \quad (3)$$

$$\left( \frac{V_c}{\sqrt{g_c d_c}} \right)^{1.835} = 55.8 \left( \frac{\sigma - \rho}{\rho} \times \frac{L_c}{d_c} \times (1-k^2) \right) \quad (4)$$

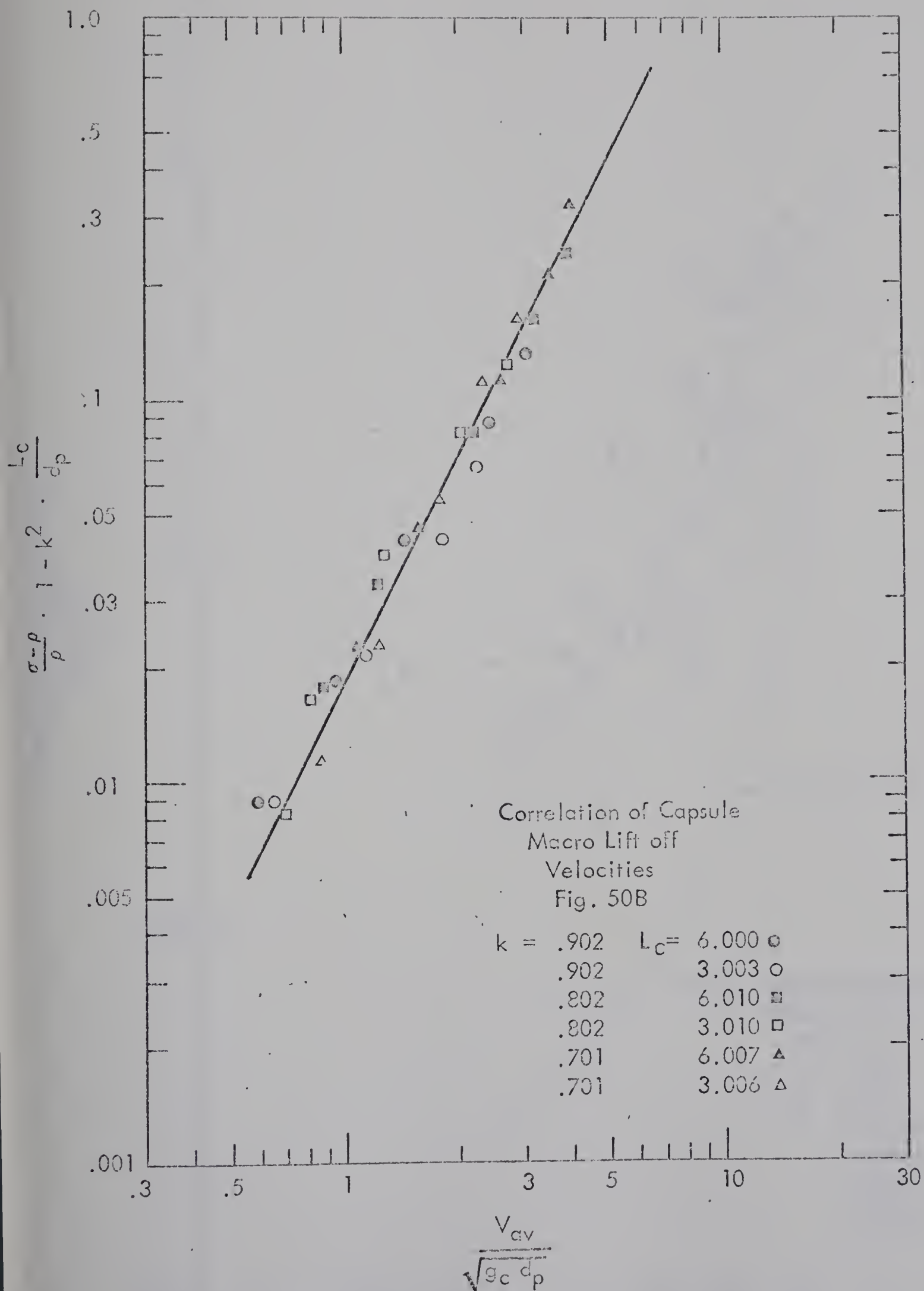
In Part 9 (9) Kruyer et al. have shown clearance as a function of velocity ratios, for different values of  $k$ . Since the theory assumes infinite capsule length, there is no consideration for capsule length. The measured clearances are plotted in this form and compared with the theoretical line for clearances in laminar flow conditions. (figs. 51 to 57.) The data for 0.90 diameter ratio show a trend to agreement with the laminar theory line. This may be the result of the flow being laminar in the annulus for this particular diameter ratio. The condition of



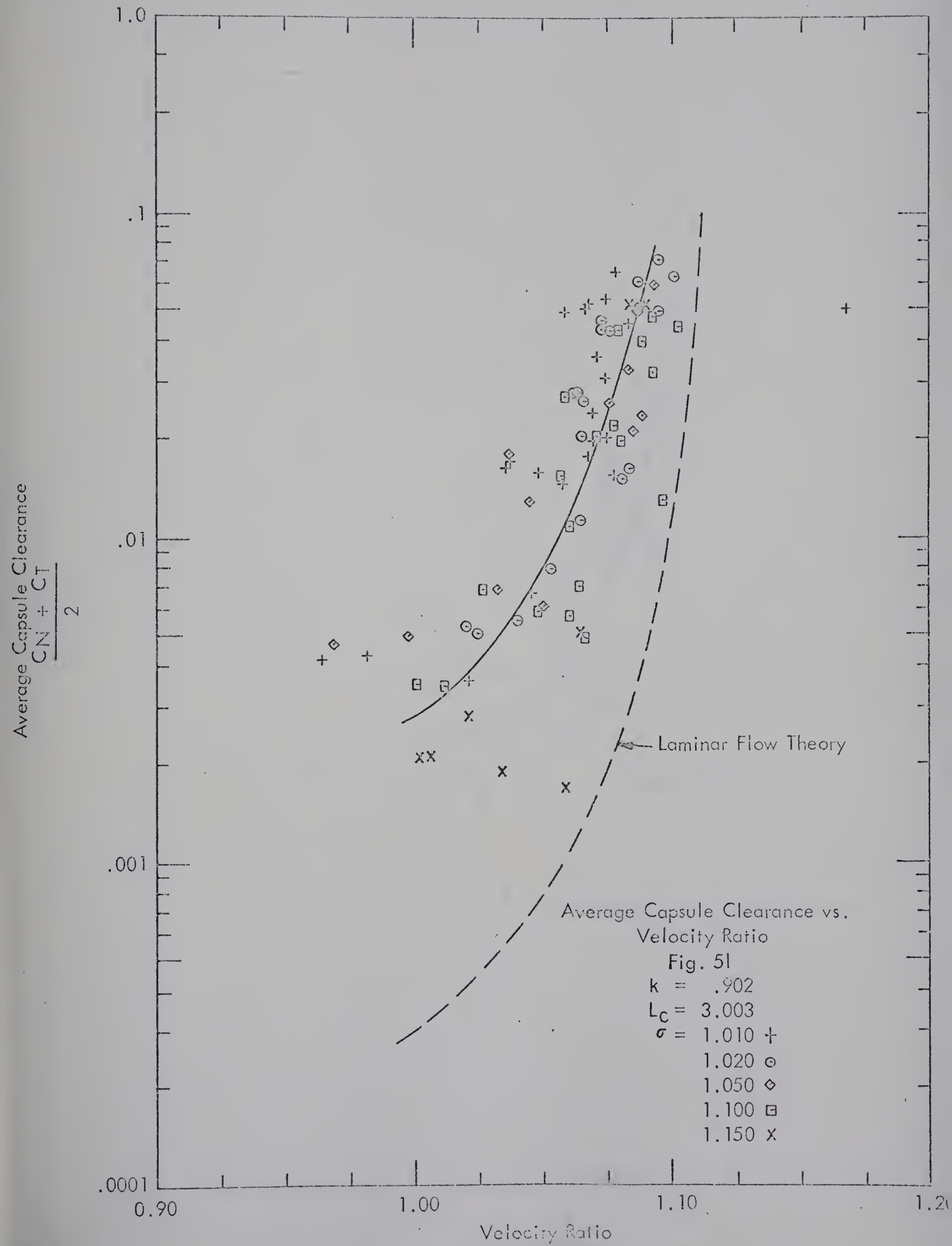




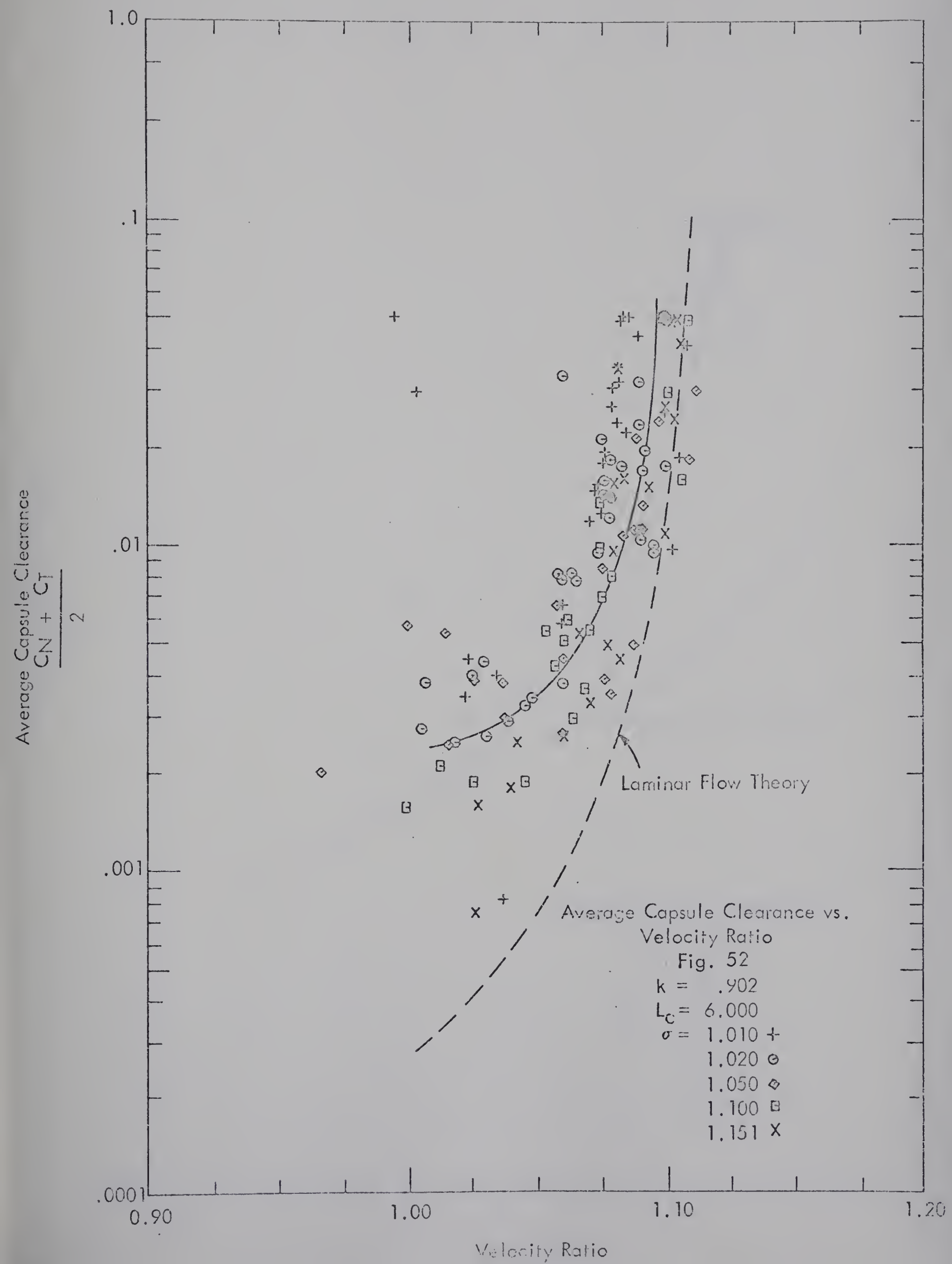






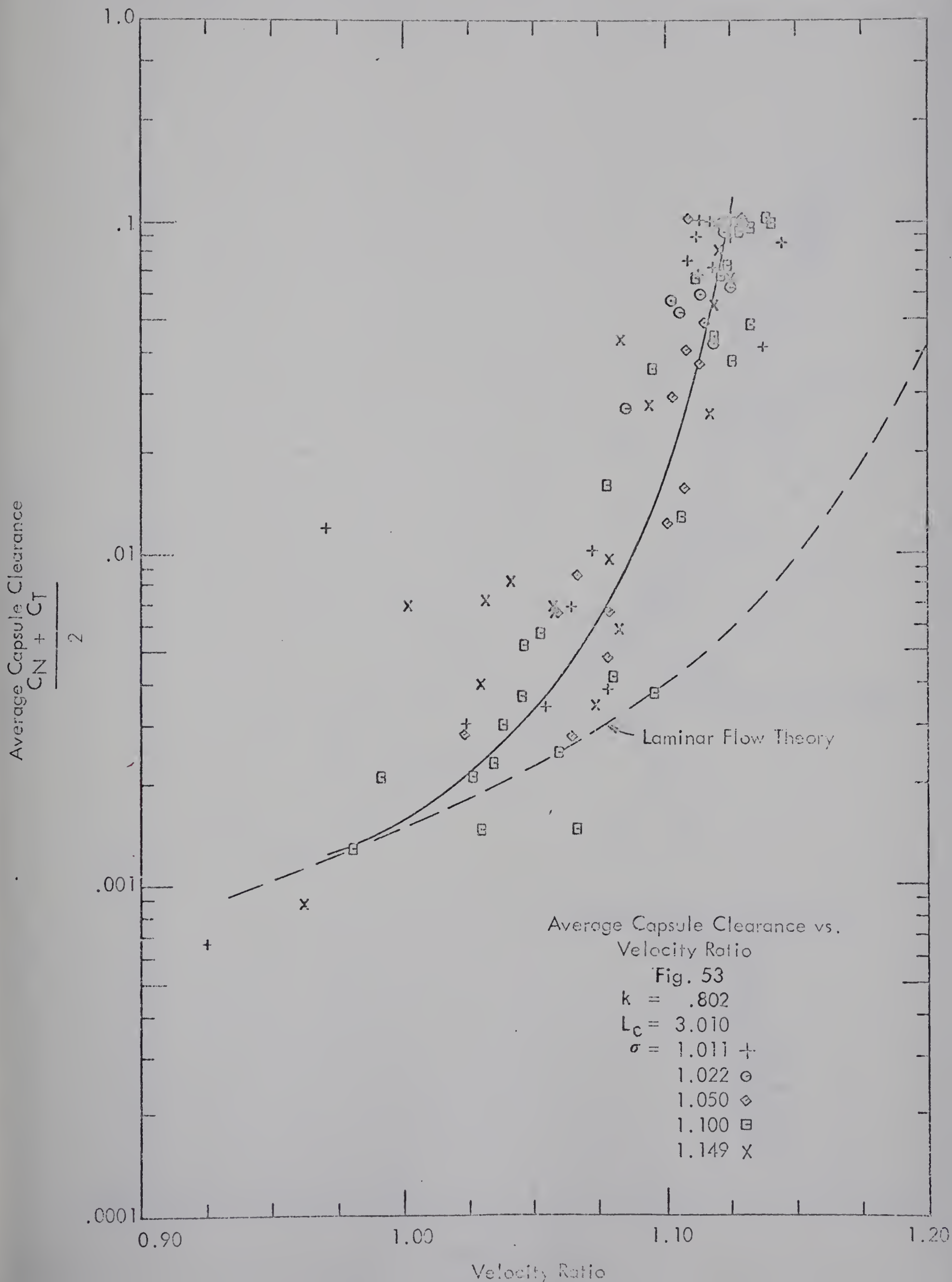




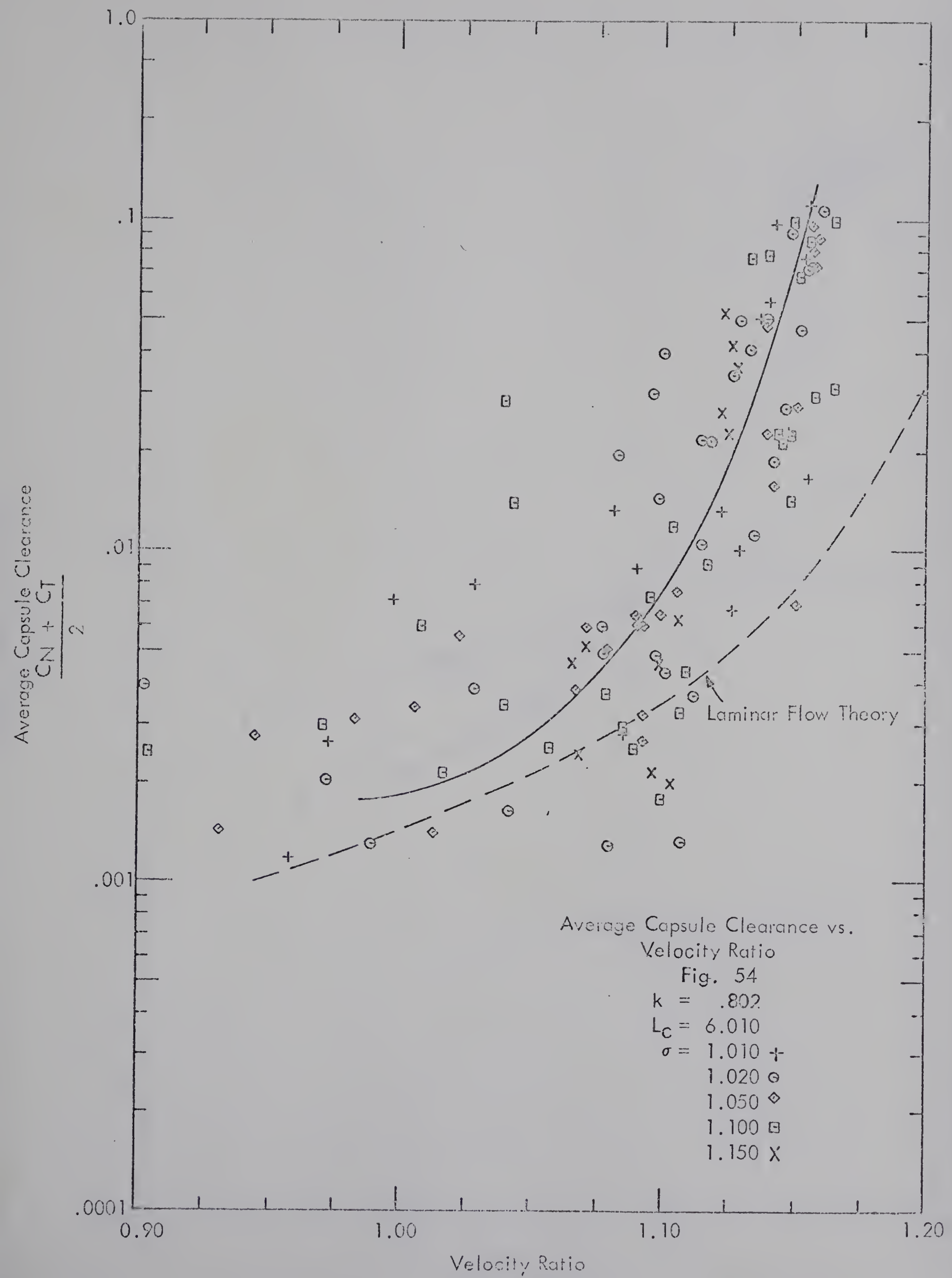




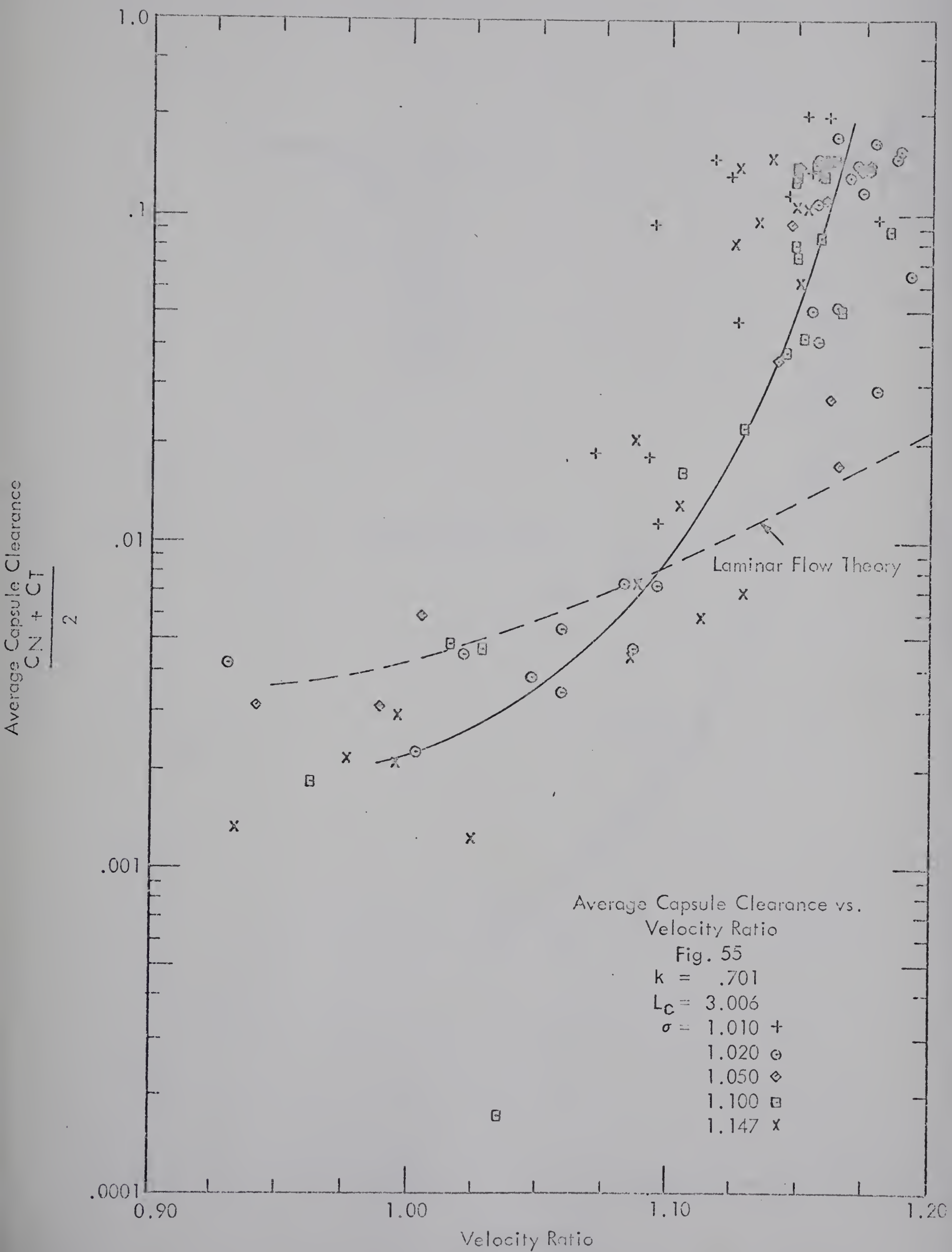






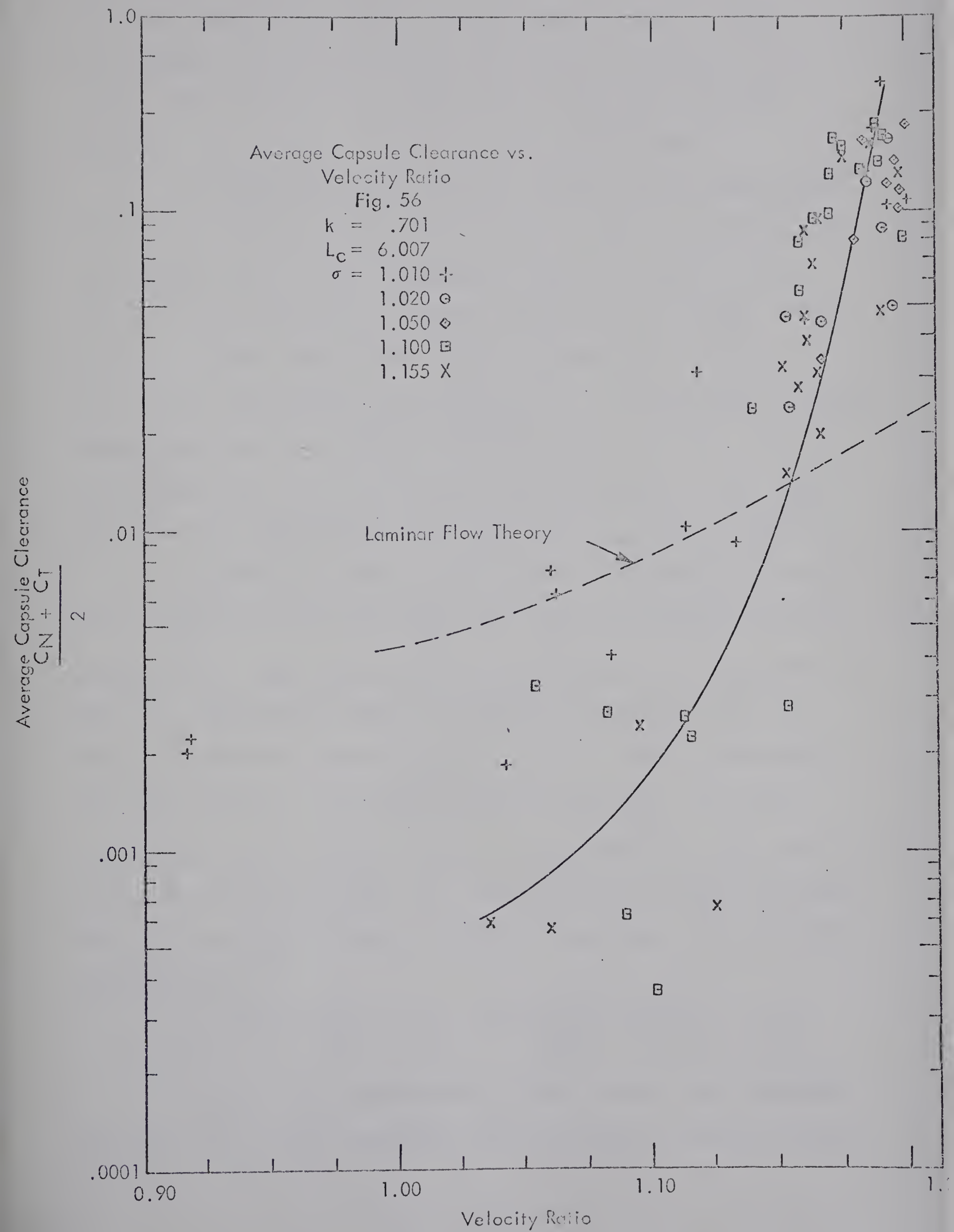














laminarity was confirmed by the fact that negative pressure readings were obtained in some cases. This will be referred to in more detail later. The plots for 0.80 and 0.70 diameter ratios show increasing departure from the laminar theory line, as would be expected.

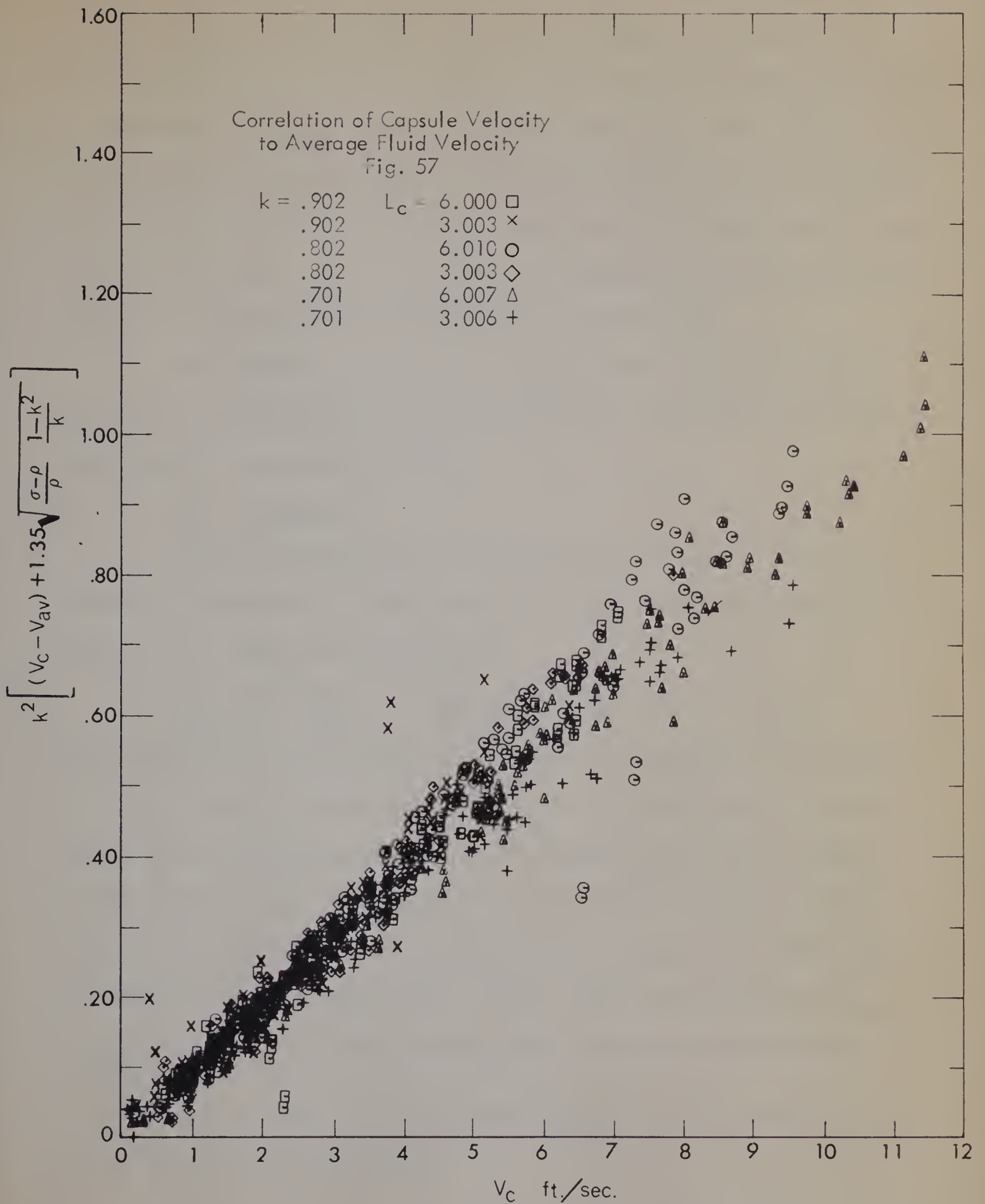
The basic data plots of capsule velocity versus average fluid velocity were linear, or very nearly so, in all cases. These plots are very similar for all cases, varying only slightly in slope and intercept of the  $V_{av}$  axis for the different values of  $k$ ,  $L_c$ , and  $\frac{\sigma - \rho}{\rho}$ . However, considerably larger differences are evident if the values of  $V_c - V_{av}$  are calculated for the various cases. At the threshold velocity, before capsule motion has begun, the capsule velocity is zero. This is now the same case as the static capsules studied earlier. There it was found that the capsule pressure drop for a given  $V_{av}$  varied as  $(\frac{1-k^2}{k})^2$ .

Following from this, we would expect the threshold velocity to vary as  $\frac{1-k^2}{k}$  and also as the  $\frac{\sigma - \rho}{\rho}$  since this is the measure of the resisting forces. This will then give us our intercept on the  $V_{av}$  axis. Once the capsule begins moving it is found that the plots of  $V_c - V_{av}$  versus  $V_c$  were linear and parallel for a given  $k$ . For the different  $k$ , the slope of the  $V_c - V_{av}$  versus  $V_c$  plots varied as  $\frac{1}{k^2}$ . With this information it was possible to prepare a single plot of  $V_c - V_{av}$  vs.  $V_c$  for all the capsules (Fig. 57). This allows us to predict the capsule velocity if the fluid velocity is known, or vice versa. The relationship obtained was:

$$V_c = 10.4k^2 \left[ (V_c - V_{av}) + 1.35 \sqrt{\frac{\sigma - \rho}{\rho} \frac{1-k^2}{k}} \right] \quad (5)$$

Pressure drop measurements were taken for all runs, but these were difficult to obtain accurately since the amount of pressure increase









caused by the capsule was very small. At higher capsule speeds, the pneumatic type pressure cells also lack sufficient response speed to obtain a pressure measurement. The pressure drop due to the capsule, above the pressure gradient of liquid alone disappeared to the extent that it could not be measured when the capsule reached the macro-lift off stage. It was particularly noticeable for the 0.90 diameter ratio and 6" length where not only did the pressure drop disappear, but in fact showed a reduction. (See fig. 58) This can be only explained by the fact that the annular flow must be predominantly laminar in this case.

This negative pressure was observed over a range of capsule velocities from 2.09 ft./sec. to 1.285 ft./sec. Using the criteria defined earlier for Reynolds number as

$$Re = \frac{u_{ann\ av} C}{\nu}$$

For the velocities at which the negative pressure drops are observed, the measured velocity ratio was = 1.08. This means that the average bulk velocity in the annulus is

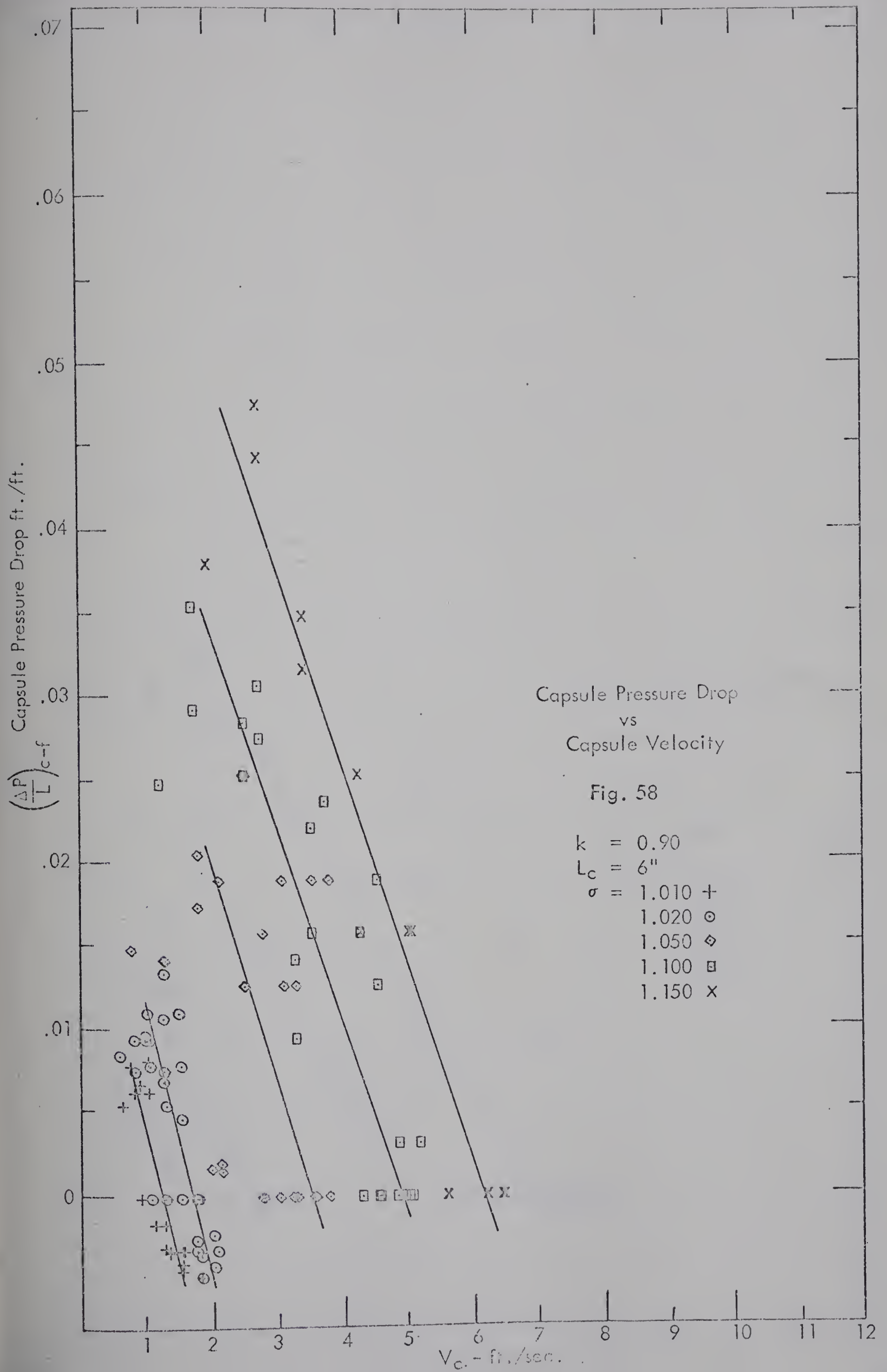
$$1 - \left( \frac{1.08 \times k^2}{1-k^2} \right) V_{av} = \left( \frac{1 - .875}{.190} \right) V_{av} = .66 V_{av}$$

The capsule motion will produce a velocity in the annulus at all points of  $1/2 V_c = .54 V_{av}$ . This leaves  $.12 V_{av}$  to be contributed by the flow caused by the pressure gradient. The "pressure" flow will be greater in the larger areas of the annulus. For 0.90 diameter ratio we could expect this flow in the widest portion of the annulus to be 1.30 times the average annulus pressure flow. In our case this would be  $.15 V_{av}$  or  $\frac{.15}{1.08} = .139 V_c$ . At the velocities where negative pressures were

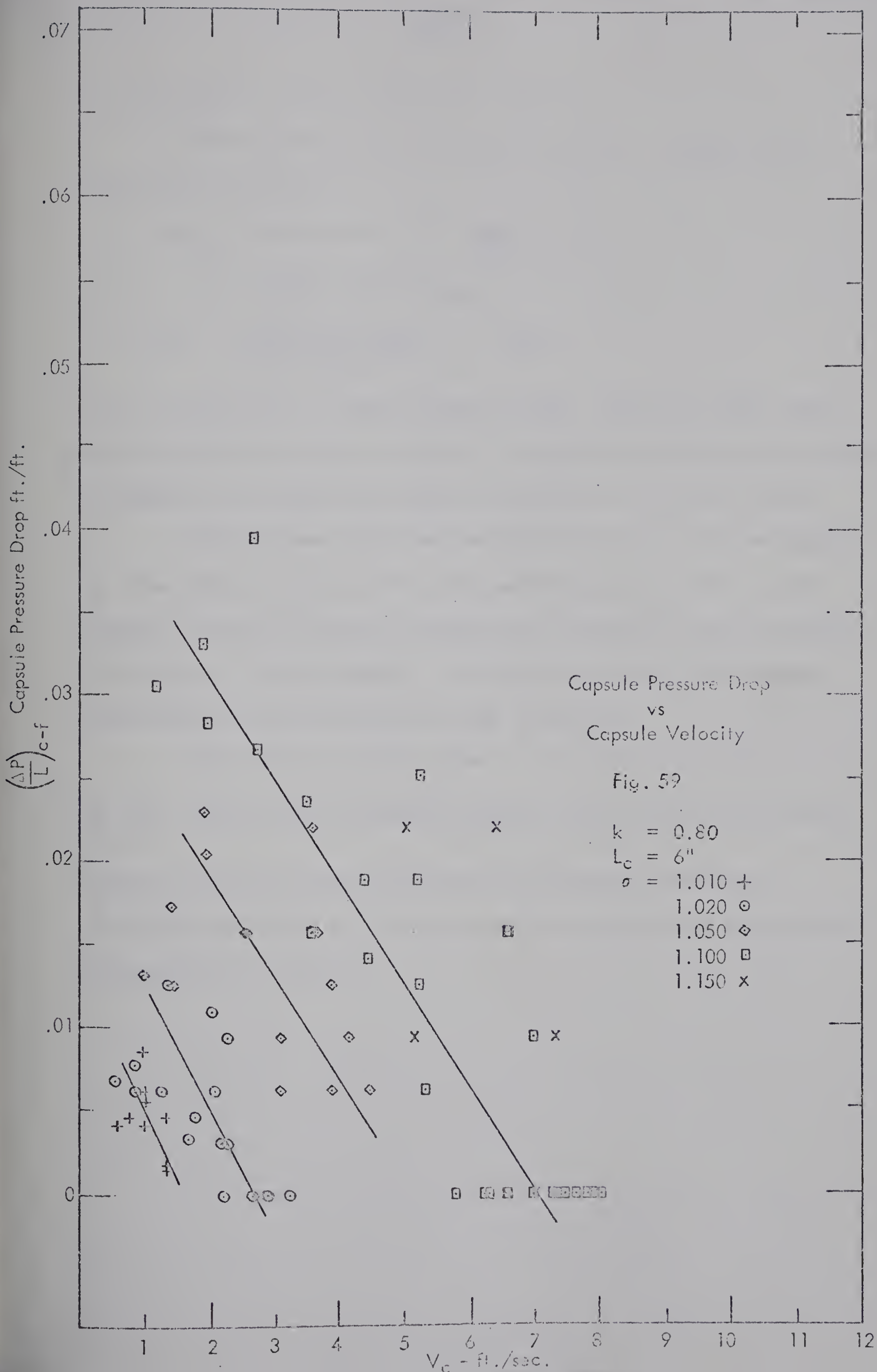
observed, the clearance was = .02 pipe diameters or .026 inches; thus the maximum gap is .1050 inches.













At this point the annulus velocity is  $.639 V_c$ .

The highest  $V_c$  at which negative pressure readings were observed was 2.09 ft.sec.

$$V_{\text{ann}} = 1.34 \text{ ft. sec.} \quad C = \frac{.1050}{12} \text{ ft.}$$

$$\nu = .9510 \times 10^{-5} \text{ ft.}^2/\text{sec.}$$

$$\therefore Re = \frac{2 \times 1.34 \times .1050}{12 \times .9510 \times 10^{-5}} = 2460.$$

This is nearly equal to our criterion of 2400. Since all other areas of the annulus will be at a lower Re, it appears that flow in the annulus is laminar, or at least, the scale of turbulence is greatly reduced.

The pressure drops measured for all runs were plotted against  $V_c$ . The data was badly scattered in most instances but did at least indicate a trend of pressure decrease with increase of capsule velocity or decrease in capsule density. The plots for .90 and .80 diameter ratios by 6" long are presented in Fig. 58 and 59.

Since we have already shown in the earlier plots that

$$\frac{C_N + C_T}{2} \text{ increases with increasing velocity, the fact that the pressure}$$

drop is shown to decrease with increasing velocities, provides a qualitative confirmation to the hypothesis of reduction of pressure drop with increase in clearance.





## IX CONCLUSIONS

1. In general, the data produced does provide qualitative answers to the particular subjects studied. However, in many instances the data is erratic and this makes it difficult to establish quantitative results. This can be attributed to some extent to the unsteady nature of the quantities being measured, but is also due no doubt to experimental error.

For future work, more data points should be taken at any given set of conditions to allow calculation of mean values, which would reduce the scatter evident in the present data.

2. The flow patterns observed around static capsules showed as principal features a toroidal vortex, and a stagnation point at the rear of the capsule, a separation of the streamlines as they passed over the sharp rear edge and a weak wake area downstream of the capsule characterized by a general backflow towards the capsule and the formation of smaller vortices in this area.

Values of vortex size, height of stagnation point and separation of the streamlines at the top of the capsule all tended to constant values with increasing velocity up to threshold.

3. Pressure drops across these static capsules showed a definite relation to average fluid velocity and were correlated for the range of diameter ratios tested.

4. Any further flow pattern work on capsules in a pipeline should concentrate on capsule trains, either cylinders or spheres and should examine conditions between the capsules.

5. For a range of densities from 1.01 to 1.15, diameter ratios 0.70, 0.80 and 0.90 and 3" and 6" lengths, clearance measurements were made,



showing that for a given capsule velocity, clearance decreases with increasing capsule density, decreases with increasing capsule length, and increases with increasing capsule diameter ratio.

6. For each capsule, there exists a specific velocity at which the capsule "lifts off" at the nose and retains a large nose clearance for any further increase in velocity. This "lift off velocity" was correlated for the range of variables tested in this study.

7. Capsule pressure drop was shown qualitatively to decrease with increasing capsule clearance. In particular, negative capsule pressure drops were recorded for the six inch long, 0.90 diameter ratio capsules, confirming that this diameter ratio does induce laminar conditions in the annulus.

8. The magnitude of the clearance is small until the macro lift off velocity is reached. Since this macro lift off is very definitely related to conditions at the capsule nose, there is doubt as to whether this macro lift off would occur in a train of capsules where nose conditions are very much different from a single finite capsule. In any case, the magnitude of the velocities required to produce the macro lift off are large, and in a practical case in a commercial line would probably never be achieved unless the capsules are very nearly equal to the density of the carrier fluid.

Thus, if a clearance is desired in a commercial pipeline, it will probably be necessary to produce it by means of modification to the basic cylindrical shape.



IX Nomenclature

a	angle of attack, - radians
A	constant (as defined in text)
b	y at which $u = 1/2 V_c$ for Couette flow, - ft.
B	constant (as defined in text)
C	clearance of capsule from pipe wall, - ft.
$c_{fr}$	coefficient of skin friction, $-\frac{lb.sec.^2}{ft.^4}$
D	distance along line orthogonal to velocity contours in the annulus, - ft.
d	diameter, - ft.
e	base of natural logarithm
f	friction factor, - dimensionless
$g_c$	gravitational constant, - ft./sec. <sup>2</sup>
j	coefficient of friction between pipe and capsule
k	diameter ratio $\frac{d_c}{d_p}$ , - dimensionless
L	length, - ft.
M	moment, - ft-lb.
$\frac{\Delta P}{L}$	pressure drop, $-\frac{lb.^2}{ft.^2}/ft.$
PR	pressure ratio $\frac{\left(\frac{\Delta P}{L}\right)_c}{\left(\frac{\Delta P}{L}\right)_f}$ - dimensionless
Q	volumetric discharge, $-\frac{ft.^3}{sec.}$
r, $\theta$	cylindrical polar coordinates, - ft. and radius
R	hydraulic radius, - ft.
Re	Reynolds number, - dimensionless
S	displacement of capsule centerline from pipe centerline, - ft.
u	axial point velocity, - ft./sec.





U	maximum point velocity at a particular radial position in the annulus, - ft./sec.
V	bulk velocity, - ft./sec.
VR	capsule velocity/average liquid velocity - dimensionless
x,y,z	cartesian coordinates, - ft.
$\alpha, \beta$	variable parameters involving k and C used in calculation of PR-VR relationship in laminar flow.
$\gamma, \phi, \omega$	angles, - degrees
$\sigma$	capsule density, - lb./ft. <sup>3</sup>
$\rho$	liquid density, - lb./ft. <sup>3</sup>
$\tau$	shear intensity, - lb./ft. <sup>2</sup>
$\epsilon$	roughness height, - ft.
$\mu$	absolute viscosity, - lb./ft. sec.
$\nu$	kinematic viscosity, - ft. <sup>2</sup> /sec.

#### Subscripts

ann.	annulus
av	average
c	capsule
f	fluid or liquid
L	laminar
Loc.	local
max.	maximum
N	nose
O	opposing
p	pipe





S	slip
t	turbulent
T	tail
z	y at which $u = 1/2 V_c$ (Couette flow)
1	pressure flow
2	Couette flow
0	radial position
$\tau$	shear



X BIBLIOGRAPHY

1. Charles, M. F., Govier, G.W. and Hodgson, G.W., Can.J.Chem.Eng., 39, 27 (1961).
2. Ellis, H.S., Can. J.Chem.Eng. 42 1 (1964).
3. Ellis, H.S., Can. J.Chem.Eng. 42, 69 (1964).
4. Charles, M.E., Can. J.Chem.Eng., 41, 46 (1963).
5. Ellis, H.S., Can. J.Chem.Eng. 42, 155 (1964).
6. Ellis, H.S. and Bolt., L.H., Can.J.Chem.Eng. 42, 201 (1964).
7. Round, G.F. and Bolt, L.H., Can.J. Chem.Eng. 43, 197 (1965).
8. Newton, R., Redberger, P.J., and Round, G.F., Can.J.Chem.Eng. 42 168 (1964).
9. Kruyer, Jan, Redberger, P.J., and Ellis, H.S., J. of Fluid Mech. 30, 513 (1967).
10. Clayton, B.R., Massey, B.S., J.Sci. Instrum 44, 2(1967).
11. Van Meel, D.A., and Vermij H. Appl. Scient.Res.A. 10, 109 (1961).
12. Popovich, A.T. and Hummel, R.L. Chem. Eng. Sci. 22, 21(1967).
13. Hodgson, G.W. and Charles, M.E., Can. J. Chem Eng. 41, 43 (1963).
14. Macagno, Enzo O., and Hung, Tin-kan, J. Fluid Mech. 28, 43 (1967).
15. Taneda, Sadatoshi, J.Phys. Soc. of Japan 11, 1104 (1956).
16. Kennedy, R.J., Can.J. Chem.Eng. 44, 354 (1966).
17. Bentwich, M., Kelly, D.A.A., and Epstein, N., J.Basic Eng. (submitted)
18. Berkowitz, N., Brown, R.A.S., and Jensen, E.J., Can.J.Chem. Eng. 43, 280 (1965).
19. Brown, R.A.S., and Jensen, E.J., Can.J. Chem. Eng. 46, (in press).
20. Berkowitz, N. Hodgson, G.W., Moreland, C., and Round, G.F., Oil in Canada, 13, 25 (1961).
21. Hodgson, G.W. and Bolt, L.H., Presented at 1962 E.I.C. General Meeting, Paper No. 15 (1962).



22. Berkowitz, N., Proc. Ann. Meeting Iron Steel Div., Am. Inst. Mining Eng.,  
Buffalo (1963).
23. Berkowitz, N. and Jensen, E.J., Can. Min. and Met. Bull. 56, 504 (1963).
24. Berkowitz, N., Proc. SRBII Inst. Fuel Cont. Brussels, 1964,  
Paper No. 4 (1964).
25. Jensen, E.J. and Berkowitz, N., Proc. Intermountain Symp.  
Fossil Hydrocarbons, 1st. Salt Lake City, 141 (1965).
26. Kruyer, J., and Ellis, H.S., J. Can. Pet. Tech. 4, 159 (1965).
27. Ellis, H.S., Redberger, P.J., and Bolt, L.H., Ind. & Eng.  
Chem. 55, 29 (1963).
28. Habgood, H.W., Oilweek 14, No. 35, 29 (1963).
29. Hodgson, G.W., Proc. Natl. Northern Develop. Conf. 3rd,  
Edmonton (1964).
30. Hodgson, G.W., Ind. Canada 68, 114 (1965).
31. Hodgson, G.W., Intern. Oil Scouts Assoc. 42 Ann. Meeting  
Issue, 14-17 (1965).
32. Hodgson, G.W., Kruyer, J., Roehl, A.A., Round, G.F., Ellis,  
H.S., J. Can. Petrol Tech. 6(1), 1 (1967).
33. Round, G.F., and Kruyer, J., Chem. Eng. Sci. 22, 1133 (1967).
34. Hodgson, G.W., and Jensen, E.J., Trans. J. 5, 31 (1966).
35. Jensen, E.J. and Ellis, H.S., Sci. Am. 216, 62 (1967).
36. Ellis, H.S., Paper 67-PET7, presented at Pet. Mech. Eng.  
Conf., Philadelphia Pa., Sept. 17-20 (1967).
37. Liddle, R.T., and Hodgson, G.W., Eng. J. 50, No. 12, (1967).
38. Ellis, H.S. and Liddle, R.T., Papers, Eighth Annual meeting  
Transportation Research Forum 411 (1967).
39. Suhr, R.W., M.Sc. Thesis, Mech. Eng. Worcester Polytechnic  
Institute (1965).





40. Jonsson, V.K. and Sparrow, F.M., J. Fluid Mech. 25, 65 (1966).
41. Couette, M. Ann. Chem. Phys. 6 433 (1890)
42. Heyda, J.F., General Electric Co. report, APEX-391 (1958).
43. Hinze, J.O. Turbulence McGraw-Hill (1959).
44. Robertson, J.M., Proc. 6th Midwestern Conference on Fluid Mechanics,  
169 (1959).
45. Von Karman, T., Jour. Aero. Sci. 4, 131 (1937).
46. Pai, S.I. Jour. Appl. Mechs., Tr ASME 75, 109 (1953).
47. Munk, M.M., Catholic Univ. of Am. Report (June 1955).
48. Wu, Yau, M.Sc. Thesis TAM Dept. Graduate College, Univ.  
of Ill. (1958).
49. Squire, W., Appl. Sci. Res. 9, 393 (1960).



Velocity Calibrations Table A-1

Orifice Size	Orifice Chart Rdg.	$\Delta P$ Orifice in. of $H_2O$	$\Delta P$ Chart rdg.	in. of $H_2O$ $\Delta P$	Weight lbs.	Time Sec.	$V_{av}$ ft./sec.	Temp. OF
2" cell								
3/16"	90.0	178.0	4.5	.145	10.25	44.943	.392	78°
	74.5	146.5	3.9	.130	10.25	49.981	.352	78°
	73.0	144.0	3.6	.125	10.25	50.444	.347	78°
	44.6	87.5	1.9	.090	10.25	67.955	.259	78°
	24.7	47.5	-	-	10.25	87.528	.202	78°
	9.8	17.5	-	-	10.25	118.329	.148	78°
	98.5	189.0	4.0	.135	35.25	150.390	.404	78°
	54.0	106.0	1.6	.085	35.25	200.797	.302	78°
	14.5	27.0	-	-	35.25	361.750	.169	78°
	97.5	193.0	13.3	.325	35.25	83.626	.728	78°
	50.0	98.0	6.5	.185	35.00	118.027	.512	78°
	10.3	18.6	1.0	.075	35.75	256.414	.241	78°
1/4"	36.0	70.0	5.4	.165	10.15	39.829	.437	78°
	19.8	37.8	2.8	.110	10.15	54.228	.322	78°
	12.4	22.5	1.7	.090	10.15	69.011	.252	78°
	93.0	184.0	13.6	.033	10.15	24.469	.713	78°
	70.5	138.5	10.2	.026	10.15	28.479	.613	78°
	74.5	146.0	50.0	1.060	10.15	12.303	1.418	79°
	53.5	104.5	39.5	.848	10.15	14.561	1.199	79°
	33.8	65.5	25.2	.560	10.15	18.417	.945	79°
	17.5	33.0	13.3	.325	10.15	25.839	.675	79°
	87.0	172.0	63.0	1.315	10.15	11.500	1.515	79°
	74.5	146.0	50.0	1.060	10.15	12.303	1.418	79°
	53.5	104.5	39.5	.848	10.15	14.561	1.199	79°
	33.8	65.5	25.2	.560	10.15	18.417	.945	79°
	17.5	33.0	13.3	.325	10.15	25.839	.675	79°
	87.0	172.0	63.0	1.315	10.15	11.500	1.515	79°
3/8"	74.5	146.0	50.0	1.060	10.15	12.303	1.418	79°
	53.5	104.5	39.5	.848	10.15	14.561	1.199	79°
	33.8	65.5	25.2	.560	10.15	18.417	.945	79°
	17.5	33.0	13.3	.325	10.15	25.839	.675	79°
	87.0	172.0	63.0	1.315	10.15	11.500	1.515	79°
	74.5	146.0	50.0	1.060	10.15	12.303	1.418	79°
	53.5	104.5	39.5	.848	10.15	14.561	1.199	79°
	33.8	65.5	25.2	.560	10.15	18.417	.945	79°
	17.5	33.0	13.3	.325	10.15	25.839	.675	79°
	87.0	172.0	63.0	1.315	10.15	11.500	1.515	79°
	74.5	146.0	50.0	1.060	10.15	12.303	1.418	79°
	53.5	104.5	39.5	.848	10.15	14.561	1.199	79°
	33.8	65.5	25.2	.560	10.15	18.417	.945	79°
	17.5	33.0	13.3	.325	10.15	25.839	.675	79°
	87.0	172.0	63.0	1.315	10.15	11.500	1.515	79°



3/8

70.0	137.5	51.0	1.075	10.15	12.839	1.359	79°
87.2	172.0	53.5	1.130	35.250	39.833	1.518	79°
42.7	83.5	27.5	.605	35.250	58.917	1.048	79°
14.2	26.5	9.5	.245	35.250	100.132	.604	79°

20" cell

1/2"

61.0	120.0	11.6	2.320	18.25	14.147	2.210	78°
43.5	85.0	8.8	1.760	18.25	16.230	1.925	78°
29.0	56.0	6.0	1.200	18.25	20.255	1.540	78°
19.6	37.0	4.2	.900	18.25	24.645	1.268	78°
92.0	182.0	16.4	3.300	35.25	22.135	2.740	78°

76.0	150.0	13.6	2.730	36.25	24.653	2.520	78°
59.0	116.0	10.8	2.180	36.25	28.493	2.180	78°
38.6	75.2	7.3	1.500	36.25	34.814	1.785	78°
10.5	19.0	21.5	.490	35.25	66.587	.909	78°
19.0	36.0	39.0	.835	18.25	24.911	1.255	78°
12.4	22.5	26.0	.575	18.25	30.784	1.019	78°

3/4"

20" cell

86.5	170.5	83.5	16.700	17.85	4.660	6.600	78°
76.5	150.5	73.5	14.700	17.85	4.951	6.200	78°
59.5	116.5	58.5	11.700	17.85	5.615	5.470	78°
46.0	90.0	46.6	9.320	17.85	6.256	4.910	78°
9.8	17.5	11.2	2.250	17.85	14.252	2.055	78°
20.3	39.0	22.0	4.400	17.85	9.358	3.280	78°
35.0	68.0	36.2	7.250	17.85	7.131	4.310	78°
10.5	19.0	11.9	2.380	35.25	26.536	2.285	78°
45.5	89.0	46.0	9.200	35.25	12.475	4.855	78°
91.0	180.0	86.0	17.200	35.25	9.193	6.600	78°

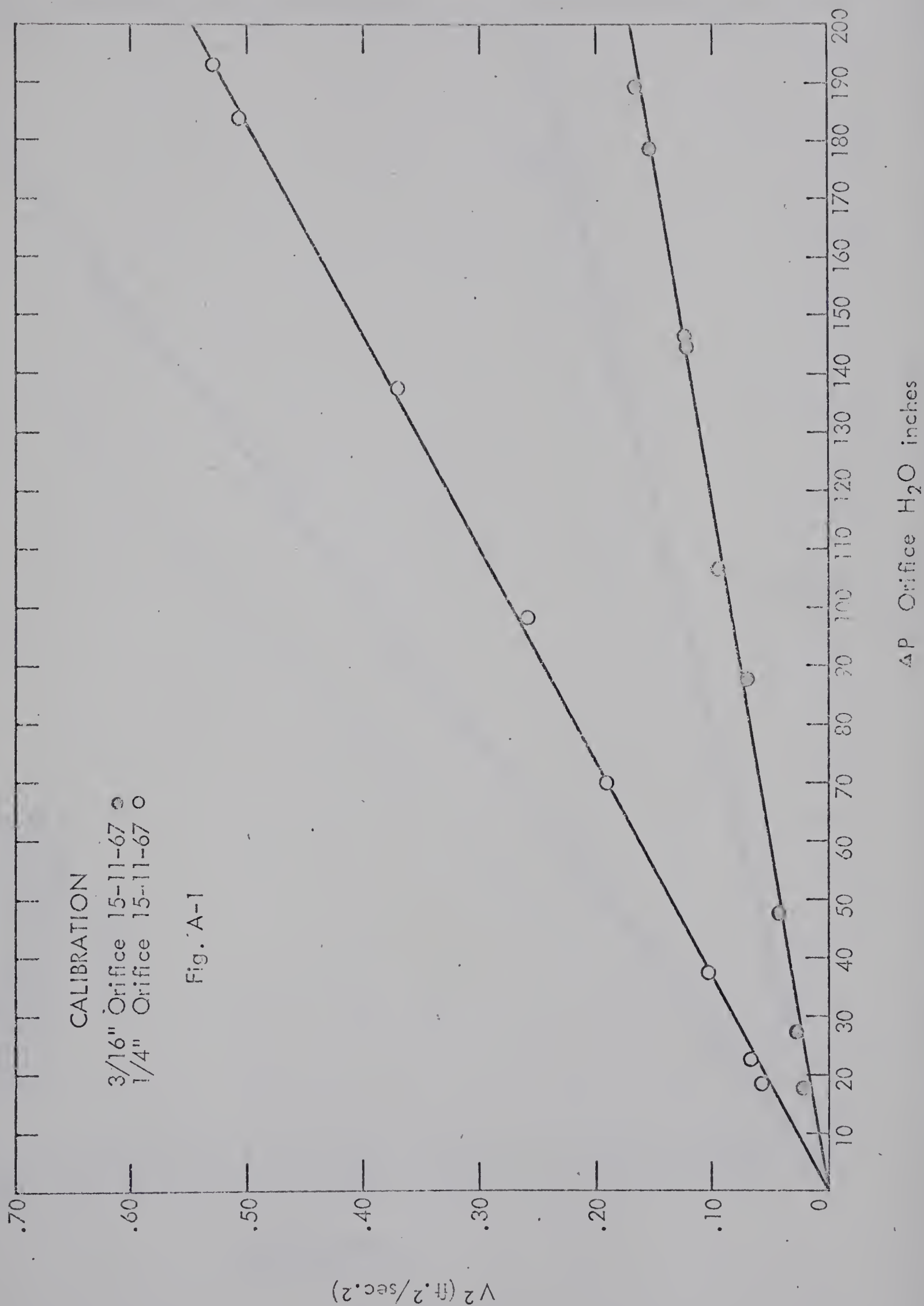


1"

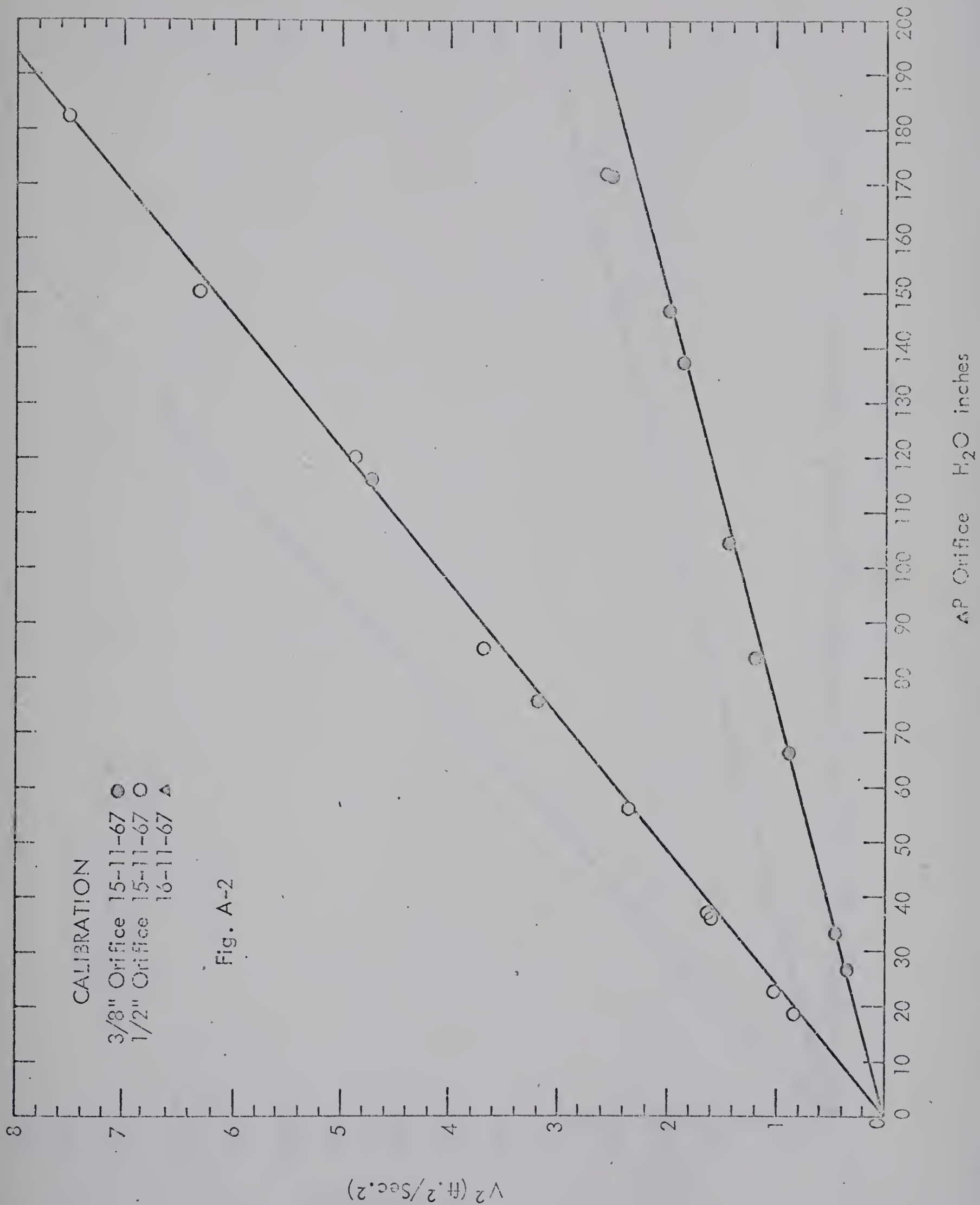
13.6	25.5	46.0	9.20	35.25	11.444	5.280	78°
28.5	55.0	92.5	18.50	35.25	8.917	6.790	78°
53.5	105.0	-	-	35.25	6.069	9.980	78°
74.6	147.0	-	-	35.25	5.153	11.710	78°
29.6	57.5	-	-	3.25	8.770	7.100	78°
50.0	98.0	-	-	36.25	5.460	9.620	78°













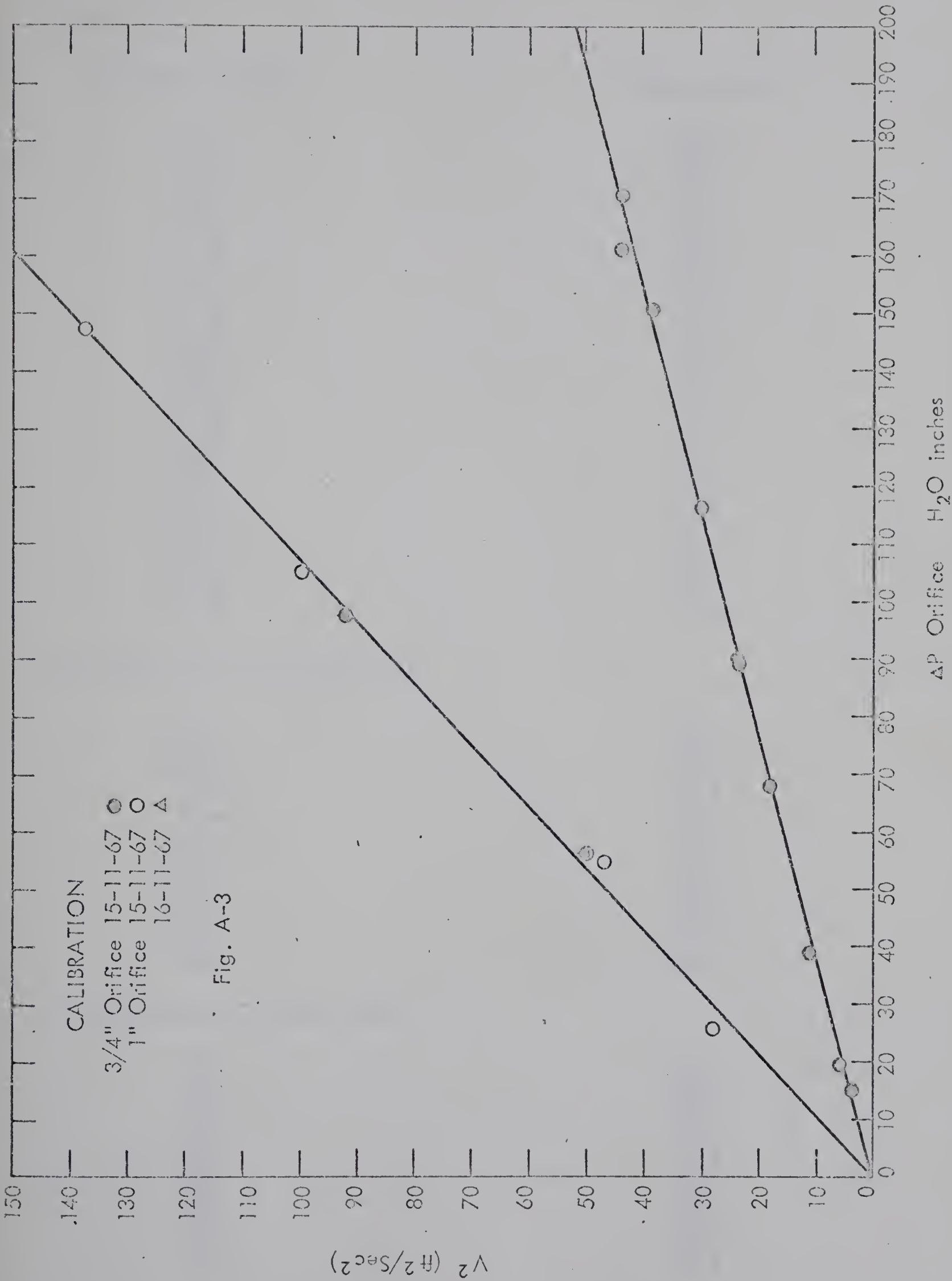






Table A-2

Calibration of Differential Pressure Cells

## 200" Cell

<u>Manometer Reading</u>	<u>Chart Reading</u>
123.60	63.0
95.60	49.2
66.90	34.7
53.90	28.1
32.35	17.0
21.90	11.8
121.30	62.0
110.20	56.3
99.55	51.2
88.23	45.5
67.59	35.1
77.28	39.9
54.96	28.8
45.50	24.0
34.13	18.0
22.45	12.0
11.32	6.2
109.30	56.2
68.30	35.4
34.50	18.2
11.37	6.8

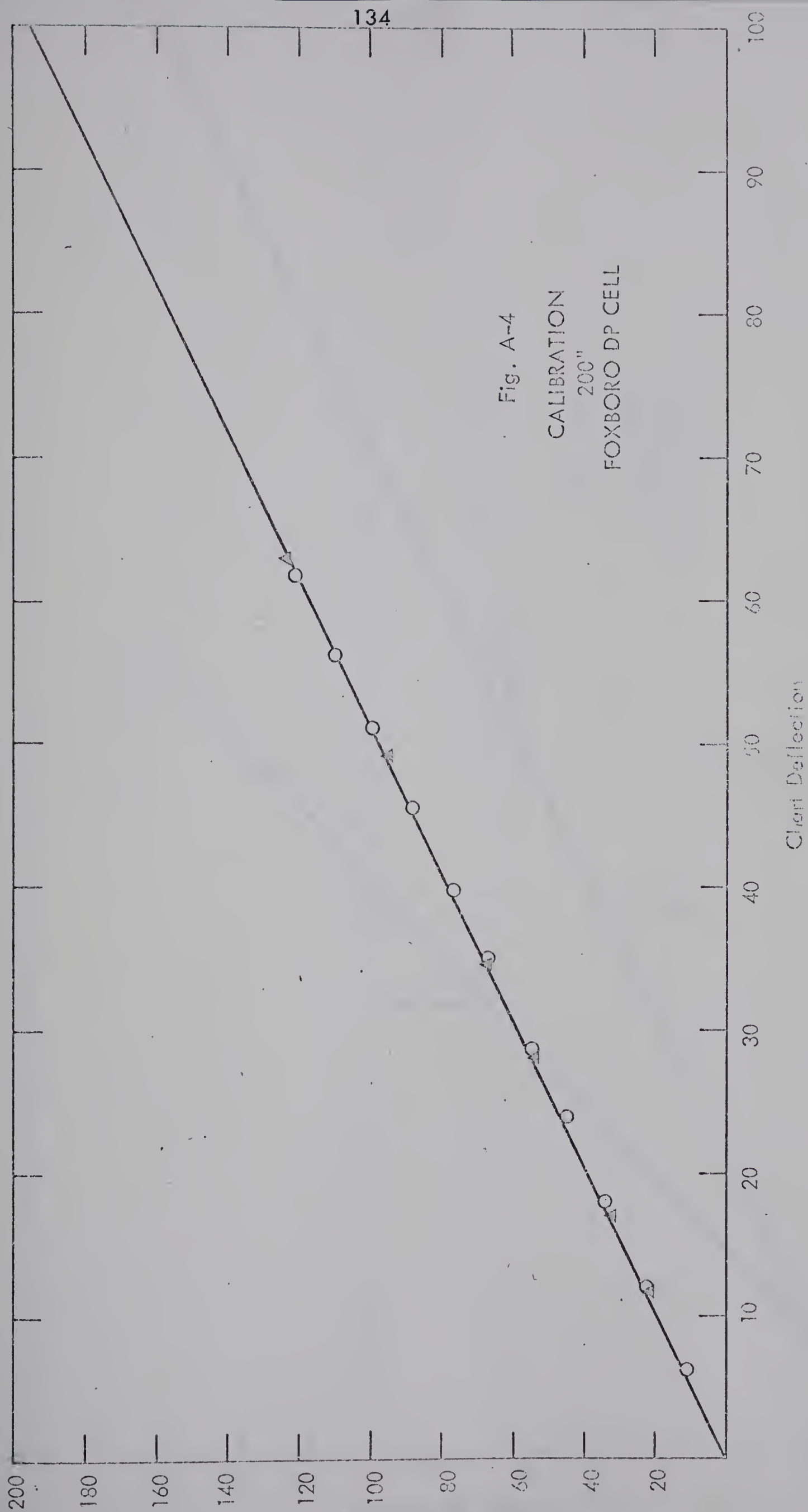
## 20" Differential Pressure Cell

11.03	55.6
15.19	77.0
19.63	99.2
7.10	35.2
2.90	14.0
3.50	17.5
10.51	53.0
13.13	66.0
15.74	79.0
19.51	97.5
6.25	31.1

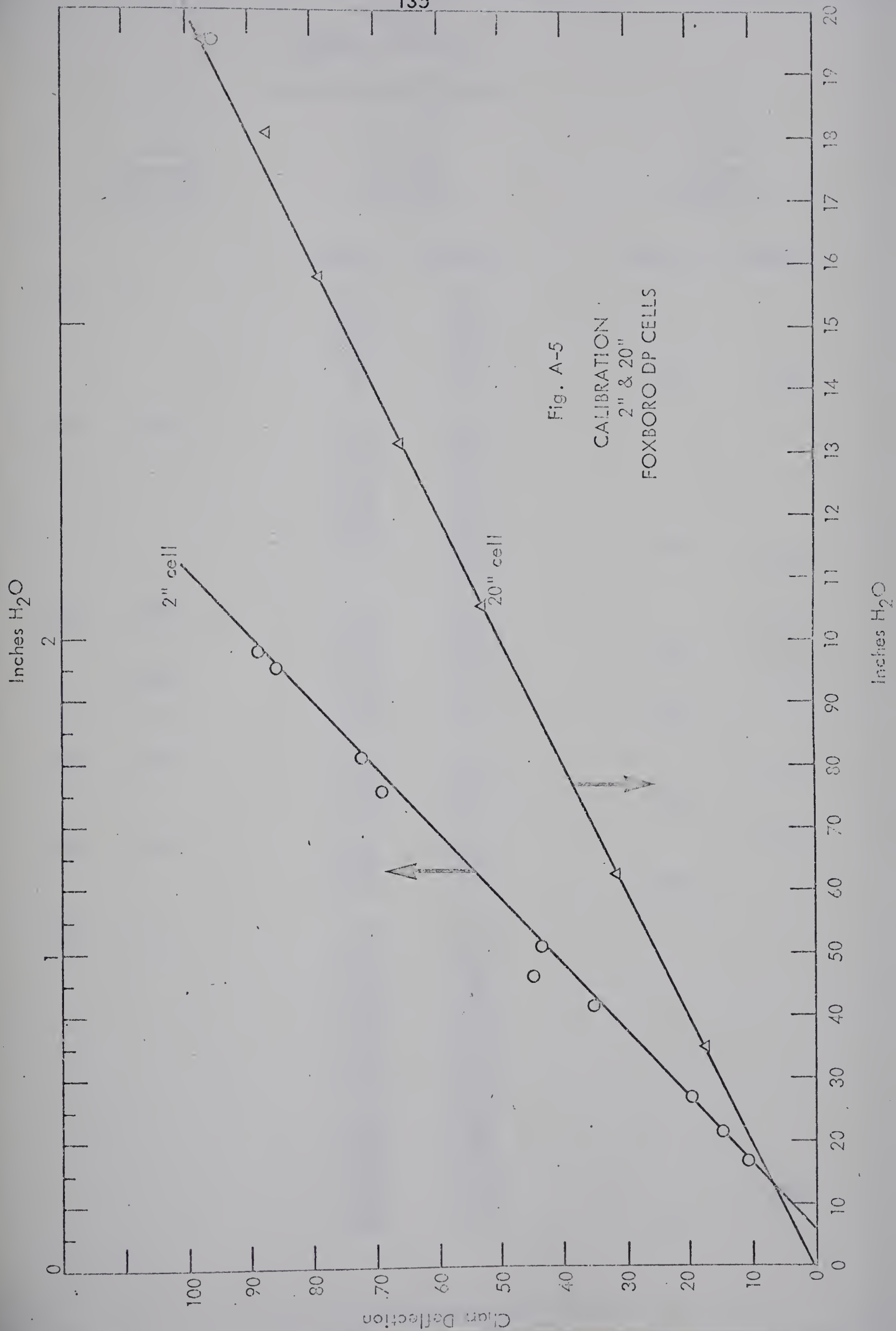
## 2" Differential Pressure Cell

0.92	45.0
1.51	69.0
1.96	89.0
0.75	28.0
0.43	14.6
1.91	85.5
1.62	72.5
1.02	43.2
.83	35.3











## APPENDIX Table A-3

Calibration of Cameras

k	Actual Clearance Thousandths of in.	Measured on Photo Thousandths of in.		Mean Value Thousandths of in.	
		<u>Camera 1</u>	<u>Camera 2</u>	<u>Camera 1</u>	<u>Camera 2</u>
.702	0	.230	.310		
		.235	.318		
		.249	.312		
		.249	.328		
		.263	.312	.245	.316
.702	.00475	.320	.408		
		.310	.400		
		.359	.419		
		.328	.455		
		.328	.420		
		.286	.450		
		.307	.440	.325	
			.410		.425
.702	.0100	.455	.648		
		.370	.526		.602
		.449	.636	.425	
	.0200	.605	.760		
		.655	.860		.811
		.627	.813	.628	
.702	.0295	.810	.990		
		.735	.985		1.012
		.737	1.061	.761	
.702	.0400	1.035	1.420		1.385
		1.045	1.420		
		1.105	1.315	1.062	
.802	.0	.195	.275		
		.177	.300		
		.240	.293		
		.185	.280		
		.215	.270		
		.205	.275		
		.182	.286		
		.212	.262		
			.253		
		.120	.342		
		.200	.287		
		.226	.300		
		.194	.270		
		.181	.246		.275
		.181	.181	.195	





k	Actual Clearance Thousandths of in.	Measured on Photo Thousandths of in.		Mean Value Thousandths of in.	
		<u>Camera 1</u>	<u>Camera 2</u>	<u>Camera 1</u>	<u>Camera 2</u>
.802	.0050	.230	.328		
		.228	.315		
		.247	.404		
		.212	.376		
		.248	.335		
		.285	.400		
		.243	.325	.243	
			.384		.365
.802	.0100	.380	.500		
		.400	.487		
		.375	.387		
		.348	.427		
		.367	.475		
		.255	.440		
		.405	.495		
		.295	.385		
		.309	.387		
		.370	.425		
			.435		
		.275	.425		.441
		.265	.467	.337	
.802	.0200	.518	.702		
		.540	.717		
		.595	.722		
		.672	.743		
		.630	.845		
		.560	.670		
		.443	.700		
		.490	.673		
		.467	.811		.726
		.525	.677	.544	
.802	.0300	.718	.935		
		.800	1.020		
		.739	.990		
		.750	.998		
		.705	1.173		
		.835	1.060		
		.724	.970		
		.623	.943		1.008
		.725	1.010		
		.698	1.080		
		.711	.914	.730	



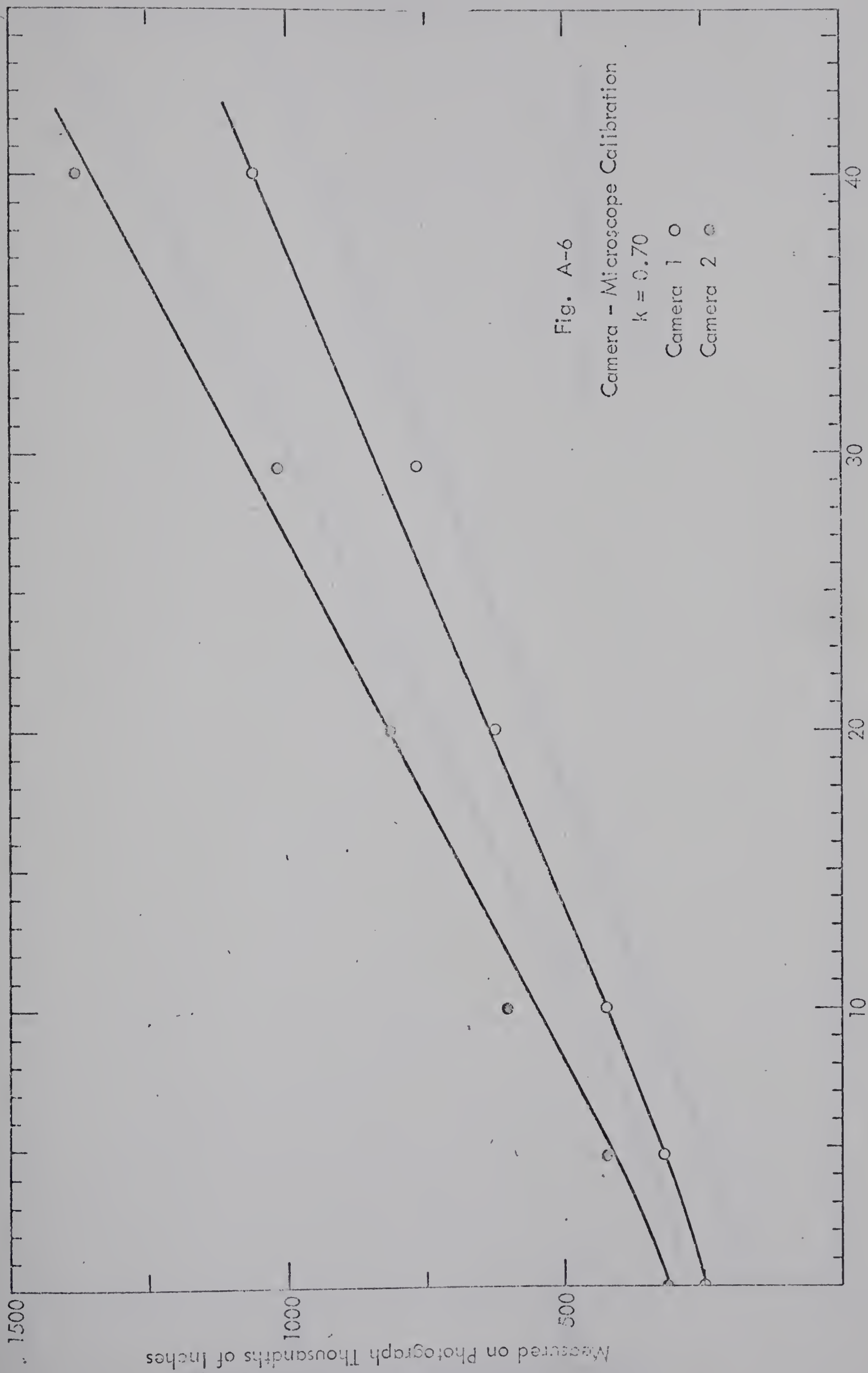
k	Actual Clearance Thousandths of in.	Measured on Photo Thousandths of in.		Mean Value Thousandths of in.	
		<u>Camera 1</u>	<u>Camera 2</u>	<u>Camera 1</u>	<u>Camera 2</u>
.802	.0400	.910	1.405		
		.885	1.208		
		.915	1.240		
		.842	1.265		
		1.007	1.461		
		.990	1.352		
		.880	1.195		
		.824	1.150		
		.890	1.180		
		.890	1.238		1.259
		.836	1.155	.897	
.901	.0	.173	.198		
		.110	.150		
		.145	.208		
		.140	.200		
		.124	.156		
		.099	.194		
		.145	.168		
		.175	.154		
		.156	.197		
		.204	.190		
			.174	.147	
			.263		.188
.901	.0045	.130	.220		
		.120	.193		
		.200	.196		
		.145	.324		
		.235	.207		
		.185	.349		
		.193	.272		.245
		.175	.201		
		.254			
		.220			
		.170			
		.180	.184		
.901	.0090	.265	.322		
		.285	.370		
		.325	.361		
		.180	.374		
		.323	.273		
		.232	.486		
		.330	.315		
		.330	.325		.347
		.260	.245	.281	
			.397		



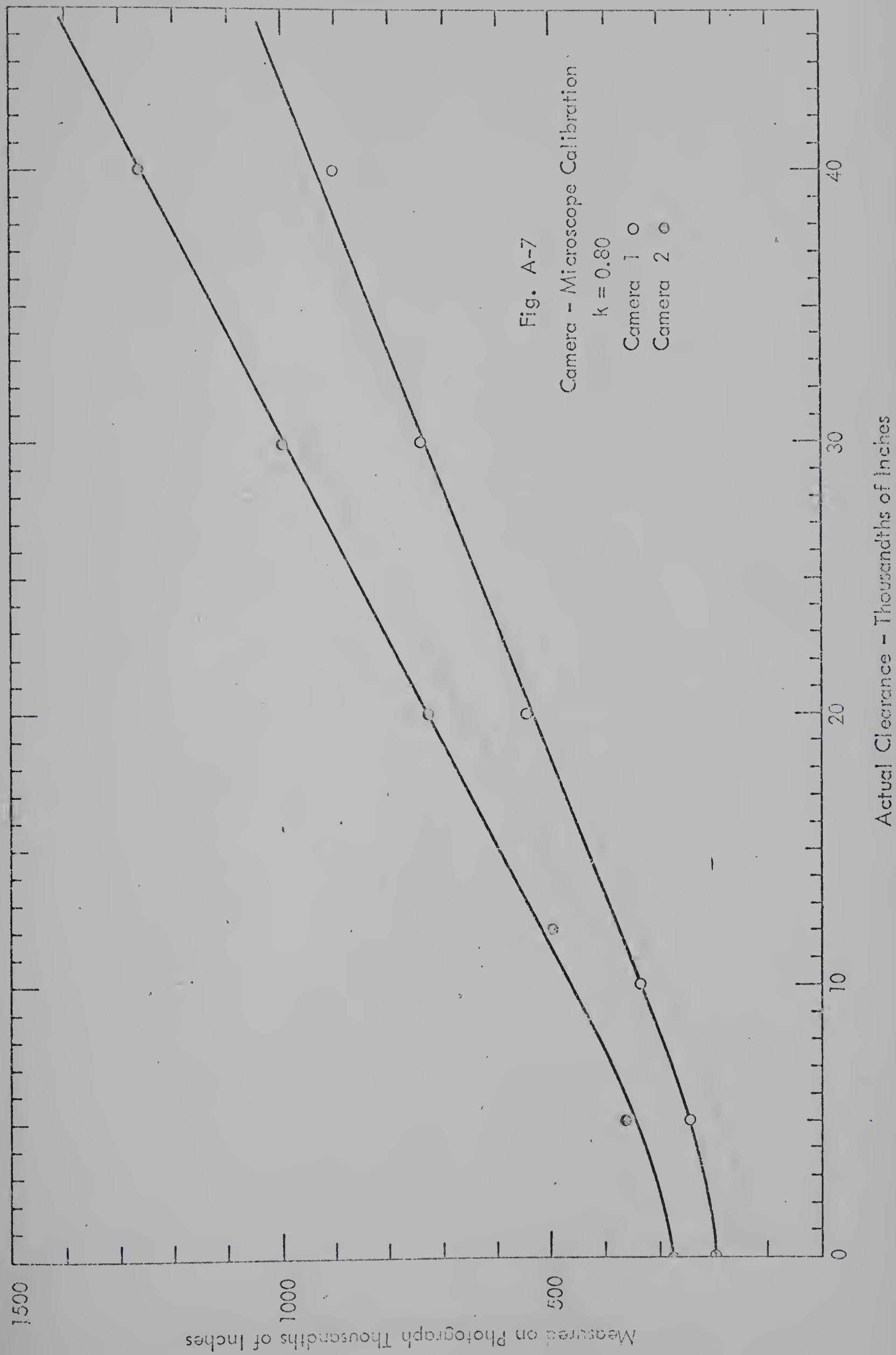
k	Actual Clearance Thousandths of in.	Measured on Photo Thousandths of in.		Mean Value Thousandths of in.	
		<u>Camera 1</u>	<u>Camera 2</u>	<u>Camera 1</u>	<u>Camera 2</u>
.901	.0200	.428	.580		
		.425	.620		
		.535	.547		
		.400	.550		
		.488	.550		
		.489	.673		
		.457	.817		.642
		.580	.748		
		.500	.712		
		.620	.593		
		.559	.668	.498	
.902	.0295	.805	.998		
		.663	1.015		
		.758	.816		
		.655	1.018		
		.860	.959		
		.710	.894		
		.809	.140		
		.620	.975		.956
		.770	.948		
		.685	.933	.734	



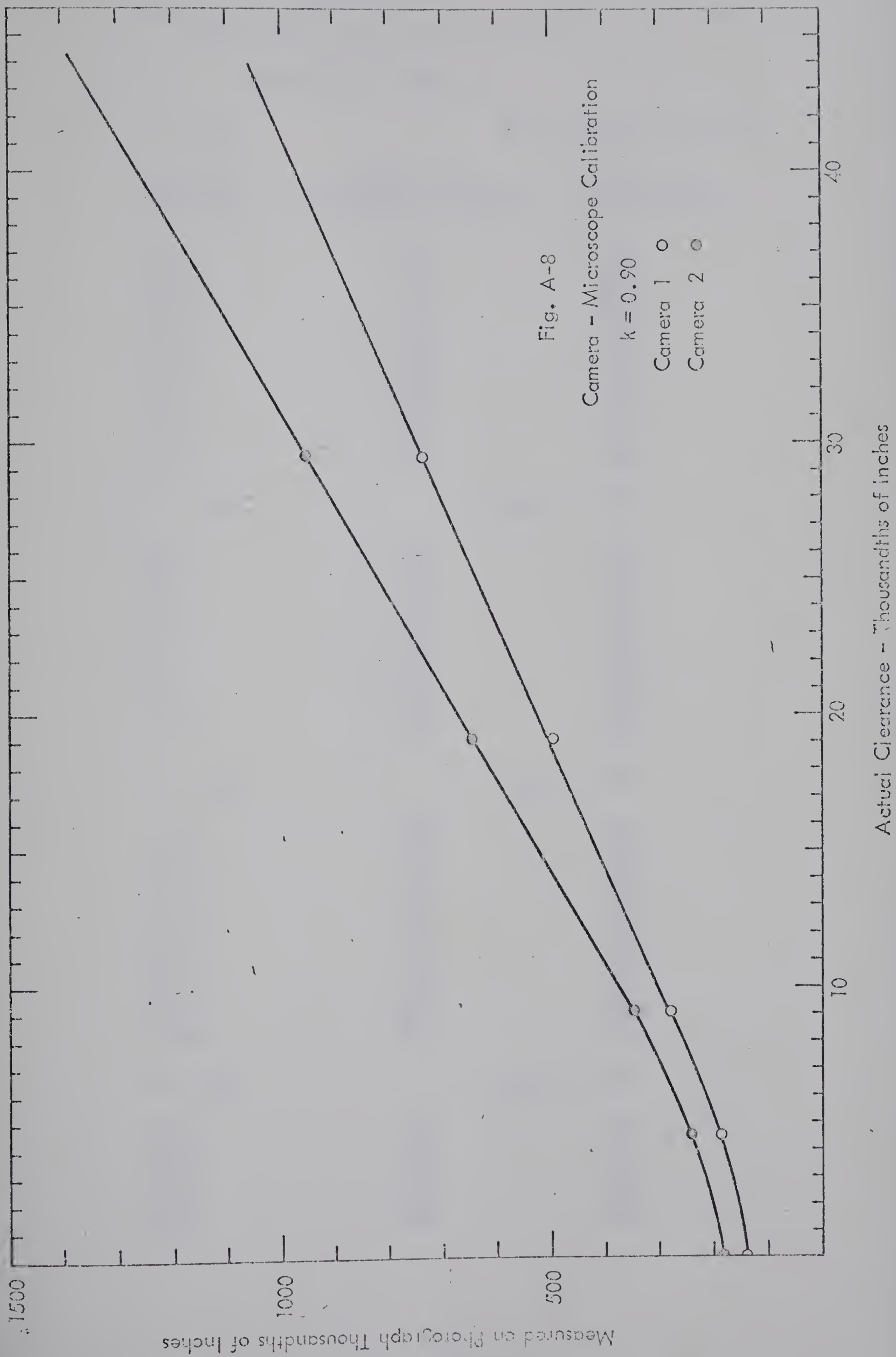














## APPENDIX A-4

## Basic Datic - Static Flow Patterns

## Separation - Velocity

$k = .625$

$dp-dc = 2300$  thousandths

Velocity ft./sec.	Separation thousandths of inches	Separation % of (dp-dc)
2.75	565	24.6
2.58	600	26.1
2.40	575	25.0
2.22	545	23.7
2.04	550	23.9
1.80	585	25.4
1.59	555	24.1
1.32	590	25.6
.95	555	24.1
.44	520	22.6

$k = .675$

$dp-dc = 1823$

2.64	525	28.8
2.50	545	29.9
2.34	545	29.9
1.95	545	29.9
1.71	560	30.7
1.47	565	31.0
1.17	502	27.5
.84	500	27.5
.48	550	30.2

$k = .718$

$dp-dc = 1574$

2.48	520	33.7
2.34	525	33.4
2.23	512	32.5
2.08	500	31.8
1.93	540	34.3
1.80	520	33.1
1.63	500	31.8
1.41	540	34.3
1.18	455	28.9
.82	405	25.7

$k = .765$

$dp-dc = 1308$

2.23	443	33.9
2.11	425	33.5
1.98	410	31.4
1.87	435	33.3
1.73	450	34.5





$$k = .765$$

$$d_p - d_c = 680 \text{ thousandths}$$

Velocity ft./sec.	Separation thousandths of inches	Separation % of $(d_p - d_c)$
1.313	161	23.7
1.168	183	26.7
1.049	210	30.9
.922	190	27.9
.686	188	27.6
.567	180	26.5
.400	165	24.3
.237	173	25.4
.242	160	23.5
.161	140	20.6
.139	180	20.5

$$k = .866$$

$$d_p - d_c = 218$$

1.262	120	32.0
1.139	140	37.5
1.028	105	28.0
.876	105	28.0
.715	105	28.0
.516	102	27.2
.502	100	26.7
.454	100	26.7
.265	97	25.8
.184	105	28.0
.161	105	28.0
.137	130	34.7
.137	110	29.3
.114	128	34.1
.114	135	36.0



# Vortex Dimensions & Stagnation Points

Film No. 11-8-67-2

Capsule Diameter = 1435

All measurements in  
thousandths of inches.k = .625      Capsule Diameter Corrected\* = 1650 = d<sub>c</sub>

Velocity ft./sec.	"X"	"X"/d <sub>c</sub> %	"Y"	Y Corr.	"Y" Corr. % d <sub>c</sub>	Stagnation Corr.	Stag. Corr. % d <sub>c</sub>
3.105	325	22.6	130	149	9.1	685	48.1
2.340	310	21.6	145	167	10.1	695	48.8
1.970	370	25.8	110	127	7.7	650	45.6
1.675	347	25.6	150	173	10.5	762	53.5
1.342	-	-	-	-	-	745	52.3
.985	300	20.9	125	144	8.7	725	50.9
.685	425	29.6	175	201	12.2	780	54.7
.551	303	21.1	157	181	10.9	755	53.0
.416	418	29.1	155	178	10.8	800	56.2
.296	420	29.2	250	288	17.4	833	58.5
.225	470	32.8	110	127	7.7	745	52.3
.115	430	30.0	215	247	15.0	798	56.0
3.000	-	-	-	-	-	610	42.8

Film No. 11-8-67-2

Capsule diameter = 1527

k = .675      Capsule diameter corrected = 1755 = d<sub>c</sub>

.098	535	30.5	265	293	17.3	963	63.5
.098	570	32.5	290	333	18.9	1015	66.5

Film No. 11-8-67-1

Capsule diameter = 1560

k = .675      Capsule diameter corrected = 1795 = d<sub>c</sub>

2.295	-	-	-	-	-	618	39.4
-------	---	---	---	---	---	-----	------

\* Corrected refers to multiplication of vertical  
measurements by .867 to account for distortion in  
vertical plane



Film No. 11-8-67-1

Capsule Diameter = 1560

All measurements in  
thousandths of inches.

k = .675

Capsule diameter corrected = 1795 = dc

Velocity ft./sec.	"X"	"X"/d <sub>c</sub> %	"Y"	Y Corr.	"Y" Corr. % dc	Stagnation Corr.	Stagnation Corr. % dc
2.415	-	-	-	-	-	780	50.0
1.970	395	21.5	147	169	9.4	810	52.0
1.678	-	-	-	-	-	775	49.7
1.272	-	-	-	-	-	750	48.1
.964	-	-	-	-	-	820	52.6
.697	240	13.4	185	203	11.9	670	43.0
.564	445	24.8	205	236	12.0	715	45.9
.454	350	19.5	170	195	10.9	685	45.0

Film No.  
k = .675

29-3-68

Capsule diameter = 1740

Capsule diameter corrected = 1998 = dc

2.810	280	14.0	170	195	9.9	780	44.8
2.680	-	-	-	-	-	720	41.4
2.495	220	11.0	170	195	9.9	730	41.9
2.315	330	16.5	210	241	12.1	780	44.8
2.115	350	17.5	200	230	11.5	830	47.7
1.922	380	19.0	170	195	9.1	850	48.9
1.731	360	18.0	220	253	12.5	900	51.7
1.462	440	22.0	250	287	14.4	880	50.6
.983	350	17.5	180	207	10.4	910	52.3
.506	620	31.0	280	322	16.1	1020	58.6
.040	550	27.5	350	402	20.1	1100	63.2





Film No. 11-8-67-1 All measurements Capsule diameter = 1670  
 k = .718 in thousandths of inches. Capsule diameter corrected = 1920 = dc

Velocity ft./sec.	"X"	"Y"/dc%	"Y"	Y Corr.	"Y" Corr.% dc	Stagnation Corr.	Stag. Corr.% dc
2.275	280	14.6	120	138	7.2	832	49.8
2.075	345	18.0	110	133	6.9	820	49.1
1.788	300	15.6	145	167	8.9	745	44.6
1.408	350	18.2	155	178	9.3	820	49.1
1.111	400	20.8	130	149	7.8	892	53.3
.701	-	-	-	-	-	800	47.9
.561	515	26.8	222	257	13.4	898	53.7
.465	470	24.5	238	274	14.3	832	49.8
.338	425	21.2	245	284	14.8	925	55.3
.225	510	26.6	325	373	19.4	992	59.4
.090	525	27.4	278	320	16.7	1005	60.2
.090	575	30.0	315	363	18.9	1058	63.3

Film No. A-10-1 Capsule diameter = 2285  
 k = .765 Capsule diameter corrected = 2630 = dc

1.313	510	19.4	205	236	23.6	1082	47.4
1.168	470	17.9	205	236	23.6	1092	48.0
1.049	485	18.4	285	328	32.8	1240	54.3
.922	455	17.8	275	316	31.7	1192	52.3
.686	-	-	-	-	-	1195	52.3
.851	-	-	-	-	-	1150	50.4
.567	550	20.9	215	247	24.8	1265	55.5
.598	580	22.1	235	270	27.1	1325	58.1
.400	555	21.1	260	299	29.9	1075	47.2
.349	685	26.1	155	178	17.8	860	37.7
.219	635	24.2	320	368	36.8	1120	49.1
.237	525	20.0	330	380	38.0	1160	50.8
.242	525	20.0	230	264	26.5	730	32.0



Film No. A-10-1 All measurements in Capsule diameter = 2285  
 k = 765 thousandths of inches. Capsule diameter corrected = 2630 =  $d_c$

Velocity ft./sec.	"X"	"X"/ $d_c$ %	"Y"	Y Corr.	"Y" Corr. % $d_c$	Stagnation	Stagnation	Stag. Corr. % $d_c$
.182	305	11.6	222	255	25.6	603	694	26.4
.201	890	33.9	335	386	38.6	1330	1530	58.3
.161	590	22.4	225	259	25.9	1127	1295	49.3
.134	590	22.4	305	351	35.1	1045	1203	45.8
.134	810	30.9	315	362	36.3	1333	1535	58.5
.139	675	25.7	395	454	45.5	1415	1628	62.0

Film No. A-3-1 Capsule diameter = 2357  
 k = .765 Capsule diameter corrected = 2710 =  $d_c$

2.225	360	13.3	267	307	11.3	1310	1508	55.7
2.075	480	17.7	310	356	13.1	1160	1335	49.3
1.740	293	10.9	300	345	12.7	1039	1194	44.1
1.950	457	16.9	316	363	13.4	1192	1372	50.7
1.505	440	16.3	300	345	12.7	1200	1380	51.1
1.205	233	8.2	233	268	9.8	745	858	31.7
1.046	580	21.4	355	408	15.1	1250	1439	53.1
.924	415	15.7	380	437	16.1	1225	1410	52.2
.778	480	17.4	275	316	11.7	1245	1432	53.0
.711	345	12.7	270	311	11.5	1365	1570	58.0
.442	657	24.3	425	488	18.0	1250	1440	53.1
.531	498	18.4	410	471	17.1	1210	1392	51.5
.951	520	19.2	295	339	12.5	1225	1410	52.2
.785	-	-	-	-	-	1240	1428	52.8
.710	392	14.5	257	296	11.0	1200	1380	51.1
.620	630	23.3	285	328	12.1	1220	1405	51.9
.458	232	8.2	237	273	10.1	1289	1471	54.8
.417	585	21.6	357	411	15.2	1318	1515	56.1
.359	487	17.9	345	397	14.6	1250	1439	53.1
.305	482	17.8	255	293	10.8	1255	1445	53.3



Film No. A-3-1 All measurements in Capsule diameter = 2357  
 k = .765 thousandths of inches. Capsule diameter corrected = 2710 =  $d_c$

Velocity  
 ft./sec. "X" "X"/ $d_c$  "Y" Y Corr. "Y" Corr. % Stagnation Stagnation  $\frac{\text{Stag. Corr. \%}}{d_c}$

.285	645	23.8	343	394	14.5	1325	1525	56.3
.187	810	29.9	365	420	15.5	1355	1560	56.7
.090	680	25.1	418	481	17.7	1435	1650	61.0

Film No. A-10-2-1 Capsule diameter = 1550  
 k = .866 Capsule diameter corrected = 1782 =  $d_c$

1.262	235	13.2	150	172	9.7	675	776	43.5
1.139	180	10.1	150	172	9.7	675	776	43.5
1.028	160	8.9	120	138	7.8	580	667	37.4
.876	300	16.8	175	201	11.3	740	851	47.7
.715	285	16.0	160	184	10.3	675	776	43.5
.516	320	17.9	170	196	11.0	690	793	44.5
.502	330	18.5	185	213	11.9	-	-	-
.454	310	17.4	155	178	10.0	640	736	41.3
.390	440	24.7	225	259	14.5	775	892	50.0
.278	400	22.4	265	305	17.1	830	955	53.6
.276	280	15.7	210	241	13.6	700	805	45.1
.265	310	17.4	195	224	12.6	800	920	51.6
.230	300	16.8	235	270	15.2	740	851	47.7
.208	375	21.1	245	282	15.8	735	845	47.4
.208	280	15.7	215	248	13.9	715	822	46.1
.184	460	25.8	290	334	18.7	890	1023	57.4
.184	380	21.3	245	282	15.8	745	856	48.1
.161	360	20.2	250	288	16.2	780	897	50.3
.161	410	23.0	260	299	16.8	910	1046	58.6
.137	410	23.0	255	294	16.5	940	1080	60.6
.137	400	22.4	260	299	16.8	920	1058	59.4
.114	410	23.0	250	288	16.2	915	1052	59.0
.114	410	23.0	245	282	15.8	945	1087	61.0





Static Capsule Pressure Drops

Capsule	k	V <sub>av</sub> ft./sec.	Inches of Water $\Delta P_c$	Inches of Water $\Delta P_f$	Inches of Water $\Delta P_{c-f}$	Inches of Water $\Delta P_{c-f} \times \left( \frac{1-k^2}{k} \right)^2$
.866		.120	.220	.043	.177	.015
.866		.215	.430	.073	.357	.030
.866		.338	.805	.116	.689	.050
.866		.355	.880	.125	.755	.063
.866		.460	1.350	.175	1.175	.099
.866		.495	1.530	.200	1.330	.111
.866		.555	1.820	.232	1.588	.133
.866		.595	1.860	.260	1.600	.134
.866		.701	2.800	.335	2.465	.206
.866		.890	4.150	.480	3.670	.307
.866		1.180	7.200	.780	6.420	.537
.765		.103	.120	.036	.084	.025
.765		.235	.240	.075	.165	.048
.765		.420	.500	.156	.344	.101
.765		.465	.535	.180	.355	.108
.765		.735	1.070	.350	.720	.211
.765		.990	1.750	.585	1.160	.337
.765		1.010	1.800	.595	1.205	.350
.765		1.430	3.480	1.100	2.380	.691
.765		1.500	3.850	1.200	2.650	.770
.765		1.820	5.350	1.540	3.810	1.113
.765		1.960	6.200	1.900	4.300	1.257
.765		2.280	8.200	2.450	5.750	1.680
.718		.145	.140	.047	.093	.043
.718		.175	.160	.056	.104	.049
.718		.260	.218	.086	.132	.062
.718		.455	.430	.175	.255	.119
.718		.475	.460	.185	.275	.129
.718		.650	.720	.292	.428	.200
.718		.680	.780	.312	.468	.219
.718		.950	1.310	.535	.775	.362
.718		1.250	2.230	.870	1.360	.635
.718		1.420	2.600	1.100	1.500	.701
.718		1.880	4.400	1.750	2.650	1.238
.718		2.120	5.750	2.200	3.550	1.660
.718		2.320	6.750	2.550	4.200	1.965





Capsule k	$V_{av}$ ft./sec.	Inches of Water $\Delta P_c$	Inches of Water $\Delta P_f$	Inches of Water $\Delta P_{c-f}$	Inches of Water $\Delta P_{c-f} \times \left(\frac{1-k^2}{k}\right)^2$
.675	.460	.360	.175	.185	.121
.675	1.000	1.130	.590	.540	.355
.675	1.150	1.480	.760	.720	.474
.675	1.430	2.050	1.110	.940	.618
.675	1.630	2.530	1.410	1.120	.736
.675	1.920	3.400	1.850	1.550	1.020
.675	1.930	3.500	1.870	1.630	1.072
.675	2.350	5.200	2.630	2.570	1.690
.675	2.620	6.300	3.150	3.150	2.070
.625	.120	.120	.040	.080	.076
.625	.228	.170	.074	.096	.091
.625	.335	.220	.115	.105	.100
.625	.550	.400	.230	.170	.162
.625	1.020	1.010	.620	.390	.371
.625	1.280	1.400	.900	.500	.476
.625	1.650	2.200	1.400	.800	.762
.625	1.950	3.050	1.880	1.170	1.113
.625	2.320	4.150	2.530	1.620	1.542
.625	2.680	5.500	3.280	2.220	2.115
.625	3.050	6.900	4.100	2.800	2.650
.625	3.280	8.400	4.600	3.800	3.620



## APPENDIX A-5

## BASIC DATA - CAPSULE CLEARANCES

<u>Heading</u>	<u>Column Letter</u>	<u>Explanation</u>
	A	Symbol indicating Full View Run 1 or Microscope Run 2
	B	Run No.
	C	Capsule Length, $L_c$ , in inches
	D	Capsule diameter ratio $k$
	E	Capsule density ratio $\frac{\sigma-\rho}{\rho}$

A	B	C	D	E
2	192	6.000	.902	1.020

<u>Data</u>	<u>Column Letter</u>	<u>Explanation</u>
	F	Symbol 1 means capsule end No. 1 downstream  Symbol 2 means capsule end No. 2 downstream
	G	Liquid velocity - $V_{av}$ ft./sec.
	H	Capsule velocity - $V_c$ ft./sec.
	I	Capsule nose clearance $\frac{C_N}{d_p}$
	J	Capsule tail clearance $\frac{C_T}{d_p}$
	K	Capsule Angle $\theta$ in radians negative sign means tail higher than nose
	L	Liquid pressure gradient $(\frac{\Delta P}{L})_f$ <u>ft. of water</u> ft.
	M	Symbol indicating pressure cell used  1 = 2" range cell 2 = 20" range cell 3 = no pressure reading taken
	N	Capsule pressure gradient $(\frac{\Delta P}{L})_{c-f}$ = total pressure gradient minus liquid pressure gradient

F	G	H	I	J	K	L	M	N
1	.984	.991	.0041	.0034	.00015	.00421	1	.01026



1 146 3.003 .901 1.000

1	.536	.571	.0180	.0180	0.00000	.00143	3	0.00000
2	.536	.570	.0325	.0201	.00543	.00143	3	0.00000
1	.976	1.051	.0850	.0451	.01738	.00415	3	0.00000
2	.966	1.018	.0866	0.0000	.03802	.00407	3	0.00000
1	1.394	1.491	.0625	.0375	.01086	.00781	3	0.00000
2	1.396	1.466	0.0000	0.0000	0.00000	.00783	3	0.00000
1	1.906	2.054	.0728	.0628	.00434	.01361	3	0.00000
2	1.906	2.028	0.0000	0.0000	0.00000	.01361	3	0.00000
1	2.561	2.758	.0602	.0652	-.00217	.02300	3	0.00000
2	2.557	2.739	0.0000	0.0000	0.00000	.02293	3	0.00000
1	3.458	3.753	.0437	.0487	-.00217	.03918	3	0.00000
2	3.458	3.761	0.0000	.0598	-.02608	.03918	3	0.00000
1	4.658	5.124	.0537	.0961	-.01847	.06649	3	0.00000
2	4.647	5.088	.0200	.0436	-.01032	.06621	3	0.00000
1	5.922	6.507	.0150	.0436	-.01249	.10181	3	0.00000
2	5.922	6.529	.0300	.0399	-.00434	.10181	3	0.00000
1	7.121	7.862	0.0000	.0249	-.01086	.14125	3	0.00000
2	7.103	7.851	.0212	.0299	-.00380	.14062	3	0.00000

1 150 3.003 .901 1.010

2	.229	.411	0.0000	0.0000	0.00000	.00031	1	.01198
1	.797	.818	0.0000	0.0000	0.00000	.00289	1	.00932
2	.793	.849	.0402	0.0000	.01789	.00287	3	0.00000
1	.996	1.074	.0314	0.0000	.01398	.00430	3	0.00000
2	.990	1.038	.0320	0.0000	.01398	.00425	3	0.00000
1	1.232	1.303	.0294	0.0000	.01286	.00628	3	0.00000
2	1.239	1.327	.0538	.0192	.01509	.00633	3	0.00000
1	1.449	1.557	.0474	.0153	.01398	.00837	3	0.00000
2	1.452	1.560	.0782	.0320	.02013	.00839	3	0.00000
1	1.927	2.057	.0141	.0217	-.00335	.01387	3	0.00000
2	1.931	2.092	.0705	.0217	.02124	.01393	3	0.00000
1	1.692	1.807	.0871	.0192	.02963	.01102	3	0.00000
2	1.697	1.810	.0961	.0064	.03912	.01108	3	0.00000
1	2.604	2.808	.0736	.0602	.00583	.02368	3	0.00000
2	3.137	3.839	.0283	.0322	-.00167	.03295	3	0.00000
1	3.137	3.793	.0645	.0542	.00447	.03295	3	0.00000
1	4.419	5.161	.0576	.0448	.00559	.06055	3	0.00000





2 174 3.000 .901 1.010

1	.239	.235	0.0000	.0007	-.00429	.00034	1	.00733
2	.235	.226	0.0000	.0004	-.00418	.00033	1	.00733
1	.473	.483	0.0000	.0072	-.00418	.00115	1	.00733
2	.473	.506	.0417	.0071	.01511	.00115	1	0.00000
1	.785	.821	0.0000	.0135	-.00603	.00282	1	0.00000
2	.763	.808	.1002	0.0000	.04180	.00263	1	0.00000
1	.687	.712	.0225	.0121	.00453	.00222	1	0.00000
2	.685	.709	.0232	.0059	.00581	.00221	1	0.00000
1	.864	.929	.0292	.0117	.00767	.00334	1	0.00000

1 154 3.003 .901 1.020

1	.986	1.027	0.0000	0.0000	0.00000	.00422	1	.00532
2	.988	.970	0.0000	0.0000	0.00000	.00424	3	0.00000
1	1.194	1.281	0.0000	0.0000	0.00000	.00593	1	.00532
2	1.194	1.265	0.0000	0.0000	0.00000	.00593	1	.00599
1	1.433	1.460	0.0000	0.0000	0.00000	.00820	3	0.00000
1	1.431	1.540	.0877	0.0000	.03802	.00318	1	.01065
1	1.431	1.525	.0531	0.0000	.02300	.00018	1	.00799
2	1.431	1.522	.0567	0.0000	.02457	.00318	1	.01132
1	1.676	1.785	.0415	0.0000	.01798	.01033	1	.01332
2	1.676	1.779	.0566	0.0000	.02451	.01063	1	.01332
1	2.126	2.281	.0945	0.0000	.04093	.01652	3	0.00000
2	2.126	2.281	.0886	0.0000	.03333	.01652	3	0.00000
1	2.812	3.040	.0305	0.0000	.01324	.02715	3	0.00000
2	2.805	3.040	.0328	0.0000	.01423	.02703	3	0.00000
1	3.480	3.811	.0696	.0319	.01643	.03962	3	0.00000
2	3.480	3.783	.1012	.0233	.03395	.03962	3	0.00000
1	4.658	5.129	.0860	.0433	.01862	.06649	3	0.00000
2	4.658	5.101	.0886	.0572	.01369	.06649	3	0.00000
1	1.347	1.445	0.0000	0.0000	0.00000	.00735	3	0.00000
2	1.347	1.434	.0227	0.0000	.00986	.00735	1	0.00000

2 373 3.002 .902 1.020

1	.646	.664	.0101	0.0000	.00441	.00200	1	.00599
2	.646	.661	.0059	.0047	.00052	.00200	1	.00746
1	.832	.876	.0144	.0016	.00556	.00312	1	0.00000
2	.832	.865	.0046	.0035	-.00001	.00312	1	.00032



1 158 3.003 .902 1.050

1	1.437	1.452	0.0000	0.0000	0.00000	.00825	1	0.00000
2	1.420	1.511	0.0000	0.0000	0.00000	.00607	1	0.00000
1	1.632	1.717	0.0000	0.0000	0.00000	.01033	3	0.00000
2	1.632	1.743	0.0000	0.0000	0.00000	.01033	1	.00566
1	1.880	1.884	0.0000	0.0000	0.00000	.01328	1	.00999
2	1.884	1.895	0.0000	0.0000	0.00000	.01334	1	.07326
2	1.884	1.962	0.0000	0.0000	0.00000	.01334	3	0.00000
1	2.105	2.217	0.0000	0.0000	0.00000	.01623	2	.01332
2	2.105	2.230	0.0000	0.0000	0.00000	.01623	2	.01332
1	2.373	2.521	0.0000	0.0000	0.00000	.02009	2	.01332
2	2.373	2.571	.0666	0.0000	.02213	.02009	2	0.00000
1	2.580	2.776	.0524	0.0000	.02298	.02330	2	0.00000
2	2.572	2.791	.0430	0.0000	.01881	.02316	2	0.00000
1	2.812	3.057	.1037	0.0000	.04528	.02715	3	0.00000
2	2.819	3.064	.1009	0.0000	.04402	.02727	3	0.00000
1	3.480	3.783	.1009	0.0000	.04402	.03962	3	0.00000
2	3.480	3.788	.0480	0.0000	.02101	.03962	3	0.00000
1	4.658	5.092	.1013	.0206	.03520	.06649	3	0.00000

1 162 3.000 .902 1.100

1	2.541	2.693	0.0000	0.0000	0.00000	.02268	2	.02000
2	2.541	2.631	0.0000	0.0000	0.00000	.02268	2	.06666
1	2.841	3.001	0.0000	0.0000	0.00000	.02765	2	.05333
2	2.841	2.986	0.0000	0.0000	0.00000	.02765	2	.06666
1	3.030	3.199	0.0000	0.0000	0.00000	.03100	2	.06666
2	3.030	3.274	.0401	0.0000	.01754	.03100	2	.04000
1	3.293	3.484	0.0000	0.0000	0.00000	.03594	2	.06666
2	3.293	3.549	.0443	0.0000	.01964	.03594	2	.02666
1	3.516	3.776	0.0000	0.0000	0.00000	.04036	2	.03333
2	3.501	3.741	0.0000	0.0000	0.00000	.04006	2	.06666
1	3.792	4.044	0.0000	0.0000	0.00000	.04615	2	.03333
2	3.799	3.939	0.0000	0.0000	0.00000	.04630	2	.13333
1	4.043	4.401	.0818	0.0000	.03578	.05172	2	.02666
2	4.031	4.351	.0884	0.0000	.03386	.05143	2	.02666
1	4.250	4.569	0.0000	0.0000	0.00000	.05651	2	.06666
2	4.232	4.533	0.0000	0.0000	0.00000	.05609	2	.06666
1	4.685	5.166	.0909	0.0000	.03975	.06717	2	0.00000
2	4.685	5.120	.0653	0.0000	.02856	.06717	2	.03333
1	5.814	6.377	.0263	0.0000	.01149	.09856	2	0.00000
2	5.636	6.377	.0974	0.0000	.04258	.09921	2	0.00000



2 170 3.000 .901 1.100

1	.550	.506	0.0000	0.0000	0.00000	.00150	1	.03600
1	.541	.495	0.0000	0.0000	0.00000	.00145	1	.03600
1	1.003	1.003	0.0000	0.0000	0.00000	.00435	1	.02600
1	2.614	3.001	0.0000	.0050	-.00430	.02719	2	0.00000
1	3.096	3.272	.0312	0.0000	.01478	.03220	2	.03466
1	3.316	3.551	.0414	0.0000	.02320	.03633	3	0.00000

2 172 3.000 .900 1.100

1	1.880	1.881	.0070	0.0000	.00542	.01328	1	.08666
2	1.882	1.996	.0115	0.0000	.00234	.01331	1	.00733
1	2.360	2.473	.0070	.0048	.00093	.01988	2	.05400
2	2.360	2.387	.0070	0.0000	.00344	.01938	2	.11066
1	2.796	2.871	0.0000	.0139	-.00607	.02688	2	.11056
2	2.805	2.975	.0218	0.0000	.01414	.02703	2	.03333
1	3.096	3.277	.0549	0.0000	.04199	.03220	3	0.00000
2	3.096	3.294	.0089	.0053	.00157	.03220	2	.02666

1 166 3.000 .901 1.150

1	3.523	3.786	0.0000	0.0000	0.00000	.04050	2	.02000
2	3.523	3.761	0.0000	0.0000	0.00000	.04050	2	.05666
1	3.779	4.032	0.0000	0.0000	0.00000	.04586	2	0.00000
2	3.779	4.099	0.0000	0.0000	0.00000	.04586	2	.02000
1	4.037	4.368	0.0000	0.0000	0.00000	.05158	2	.02000
2	4.037	4.384	0.0000	0.0000	0.00000	.05158	2	0.00000
1	4.250	4.606	.1060	0.0000	.04632	.05651	2	0.00000
2	4.256	4.639	.1060	0.0000	.04632	.05665	2	0.00000
1	4.470	4.839	0.0000	0.0000	0.00000	.06180	2	0.00000
2	4.470	4.872	0.0000	0.0000	0.00000	.06180	2	0.00000

2 168 3.000 .901 1.150

1	1.958	1.962	.0042	0.0000	.00289	.01428	1	.03333
2	1.958	1.971	.0042	0.0000	.00231	.01428	1	.04000
1	2.541	2.628	.0038	0.0000	.00197	.02268	2	.05333
2	2.551	2.605	0.0000	.0056	-.00289	.02284	2	.06666
1	3.239	3.430	0.0000	.0033	-.00231	.03490	2	.02000
2	3.232	3.441	.0008	.0093	-.00371	.03475	2	.01333





1 147 6.000 .901 1.000

1	7.096	7.894	0.0000	.0450	-.00983	.14037	3	0.00000
2	7.103	7.916	.0160	.0223	-.00135	.14062	3	0.00000
1	5.875	6.514	.0450	.0450	0.00000	.10030	3	0.00000
2	5.866	6.463	.0597	.0509	.00191	.10012	3	0.00000
1	4.685	5.143	0.0000	0.0000	0.00000	.06717	3	0.00000
1	4.674	5.189	.0109	.0424	-.00688	.06690	3	0.00000
2	4.685	5.194	.0366	.0397	-.00068	.06717	3	0.00000
1	3.573	3.936	.0731	.0649	.00178	.04152	3	0.00000
2	3.573	3.936	.0506	.0315	.00418	.04152	3	0.00000
1	2.565	2.816	.0889	.0537	.00770	.02305	3	0.00000
2	2.572	2.821	.0644	.0276	.00804	.02318	3	0.00000
1	1.935	2.100	.0902	.0744	.00346	.01398	3	0.00000
2	1.937	2.104	.0925	.0286	.01393	.01401	3	0.00000
1	1.459	1.574	.0297	0.0000	.00655	.00847	3	0.00000
2	1.406	1.528	.0856	.0518	.00737	.00793	3	0.00000
1	1.003	1.073	.0937	.0537	.00874	.00435	3	0.00000
2	1.012	1.101	.0297	.0247	.00109	.00442	3	0.00000
1	.587	.611	.0833	.0532	.00655	.00168	3	0.00000
2	.589	.630	.0250	.0250	0.00000	.00169	3	0.00000

1 151 6.000 .901 1.010

2	4.712	5.227	.0410	.0410	0.00000	.06786	3	0.00000
1	3.551	3.872	.0880	0.0000	.01932	.04109	3	0.00000
2	3.551	3.909	.0509	0.0000	.01104	.04109	3	0.00000
1	2.576	2.791	.0975	0.0000	.02180	.02323	3	0.00000
2	2.565	2.787	.1006	0.0000	.02203	.02305	3	0.00000
1	2.325	2.336	.0594	0.0000	.01297	.01937	3	0.00000
2	2.325	2.316	.1012	0.0000	.02208	.01937	3	0.00000
1	1.873	1.991	.0113	0.0000	.00248	.01326	3	0.00000
2	1.873	2.032	.1012	0.0000	.02208	.01320	3	0.00000
1	1.692	1.831	.0473	0.0000	.01021	.01102	1	-.00500
2	1.692	1.837	.0443	0.0000	.00966	.01102	1	-.00500
1	1.426	1.577	.0369	0.0000	.00800	.00813	1	-.00333
2	1.420	1.567	.0192	0.0000	.00414	.00807	1	-.00333
1	1.215	1.313	.0277	0.0000	.00607	.00612	1	0.00000
2	1.215	1.304	0.0000	0.0000	0.00000	.00612	3	0.00000
1	.999	1.037	0.0000	0.0000	0.00000	.00432	1	.00866
2	1.001	1.044	0.0000	0.0000	0.00000	.00434	1	.00866
1	.800	.827	0.0000	0.0000	0.00000	.00291	1	.00866





2 193 6.000 .901 1.010

1	.629	.544	.0068	0.0000	.00202	.00190	1	.00533
1	.874	.905	.0078	0.0000	.00232	.00341	1	.00716
2	.874	.927	.0090	.0039	.00110	.00341	1	0.00000
1	1.193	1.284	.0243	.0113	.00232	.00592	1	-.00316
2	1.193	1.280	.0234	.0058	.00385	.00592	1	-.00166
1	1.429	1.544	.0460	.0072	.00346	.00316	1	-.00416
2	1.427	1.542	.0441	.0166	.00599	.00315	1	-.00460

2 302 6.000 .901 1.010

1	.743	.761	.0038	0.0000	.00244	.00255	1	.00833
2	.743	.771	0.0000	.0016	-.00053	.00255	3	0.00000
1	1.056	1.136	.0193	.0055	.00301	.00477	1	-.00166
2	1.056	1.131	.0143	.0091	.00114	.00477	1	-.00166
1	1.257	1.351	.0179	.0127	.00112	.00650	1	-.00343
2	1.256	1.354	.0285	.0099	.00404	.00649	1	-.00333
1	1.431	1.549	.0481	.0152	.00717	.00818	1	-.00416
2	1.431	1.549	.0549	.0155	.00858	.00818	1	-.00333

1 155 6.000 .901 1.020

2	.992	1.029	0.0000	0.0000	0.00000	.00427	1	.01166
1	1.205	1.274	0.0000	0.0000	0.00000	.00603	1	.00500
2	1.202	1.267	0.0000	0.0000	0.00000	.00601	1	.01133
1	1.414	1.500	0.0000	0.0000	0.00000	.00802	1	.01166
2	1.408	1.494	0.0000	0.0000	0.00000	.00795	1	.01166
1	1.649	1.795	0.0000	0.0000	0.00000	.01052	1	0.00000
2	1.639	1.763	0.0000	0.0000	0.00000	.01041	1	0.00000
1	1.906	2.089	.0198	0.0000	.00435	.01361	1	-.00333
2	1.906	2.089	.0187	0.0000	.00411	.01361	1	-.00333
1	2.126	2.319	.0466	0.0000	.01021	.01652	3	0.00000
2	2.126	2.321	.0337	0.0000	.00737	.01652	3	0.00000
1	2.339	2.552	.0220	0.0000	.00484	.01958	3	0.00000
2	2.325	2.560	.0349	0.0000	.00764	.01937	3	0.00000
1	2.557	2.759	.0240	0.0000	.00529	.02293	3	0.00000
2	2.557	2.794	.0388	0.0000	.00851	.02293	3	0.00000
1	2.812	3.069	.0206	0.0000	.00451	.02715	3	0.00000
2	2.812	3.067	.0579	.0054	.01147	.02715	3	0.00000
1	3.779	4.159	.0630	.0384	.00537	.04586	3	0.00000



2 202 6.000 .901 1.020

1	.984	.991	.0041	.0034	.00015	.00421	1	.01026
2	.984	.990	.0019	.0035	-.00036	.00421	1	.01000
1	1.245	1.202	.0045	.0017	.00061	.00639	1	.00503
2	1.245	1.277	0.0000	.0075	-.00251	.00639	1	.01416
1	1.448	1.542	.0141	.0022	.00257	.00639	1	0.00000
2	1.448	1.536	.0095	.0050	.00076	.00639	1	0.00000
1	1.709	1.841	.0237	.0076	.00351	.01122	1	-.00500
2	1.943	2.091	.0332	.0090	.00526	.01409	3	0.00000
2	1.709	1.836	0.0000	0.0000	-.00477	.01122	1	-.00366

2 192 6.000 .902 1.020

2	.606	.605	0.0000	0.0000	0.00000	.00178	1	.00900
1	.805	.820	.0015	.0033	-.00037	.00294	1	.01000
2	.805	.830	0.0000	.0051	-.00159	.00294	1	.00200
1	1.024	1.087	.0074	0.0000	.00170	.00452	1	0.00000
2	1.024	1.065	0.0000	.0057	-.00166	.00452	1	.00033
1	1.024	1.056	0.0000	.0037	-.00242	.00452	1	.01000
1	1.210	1.210	.0154	0.0000	.00400	.00608	1	0.00000
2	1.210	1.268	0.0000	0.0000	0.00000	.00608	1	.00733
1	1.467	1.539	0.0000	.0067	-.00181	.00655	1	.00333
2	1.462	1.549	0.0000	.0162	-.00469	.00650	1	.00500
1	1.639	1.769	.0238	.0042	.00427	.01041	1	-.00266
2	1.639	1.765	.0241	.0043	.00431	.01041	1	-.00333
1	1.884	2.034	.0191	.0173	.00037	.01334	1	-.00433
2	1.884	2.025	.0083	.0104	-.00045	.01334	1	-.00233
1	2.087	2.254	.0151	.0127	.00053	.01600	3	0.00000
2	2.087	2.263	.0304	.0043	.00568	.01600	3	0.00000
1	2.370	2.515	.0663	0.0000	.01719	.02004	3	0.00000



1 159 6.000 .902 1.050

1	4.576	5.070	0.0000	0.0000	0.00000	.06442	3	0.00000
2	4.587	5.082	.0364	0.0000	.00770	.06470	3	0.00000
1	3.759	4.123	.0593	0.0000	.01255	.04543	3	0.00000
2	3.759	4.129	.0479	0.0000	.01014	.04543	3	0.00000
1	3.263	3.533	.0211	0.0000	.00447	.03534	2	.02000
2	3.263	3.562	.0202	.0019	.00399	.03534	2	0.00000
1	3.480	3.601	.0133	.0099	.00140	.03962	2	.02000
2	3.480	3.788	.0220	0.0000	.00466	.03962	2	.02000
1	3.055	3.291	.0076	0.0000	.00162	.03145	2	.01333
2	3.030	3.302	.0425	0.0000	.00900	.03100	2	0.00000
1	2.850	3.102	.0097	0.0000	.00205	.02780	2	.01333
2	2.850	3.077	.0066	0.0000	.00145	.02780	2	.02000
1	2.580	2.795	0.0000	0.0000	0.00000	.02331	2	0.00000
2	2.561	2.764	0.0000	0.0000	0.00000	.02299	2	0.00000
1	2.351	2.518	0.0000	0.0000	0.00000	.01976	2	.02666
2	2.346	2.479	0.0000	0.0000	0.00000	.01971	2	.02666
1	2.126	2.157	0.0000	0.0000	0.00000	.01652	1	.00166
2	2.126	2.145	0.0000	0.0000	0.00000	.01652	1	.00216
1	1.880	1.996	0.0000	0.0000	0.00000	.01328	1	.00183

2 200 6.000 .901 1.050

2	.813	.786	.0019	.0020	-.00003	.00300	1	.01566
1	1.257	1.278	.0018	.0029	-.00022	.00650	1	.01500
2	1.257	1.291	.0062	.0013	.00106	.00650	1	.01500
1	1.722	1.793	.0057	.0017	.00087	.01144	1	.01833
2	1.723	1.790	.0058	0.0000	.00129	.01138	1	.02166
1	2.112	2.145	.0097	.0003	.00194	.01634	3	0.00000
2	2.116	2.117	.0077	.0035	.00091	.01639	2	.02000
1	2.356	2.500	.0013	.0074	-.00133	.01983	2	.01333
2	2.355	2.493	0.0000	.0129	-.00282	.01981	2	.01333
2	2.614	2.774	.0050	.0001	.00106	.02385	2	.01666
2	2.822	3.038	.0163	0.0000	.00694	.02732	2	0.00000
1	1.222	3.248	.0078	.0071	.00015	.00618	2	0.00000
2	1.222	3.285	.0097	.0022	.00164	.00618	2	-.01000
1	1.326	3.593	.0773	0.0000	.01747	.00715	2	0.00000
2	1.323	3.564	.0332	.0055	.00603	.00712	2	0.00000
1	1.414	3.800	0.0000	.0227	-.00725	.00802	2	0.00000

2 173 3.002 .902 1.050

1	.963	.561	.0100	0.0000	.00442	.00405	1	.02664
2	.950	.921	.0071	.0022	.00215	.00396	1	.04663
1	1.656	1.740	.0123	0.0000	.00941	.01061	1	.01399
2	1.656	1.710	0.0000	.0139	-.00709	.01061	1	.02265
1	1.895	1.900	.0261	0.0000	.01988	.01347	1	.01998
1	2.107	2.104	.0366	0.0000	.02360	.01626	2	.06662
2	2.110	2.224	0.0000	0.0000	-.02470	.01631	2	.06662





1 163 6.000 .902 1.100

1	5.879	6.478	.0589	0.0000	.01238	.10051	3	0.00000
2	5.836	6.478	.0981	0.0000	.02196	.09921	3	0.00000
1	5.098	5.643	.0316	0.0000	.00692	.07803	3	0.00000
2	5.122	5.643	.0987	0.0000	.02160	.07870	3	0.00000
1	4.765	5.241	.1000	0.0000	.02187	.06922	3	0.00000
2	4.770	5.189	0.0000	0.0000	0.00000	.06936	2	.00333
1	4.464	4.918	0.0000	0.0000	0.00000	.06166	2	0.00000
2	4.464	4.859	0.0000	0.0000	0.00000	.06166	2	.00333
1	4.178	4.544	0.0000	0.0000	0.00000	.05432	2	.01333
2	4.178	4.530	0.0000	0.0000	0.00000	.05432	2	.02000
1	3.923	4.270	0.0000	0.0000	0.00000	.04702	2	.01666
2	3.923	4.276	0.0000	0.0000	0.00000	.04902	2	.01666
1	3.278	3.529	0.0000	0.0000	0.00000	.03564	2	.02333
2	3.286	3.532	0.0000	0.0000	0.00000	.03579	2	.01666
1	2.356	2.491	0.0000	0.0000	0.00000	.01998	2	.03000
2	2.356	2.495	0.0000	0.0000	0.00000	.01982	2	.02666

2 193 4.000 .902 1.100

2	1.212	1.212	.0031	0.0000	.00091	.00509	1	.02516
1	1.692	1.737	.0020	.0016	.00007	.01102	1	.03083
2	1.692	1.715	.0041	0.0000	.00129	.01102	1	.03733
1	2.593	2.734	0.0000	.0105	-.00236	.02350	2	.02900
2	2.593	2.713	.0036	.0001	.00076	.02350	2	.03233
1	3.096	3.276	.0034	0.0000	.00266	.03220	2	.01500
2	3.096	3.291	.0116	0.0000	.00365	.03220	2	.01000
1	3.509	3.736	.0053	0.0000	.00140	.04021	2	.02500
2	3.509	3.724	0.0000	.0100	-.00277	.04021	2	.02500
2	3.987	4.305	.0159	0.0000	.00480	.05044	2	0.00000
1	4.256	4.580	.0010	.0127	-.00254	.05665	2	0.00000
2	4.256	4.551	0.0000	.0071	-.00219	.05665	2	0.00000
1	4.492	4.831	.0269	0.0000	.00016	.06235	2	0.00000
2	4.492	4.831	.0012	.0132	-.00371	.06235	2	0.00000
1	4.690	5.025	.0108	0.0000	.00540	.06731	2	0.00000
2	4.690	5.074	0.0000	0.0000	-.00219	.06731	2	0.00000



1 167 6.000 .901 1.150

1	5.353	5.886	0.0000	0.0000	0.00000	.03538	3	0.00000
2	5.353	5.880	0.0000	0.0000	0.00000	.03538	3	0.00000
1	5.660	6.231	.0532	0.0000	.01163	.09397	3	0.00000
2	5.660	6.252	.0418	0.0000	.01571	.09397	3	0.00000
1	5.866	6.420	.0300	0.0000	.00657	.10012	3	0.00000
2	5.879	6.470	.0215	0.0000	.00470	.10051	3	0.00000
1	6.193	6.832	.0974	0.0000	.02129	.11022	3	0.00000
2	6.172	6.832	0.0000	0.0000	0.00000	.10958	3	0.00000
1	6.393	7.077	.0833	0.0000	.01820	.11664	3	0.00000
2	6.393	7.066	.0984	0.0000	.02151	.11664	3	0.00000

2 196 6.000 .902 1.150

2	1.888	1.940	.0014	0.0000	.00045	.01339	2	.04000
1	2.611	2.713	0.0000	.0035	-.00099	.02380	2	.05000
2	2.611	2.725	.0003	.0040	-.00068	.02380	2	.04666
1	3.316	3.410	.0031	0.0000	.00091	.03638	2	.03333
2	3.324	3.403	0.0000	0.0000	0.00000	.03653	2	.03666
1	3.974	4.276	0.0000	0.0000	0.00000	.05016	2	.01666
2	3.974	4.242	.0106	0.0000	.00427	.05016	2	.02666
1	4.722	5.061	.0064	0.0000	.00213	.06813	2	.01666
2	4.722	5.012	0.0000	.0051	-.00129	.06813	2	.01666
1	5.176	5.594	0.0000	.0190	-.00488	.08013	2	0.00000
2	5.171	5.610	.0043	.0270	-.00484	.08005	2	0.00000
1	5.740	6.218	.0077	.0010	.00145	.09633	2	0.00000
2	5.740	6.204	.0309	0.0000	.00763	.09633	2	0.00000
1	5.977	6.470	.0576	.0121	.00992	.10350	2	0.00000
2	5.973	6.441	.0087	0.0000	.00255	.10337	2	0.00000



1 144 3.010 .802 1.000

1	.509	.557	.1935	.0202	.07527	.00130	3	0.00000
2	.501	.533	0.0000	.1758	-.07638	.00127	3	0.00000
1	1.005	1.027	.2129	.0267	.08082	.00437	3	0.00000
1	.999	1.036	.1883	.0125	.07638	.00432	3	0.00000
2	.999	1.025	0.0000	.1604	-.06971	.00432	3	0.00000
1	1.435	1.612	.1806	.0522	.05580	.00823	3	0.00000
2	1.431	1.556	.2012	.0151	.08082	.00818	3	0.00000
1	1.916	2.140	.1935	.1267	.02904	.01374	3	0.00000
2	1.920	2.133	.0651	.1434	-.03406	.01379	3	0.00000
1	2.565	2.881	.1217	.0704	.02234	.02305	3	0.00000
2	2.580	2.881	.2015	.0179	.07971	.02330	3	0.00000
1	3.573	4.039	.2046	.0505	.06693	.04152	3	0.00000
2	3.587	4.053	.0952	.0760	.00837	.04181	3	0.00000
1	4.685	5.275	.0957	.0629	.00558	.06717	3	0.00000
2	4.685	5.314	.1093	.0965	.00558	.06717	3	0.00000
1	5.879	6.666	.1847	.0627	.05302	.10051	3	0.00000
2	5.900	6.658	.2046	.0210	.07971	.10116	3	0.00000

1 148 3.010 .802 1.010

1	.788	.743	0.0000	0.0000	0.00000	.00284	3	0.00000
2	.793	.738	0.0000	0.0000	0.00000	.00287	3	0.00000
1	.992	1.026	0.0000	0.0000	0.00000	.00427	3	0.00000
2	.996	1.002	0.0000	0.0000	0.00000	.00430	3	0.00000
1	1.145	1.302	.0650	0.0000	.03739	.00551	3	0.00000
2	1.155	1.201	0.0000	0.0000	0.00000	.00560	3	0.00000
1	1.417	1.576	.1404	0.0000	.06156	.00804	3	0.00000
2	1.417	1.483	0.0000	0.0000	0.00000	.00804	3	0.00000
1	1.671	1.857	.1829	0.0000	.07836	.01077	3	0.00000
2	1.671	1.791	.0206	0.0000	.00895	.01077	3	0.00000
2	1.884	2.106	.1478	0.0000	.06413	.01334	3	0.00000
1	2.118	2.357	.2043	0.0000	.08932	.01642	3	0.00000
1	1.884	2.038	.1551	0.0000	.06733	.01334	3	0.00000
2	2.145	2.395	.2035	0.0000	.08932	.01678	3	0.00000
1	3.255	3.660	.1818	0.0000	.07886	.03519	3	0.00000
2	3.286	3.753	.1197	.0555	.02791	.03579	3	0.00000
1	2.796	3.132	.1807	.0172	.07100	.02688	3	0.00000
2	2.805	3.155	.1878	.0220	.07205	.02703	3	0.00000





2 379 3.000 .802 1.010

1	.585	.622	.0092	.0047	.00197	.00167	3	0.00000
2	.580	.537	0.0000	.0013	-.00059	.00165	1	-.01020
1	.772	.832	0.0000	.0078	-.00372	.00273	1	0.00000
2	.777	.795	0.0000	.0061	-.00372	.00277	1	.00333
1	1.005	1.060	.0014	.0054	-.00174	.00437	1	0.00000
2	1.010	.980	.0059	.0182	-.00535	.00441	1	.01933

1 152 3.010 .802 1.022

1	1.198	1.226	0.0000	0.0000	0.00000	.00597	1	.01262
2	1.205	1.244	0.0000	0.0000	0.00000	.00603	1	.01196
1	1.429	1.589	0.0000	0.0000	0.00000	.00816	3	0.00000
2	1.417	1.563	0.0000	0.0000	0.00000	.00804	1	.01063
1	1.685	1.862	.1081	0.0000	.04946	.01094	3	0.00000
2	1.680	1.796	0.0000	0.0000	0.00000	.01088	1	.01461
1	1.869	2.090	.0869	0.0000	.03978	.01315	1	.00930
2	1.863	1.919	0.0000	0.0000	0.00000	.01307	3	0.00000
2	2.099	2.313	.1173	0.0000	.05367	.01615	3	0.00000
1	2.368	2.569	.0555	0.0000	.02524	.02001	3	0.00000
2	2.368	2.657	.1888	0.0000	.08564	.02001	3	0.00000
1	2.805	3.150	.2000	0.0000	.09065	.02703	3	0.00000
2	2.805	3.122	.1222	0.0000	.05549	.02703	3	0.00000
1	3.544	3.935	.0989	.0299	.02999	.04094	3	0.00000
2	3.530	3.958	.2000	0.0000	.09065	.04065	3	0.00000
1	4.765	5.344	.2000	0.0000	.08650	.06922	3	0.00000
2	4.754	5.369	.2000	0.0000	.08650	.06895	3	0.00000

2 179 3.010 .802 1.050

1	1.429	1.462	.0057	0.0000	.00436	.00816	3	0.00000
1	2.334	2.516	.0097	0.0000	.00710	.01950	2	.01993
2	2.330	2.480	.0056	0.0000	.00372	.01945	2	.01661
1	2.827	2.992	0.0000	.0133	-.00551	.02740	2	.02524
1	2.604	2.800	.0134	0.0000	.00836	.02368	3	0.00000
2	2.600	2.772	0.0000	.0173	-.00755	.02363	3	0.00000





1 156 3.010 .902 1.050

1	1.434	1.440	0.0000	0.0000	0.00000	.00322	1	.01193
1	1.440	1.404	0.0000	0.0000	0.00000	.00327	1	.02325
2	1.437	1.435	0.0000	0.0000	0.00000	.00325	1	.02325
1	1.895	1.989	0.0000	0.0000	0.00000	.01347	1	.01326
2	1.888	1.999	0.0000	0.0000	0.00000	.01339	1	.01328
1	2.334	2.483	0.0000	0.0000	0.00000	.01950	2	.01328
2	2.334	2.483	0.0000	0.0000	0.00000	.01950	2	.01328
1	2.783	3.051	0.0000	0.0000	0.00000	.02666	3	0.00000
2	2.783	3.057	.0756	0.0000	.01648	.02666	3	0.00000
1	2.580	2.795	0.0000	0.0000	0.00000	.02330	3	0.00000
2	2.583	2.859	.0318	0.0000	.00693	.02335	3	0.00000
1	3.055	3.268	0.0000	0.0000	0.00000	.03145	3	0.00000
2	3.030	3.356	.0829	0.0000	.01509	.03100	3	0.00000
1	3.309	3.521	0.0000	0.0000	0.00000	.03623	3	0.00000
2	3.276	3.607	.0246	0.0000	.00541	.03564	3	0.00000
1	3.480	3.828	.2074	0.0000	.04521	.03962	3	0.00000
2	3.480	3.857	.2068	0.0000	.04500	.03962	3	0.00000
1	3.779	4.211	.0622	.0379	.01055	.04586	3	0.00000
2	3.759	4.144	.0354	.0245	.00475	.04543	3	0.00000

1 160 3.000 .800 1.100

1	2.796	2.926	0.0000	0.0000	0.00000	.02688	2	.05333
2	2.786	2.878	0.0000	0.0000	0.00000	.02688	2	.05666
1	3.247	3.445	0.0000	0.0000	0.00000	.03505	2	.04000
2	3.239	3.542	0.0000	0.0000	0.00000	.03490	2	.02666
1	3.738	4.064	0.0000	0.0000	0.00000	.04500	2	0.00000
2	3.738	4.062	0.0000	0.0000	0.00000	.04500	2	.02000
1	3.955	4.449	.0771	0.0000	.03368	.04973	2	0.00000
2	3.948	4.415	.0917	0.0000	.04004	.04959	2	.02666
1	4.262	4.727	0.0000	0.0000	0.00000	.05679	3	0.00000
2	4.262	4.712	.0260	0.0000	.01137	.05679	3	0.00000
1	4.515	5.017	.1372	0.0000	.05989	.06291	3	0.00000
2	4.492	5.034	.1397	0.0000	.06104	.06235	3	0.00000
1	4.738	5.364	.0992	0.0000	.04337	.06854	3	0.00000
2	4.738	5.265	0.0000	0.0000	0.00000	.06854	3	0.00000
1	5.152	5.862	.2091	0.0000	.09112	.07951	3	0.00000
2	5.220	5.862	.1501	0.0000	.06546	.08138	3	0.00000
2	5.801	6.567	.1948	0.0000	.08502	.09617	3	0.00000
1	5.771	6.507	.1895	0.0000	.08262	.09725	3	0.00000
2	6.687	7.851	.2013	0.0000	.08765	.13311	3	0.00000



2 178 3.010 .802 1.100

1	1.884	1.863	.0042	0.0000	.00325	.01334	1	.03607
2	1.878	1.841	.0025	0.0000	.00197	.01326	1	.04385
1	2.334	2.414	0.0000	.0047	-.00220	.01950	2	.04318
2	2.334	2.403	.0020	.0009	.00043	.01950	2	.04318
1	2.812	2.998	.0029	0.0000	.00197	.02715	2	.03986
2	2.812	2.919	0.0000	.0061	-.00272	.02715	2	.04518
1	3.030	3.210	0.0000	.0050	-.00220	.03100	2	.02790
2	3.030	3.110	0.0000	.0042	-.00185	.03100	2	.05647
1	3.286	3.436	.0106	0.0000	.00812	.03579	2	.05647
2	3.278	3.426	.0074	0.0000	.00569	.03564	2	.03986
1	3.551	3.826	0.0000	.0325	-.01416	.04109	2	0.00000
2	3.551	3.736	.0116	0.0000	.00882	.04109	2	.04651
1	3.759	4.059	0.0000	.0085	-.00371	.04543	3	0.00000
2	3.759	4.117	.0076	0.0000	.00581	.04543	3	0.00000
1	4.006	4.384	.0572	.0150	.01802	.05087	3	0.00000

2 171 3.010 .802 1.100

1	1.000	.895	.0067	0.0000	.00293	.00433	1	.02330
2	1.024	.904	.0102	0.0000	.00446	.00452	1	.03322
1	1.863	1.803	.0085	.0026	.00253	.01307	1	.03083
2	1.863	1.894	.0057	.0011	.00199	.01307	1	.02591
1	2.343	2.320	.0060	.0045	.00064	.01963	2	.06312
2	2.330	2.439	.0111	0.0000	.00669	.01945	2	.02524
1	2.814	2.957	.0097	0.0000	.00751	.02719	2	.03853
2	2.823	2.904	0.0000	.0164	-.00716	.02734	2	.04983
1	3.332	3.681	.0343	.0374	-.00134	.03668	2	0.00000
1	3.523	3.831	.0207	0.0000	.01596	.04050	2	.02325
2	3.516	3.753	0.0000	.0156	-.00680	.04036	2	.03322

1 164 3.010 .802 1.150

1	4.859	5.251	0.0000	0.0000	0.00000	.07168	2	.03986
2	4.859	5.256	0.0000	0.0000	0.00000	.07168	2	.03322
1	5.171	5.739	0.0000	0.0000	0.00000	.08005	2	.03986
2	5.171	5.774	.0534	0.0000	.02336	.08005	2	.02657
1	5.465	6.145	.1373	0.0000	.05986	.08830	2	0.00000
2	5.456	6.112	0.0000	0.0000	0.00000	.08804	2	0.00000
1	5.633	6.314	.1666	0.0000	.07271	.09332	2	0.00000
2	5.647	6.314	.1136	0.0000	.04962	.09358	2	0.00000





2 169 3.010 .802 1.150

1	.823	.643	.0022	0.0000	.00367	.00306	1	.03654
2	.813	.619	.0055	.0023	.00139	.00300	1	.03986
1	1.976	1.901	0.0000	.0017	-.00104	.01451	1	.05980
2	1.974	1.977	.0140	0.0000	.00641	.01449	1	.02990
1	2.565	2.644	.0146	0.0000	.00642	.02305	2	.03986
2	2.565	2.669	.0147	.0018	.00559	.02305	2	.03986
1	3.309	3.487	.0139	0.0000	.00583	.03623	2	.01993
2	3.316	3.414	.0091	0.0000	.00373	.03638	2	.05315
1	3.759	3.974	.0133	0.0000	.00612	.04543	2	.05315
2	3.759	4.067	.0078	.0040	.00169	.04543	2	.03986
2	4.214	4.522	.0070	0.0000	.00291	.05567	2	.03322
2	4.685	5.052	.0194	0.0000	.00851	.06717	2	.01993
2	4.972	5.384	.0864	.0031	.03624	.07466	2	.01993
1	5.248	5.739	.0534	.0033	.02180	.08219	2	.01993

1 145 6.010 .802 1.000

1	7.157	8.342	.1922	.1264	.01434	.14249	3	0.00000
1	5.900	6.873	.1861	.0780	.02354	.10116	3	0.00000
2	5.866	6.768	.1302	.0606	.01515	.10012	3	0.00000
1	4.722	5.487	.0473	.1057	-.01271	.06813	3	0.00000
2	4.733	5.466	.0738	.0987	-.00541	.06841	3	0.00000
1	3.161	4.114	.1345	.0812	.01161	.03340	3	0.00000
2	3.153	4.079	.2028	.1331	.01519	.03325	3	0.00000
1	2.588	2.963	.0338	.1156	-.01782	.02343	3	0.00000
2	2.579	2.966	.1287	.0998	.00630	.02328	3	0.00000
1	1.852	2.089	.1572	.1026	.01190	.01293	3	0.00000
2	1.852	2.099	.1980	.0279	.03706	.01293	3	0.00000
1	1.454	1.654	0.0000	.0273	-.00595	.00342	3	0.00000
2	1.459	1.639	.1992	.0539	.03165	.00847	3	0.00000
1	.992	1.102	0.0000	0.0000	0.00000	.00427	3	0.00000
2	.986	1.113	.1975	0.0000	.04327	.00422	3	0.00000
1	.569	.608	0.0000	0.0000	0.00000	.00159	3	0.00000

2 393 6.010 .802 1.010

1	.606	.590	.0052	0.0000	.00171	.00178	1	.00449
2	.606	.581	0.0000	.0023	-.00062	.00178	1	.00449
1	.979	1.006	.0158	0.0000	.00445	.00417	1	.00449
2	.979	.976	.0141	0.0000	.00390	.00417	1	.00915
1	1.231	1.336	.0016	.0039	-.00050	.00627	1	.00199
2	1.233	1.344	.0177	0.0000	.00555	.00628	1	.00166





1 149 6.010 .802 1.010

1	.767	.771	0.0000	0.0000	0.00000	.00270	3	0.00000
2	.767	.770	0.0000	0.0000	0.00000	.00270	1	.00499
1	.992	1.019	0.0000	0.0000	0.00000	.00427	1	.00665
2	.979	1.027	0.0000	0.0000	0.00000	.00417	1	.00599
1	1.237	1.331	0.0000	0.0000	0.00000	.00631	1	.00499
2	1.221	1.292	0.0000	0.0000	0.00000	.00617	3	0.00000
1	1.413	1.556	0.0000	0.0000	0.00000	.00800	3	0.00000
2	1.423	1.574	0.0000	0.0000	0.00000	.00815	3	0.00000
1	1.644	1.831	0.0000	0.0000	0.00000	.01047	3	0.00000
2	1.632	1.763	.0266	0.0000	.00582	.01033	3	0.00000
1	1.884	2.113	.0264	0.0000	.00582	.01334	3	0.00000
2	1.880	2.121	.0202	0.0000	.00436	.01328	3	0.00000
1	2.145	2.414	.0133	0.0000	.00291	.01673	3	0.00000
2	2.130	2.442	.0463	0.0000	.01013	.01657	3	0.00000
1	2.363	2.684	.1020	0.0000	.02183	.01994	3	0.00000
2	2.351	2.684	.1960	0.0000	.04276	.01976	3	0.00000
1	2.588	2.949	.1140	0.0000	.02474	.02343	3	0.00000
2	2.593	2.989	.1203	.0339	.01892	.02350	3	0.00000
1	3.516	4.059	0.0000	.0333	.00727	.04036	3	0.00000
2	3.530	4.076	.2021	.0218	.03928	.04065	3	0.00000

1 153 6.010 .802 1.020

1	4.765	5.487	.0691	.0250	.00961	.06922	3	0.00000
2	4.754	5.513	.1849	.0311	.03350	.06895	3	0.00000
1	3.480	3.958	0.0000	0.0000	0.00000	.03962	3	0.00000
2	3.480	3.994	.1537	.0309	.02676	.03962	3	0.00000
1	2.859	3.143	.0797	0.0000	.01740	.02795	3	0.00000
2	2.859	3.237	.0819	0.0000	.01788	.02795	3	0.00000
1	3.096	3.525	.1017	0.0000	.02217	.03220	3	0.00000
2	3.096	3.499	0.0000	0.0000	0.00000	.03220	3	0.00000
1	3.255	3.756	.1431	0.0000	.03123	.03519	3	0.00000
2	3.255	3.761	.1455	0.0000	.03175	.03519	3	0.00000
1	2.557	2.806	.0289	0.0000	.00631	.02293	3	0.00000
2	2.541	2.881	.0225	0.0000	.00491	.02267	3	0.00000
1	2.348	2.600	0.0000	0.0000	0.00000	.01971	3	0.00000
2	2.351	2.653	.1006	0.0000	.02197	.01976	3	0.00000
1	2.080	2.265	0.0000	0.0000	0.00000	.01589	1	.00998
2	2.068	2.272	0.0000	0.0000	0.00000	.01573	1	.00332
1	1.897	2.076	0.0000	0.0000	0.00000	.01350	1	.00665
2	1.897	2.025	0.0000	0.0000	0.00000	.01350	1	.01164
1	1.420	1.476	0.0000	0.0000	0.00000	.00807	3	0.00000



2 151 6.010 .802 1.020

1	.617	.557	0.0000	.0073	-.00212	.00184	1	.00732
1	.876	.866	0.0000	.0025	-.00086	.00342	1	.00665
2	.874	.850	0.0000	.0040	-.00074	.00341	1	.00831
1	1.219	1.269	0.0000	.0032	-.00102	.00615	1	.00665
2	1.220	1.254	.0076	0.0000	.00223	.00616	1	.00665
2	1.553	1.675	.0014	.0011	.00007	.00946	1	.00366
2	2.165	2.332	0.0000	.0093	-.00259	.01707	3	0.00000
1	2.394	2.622	.0602	0.0000	.02032	.02040	3	0.00000
2	2.733	3.188	.0544	0.0000	.01319	.02666	3	0.00000
1	2.619	2.826	.0192	.0234	-.00078	.02393	3	0.00000
2	2.619	2.872	0.0000	.0057	-.00275	.02393	3	0.00000
1	2.791	3.109	0.0000	.0210	-.00543	.02678	3	0.00000

2 201 6.000 .802 1.020

1	1.215	1.350	.0031	.0041	-.00022	.00612	1	.01333
2	1.645	1.775	.0118	0.0000	.00390	.01052	1	.00500
1	2.013	2.176	.0017	.0375	-.00781	.01499	2	.00333
2	2.009	2.210	.0085	0.0000	.00169	.01494	2	0.00000
1	2.355	2.651	0.0000	.0605	-.01683	.01901	2	0.00000
1	2.596	2.872	0.0000	.0026	-.00068	.02355	2	0.00000
2	2.596	2.891	.0435	0.0000	.01429	.02355	2	0.00000
1	2.827	3.226	.0375	0.0000	.01516	.02740	2	0.00000

1 157 6.010 .802 1.050

1	4.765	5.424	.0345	.0111	.00510	.06922	3	0.00000
2	4.765	5.513	.1462	0.0000	.03175	.05922	3	0.00000
1	3.752	4.177	0.0000	0.0000	0.00000	.04529	3	0.00000
2	3.759	4.200	0.0000	0.0000	0.00000	.04543	3	0.00000
1	4.031	4.510	0.0000	0.0000	0.00000	.05143	3	0.00000
2	4.037	4.595	.0965	0.0000	.02095	.05150	3	0.00000
1	4.262	4.876	0.0000	0.0000	0.00000	.05679	3	0.00000
2	4.262	4.864	.0317	0.0000	.00508	.05679	3	0.00000
1	4.492	5.166	.0137	0.0000	.00299	.06235	3	0.00000
2	4.492	5.166	.0551	0.0000	.01197	.06235	3	0.00000
1	4.952	5.733	.1634	.0139	.03257	.07412	3	0.00000
2	4.921	5.688	.1627	0.0000	.03531	.07331	3	0.00000
1	5.879	6.792	.1662	.0254	.03112	.10051	3	0.00000



2 199 6.010 .802 1.050

1	1.051	.993	.0054	0.0000	.00114	.00473	1	.01397
2	1.051	.979	.0028	0.0000	.00051	.00473	1	.01397
1	1.429	1.447	.0023	.0001	.00053	.00816	1	.01331
2	1.429	1.404	.0051	0.0000	.00157	.00816	1	.01830
1	1.891	1.933	.0110	0.0000	.00245	.01342	1	.02163
2	1.891	1.901	.0067	0.0000	.00160	.01342	1	.02429
1	2.365	2.550	.0101	0.0000	.00256	.01995	2	.01663
2	2.363	2.520	.0076	0.0000	.00303	.01994	2	.01663
1	2.812	3.070	.0053	0.0000	.00160	.02715	2	.00665
2	2.819	3.070	.0128	0.0000	.00459	.02727	2	.00998
1	3.332	3.630	.0119	0.0000	.00405	.03588	2	.01663
2	3.324	3.558	.0118	0.0000	.00344	.03653	2	.02329
1	3.537	3.862	.0053	0.0000	.00237	.04079	2	.00665
2	3.537	3.852	.0128	0.0000	.00536	.04079	2	.01331
1	3.759	4.129	.0123	0.0000	.00520	.04543	2	.00998
2	3.772	4.120	.0118	0.0000	.00482	.04572	2	.00998
1	4.024	4.445	.0009	.0141	-.00269	.05129	2	.00665

1 161 6.010 .502 1.100

1	6.905	7.916	0.0000	0.0000	0.00000	.13374	2	0.00000
2	6.887	8.016	.2005	0.0000	.04331	.13311	2	0.00000
1	6.549	7.454	0.0000	0.0000	0.00000	.12173	2	0.00000
2	6.549	7.622	.0626	0.0000	.01361	.12173	2	0.00000
1	6.828	7.884	.1746	0.0000	.03800	.13109	2	0.00000
2	6.824	7.798	.0457	0.0000	.00994	.13097	2	0.00000
1	6.314	7.265	.1363	0.0000	.02956	.11408	2	0.00000
2	6.330	7.320	.0592	0.0000	.01274	.11459	2	0.00000
1	6.069	6.965	.0285	0.0000	.00619	.10635	2	0.00000
2	6.069	6.965	.0453	0.0000	.00983	.10635	2	.00998
1	5.814	6.559	0.0000	0.0000	0.00000	.09856	2	.01663
2	5.793	6.532	0.0000	0.0000	0.00000	.09790	2	.01663
1	4.712	5.217	0.0000	0.0000	0.00000	.06736	2	.02662
2	4.706	5.304	0.0000	0.0000	0.00000	.06772	2	.00665
1	7.475	8.553	.0428	0.0000	.00729	.15394	3	0.00000
2	7.475	8.465	.1546	0.0000	.03341	.15394	3	0.00000
1	8.330	9.486	.1582	0.0000	.04319	.18656	3	0.00000
2	8.330	9.566	.1994	0.0000	.04319	.18656	3	0.00000





2 197 6.010 .602 1.100

2	1.302	1.177	0.0000	.0049	-.00176	.00692	1	.03227
1	1.937	1.879	.0015	.0043	-.00061	.01401	1	.03494
2	1.937	1.952	0.0000	.0118	-.00295	.01401	2	.02995
1	2.616	2.658	0.0000	.0042	-.00103	.02388	2	.04159
2	2.616	2.718	.0038	0.0000	.00268	.02388	2	.02828
1	3.278	3.534	0.0000	.0073	-.00206	.03564	2	.01663
2	3.278	3.463	.0050	0.0000	.00199	.03564	2	.02495
1	4.018	4.415	.0018	.0016	.00003	.05115	2	.01497
2	4.018	4.358	0.0000	.0058	-.00153	.05115	2	.01996
1	4.754	5.203	.0145	0.0000	.00463	.06295	2	.01331
2	4.754	5.175	.0040	.0010	.00065	.06295	2	.01996
1	5.210	5.762	.0051	.0013	.00024	.08112	2	.19966
2	5.210	5.774	0.0000	.0016	-.00356	.08112	2	0.00000
1	5.638	6.218	.0233	0.0000	.00551	.08332	2	0.00000
2	5.638	6.293	0.0000	.0183	-.00444	.08332	2	0.00000
1	6.314	6.582	.0279	0.0000	.00701	.11403	2	0.00000
2	6.314	6.559	0.0000	.0568	.00819	.11403	2	0.00000

1 165 6.010 .802 1.150

1	7.150	7.927	0.0000	0.0000	0.00000	.14227	3	0.00000
2	7.150	8.016	.0530	0.0000	.01158	.14227	3	0.00000
1	7.680	8.618	.1055	0.0000	.02312	.16150	3	0.00000
2	7.715	8.696	.0723	0.0000	.01566	.16283	3	0.00000
1	8.330	9.363	.0458	0.0000	.00996	.18656	3	0.00000
2	8.363	9.409	.0842	0.0000	.01833	.18787	3	0.00000
1	7.352	8.152	0.0000	0.0000	0.00000	.14946	3	0.00000
2	7.352	8.199	0.0000	0.0000	0.00000	.14946	3	0.00000

2 195 6.010 .802 1.150

1	4.690	5.138	.0011	.0032	-.00045	.06731	2	.00998
2	4.690	5.000	.0032	.0015	.00033	.06731	2	.02329
1	5.814	6.334	.0063	.0028	.00076	.09856	2	.02329
1	6.342	7.008	.0124	0.0000	.00289	.11497	2	0.00000
2	6.357	7.008	0.0000	.0039	-.00103	.11548	2	0.00000
1	6.858	7.339	.0103	0.0000	.00289	.13210	2	0.00000
2	6.858	7.302	0.0000	.0092	-.00303	.13210	2	.00990





1 108 3.006 .701 1.010

1	.235	.176	0.0000	0.0000	0.00000	.00033	3	0.00000
2	.236	.173	0.0000	0.0000	0.00000	.00033	3	0.00000
1	.475	.423	0.0000	0.0000	0.00000	.00115	3	0.00000
2	.474	.420	0.0000	0.0000	0.00000	.00115	3	0.00000
2	.690	.637	0.0000	0.0000	0.00000	.00224	3	0.00000
1	.986	.961	0.0000	0.0000	0.00000	.00422	3	0.00000
2	.986	1.005	0.0000	0.0000	0.00000	.00422	3	0.00000
1	1.200	1.243	0.0000	0.0000	0.00000	.00599	3	0.00000
2	1.215	1.277	0.0000	0.0000	0.00000	.00612	3	0.00000
1	1.435	1.536	.0306	.0070	.01030	.00823	3	0.00000
2	1.440	1.571	0.0000	.0367	-.01599	.00827	3	0.00000
1	1.646	1.779	0.0000	0.0000	0.00000	.01050	3	0.00000
2	1.646	1.843	0.0000	0.0000	0.00000	.01050	3	0.00000
1	1.884	2.120	.0461	.0492	-.00133	.01334	3	0.00000
2	1.884	2.114	.2461	.0205	.09801	.01334	3	0.00000
1	2.116	2.313	.0950	.0950	0.00000	.01639	3	0.00000
2	2.107	2.305	0.0000	.0229	-.00999	.01626	3	0.00000
1	2.360	2.700	.1484	.0349	.02764	.01988	3	0.00000
2	2.414	2.779	.3000	.1087	.03314	.02070	3	0.00000
1	2.650	3.056	.1370	.1370	0.00000	.02443	3	0.00000
2	2.650	2.957	.3000	0.0000	.12927	.02443	3	0.00000
1	2.824	3.276	.3000	.1049	.08479	.02735	3	0.00000
2	2.812	3.315	.0980	.0980	0.00000	.02715	3	0.00000

1 115 3.006 .701 1.020

1	2.823	3.306	.2773	.0116	.11527	.02734	3	0.00000
2	2.823	3.352	.2616	.0565	.08912	.02734	3	0.00000
1	3.055	3.532	.0650	.0182	.02042	.03145	3	0.00000
2	3.055	3.623	.3002	0.0000	.13310	.03145	3	0.00000
1	3.255	3.826	.2588	.0196	.10388	.03519	3	0.00000
2	3.255	3.878	.0854	.0463	.01701	.03519	3	0.00000
1	3.494	4.030	.0735	.0295	.01914	.03992	3	0.00000
2	3.501	4.047	.2755	.0244	.10903	.04006	3	0.00000
1	3.711	4.374	0.0000	.0585	-.02552	.04442	3	0.00000
2	3.759	4.371	.2523	.0990	.06670	.04543	3	0.00000
1	3.923	4.755	.1590	.0784	.03511	.04902	3	0.00000
2	3.923	4.783	.2742	.0560	.09483	.04902	3	0.00000
1	4.285	4.952	.2195	0.0000	.16383	.05735	3	0.00000
2	4.297	5.061	.2122	.1253	.03736	.05763	3	0.00000
1	4.576	5.344	.2644	0.0000	.11649	.06442	3	0.00000
2	4.565	5.309	0.0000	.1054	-.04592	.06415	3	0.00000
1	4.770	5.529	.2995	0.0000	.13366	.06936	3	0.00000
2	4.765	5.492	0.0000	0.0000	0.00000	.06922	3	0.00000
1	4.998	5.751	0.0000	0.0000	0.00000	.07534	3	0.00000
2	4.972	5.832	.1380	.0990	.01701	.07466	3	0.00000



2 113 3.006 .701 1.020

1	.230	.135	.0096	.0014	.00357	.00032	3	0.00000
2	.230	.146	0.0000	.0075	-.00369	.00032	3	0.00000
1	.458	.385	.0035	0.0000	.00305	.00108	1	.00399
1	.731	.656	.0013	.0074	-.00266	.00242	3	0.00000
2	.733	.681	0.0000	.0084	-.00409	.00249	1	.00452
2	1.018	1.020	.0001	.0044	-.00188	.00447	1	.00532
1	1.257	1.330	.0059	.0009	.00214	.00650	1	.00339
2	1.253	1.311	.0035	.0041	-.00025	.00647	1	.00499
2	1.656	1.812	0.0000	.0147	-.00621	.01061	1	.00565
1	1.888	2.049	0.0000	.0093	-.00694	.01339	1	.00565
1	1.414	1.443	.0090	0.0000	.00530	.00802	3	0.00000
1	1.659	1.754	.0102	0.0000	.00667	.01064	3	0.00000
2	1.656	1.791	.0130	.0018	.00490	.01061	3	0.00000
2	2.377	2.604	0.0000	0.0000	-.00091	.02014	3	0.00000

1 127 3.006 .701 1.050

2	4.379	5.074	.2254	0.0000	.09816	.05958	3	0.00000
1	4.190	4.864	.0551	0.0000	.02423	.05510	3	0.00000
2	4.184	4.807	.2855	0.0000	.12311	.05496	3	0.00000
1	3.923	4.599	.2749	0.0000	.12062	.04902	3	0.00000
2	3.942	4.636	.2878	0.0000	.12510	.04944	3	0.00000
1	3.745	4.289	.1896	0.0000	.08314	.04514	3	0.00000
2	3.725	4.248	.0724	0.0000	.03180	.04471	3	0.00000
1	3.443	3.834	0.0000	0.0000	0.00000	.03889	3	0.00000
2	3.443	4.003	.0344	0.0000	.01515	.03889	3	0.00000
2	3.239	3.621	0.0000	0.0000	0.00000	.03490	3	0.00000
1	2.946	3.237	0.0000	0.0000	0.00000	.02948	3	0.00000
2	2.946	3.296	0.0000	0.0000	0.00000	.02948	3	0.00000
1	2.714	2.981	0.0000	0.0000	0.00000	.02548	3	0.00000
2	2.705	2.994	0.0000	0.0000	0.00000	.02533	3	0.00000
1	2.541	2.722	0.0000	0.0000	0.00000	.02267	3	0.00000
2	2.533	2.816	0.0000	0.0000	0.00000	.02255	3	0.00000

1 124 3.006 .701 1.050

1	.455	.244	0.0000	0.0000	0.00000	.00107	1	.01796
2	.452	.271	.0002	.0002	0.00000	.00106	1	.01596
1	.452	.196	.0006	.0012	-.00026	.00106	1	.00996
1	.976	.841	.0069	0.0000	.00547	.00414	1	.01197
2	1.174	1.111	0.0000	0.0000	0.00000	.00576	1	.01131
1	1.406	1.322	.0040	.0022	.00079	.00793	1	.01330
1	1.646	1.626	.0062	0.0000	.00290	.01090	1	.01330
2	1.644	1.650	.0118	0.0000	.00541	.01047	1	.01131
2	1.906	1.951	0.0000	0.0000	-.00369	.01361	1	.01330





1 129 3.005 .701 1.100

1	4.685	5.170	.0323	0.0000	.01435	.06717	3	0.00000
2	4.685	5.246	0.0000	0.0000	0.00000	.06717	3	0.00000
1	4.947	5.577	.0447	0.0000	.01949	.07398	3	0.00000
2	4.942	5.671	.1504	0.0000	.06540	.07385	3	0.00000
2	5.102	5.856	.2667	0.0000	.11581	.07817	3	0.00000
1	5.386	6.178	.2565	0.0000	.11147	.09605	3	0.00000
2	5.386	6.178	.1634	0.0000	.07102	.09605	3	0.00000
1	5.638	6.522	.1726	0.0000	.07473	.09332	3	0.00000
2	5.638	6.448	.0767	0.0000	.03348	.09332	3	0.00000
1	5.879	6.849	.1028	0.0000	.04493	.10051	3	0.00000
2	5.840	6.744	.2891	0.0000	.12278	.09934	3	0.00000
1	6.111	7.103	.2997	0.0000	.13044	.10764	3	0.00000
2	6.111	7.077	.2668	0.0000	.11647	.10764	3	0.00000
1	6.373	7.386	.2965	0.0000	.12829	.11600	3	0.00000
2	6.373	7.542	.1799	0.0000	.07057	.11600	3	0.00000
1	6.679	7.663	.2831	0.0000	.12313	.12605	3	0.00000
2	6.679	7.683	.0625	.0227	.01732	.12605	3	0.00000

2 120 3.005 .701 1.110

1	.452	.161	0.0000	.0187	-.00925	.00106	1	.02152
2	.452	.179	.0020	0.0000	.00105	.00105	1	.01996
1	1.405	1.222	.0036	0.0000	.00317	.00792	1	.02661
1	1.884	1.811	.0010	.0025	-.00066	.01334	1	.02062
1	2.791	2.832	.0097	0.0000	.00542	.02678	2	.02661
2	2.794	2.869	0.0000	.0093	-.00489	.02683	3	0.00000
1	3.208	3.317	0.0000	.0005	.00052	.03430	2	.02322

1 120 3.005 .701 1.147

1	4.701	5.198	0.0000	0.0000	0.00000	.06758	3	0.00000
2	4.712	5.194	0.0000	0.0000	0.00000	.06786	3	0.00000
1	5.147	5.803	.0140	0.0000	.00612	.07937	3	0.00000
2	5.161	5.492	0.0000	0.0000	0.00000	.07978	3	0.00000
2	5.147	5.632	0.0000	0.0000	0.00000	.07937	3	0.00000
1	5.700	6.286	.0260	0.0000	.01137	.09515	3	0.00000
1	6.176	6.776	0.0000	0.0000	0.00000	.10971	3	0.00000
2	6.172	7.059	0.0000	0.0000	0.00000	.10958	3	0.00000
2	6.641	7.522	.1941	0.0000	.08466	.12473	3	0.00000





1 112 3.006 .701 1.147

1	6.069	6.681	0.0000	0.0000	0.00000	.10635	3	0.00000
2	6.131	7.033	.2151	0.0000	.09448	.10829	3	0.00000
1	6.549	7.542	.2126	0.0000	.09200	.12173	3	0.00000
2	6.549	7.522	.1261	0.0000	.05529	.12173	3	0.00000
1	6.978	7.927	0.0000	0.0000	0.00000	.13625	3	0.00000
2	6.978	8.072	.2708	0.0000	.11765	.13625	3	0.00000
2	7.715	8.683	.2845	0.0000	.12159	.16233	3	0.00000
1	8.406	9.566	.3027	0.0000	.12989	.18961	3	0.00000
2	8.471	9.518	.1657	0.0000	.08660	.19222	3	0.00000

2 117 3.006 .701 1.147

1	.462	.103	.0052	.0010	.00184	.00110	1	.02661
2	.460	.102	.0022	.0035	-.00059	.00109	1	.02661
1	1.034	.692	.0024	0.0000	.00144	.00460	1	.04457
2	1.038	.767	.0017	0.0000	.00105	.00463	1	.02994
2	1.431	1.218	0.0000	.0056	-.00263	.00318	1	.02994
1	1.873	1.747	.0026	0.0000	.00230	.01320	3	0.00000
1	2.325	2.268	.0033	.0009	.00105	.01937	2	.03326
2	2.343	2.329	.0023	.0013	.00065	.01963	2	.02661
1	2.819	2.805	.0058	0.0000	.00480	.02727	2	.02326
1	3.255	3.331	.0024	0.0000	.00171	.03519	2	.02661
2	3.759	4.065	0.0000	.0149	-.00382	.04543	3	0.00000
1	4.625	5.021	.0414	0.0000	.01816	.06566	3	0.00000
1	4.603	4.990	.0073	.0014	.00257	.06511	3	0.00000
2	4.625	5.170	0.0000	0.0000	0.00000	.06566	3	0.00000
1	5.186	5.762	0.0000	.0117	-.00523	.08045	3	0.00000
1	6.077	6.974	0.0000	0.0000	-.02936	.10661	3	0.00000



1 130 6.007 .701 1.000

1	.236	.297	.1518	0.0000	.03550	.00033	3	0.00000
2	.232	.216	0.0000	0.0000	0.00000	.00032	3	0.00000
1	.238	.273	.2578	.0167	.05254	.00033	3	0.00000
2	.238	.274	0.0000	.2251	-.04506	.00033	3	0.00000
1	.401	.476	.3070	.0536	.05520	.00035	3	0.00000
2	.403	.396	0.0000	0.0000	0.00000	.00036	3	0.00000
1	.805	.926	.2893	.0256	.05744	.00294	3	0.00000
2	.805	.967	.1500	.0751	.01631	.00294	3	0.00000
1	1.213	1.401	.0377	.0300	.00167	.00610	3	0.00000
2	1.217	1.421	.1823	.0871	.02077	.00614	3	0.00000
1	1.922	2.223	.0607	.0416	.00416	.01382	3	0.00000
2	1.922	2.263	.0264	.2012	-.03809	.01382	3	0.00000
1	2.557	3.138	.1922	.1138	.01709	.02358	3	0.00000
2	2.557	3.072	.1682	.1229	.00988	.02358	3	0.00000
1	3.523	4.229	.1100	.1100	0.00000	.04050	3	0.00000
2	3.523	4.245	.1307	.1493	-.00405	.04050	3	0.00000
2	4.701	5.627	.2882	.1963	.01960	.06758	3	0.00000

1 131 6.000 .701 1.010

1	5.836	6.923	.2439	.1159	.02791	.09921	3	0.00000
2	5.840	7.008	.0306	.1837	-.03341	.09934	3	0.00000
1	4.701	5.605	.0294	.1776	-.03233	.06758	3	0.00000
2	4.701	5.643	.2858	.1522	.02916	.06758	3	0.00000
2	3.622	4.361	.2486	.0861	.03548	.04254	3	0.00000
1	3.622	4.286	.1951	.0675	.02783	.04254	3	0.00000
1	2.591	3.005	.0243	.0663	-.00916	.02348	3	0.00000
2	2.596	3.039	.0583	.4430	-.08379	.02355	3	0.00000
1	2.112	2.346	0.0000	0.0000	0.00000	.01634	3	0.00000
2	2.112	2.364	0.0000	0.0000	0.00000	.01634	3	0.00000
1	1.916	2.169	.0182	0.0000	.00439	.01374	3	0.00000
2	1.916	2.035	0.0000	0.0000	0.00000	.01374	3	0.00000
1	1.910	2.173	0.0000	0.0000	0.00000	.01366	1	0.00000
1	1.680	1.820	0.0000	0.0000	0.00000	.01038	1	.00333
2	1.762	1.969	.0599	.0024	.01253	.01185	1	0.00000
1	1.454	1.550	0.0000	0.0000	0.00000	.00842	1	0.00000



2 132 6.000 .701 1.010

1	.238	.165	-.0023	.0005	.00038	.00033	3	0.00000
2	.238	.167	0.0000	.0016	-.00038	.00033	3	0.00000
1	.398	.334	.0020	.0004	.00034	.00034	3	0.00000
2	.399	.328	.0021	.0043	-.00049	.00034	3	0.00000
1	.751	.690	.0026	.0019	.00015	.00261	3	0.00000
2	.750	.687	.0039	.0001	.00083	.00260	3	0.00000
2	1.196	1.246	0.0000	.0036	-.00129	.00595	3	0.00000
1	1.427	1.515	.0126	0.0000	.00511	.00315	3	0.00000
2	1.427	1.512	0.0000	.0149	-.00511	.00315	3	0.00000
1	1.660	1.820	0.0000	.0001	-.00339	.01008	3	0.00000
2	1.678	1.867	0.0000	.0205	-.00725	.01008	3	0.00000

1 134 6.007 .701 1.020

1	7.063	8.566	.0446	.1463	-.02213	.13937	3	0.00000
2	7.063	8.440	.0153	.0845	-.01509	.13937	3	0.00000
2	6.314	7.663	.3000	0.0000	.05550	.11408	3	0.00000
1	6.314	7.642	.0730	.0730	0.00000	.11408	3	0.00000
1	5.683	6.882	.2960	.0362	.05658	.09463	3	0.00000
2	5.683	6.857	.3000	.0211	.05091	.09463	3	0.00000
1	4.952	6.035	.1065	.0699	.00798	.07412	3	0.00000
2	4.957	5.966	0.0000	.0601	-.01311	.07425	3	0.00000
1	4.515	5.374	.1262	.0489	.01635	.06291	3	0.00000
2	4.520	5.435	.2450	0.0000	.05340	.06304	3	0.00000
1	3.967	4.794	.0433	0.0000	.00944	.05044	3	0.00000
2	3.980	4.591	.0290	.0193	.00211	.05030	3	0.00000
2	3.974	4.794	.3000	0.0000	.05550	.05016	3	0.00000
1	3.494	4.138	.2113	.0325	.03898	.03992	3	0.00000
2	3.487	4.159	.2693	.0628	.04500	.03977	3	0.00000
1	3.309	3.783	0.0000	0.0000	0.00000	.03623	3	0.00000
2	3.316	3.821	.0764	.0162	.01311	.03638	3	0.00000
1	3.055	3.504	0.0000	0.0000	0.00000	.03145	3	0.00000
2	3.055	3.562	.0764	.0130	.01302	.03145	3	0.00000
1	2.796	3.131	0.0000	0.0000	0.00000	.02688	3	0.00000





1 137 6.000 .701 1.050

2	7.068	8.477	.3418	.0256	.06093	.13937	3	0.00000
1	6.607	7.982	.3073	.0384	.05862	.12364	3	0.00000
2	6.603	8.063	.0776	.0356	.00916	.12351	3	0.00000
1	6.253	7.483	.1872	.0142	.03775	.11215	3	0.00000
2	6.253	7.522	.3198	.0648	.05561	.11215	3	0.00000
1	5.849	6.990	.1979	.0863	.02435	.09960	3	0.00000
2	5.849	6.915	0.0000	0.0000	0.00000	.09960	3	0.00000
1	5.709	6.800	0.0000	0.0000	0.00000	.09542	3	0.00000
2	5.709	6.752	.2575	.0724	.04039	.09542	3	0.00000
1	5.410	6.514	.1811	.0434	.03005	.08671	3	0.00000
2	5.410	6.448	.2109	.0220	.04296	.08671	3	0.00000
1	5.122	6.016	0.0000	0.0000	0.00000	.07870	3	0.00000
2	5.122	6.132	.2302	0.0000	.05019	.07870	3	0.00000
1	4.921	5.739	.0507	.0173	.00727	.07331	3	0.00000
2	4.911	5.791	.1611	0.0000	.03515	.07303	3	0.00000
1	4.712	5.399	0.0000	0.0000	0.00000	.06786	3	0.00000
2	4.701	5.424	0.0000	0.0000	0.00000	.06753	3	0.00000

1 138 6.000 .701 1.100

1	11.664	13.863	.2558	.0263	.04095	.33909	3	0.00000
2	11.742	13.731	.2059	.0533	.03332	.34312	3	0.00000
1	10.554	12.531	.3486	.0225	.07106	.28395	3	0.00000
2	10.528	12.531	.2976	.0439	.05533	.28271	3	0.00000
1	8.912	10.435	.3357	0.0000	.07296	.21034	3	0.00000
2	8.861	10.360	.1515	.0435	.02353	.20819	3	0.00000
1	9.697	11.456	.2245	.0437	.03945	.24434	3	0.00000
2	9.697	11.388	.2843	.0327	.05487	.24434	3	0.00000
1	8.051	9.317	.1593	0.0000	.03468	.17563	3	0.00000
2	8.051	9.363	.1889	0.0000	.04117	.17563	3	0.00000
1	7.150	8.316	0.0000	0.0000	0.00000	.14227	3	0.00000
2	7.150	8.566	.1640	0.0000	.03575	.14227	3	0.00000
1	6.756	7.613	.0480	0.0000	.01044	.12866	3	0.00000
2	6.756	7.819	.1120	0.0000	.02437	.12866	3	0.00000

2 142 6.000 .701 1.100

1	5.254	6.054	0.0000	.0055	-.00161	.08232	3	0.00000
2	5.410	6.028	0.0000	.0045	-.00133	.08671	3	0.00000
1	4.932	5.481	0.0000	.0052	-.00165	.07358	3	0.00000
2	4.947	5.445	0.0000	.0007	-.00023	.07398	3	0.00000
1	4.244	4.621	.0012	0.0000	.00038	.05637	3	0.00000
2	4.232	4.577	0.0000	.0053	-.00146	.05601	2	.02000
1	3.400	3.665	0.0000	.0065	-.00165	.03962	2	.02333
2	3.400	3.662	0.0000	0.0000	0.00000	.03962	2	.02333





1 143 6.007 .701 1.147

1	7.099	8.005	0.0000	0.0000	0.00000	.14046	3	0.00000
2	7.099	7.862	0.0000	0.0000	0.00000	.14046	3	0.00000
1	7.703	8.912	.0508	.0052	.00829	.16239	3	0.00000
2	7.703	8.940	.0784	0.0000	.01712	.16239	3	0.00000
1	8.374	9.761	.0400	0.0000	.00374	.18830	3	0.00000
2	8.395	9.761	.1358	0.0000	.02866	.18817	3	0.00000
1	8.892	10.231	.0647	0.0000	.01414	.20840	3	0.00000
2	8.831	10.323	.1878	0.0000	.04084	.20819	3	0.00000
1	9.612	11.433	.0966	0.0000	.02109	.24055	3	0.00000
2	9.612	11.144	.0933	0.0000	.02142	.24055	3	0.00000
1	10.076	12.053	.2312	.0286	.04388	.26153	3	0.00000
2	10.130	12.007	.3039	.0180	.06225	.26403	3	0.00000
1	10.810	12.698	.2929	0.0000	.06329	.29631	3	0.00000
2	10.810	12.586	.0419	.0202	.00474	.29631	3	0.00000
1	11.506	13.255	.0150	.0150	0.00000	.33089	3	0.00000
1	11.648	13.504	.1239	.0490	.01634	.33828	3	0.00000

2 342 6.000 .701 1.150

1	3.566	3.776	0.0000	.0011	-.00038	.04138	2	.02000
2	3.551	3.676	0.0000	.0011	-.00038	.04107	2	.02333
2	4.685	5.124	0.0000	.0048	-.00153	.08717	3	0.00000
1	6.006	6.752	.0013	0.0000	.00053	.10441	3	0.00000





**B29883**